Importance of thermosensitive ion channel (TRPV2 and TRPV3) in cellular functions

By
Manoj Yadav
LIFE11201104006

National Institute of Science Education and Research,
Bhubaneswar

A thesis submitted to the
Board of Studies in Life Sciences
In partial fulfillment of the requirements
For the Degree of

DOCTOR OF PHILOSOPHY

of

HOMI BHABHA NATIONAL INSTITUTE

April, 2018

Homi Bhabha National Institute

Recommendations of the Viva Voce Committee

As members of the Viva Voce Committee, we certify that we have read the dissertation prepared by **Manoj Yadav** entitled "**Importance of thermosensitive ion channel (TRPV2 and TRPV3) in cellular functions**" and recommend that it may be accepted as fulfilling the thesis requirement for the award of Degree of Doctor of Philosophy.

Chairman: Dr. Sanjib Kar	**Date:** 05/04/2018
Guide / Convener: Dr. Chandan Goswami	**Date:** 5/4/2018
Examiner: Prof. M. K. Mathew	**Date:** 5/4/2018
Member 1: Dr. Praful Singru	**Date:** 5.4.2018
Member 2: Dr. Kishore CS Panigrahi	**Date:** 5.4.2018
Member 3: Prof. Avinash Sonawane	**Date:** 05.04.2018

Final approval and acceptance of this thesis is contingent upon the candidate's submission of the final copies of the thesis to HBNI.

I hereby certify that I have read this thesis prepared under my direction and recommend that it may be accepted as fulfilling the thesis requirement.

Place: Bhubaneswar **Signature** 5/4/2018

Date: 5/4/2018 **Guide**

Also, I would like to thank Dr. Luna Goswami (KIIT University, Bhubaneswar), Dr. Apratim Maity (OUAT, Bhubaneswar), Dr. Abhishek Kumar (Heidelberg, Germany) for their help during this time. I would also like to thank all funding agencies (DAE) for extending their financial support during my PhD tenure.

Special thanks to all my present lab mates Rakesh, Somdatta, Rashmita, Ram prasad, Tushar and Nishant for their help and support. Also, thankful to my former lab mates Ashutosh, Shikha, Arijit for their help and scientific input for thesis work. Special thanks to Nikhil for his help in the bioinformatics analysis for this thesis work. Also thankful to Divyanshi for her help in data analysis, SBS students (Ankit, Mitali, Tapas, Shubhransu, Shrikant, Anoop) and friends for their support during my PhD time for making this journey wonderful.

I would like to thank to my parents and family members for their continuous help and support in this time of PhD. Without their support this journey would have been impossible.

Manoj Yadav

ACKNOWLEDGEMENTS

I acknowledge each and every one who is directly or indirectly associated with me during this time, without their guidance, help and blessing this thesis would not have been completed.

I would like to acknowledge my thesis supervisor Dr. Chandan Goswami who guided me throughout this time. Without his guidance this thesis seemed impossible. Also, I would like to acknowledge my thesis monitoring committee and doctoral committee member Dr. Sanjib Kar (NISER Bhubaneswar), Dr. Praful Singru (NISER Bhubaneswar), Dr. Kishore C.S. Panigrahi (NISER Bhubaneswar), Dr. Abdur Rahaman (NISER Bhubaneswar), and Prof. Avinash Sonawane (KIIT Bhubaneswar) for their scientific advises during this time. I would like to acknowledge all the faculty members, and staff from school of biological sciences for their constant help and support. I acknowledge the Imaging facility, FACS facility and other central instrumentation facility from school of biological science.

Also, I would like to acknowledge the help from other scientist across the world for providing constructs. Dr. Yong Yang (Beijing China) for providing TRPV3-Wt and OS mutant construct, Prof. Jon D Levine (UCSF, San Francisco) for sending pCDNA 3.1 construct, Prof. J. Berreiter-Hahn (Frankfurt, Germany) for pEGFPN3 construct, Dr. P V Alone (NISER, India) for pGEX6P1, Prof. R. Y. Tsien (Sen Diego, California) for tubulin-mCherry, Prof. F. Hucho (FU, Berlin) for TRPV2-GFP and MBP-TRPV2-Ct, and Prof. Kees Jalink (Netherlands Cancer Institute, NKI-AVL) for providing cAMP sensor.

My sincere thanks to Prof. Eckart D. Gundelfinger and Dr. Karl-Heinz Smalla (Magdeburg, Germany) for providing Synaptosome fractions of rat fore brain. I am thankful to Prof. H. H. Ropers, Dr. Tim Hucho, Dr. Rudi Lurz and other lab members (Max Planck Institute of Molecular Genetics, Berlin) for sending cell lines.

Dedicated to…

My Parents

Conference, Symposium and workshop attended:

1. Participated in SERB School in Neuroscience - VIth Edition, from Dec 10th- 23rd 2012 at NISER, Bhubaneswar, Orissa.
2. XXXVll All India Cell Biology Conference, Bangalore, 2013.
3. Indian Immunology Society - Odisha Chapter, Aug 11, 2012, NISER, Bhubaneswar.
4. Participated in Welcome trust / DBT India Alliance, Science communication workshop, held on 11 September 2014 at ILS, Bhubaneswar.
5. Participated in Orientation workshop on laboratory animal sciences, held on July 13-15, 2015 at ILS, Bhubaneswar.
6. Participated in International conference on Electron Microscopy (EMSI- 2015) held on July 8-10, 2015, at Bhabha Atomic research center (BARC), Tromby, Mumbai.
7. Participated in 83rd annual meeting of the society of biological chemist (India), Haldane memorial symposium on evolutionary biology, held on 17th Dec. 2014, NISER, Bhubaneswar.
8. Participated in International conference on neurosciences on brain plasticity and neurological disorders. Ravenshaw University, Cuttack. 9-11th Nov 2013.
9. Participated in International symposium on genetic analysis, from 21st -23rd November 2014, department of zoology, the university of Burdwan.
10. Participated in the Bangalore Microscopy Course, 2014 held at NCBS, Bangalore from 21st to 28th 2014.
11. Participated in 2nd International Conference on Translation Research (ICTR-2016) from 14th -16th October 2016 at KIIT University, Bhubaneswar.

Manoj Yadav

List of Publications arising from the thesis:

1. Yadav M, Goswami C. (2016) TRPV3 mutants causing *Olmsted Syndrome* induce impaired cell adhesion and nonfunctional lysosomes. *Channels (Austin)*. 18:1-13.

2. Majhi RK*, Sahoo SS*, **Yadav M**, Pratheek BM, Chattopadhyay S, Goswami C. (2015) Functional expression of TRPV channels in T cells and their implications in immune regulation. *FEBS J*. **282**:2661-2681.

3. Kumar A, Kumari S, Majhi RK, Swain N, **Yadav M**, Goswami C. (2015) Regulation of TRP channels by steroids: Implications in physiology and diseases. *General and Comparative Endocrinology* **220**:23-32.

4. *Kumari S, *Kumar A, *Sardar P, **Yadav M**, Majhi RK, Kumar A, Goswami C. (2015) Influence of membrane cholesterol in the molecular evolution and functional regulation of TRPV4. *Biochem Biophys Res Commun*. **456**: 312-9.

Communicated: (From thesis)

1. Yadav M, Goswami C. (2017) Activation of TRPV2 induces neurite initiation and branching. *Journal of Neurochemistry*.

2. Yadav M, Saha S. &Goswami C. (2017) From neuropathy to naturopathy: Plant and natural products as modulators of TRP channels.

Other Publications:

1. Singh U, Kumar S, Shelkar GP, **Yadav M**, Kokare DM, Goswami C, Lechan RM, Singru PS. (2016) Transient receptor potential vanilloid (TRPV3) in the ventral tegmental area of rat: Role in modulation of the mesolimbic-dopamine reward pathway. 110:198-210.

2. ‡ *Majhi RK, Kumar A, **Yadav M**, Swain N, Kumari S, Saha A, Pradhan A, Goswami L, Saha S, Samanta L, Maity A, Nayak TK, Chattopadhyay S, Rajakuberan C, Kumar A, Goswami C. (2013) Thermosensitive ion channel TRPV1 is endogenously expressed in the sperm of a fresh water teleost fish (*Labeo rohita*) and regulates sperm motility. *Channels* **7**: 1-10.

3. Majhi R K, Kumar A, **Yadav M**, Kumar P, Maiti A, Giri S.C., Goswami C. (2015) Light and electron microscopic study of mature spermatozoa from white pekin duck (*Anas platyrhynchos*): An ultrastructural and molecular analysis. ***Andrology***. 4:232-244.

Chapters in books and lectures notes:

1. Kumar A, Majhi R, **Yadav M**, Szallasi A, Goswami C. (2013) TRPV1 activators ("vanilloids") as neurotoxins. Book chapter (*Springer*), pp 611-636.

Awards and recognition

1. "**Oral presentation**" at International conference on neurosciences on brain plasticity and neurological disorders. Ravenshaw University, Cuttack. 9-11th Nov 2013.

2. "1st prize in Oral presentation" at International symposium on genetic analysis, from 21st -23rd November 2014, department of zoology, the university of Burdwan.

3. "2nd runner-up Poster award" DSS- NCBS MicroImaging awards-2014 The Zeeshan Khan Memorial award for excellence in light microscopy, at the Bangalore Microscopy Course, 2014 held at NCBS, Bangalore from 21st to 28th 2014.

4. Special Jury Award for poster presentation in 2nd International Conference on Translation Research (ICTR-2016) from 14th -16th October 2016 at KIIT University, Bhubaneswar.

DECLARATION

I, hereby declare that the investigation presented in the thesis has been carried out by me. The work is original and has not been submitted earlier as a whole or in part for a degree / diploma at this or any other Institution / University.

Manoj Yadav

STATEMENT BY AUTHOR

This dissertation has been submitted in partial fulfillment of requirements for an advanced degree at Homi Bhabha National Institute (HBNI) and is deposited in the Library to be made available to borrowers under rules of the HBNI.

Brief quotations from this dissertation are allowable without special permission, provided that accurate acknowledgement of source is made. Requests for permission for extended quotation from or reproduction of this manuscript in whole or in part may be granted by the Competent Authority of HBNI when in his or her judgment the proposed use of the material is in the interests of scholarship. In all other instances, however, permission must be obtained from the author.

Manoj Yadav

Content

Doctoral Committee:

S. No.	Name	Designation	Signature	Date
1.	Dr. Sanjib Kar	Chairman		
2.	Dr. Chandan Goswami	Guide/ Convener		
3.		Co-guide (if any)		
4.	Dr. Prafull Singru	Member		
5.	Prof. Avinash Sonawane	Member		
6.	Dr. Kishore C.S. Panigrahi	Member		

Awards and recognition

1. **"Oral presentation"** at International conference on neurosciences on brain plasticity and neurological disorders. Ravenshaw University, Cuttack. 9-11th Nov 2013.

2. **"1st prize in Oral presentation"** at International symposium on genetic analysis, from 21st -23rd November 2014, department of zoology, the university of Burdwan.

3. **"2nd runner-up Poster award"** DSS- NCBS MicroImaging awards-2014 The Zeeshan Khan Memorial award for excellence in light microscopy, at the Bangalore Microscopy Course, 2014 held at NCBS, Bangalore from 21st to 28th 2014.

4. **Special Jury Award for poster presentation** in 2nd International Conference on Translation Research (ICTR-2016) from 14th -16th October 2016 at KIIT University, Bhubaneswar.

Conference, Symposium and workshop attended:

1. Participated in SERB School in Neuroscience - VIth Edition, from Dec 10th- 23rd 2012 at NISER, Bhubaneswar, Orissa.
2. XXXVII All India Cell Biology Conference, Bangalore, 2013.
3. Indian Immunology Society - Odisha Chapter, Aug 11, 2012, NISER, Bhubaneswar.
4. Participated in Welcome trust / DBT India Alliance, Science communication workshop, held on 11 September 2014 at ILS, Bhubaneswar.
5. Participated in Orientation workshop on laboratory animal sciences, held on July 13-15, 2015 at ILS, Bhubaneswar.
6. Participated in International conference on Electron Microscopy (EMSI- 2015) held on July 8-10, 2015, at Bhabha Atomic research center (BARC), Tromby, Mumbai.
7. Participated in 83rd annual meeting of the society of biological chemist (India), Haldane memorial symposium on evolutionary biology, held on 17th Dec. 2014, NISER, Bhubaneswar.
8. Participated in International conference on neurosciences on brain plasticity and neurological disorders. Ravenshaw University, Cuttack. 9-11th Nov 2013.
9. Participated in International symposium on genetic analysis, from 21st -23rd November 2014, department of zoology, the university of Burdwan.
10. Participated in the Bangalore Microscopy Course, 2014 held at NCBS, Bangalore from 21st to 28th 2014.
11. Participated in 2nd International Conference on Translation Research (ICTR-2016) from 14th -16th October 2016 at KIIT University, Bhubaneswar.

Signature of Student:

Date: 15/05/2017

Publications in Refereed Journal:

Published:

***1. Yadav M,** Goswami C. (2016) TRPV3 mutants causing *Olmsted Syndrome* induce impaired cell adhesion and nonfunctional lysosomes. *Channels (Austin)*. 18:1-13.

2. Singh U, Kumar S, Shelkar GP, **Yadav M**, Kokare DM, Goswami C, Lechan RM, Singru PS. (2016) Transient receptor potential vanilloid (TRPV3) in the ventral tegmental area of rat: Role in modulation of the mesolimbic-dopamine reward pathway. 110:198-210.

***3.** Majhi RK*, Sahoo SS*, **Yadav M**, Pratheek BM, Chattopadhyay S, Goswami C. (2015) Functional expression of TRPV channels in T cells and their implications in immune regulation. *FEBS J*. **282**:2661-2681.

4. ‡ *Majhi RK, Kumar A, **Yadav M**, Swain N, Kumari S, Saha A, Pradhan A, Goswami L, Saha S, Samanta L, Maity A, Nayak TK, Chattopadhyay S, Rajakuberan C, Kumar A, Goswami C. (2013) Thermosensitive ion channel TRPV1 is endogenously expressed in the sperm of a fresh water teleost fish (*Labeo rohita*) and regulates sperm motility. *Channels* **7**: 1-10.

***5.** Kumar A, Kumari S, Majhi RK, Swain N, **Yadav M**, Goswami C. (2015) Regulation of TRP channels by steroids: Implications in physiology and diseases. *General and Comparative Endocrinology* **220**:23-32.

***6.** *Kumari S, *Kumar A, *Sardar P, **Yadav M**, Majhi RK, Kumar A, Goswami C. (2015) Influence of membrane cholesterol in the molecular evolution and functional regulation of TRPV4. *Biochem Biophys Res Commun*. **456**: 312-9.

7. Majhi R K, Kumar A, **Yadav M**, Kumar P, Maiti A, Giri S.C., Goswami C. (2015) Light and electron microscopic study of mature spermatozoa from white pekin duck (*Anas platyrhynchos*): An ultrastructural and molecular analysis. ***Andrology***. 4:232-244.

*8. Kumar A, Majhi R, **Yadav M**, Szallasi A, Goswami C. (2013) TRPV1 activators ("vanilloids") as neurotoxins. Book chapter (*Springer*), pp 611-636.

Communicated:

***9. Yadav M,** Goswami C. (2017) Activation of TRPV2 induces neurite initiation and branching. *Journal of Neurochemistry*.

*10. **Yadav M**, Saha S. &Goswami C. (2017) From neuropathy to naturopathy: Plant and natural products as modulators of TRP channels.

*Pertaining to this thesis

30. Dong, X.P. et al. The type IV mucolipidosis-associated protein TRPML1 is an endolysosomal iron release channel. Nature 455, 992-996 (2008).
31. Krapivinsky, G., Mochida, S., Krapivinsky, L., Cibulsky, S.M. & Clapham, D.E. The TRPM7 ion channel functions in cholinergic synaptic vesicles and affects transmitter release. Neuron 52, 485-496 (2006).
32. Lange, I. et al. TRPM2 functions as a lysosomal Ca2+-release channel in beta cells. Sci Signal 2, ra23 (2009).
33. Turner, H., Fleig, A., Stokes, A., Kinet, J.P. & Penner, R. Discrimination of intracellular calcium store subcompartments using TRPV1 (transient receptor potential channel, vanilloid subfamily member 1) release channel activity. Biochem J 371, 341-350 (2003).
34. Goswami, C. Structural and functional regulation of growth cone, filopodia and synaptic sites by TRPV1. Commun Integr Biol 3, 614-618.
35. Goswami, C. et al. Identification and characterization of a Ca2+ -sensitive interaction of the vanilloid receptor TRPV1 with tubulin. J Neurochem 91, 1092-1103 (2004).
36. Goswami, C. & Hucho, T. TRPV1 expression-dependent initiation and regulation of filopodia. J Neurochem 103, 1319-1333 (2007).
37. Goswami, C. et al. Estrogen destabilizes microtubules through an ion-conductivity-independent TRPV1 pathway. J Neurochem 117, 995-1008.
38. Goswami, C., Kuhn, J., Heppenstall, P.A. & Hucho, T. Importance of non-selective cation channel TRPV4 interaction with cytoskeleton and their reciprocal regulations in cultured cells. PLoS One 5, e11654.
39. Goswami, C. et al. TRPV1 acts as a synaptic protein and regulates vesicle recycling. J Cell Sci 123, 2045-2057.
40. Goswami, C., Schmidt, H. & Hucho, F. TRPV1 at nerve endings regulates growth cone morphology and movement through cytoskeleton reorganization. FEBS J 274, 760-772 (2007).
41. Dehmelt, L. & Halpain, S. Actin and microtubules in neurite initiation: are MAPs the missing link? J Neurobiol 58, 18-33 (2004).
42. Sainath, R. & Gallo, G. Cytoskeletal and signaling mechanisms of neurite formation. Cell Tissue Res 359, 267-278.
43. Bedlack, R.S., Jr., Wei, M. & Loew, L.M. Localized membrane depolarizations and localized calcium influx during electric field-guided neurite growth. Neuron 9, 393-403 (1992).
44. Hutchins, B.I. Competitive outgrowth of neural processes arising from long-distance cAMP signaling. Sci Signal 3, jc1.
45. Nishiyama, M. et al. Cyclic AMP/GMP-dependent modulation of Ca2+ channels sets the polarity of nerve growth-cone turning. Nature 423, 990-995 (2003).
46. Oyama, K. et al. Triggering of high-speed neurite outgrowth using an optical microheater. Sci Rep 5, 16611.
47. Xiong, Y., Lee, A.C., Suter, D.M. & Lee, G.U. Topography and nanomechanics of live neuronal growth cones analyzed by atomic force microscopy. Biophys J 96, 5060-5072 (2009).
48. Neumann, S., Doubell, T.P., Leslie, T. & Woolf, C.J. Inflammatory pain hypersensitivity mediated by phenotypic switch in myelinated primary sensory neurons. Nature 384, 360-364 (1996).
49. Tojima, T. & Ito, E. A cyclic AMP-regulated negative feedforward system for neuritogenesis revealed in a neuroblastomaxglioma hybrid cell line. Neuroscience 104, 583-591 (2001).
50. Tojima, T., Takahashi, M. & Ito, E. Dual regulation of LIM kinase 1 expression by cyclic AMP and calcium determines cofilin phosphorylation states during neuritogenesis in NG108-15 cells. Brain Res 985, 43-55 (2003).
51. Li, C. et al. Sorting Nexin 11 Regulates Lysosomal Degradation of Plasma Membrane TRPV3. Traffic 17, 500-514.
52. Bargal, R. et al. Identification of the gene causing mucolipidosis type IV. Nat Genet 26, 118-123 (2000).
53. Bassi, M.T. et al. Cloning of the gene encoding a novel integral membrane protein, mucolipidin-and identification of the two major founder mutations causing mucolipidosis type IV. Am J Hum Genet 67, 1110-1120 (2000).
54. Sun, M. et al. Mucolipidosis type IV is caused by mutations in a gene encoding a novel transient receptor potential channel. Hum Mol Genet 9, 2471-2478 (2000).
55. Baier, C.J., Fantini, J. & Barrantes, F.J. Disclosure of cholesterol recognition motifs in transmembrane domains of the human nicotinic acetylcholine receptor. Sci Rep 1, 69.
56. Fantini, J. & Barrantes, F.J. How cholesterol interacts with membrane proteins: an exploration of cholesterol-binding sites including CRAC, CARC, and tilted domains. Front Physiol 4, 31.

References:

1. Cosens, D.J. & Manning, A. Abnormal electroretinogram from a Drosophila mutant. Nature 224, 285-287 (1969).

2. Montell, C. & Rubin, G.M. Molecular characterization of the Drosophila trp locus: a putative integral membrane protein required for phototransduction. Neuron 2, 1313-1323 (1989).

3. Matsuura, H., Sokabe, T., Kohno, K., Tominaga, M. & Kadowaki, T. Evolutionary conservation and changes in insect TRP channels. BMC Evol Biol 9, 228 (2009).

4. Stowers, L., Holy, T.E., Meister, M., Dulac, C. & Koentges, G. Loss of sex discrimination and male-male aggression in mice deficient for TRP2. Science 295, 1493-1500 (2002).

5. Zhang, Y. et al. Coding of sweet, bitter, and umami tastes: different receptor cells sharing similar signaling pathways. Cell 112, 293-301 (2003).

6. Montell, C., Jones, K., Hafen, E. & Rubin, G. Rescue of the Drosophila phototransduction mutation trp by germline transformation. Science 230, 1040-1043 (1985).

7. Hofmann, T., Schaefer, M., Schultz, G. & Gudermann, T. Subunit composition of mammalian transient receptor potential channels in living cells. Proc Natl Acad Sci U S A 99, 7461-7466 (2002).

8. Caterina, M.J., Rosen, T.A., Tominaga, M., Brake, A.J. & Julius, D. A capsaicin-receptor homologue with a high threshold for noxious heat. Nature 398, 436-441 (1999).

9. Nilius, B. & Owsianik, G. The transient receptor potential family of ion channels. Genome Biol 12, 218.

10. Iwata, Y. et al. A novel mechanism of myocyte degeneration involving the Ca2+-permeable growth factor-regulated channel. J Cell Biol 161, 957-967 (2003).

11. Peralvarez-Marin, A., Donate-Macian, P. & Gaudet, R. What do we know about the transient receptor potential vanilloid 2 (TRPV2) ion channel? FEBS J 280, 5471-5487.

12. Peier, A.M. et al. A heat-sensitive TRP channel expressed in keratinocytes. Science 296, 2046-2049 (2002).

13. Smith, G.D. et al. TRPV3 is a temperature-sensitive vanilloid receptor-like protein. Nature 418, 186-190 (2002).

14. Xu, H. et al. TRPV3 is a calcium-permeable temperature-sensitive cation channel. Nature 418, 181-186 (2002).

15. Cheng, X. et al. TRP channel regulates EGFR signaling in hair morphogenesis and skin barrier formation. Cell 141, 331-343.

16. Denda, M., Sokabe, T., Fukumi-Tominaga, T. & Tominaga, M. Effects of skin surface temperature on epidermal permeability barrier homeostasis. J Invest Dermatol 127, 654-659 (2007).

17. Ferby, I. et al. Mig6 is a negative regulator of EGF receptor-mediated skin morphogenesis and tumor formation. Nat Med 12, 568-573 (2006).

18. Murillas, R. et al. Expression of a dominant negative mutant of epidermal growth factor receptor in the epidermis of transgenic mice elicits striking alterations in hair follicle development and skin structure. EMBO J 14, 5216-5223 (1995).

19. Danso-Abeam, D. et al. Olmsted syndrome: exploration of the immunological phenotype. Orphanet J Rare Dis 8, 79.

20. Duchatelet, S. et al. Olmsted syndrome with erythromelalgia caused by recessive transient receptor potential vanilloid 3 mutations. Br J Dermatol 171, 675-678.

21. Duchatelet, S. et al. A new TRPV3 missense mutation in a patient with Olmsted syndrome and erythromelalgia. JAMA Dermatol 150, 303-306.

22. Eytan, O. et al. Olmsted syndrome caused by a homozygous recessive mutation in TRPV3. J Invest Dermatol 134, 1752-1754.

23. He, Y. et al. A gain-of-function mutation in TRPV3 causes focal palmoplantar keratoderma in a Chinese family. J Invest Dermatol 135, 907-909.

24. Kariminejad, A., Barzegar, M., Abdollahimajd, F., Pramanik, R. & McGrath, J.A. Olmsted syndrome in an Iranian boy with a new de novo mutation in TRPV3. Clin Exp Dermatol 39, 492-495.

25. Konathan, R. & Alur, S.K. Olmsted Syndrome in a Family. Int J Trichology 8, 168-170.

26. Lai-Cheong, J.E. et al. Recurrent heterozygous missense mutation, p.Gly573Ser, in the TRPV3 gene in an Indian boy with sporadic Olmsted syndrome. Br J Dermatol 167, 440-442.

27. Lin, Z. et al. Exome sequencing reveals mutations in TRPV3 as a cause of Olmsted syndrome. Am J Hum Genet 90, 558-564.

28. Klein, A.S., Tannert, A. & Schaefer, M. Cholesterol sensitises the transient receptor potential channel TRPV3 to lower temperatures and activator concentrations. Cell Calcium 55, 59-68.

29. Bezzerides, V.J., Ramsey, I.S., Kotecha, S., Greka, A. & Clapham, D.E. Rapid vesicular translocation and insertion of TRP channels. Nat Cell Biol 6, 709-720 (2004).

both *in silico* as well as in biochemical experiments. This can be extrapolated as TRPV3-induced channelopathy due to reduced/loss of cholesterol interaction.

In conclusion, this study establishes the important role of TRPV2 in neuronal cell function, especially in neuritogenesis process. TRPV3 is a lysosomal protein and regulates lysosomal functions. *Olmsted Syndrome* causing TRPV3 mutants cause the lysosomal disorder. However, further investigations are needed to understand the molecular mechanisms in details.

problem in terms of the structure and function of different subcellular organelles. Among all, lysosomes are most affected due to the expression of OS mutants, even at a very low level. This thesis work suggests that TRPV3 (both wild type and OS mutants) are present in the lysosome and are involved in the ionic homeostasis of the lysosome. This accord well with a recent report suggesting that TRPV3 is present in lysosome and interacts with lysosomal protein [51]. TRPV3 seem to be involved in the Ca^{2+}-release from the lysosome. In fact, pharmacological inhibition of TRPV3 leads to increased Ca^{2+}-level in cell and more in intracellular organelles suggesting that TRPV3 is involved in the Ca^{2+}-buffering by intracellular organelles. In that context, TRPV3 is involved in similar functions reported for other TRP family members that are present in the lysosome. For example, TRPML1-3 are present in lysosome and any abnormalities in TRPML results in pathophysiological conditions. Mutation in TRPML1 has been associated with mucolipidosis IV, which is a lysosomal storage disorder that leads to neurodegeneration, mental retardation and blindness [52-54].

At the molecular level, TRPV3 mutants are constitutively active suggesting that these channels have a high probability of spontaneous opening [27]. The spontaneous opening of TRPV3 in physiological temperature seem to be modulated by cholesterol present in the lipid bilayer. Multiple cholesterol molecules may interact with different positions of tetrameric TRPV3 and may form an annular belt-like structure [55, 56]. Such annular-belt of cholesterol and occupancy of individual cholesterol molecule on the TRPV3 surface may be a critical parameter for preventing spontaneous channel opening. In this regard, it is important to note that TRPV3 contains several putative cholesterol-binding motif sequences and some of these motifs are well conserved throughout the vertebrate evolution. This strongly suggests that TRPV3 has co-evolved during vertebrate evolution and interaction with cholesterol can be a selection pressure. Indeed, the OS mutants reveal altered probability of cholesterol interaction,

interaction with actin and tubulin cytoskeleton helps to form signaling complex/s at the plasma membrane which is relevant for different cell functions. In that regard, it seems that cAMP, Ca^{2+} ion and Tyrosine kinase are important factors that are involved in this neuritogenesis process regulated by TRPV2. This accord well with previous reports demonstrating that cAMP and Ca^{2+} oppositely regulate neuritogenesis [44, 45]. Increased amount of cAMP and Ca^{2+} correlates with increased and decreased number of neurites respectively [49]. Such neurite numbers are regulated by cAMP or Ca^{2+} through regulation of Actin cytoskeleton, mainly by cofilin which controls the dynamics of actin cytoskeleton [50]. Similarly, the involvement of Tyrosine kinase in the regulation of dynamics of leading edge is well established and TRPV2 may have importance in that function too.

Ion channels are not only critical regulators of cellular ionic homeostasis, but also for other important processes such as vesicular recycling, vesicle fusion, pH regulation etc. Trafficking of protein from ER to plasma membrane and other subcellular organelles is an important process. Such constant protein trafficking from ER to the plasma membrane and vice versa maintains the cellular dynamics and thereby maintain the cellular homeostasis. These dynamic and bi-directional processes are maintained at a steady state and changes in these events leads to an imbalance in vesicular trafficking process causing pathophysiological conditions. In this context, unique point mutations in TRPV3 that are linked with the development of *Olmsted Syndrome*, offers suitable molecular tools to characterize the above mentioned critical cellular events in details.

At the cellular level, OS mutants have severe defects in terms of protein sorting. The OS-mutants are primarily retained in the ER and presence of these mutants in the plasma membrane is very less compared to the wild type. Expression of OS-mutants induce a general defect for protein sorting and as a result of that, other membrane proteins are also not trafficked to the plasma membrane. The cells loose tight focal adhesion properties and also induce severe

TRPV3, as these two channels are poorly characterized with respect to other thermosensitive TRPV channels such as TRPV1 and TRPV4.

Previously, the importance of TRP channels, especially in TRPV1 and TRPV4 in the regulation of submembranous cytoskeleton and regulation of critical cellular structures such as filopodia, neurites and growth cones have been established before [34-40]. The neuronal cells have a precise mechanism of neuritogenesis which is accompanied by neurite sprouting, neurite elongation, and neurite maintenance, all these processes are tightly regulated by a large number of factors [41, 42]. These neuronal processes mainly, filopodia, lamellipodia, growth cone are very dynamic structures and very little change in temperature, mechanical pressure and Ca^{2+} can cause an abrupt change in all these structures [43-47]. Function, as well as maintenance of these structures, are tightly regulated and any abnormalities in these steps result in the development of pathophysiological conditions, though such processes are complex and not well-understood events [48].

This work established the importance of TRPV2 in the initiation, extension and further branching pattern of peripheral neurites, at least in the F11 cell. Such aspects define the density of terminal nerve ends and also the response received or triggered by sensory nerves from peripheral tissues. Such aspects are complex and are also relevant for precise neuronal networking and neural plasticity. For example, activation of TRPV1 or TRPV4 leads to a reduction in neurites while activation of TRPV2 leads to neurite extension, a phenomenon that is different than that of TRPV1 or TRPV4 [36, 38]. At the cellular level, activation of TRPV2 results in the formation of growth cone. Neurite extension demands insertion of extra-lipid bilayers and TRPV2 activation may be important steps for that purpose. Rapid vesicle fusion at the peripheral membrane may be a critical step observed towards initiation of neurites. Like TRPV1 and TRPV4 channels, TRPV2 also interact with different cytoskeleton components such as tubulin, modified tubulins and actin through its C-terminus region. It seems that TRPV2

binds to the OS-mutants with different energy parameters. Biochemical experiments with a MBP-tagged TM4-loop4-TM5 fragment of the TRPV3 wild type as well as OS mutants also suggest that OS mutants have reduced interaction with cholesterol. This TRPV3-cholesterol interaction study may have importance in the context of regulation of channel function. Reduced occupancy of cholesterol on OS mutants may be relevant for the constitutive opening of channels and therefore relevant in the context of pathophysiology.

Discussion and conclusion:

So far, a large number of studies suggests that members belong to TRP family are localized primarily in the plasma membrane. However, apart from the plasma membrane, there is evidence which suggests the presence of TRP channel members in the intracellular organelles where these channels play a crucial role such as membrane trafficking, signal transduction, and ionic homeostasis, etc. [29-33]. Such functions are important for normal growth, development and several physiological processes. Abnormalities in any of such aspects lead to severe pathophysiological disorders. Such abnormalities may appear due to mislocalization, changes in cell signaling events, or even by point mutations resulting in different channel behaviour. Notably, proper function of TRP channels largely depends on the proper localization which ensures the molecular environments in which these channels are regulated in a precise manner. In the case of TRP channels, extracellular matrix components, different membrane lipids, and submembranous cytoskeleton forms a proper microenvironment where these channels become functional. In most cases, changes in these localizations and/or microenvironment correlate with the changes in channel function and such changes are the hallmarks of pathophysiological conditions too. Therefore, understanding of the molecular and cellular mechanisms involved in these processes are important. A major focus of this thesis work was to explore the localization-mislocalization and trafficking of TRPV members, namely for TRPV2 and

In silico analysis reveals that TRPV3 have few lysosomal targeting sequences among which one is highly conserved in all vertebrates. Expression of these lysosomal targeting sequences as GFP-tagged protein and live cell imaging suggest the localization of these sequences in the lysosome. Further western blot analysis confirmed the presence of TRPV3 in the lysosomal and mitochondrial fraction isolated from cattle brain.

Ca^{2+}-imaging experiments using specific activator and inhibitor shows a modest increment in Ca^{2+}-level while inhibition of TRPV3 causes much robust and an abrupt increase in the cytoplasmic Ca^{2+}, suggesting the importance of TRPV3 in the regulation of intracellular pH. Live cell experiments with pH-sensitive dye further reveal that stable cells expressing OS mutants have increased cytoplasmic pH while cells expressing TRPV3-Wt have pH at the physiological range. Obtained results strongly suggest that OS-causing mutants affect lysosomal functions and intracellular pH regulation drastically, confirming that OS is a lysosomal disorder.

4. Importance of cholesterol in the regulation of TRPV3

Previously cholesterol-mediated regulation of TRPV3 channel functions and therefore alteration in Ca^{2+}-influx was reported [28]. However, the detailed molecular mechanism of cholesterol-mediated regulation is yet to be established. Using *in silico* methods, Cholesterol recognition amino acid consensus motifs (CRAC-motifs, defined as L/V-$X_{(1-5)}$-Y-$X_{(1-5)}$-R/K), cholesterol-binding motif (CARC-motifs defined as the inverted CRAC) sequences present in TRPV3 were identified. Conservation study reveals that CRAC (357-363) and CARC (376-385) regions are highly conserved throughout the vertebrate evolution. These suggest a possible interaction of cholesterol with TRPV3 which in turn may have importance during the vertebrate evolution. Docking experiments suggest that cholesterol can bind to the TRPV3 through its intracellular loop-4 region. Similar docking analysis reveals that cholesterol

G573A, G573S, G573C and W692G) have reduced surface expression whereas TRPV3-Wt localises properly in the plasma membrane. This study reveals that the OS mutants cause damage to different subcellular organelles including ER, mitochondria, Golgi and lysosome as analyzed by using different antibodies detecting KDEL, HSP60, GM130, and Lamp1 respectively as different subcellular organelle markers. Use of specific organelle-labelling probes such as MitoTracker-Red and LysoTracker-Red also confirms that OS-causing mutants damage normal mitochondrial and lysosomal structures as well as functions. Both qualitative and quantitative data indicates that these naturally occurring TRPV3 mutants are mainly restricted in the ER. Expression of OS-mutants cause impaired vesicular trafficking resulting reduced surface localization of these mutants and other membrane proteins too. OS-mutants also cause reduced cell adhesion. Both wild-type and OS mutants of TRPV3 can be detected in the lysosome. The data suggests that TRPV3 is a lysosomal protein and thus also suggest that *Olmsted Syndrome* is a lysosomal disorder. These findings may have a broad implication in the context of keratinocyte functions, skin degeneration and in skin cancer.

3. Importance of TRPV3 in regulation of intracellular organelle

HaCaT cells expressing low levels of TRPV3-Wt and OS-mutants were generated after stable cell selection. Subsequently, expression, localization and function of OS-mutants along with TRPV3-Wt were studied in these stable cell lines. Stable cell lines expressing OS-mutants have low mitochondrial potentiality whereas TRPV3-Wt expressing cells shows normal potentiality. In the same manner, stable cell lines expressing OS-mutants have less number of lysosomes, less LysoTracker labelling and less lysosomal movement. In contrast, untransfected control cells, or stable cells expressing TRPV3-Wt, or EGFP show normal lysosomal numbers, lysosomal labelling and movement.

Results:

1. **Exploring the importance of TRPV2 in neuronal cell: Importance in neuritogenesis and cross-talk between TRPV2 and cytoskeleton**

For this objective, neuronal cell line F11 and Neuro2A were chosen. The importance of TRPV2 in the regulation of neuronal cytoskeleton has been investigated by transient overexpression of TRPV2-GFP. Similarly, endogenous TRPV2 was modulated by using specific agonist or antagonist. Confocal imaging of live cells expressing TRPV2-GFP was performed to study the localisation of TRPV2 at specific sites such as in filopodia, growth cone and neurites and also to study the dynamics of TRPV2. Fixed cells immunostained with different modified tubulin were analyzed. Endogenous expression of TRPV2 in the F11 cell was confirmed by western blot analysis and immunofluorescence analysis. Live cell Ca^{2+}-imaging experiments with specific activator and inhibitor confirmed the functional nature of endogenous TRPV2. Both endogenous as well as overexpressed TRPV2 play important role in the process of neuritogenesis. Experimental data suggest that activation of TRPV2 correlates with enhanced neuritogenesis, and in particular specific processes such as neurite initiation and branching. Experimental data confirmed the colocalization of TRPV2 with Actin and tubulin in specific cellular structures and presence of these two important cytoskeleton proteins in the complex formed by MBP-TRPV2-Ct. Such findings correlate well with the involvement of TRPV2 in sensory and pain functions.

2. Characterization of naturally occurring and clinically important –TRPV3 mutants

The localization of TRPV3 wild type, as well as mutants causing OS, were analyzed by transient overexpression studies. These were performed in HaCaT cells, a human keratinocyte cell line suitable model system for this study. Both wild-type and OS mutants of TRPV3 were expressed by transient overexpression. This study strongly confirmed that OS mutants (namely

lysosomes of keratinocyte cell lines. This work establishes that TRPV3 is a lysosomal protein and it has importance in the regulation of lysosomal functions. This work also establishes that *Olmsted Syndrome* is a lysosomal disorder.

Aims of the present study:

1. Establishing the importance of TRPV2 in the regulation of neuronal functions.
2. Characterization of wild-type and naturally occurring clinically important –TRPV3 mutants in cellular functions.
3. The importance of TRPV3 in the regulation of intracellular organelle functions.
4. The importance of cholesterol in the regulation of TRPV3.

Organization of the thesis:

This thesis work is embodied into different chapters. The chapter 1 deals with general introduction and review of the literature with current scientific information relevant to concerned work and aims of the study. The chapter 2 deals with all the results obtained in order to justify the above-mentioned objectives. The chapter 3 includes a detailed discussion on the results obtained in this work in the light of pre-existing literature. The chapter 4 summarizes the entire work done, conclusions and future direction in the light of the present study. The chapter 5 includes materials and methodologies used in this current study. The chapter 6 includes all the bibliographic information mentioned in this study.

genodermatosis where TRPV3 mutant channels remain constitutively active and these result in the development of OS. As TRPV3 is involved in the regulation of skin keratinocyte and hair cells, the OS patients suffer from loss of hair, defects in keratinocytes, specific loss of bones from peripheral parts, periorphesial plaques, and severe itching [27]. TRPV3 has few endogenous modulators and these are mainly metabolites such as Farnesyl pyrophosphate (FPP). In addition, TRPV3 can be activated by different chemical modulators, such as camphor, carvacrol, eugenol, menthol, thymol, borneol, cresol, carveol, gerianool and 2-APB which potentiates its activity. The antagonists include ruthenium red, icilin, isopentenyl pyrophosphate, DPTHF and 17-R resolving D1.

A large number of research articles available till date suggest that TRPV1 and TRPV4 have been investigated widely. Both TRPV1 and TRPV4 have significant roles in neuronal and non-neuronal cells and related tissues. It is important to note that the expression, localization, precise regulation and function of different channels are expected to be unique and relevant to different physiological functions. In this context, the most of the understandings are based on the studies with TRPV1 and TRPV4. Among all members belong to TRPV subfamily, TRPV2 and TRPV3 are relatively less characterized and not much is known about these two channels. Moreover, mutations in TRPV3 cause severe pathophysiological conditions, through the molecular and cellular mechanisms for this are not known. This impose the challenges to pursue this thesis work on TRPV2 and TRPV3.

In this thesis work, localisation, subcellular distribution and specific function of TRPV2 and TRPV3 were investigated. In specific, localization and importance of TRPV2 has been investigated in F11 cell lines, a model system used as peripheral neurons. This study reveals that endogenous and functional TRPV2 has importance in the regulation of different aspects of neuritogenesis. Similarly, wild type TRPV3 and OS-mutants were characterized in HaCaT cell, a keratinocytes cell line. Both wild-type and OS-mutants of TRPV3 are present in the

ranging from (27ºC-52ºC) [2]. In experimental conditions, TRPV2 is activated at a noxious temperature at 52ºC [8] and its presence has been reported in all tissues including neuronal and non-neuronal origin. For example, it is present in the brain and in CNS neurons, Dorsal root ganglia. In addition it is also expressed in macrophage, cardiac tissue, gastro-intestinal tract, spleen, mast cells, smooth, cardiac and skeletal muscle cells [9]. Other regulatory function of TRPV2 includes axon outgrowth in spinal motor neurones, phagocytosis in macrophages, and structure-function regulation in cardiac cells [8-10]. Chemical modulators of TRPV2 includes 2-APB, plant products such as Cannabidiol, Cannabinol, Cannabigerol, Cannabidivaril, Cannabigivarin, Diphenylboronic anhydride, Δ9-tetrahydrocannabinola, Tetrahydrocannabinol acid, and Probenecid. In contrast, Ruthenium Red, SKF96365, and Tranilast act as an inhibitor of TRPV2 [11].

Another member of TRPV subfamily is TRPV3 which acts as a “warmth sensor” and it is activated at 28ºC. A specific feature of this ion channel is its abundant expression in skin keratinocyte and hair cells while relative low expression in the neuronal systems [12-14]. Expression of TRPV3 is also reported from Dorsal Root and Trigeminal Ganglion neurones, brain, tongue, testis and also from breast cancer tissue [9]. Two important regulatory proteins for skin morphogenesis and hair development are TGFα and EGFR which form a signaling network with TRPV3 [15, 16]. TGFα and EGFR play very important role in skin function [17, 18]. Also, loss-of-function for TGFα and EGFR results in wavy hair phenotype [15]. Indeed, EGFR and TRPV3 signaling paly important role for epidermal barrier formation and skin morphogenesis. A study in mice reported that increased activity of TGFα and EGFR results in hairless phenotype and skin cancer suggesting that TRPV3 complex might also be involved in such functions [17, 18].

Several unique point mutations in TRPV3 have been associated with the development of *Olmsted Syndrome* (OS), a rare genetic disorder, i.e. a channelopathy [19-27]. OS is a rare

Introduction:

Transient receptor potential (TRP) family of ion channels are members of a non-selective Ca^{2+} ion channels and these channels are present in single cell eukaryotes to human but are absent in plants. These channels have been classified into six subfamilies based on the presence of certain domains as well as motif sequences, homology and sequence similarity. These subfamilies include TRPV (Vanilloids), TRPC (Canonical), TRPM (Melastatin), TRPML (Mucolipins), TRPA (Ankyrin), and TRPP (Polycystins). In 1969 these ion channels were first discovered in *Drosophila melanogaster* where mutant animals show transient voltage in response to continuous light [1]. Later on, the gene harboring the mutation was named as Transient Receptor Potential (TRP) [2]. Subsequent characterization revealed that these channels are involved in diverse cellular functions including thermosensation, pheromone sensing, mechanosensation, taste, vision, etc. [3-5]. Apart from different cellular functions, these channels represent some characteristic features which are similar in all cases. For example, all TRP ion channels have six transmembrane segments flanked by intracellular N- and C-terminus domains and the "functional pore" is formed by the amino acids that are present between 5^{th} and 6^{th} transmembrane segment [6]. Some TRP channels (namely the members belong to TRPA, TRPV and TRPC) contains Ankyrin repeat sequences in the N-terminus and a consensus amino acid sequence known as "TRP-box" at the C-terminus (especially in members belong to TRPV, TRPC and TRPM subfamily members). Functional TRP channels form homotetramer or heterotetramer [7].

Vanilloid subfamily is represented by 6 members, namely TRPV1, TRPV2, TRPV3, TRPV4 in one subgroup and TRPV5 and TRPV6 (which are highly Ca^{2+}-selective channels) in another subgroup [2]. Among all the Vanilloid family members, TRPV1-TRPV4 are thermosensitive in nature and these channels become activated at a very specific temperature

Homi Bhabha National Institute

SYNOPSIS OF Ph. D. THESIS

1. **Name of the Student: Manoj Yadav**

2. **Name of the Constituent Institution: National Institute of Science Education and Research (NISER)**

3. **Enrolment No.: LIFE11201104006**

4. **Title of the Thesis: Importance of thermosensitive ion channel (TRPV2 and TRPV3) in cellular functions**

5. **Board of Studies: Life Science**

SYNOPSIS

(Limited to 10 pages in double spacing)

PGE2	Prostaglandin E2
PLC	Phospholipase C
PMSF	Phenylmethanesulfonyl fluoride
PIPES	1,4-Piperazinediethanesulfonic acid
PIP_2	Phosphatidylinositol 4,5-bisphosphate
PKA	Protein Kinase A
PTM	Post-translational modifications
PKC	Protein Kinase C
PPK	Palmoplantar Keratoderma
PPM	Parts per million
PSD	Post synaptic density
PVDF membrane	Polyvinylidene difluoride membrane
ROS	Reactive oxygen species
RPM	Revolution-Per-Minute
RT	Room temperature
RT-PCR	Reverse transcription- polymerase chain reaction
RTX	Resiniferatoxin
SDS	Sodium Dodecyl Sulphate
SNX11	Sorting nexin 11
SOCE	Store operated Ca^{2+} entry
TAE	Tris-Acetic Acid-EDTA
TEMED	N,N,N′,N′-Tetramethylethylenediamine
TG	Trigeminal ganglion
TGF-α	Transforming growth factor-α
TM	Transmembrane
Tris	Tris Hydroxymethylaminoethane
TRP	Transient Receptor Potential
UVR	Ultra violet radiation
v/v	Volume per volume
w/v	Weight per volume

GJB2	Gap junction protein beta 2
GPCR	G protein coupled receptor
GTP	Guanosine 5′-triphosphate
H	hour (Time unit)
HCl	Hydrogen Chloride
HEPES	4-(2-Hydroxyethyl)piperazine-1-ethanesulfonic acid
HRP	Horseradish Peroxidase
Hz	Hertz
IGF	Insulin growth factor
InsP3	Inositol-1,4,5-trisphosphate
IPP	Isopentenyl pyrophosphate
IPTG	Isopropyl thiogalactose
IRTX	5'-iodoresiniferatoxin
JC-1	5,5′,6,6′-tetrachloro-1,1′,3,3′-tetraethylbenzimidazolocarbocyanine iodide
Kan	Kanamycin
Kb	Kilo base
kDa	Kilo Dalton
KO	Knock out
KOH	Potassium Hydroxide
L	Litre (volume unit)
L2	Loop2
L4	Loop4
LB	Luria-Bertani
LTS	Lysosomal targeting sequence
LWI	Lipid-water interface
MBP	Maltose Binding Protein
MFI	Mean Fluorescence Intensity
Min	Minutes (Time unit)
MT	Microtubules
MitoTracker Red	MitoTracker Red FM
NA	Numerical aperture
NaCl	Sodium Chloride
NaOH	Sodium Hydroxide
NADH	Nicotinamide adenine dinucleotide (reduced form)
NGF	Nerve growth factor
NOS	Nitric oxide synthase
OS	*Olmsted Syndrome*
PAGE	Poly Acrylamide Gel Electrophoresis
PBS	Phosphate buffer saline
PCR	Polymerase Chain Reaction

List of abbreviations:

4αPDD	4α-Phorbol 12,13-didecanoate
ACBD	Acyl-CoA binding domain protein
AKAP-5	A kinase anchor protein 5
Amp	Ampicillin
APS	Ammonium persulphate
2-APB	Aminoethoxydiphenyl borate
ARD	Ankyrin repeat domain
ATP	Adenosine triphosphate
BCECF	2',7'-Bis-(2-Carboxyethyl)-5-(and-6)-Carboxyfluorescein, Acetoxymethyl Ester
Bp	Base pair
BSA	Bovine serum albumin
CaM	Calmodulin
CBB	Coomassie Brilliant Blue G250
CCM	Cholesterol Consensus Motif
CHOK1-Mock	Chinese Hamster Ovary K1-Mock
CIPN	Chemotherapy induced neuropathic pain
CRAC	Cholesterol recognition amino acid consensus
DAPI	4',6-diamidino-2-phenylindole
DAG	Di acyl glycerol
DMSO	Dimethyl Sulfoxide
DPTHF	2,2-diphenyltetrahydrofuran
DNA	Deoxyribonucleic acid
dNTP	deoxy Nucleotide Tri Phosphate
DRG	Dorsal root ganglion
ECL	Enhanced Chemiluminescent
EDTA	Ethylenediaminetetraacetic acid
EGTA	Ethylene glycol bis(2-aminoethyl ether)tetraacetic acid
EGFR	Epidermal growth factor receptor
EM	Electron Microscopy
ER	Endoplasmic Reticulam
EtBr	Ethidium Bromide
FBS	Fetal calf serum
Fluo-4 AM	Non-fluorescent acetoxymethyl ester
FPP	Farnesyl pyrophosphate
PI	Complete protease inhibitor
PFA	Paraformaldehyde
GFP	Green Fluorescence Protein

1.6. The aim of the study:

In this thesis work I have characterized the importance of TRPV channels in the different cellular systems. Such understandings are important in order to elucidate the importance of TRPV channels in physiology, pathophysiology and in channelopathy.

For that purpose, F11 cell was used as a model system and spatiotemporal localization of TRPV2 as well as importance of TRPV2 in neuritogenesis was investigated (Chapter 1). Different events related to neuritogenesis needs extensive remodelling of actin and microtubule cytoskeleton. Therefore, physical interaction of TRPV2 with actin and microtubule was explored. Also, remodelling of cytoskeleton and membrane dynamics induced by TRPV2 activation or inhibition was characterized.

Recently TRPV3 has been linked with the development of skin disorder as mis-regulation and/or mutations in TRPV3 can cause hair-loss and develop a pathophysiological condition known as *Olmsted Syndrome*. However, the cellular and molecular mechanisms are not known. Therefore, importance of TRPV3 in keratinocytes was investigated using HaCat as a cellular model system. Alternation of subcellular functions and ionic homeostasis induced by TRPV3 mutations and modulation was explored (Chapter 2 and Chapter 3).

High-resolution molecular structure of TRPV3 in open and closed condition was developed. *In silico* analysis of TRPV3 structure was analysed. Evolutionary significance of such structures, different domains and motifs was analysed. Possible regulation of TRPV3 by membrane components such as by Cholesterol was explored (Chapter 4).

defined background in TRPV3 knockout Mice reveals contradictory results where they have found no difference in thermosensation. This strongly suggests that role of TRPV3 in thermosensation is very limited [257].

1.5.8. The behavior of TRPV2 and TRPV3 knockout animals:

Importance of TRPV channels lies in the fact that elimination/alteration of these genes from animals, or tissue or even at the cellular level can alter animal behavior, tissue and cellular functions such as change in detection ability for noxious chemicals and temperature. However, though TRPV channels are involved in several functions, certain functions can also be complemented or reciprocated by the presence of other similar or homologues channels. For example, Mice which are ablated off TRPV2 shows change in cardiac structure and function in the very early stages suggesting the importance of TRPV2 in maintaining cardiac structure and function [255]. However, TRPV2 knockout mice do not show any change in thermal and mechanical behavior suggesting that such functions can be compensated by other channels [121]. Further analysis also reveals that distribution of different sensory neurons including, dorsal root ganglion and trigeminal ganglion are normal in knockout animals [121]. To rule out the possibility of involvement of other TRPV channel double knockouts of TRPV1 and TRPV2, Mice was studied and no significant difference in thermal hyperalgesia as compared to TRPV1 knockout only is observed [121]. Mice lacking TRPV2 shows a clear difference in reduced perinatal viability, embryo, and adult body weight. Other functions which are affected in the TRPV2 knockout Mice is the immune activity of Macrophage cells. It has been shown that Macrophage cells genetically devoid of TRPV2 have impaired particle binding and phagocytosis ability [239]. Macrophage cells devoid of TRPV2 also show impaired chemo-attractant-elicited motility and increased mortality and organs show high bacterial load [239].

Initially, it was shown that TRPV3 knockout Mice have different abnormality in the detection of noxious and innocuous temperature but have other sensory functions normal [75]. Keratinocytes are known to release ATP in the medium in response to heating and the released ATP acts on the sensory nerves as itching stimuli [256]. TRPV3 knockout Mice show impaired phenomenon of ATP release from keratinocyte due to heating [256]. Another study with

1.5.7. The importance of TRPV2 and TRPV3 channels in pain and other pathophysiology:

TRPV channels are functionally present in diverse cellular systems including neuronal and non-neuronal cells/tissues. Any change in the functioning of these proteins due to alteration of sequence, mutation, or other defects result in pathophysiological conditions. There are increasing evidence which suggest role of many TRPV channels (TRPV1, TRPV3, TRPV4) in such pathophysiology. For example, cardiomyocytes functionally express TRPV2 and it is very crucial for maintenance of cardiac structure and function. Ablation or deletion of TRPV2 from cardiac cells severely affects cardiac structure and function. Transgenic expression of TRPV2 leads to cardiomyopathy [240]. Rosacea, a chronic inflammatory skin disease of unknown etiology is primarily characterized by neurological inflammation and different TRPV channels have been found to be involved in such pathophysiology. Rosacea affected samples have immunofluorescence for TRPV2 and TRPV3. Gene expression of TRPV1 and TRPV4 has been shown to increase in the disease sample.

Importance of Vanilloid Receptor (VRL-3) in skin morphogenesis and hair growth is reported. In mouse model, “loss-of-function” in TGFα and EGFR results in the wavy hair phenotype. Also, increased activity of both genes results in hairless phenotype and skin cancer [108, 109]. Genetic ablation of TRPV3 in Mice also results in similar phenotypes, i.e. wavy hair and curly whiskers [107]. TRPV3 role in other Human skin pathophysiology is also reported, where constitutively active Human TRPV3 mutants result in *Olmsted Syndrome* (OS). So far, worldwide 75 patients have been reported with OS and TRPV3 point mutations involved in OS are Gly573Ala, Gly573Cys, Gly573Ser, Try692Gly, Met672lle, Gly573Val, Gly568Asp, Gly568Val, Gln580Pro, Trp521Ser, Gly568Cys, Leu673Phe [243].

1.5.6. Different physiological functions of TRPV channels:

Presence of Vanilloid subfamily members in different excitable and non-excitable cells and tissue allows their diverse physiological functions. TRPV family members possess a common function of thermosensation with an exception of TRPV5 and TRPV6. The diverse functions of these ion channels include thermos-sensation, vision, taste, pheromone sensing etc. [12-16]. TRPV1 has a role in thermosensation (heat), autonomic thermoregulation, nociception, pain sensation, synaptic plasticity in the brain, endocannabinoid signaling in the brain, food intake regulation, growth cone guidance in the brain, osmosensing in the brain by a particular TRPV1 variant, multiple functions in the gut, and it also has a role in purinergic signaling through bladder urothelium [32, 96, 136, 138]. TRPV2, another member of Vanilloid family plays an important role in detection of noxious temperature, nociception, axon outgrowth in spinal motor neurons, phagocytosis in Macrophages, release of Ca^{2+} mediated through Insulin Growth Factor (IGF-1) [96, 110, 217]. Constitutively active TRPV3 has been linked with the pathophysiological condition in Humans called as *Olmsted Syndrome* [243]. Other function of this warmth sensor includes thermo-sensation (moderate heat), nociception, skin integrity, wound healing, hair growth and sebocyte function [96]. Similarly, TRPV4 has been linked with different pathophysiological conditions including bone growth, Brachyolmias and Skeletal Dysplasia, neurodegenerative disorders known as Scapuloperoneal Spinal Muscular Atrophy (SPSMA) and Charcot-Marie-Tooth disease type 2C (CMT2C) [127, 129, 130, 253, 254]. TRPV4 has role in thermos-sensation, mechanosensation osmosensation, nociception, cell migration, endothelium vaso-motor control and possible shear stress response. TRPV4 acts as mechanoreceptor in urothelium. It is also involved in osteogenesis and osteoclast function. TRPV4 is also important in the context of Human bone and neurodegenerative diseases. It also controls adherens junctions in skin and cochlea [96].

1.5.5. Tissue-wise distribution of TRPV2 and TRPV3 channels:

Ample evidences are available for the presence and distribution of TRPV channels in different cell types and tissues. Most of these studies have used antibody-based approaches such as immunofluorescence, immunohistochemistry and western blot or RT-PCR based approach to detect the expression profile of TRPV channels. Due to technical difficulty, all these studies provide variable expression profile. Importance of TRPV2 has been studied extensively in embryonic tissue, brain, pancreas, spleen, liver, lung tissue and also in cardiac tissue. Presence of TRPV2 in the early embryonic days from 10.5 to 13.5 has been reported [238]. Furthermore, it is also present in sensory fibres from central and peripheral nervous system which helps in the detection and propagation of different stimuli [64-69, 251]. It plays an important role in the pancreas and in insulin secretion. It is also reported to act as a receptor of IGF-1 [110]. Immune regulation of TRPV2 have been studied widely where its expression has been reported in the spleen, lung and different Macrophage populations such as liver Kupffer cells, skin epidermal Langerhans cells and lung alveolar Macrophage [217, 239]. Some of its immune related functions involve Mast cell degranulation and phagocytosis. TRPV2 is functionally present in the cardiac tissue and muscle tissue where it maintains the heart structure and function [240].

TRPV3 is present in many tissues including skin, hair, testis, tongue, and some amount in brain (Alex 2013). In skin, TRPV3 plays an important role in the formation of physical-chemical skin barrier [107-109, 227, 252]. It forms a signaling network with EGFR and TGF-α to form the epidermal barrier [107]. Other important physiological functions regulated by TRPV3 include hair morphogenesis and hair recycling. TRPV3 is also involved in cutaneous growth and survival, skin inflammation, cutaneous pain, and proprioceptive itch [108, 109, 252]. “Gain-of-function” mutations in TRPV3 also results in dermatitis.

Table 3. TRPV2 modulators Taken from [231].

Ion channel	Activators	blockers	Reference
TRPV2	2-APB, Diphenylboronic anhydride, Cannabidiol, Cannabigerol, Cannabinol, Cannabidivarin, Cannabigivarin, Δ9-tetrahydrocannabinol, Tetrahydrocannabinol acid, Tetrahydrocannabivarin, Lysophosphatidylcholine, Lysophosphatidylinositol, Probenecid	Ruthenium Red, SKF96365, Tranilast	[144, 217-223]

Another compound which modulates TRPV3 activity is 17(R)-resolvin D1 (17R-RvD1), a lipid that specifically inhibits TRPV3 activity. Another modulator namely, farnesyl pyrophosphate (FPP, an intermediate of the mevalonate pathway) acts as an activator of TRPV3. It is involved in many biosynthetic pathways such as terpenoid synthesis, protein prenylation, cell membrane maintenance, protein anchoring and N-glycosylation. In several studies FPP has been reported as a specific activator of TRPV3. Also, isopentenyl pyrophosphate (IPP), which is an upstream metabolite in the same pathway, shows inhibitory effect on TRPV3 indicating that the mevalonate pathway may even mediate a negative feedback through TRPV3 [140, 224] **(Tab. 4)**.

Table 4. TRPV3 modulators

Ion channel	Activators	blockers	Reference
TRPV3	2-APB, 17(R)-resolvin D1, PIP_2, diphenyl boronic anhydride, farnesyl pyrophosphate camphor, carvacrol, eugenol, menthol, thymol, borneol, cresol, carveol, gerianool, propofol, linalool, incensole, citral.	Ruthenium red, icilin, isopentenyl pyrophosphate chromane-, fused pyrimidine-, fused pyrimidinones-, chromanone- and fused imidazole-derivatives.	[75, 143, 220, 225, 226, 247-250]

thresholds of temperature, physical and chemical stimuli. TRPV2 is known to be activated by high temperature exceeding 52°C [63, 119, 215, 216] and it is also reported to be mechanosensitive which gets stimulated on stretching of membrane [240]. The temperature threshold for TRPV2 is very high and unusual since physiological temperature is around 37°C. There are some other modulators which are of natural and synthetic origin and they act via TRPV2. Some of the chemical compounds which modulate TRPV2 activity are *Cannabis sativa* derivatives, and these have been proved to be the most potent TRPV2 activators so far, but these compounds are nonspecific in nature [219, 245]. Some of the other compounds which have shown promising results are Probenecid (agonist) and Tranilast (antagonist). Another compound, namely 2-APB is also used as one of the most important agonist for TRPV2 but it shows species specific variations. Such as, Human TRPV2 is insensitive to 2-APB [221, 246]. Agonists and antagonists of TRPV2 have been enlisted below Taken from [231] **(Tab. 3)**.

TRPV3, which is also a polymodal ion channel, is regulated by many physical and chemical stimuli. The temperature threshold for activation of this ion channel is around 28°C. However, there are many endogenous and exogenous compounds which seem to regulate this protein. For example, depletion of phosphatidyl inositol (4,5) bisphosphate (PIP_2) results in the activation of TRPV3 [140].

TRPV2. Mast cell TRPV2 activation is also reported to be mediated by protein kinase A signaling. In a similar report, human cell line HMC-1 shows Mast cell degranulation upon stimulation at noxious temperature >52ºC, exposure to red light and mechanical stress [174]. This observation contradicts the previously reported study where TRPV2 was shown to be non-responsive to temperature [174]. In another study, importance of TRPV2 in phagocytosis has been shown in Macrophages where the process is mediated via PI3K signaling [239]. Importance of TRPV2 in circulatory organ and muscle function has also been studied. In a normal heart, TRPV2 is localized in intercalated discs and it detects the mechanical force generated through Myocytes [240].

TRPV3 ion channel is largely expressed and present in specialized sensory neurons and the end terminals are located in different layers of the skin [241]. TRPV3 has an activation temperature in a physiological range and its activation results in Ca^{2+}-influx. Regulatory proteins of this ion channel are A-kinase anchor protein 5 (AKAP5) [236], epithelial growth factor receptor (EGFR) [107], Calmodulin (CaM) [164] and TRPV1 [30]. Other known TRP partners of TRPV3 are TRPV1 [40], TRPC1, and TRPP2 [229, 237, 242]. The thermosensory behavior of TRPV3 is always debatable but it shows a very precise regulated mechanism in cutaneous sensation, hair morphogenesis, and skin barrier formation [107, 227]. In 2012 TRPV3 has been linked with the pathophysiology of skin disorder where constitutive activation of TRPV3 mutants shows rare genodermatosis known as *Olmsted Syndrome* [243]. Recent finding revealed that vesicular trafficking protein sorting nexin 11 (SNX11) regulate the lysosomal degradation of plasma membrane TRPV3. In this study, the authors have revealed that SNX11 direct the plasma membrane TRPV3 to lysosome for degradation through protein-protein interaction [244].

1.5.4. Activation of TRPV2 and TRPV3 in response to physical and chemical stimuli: Vanilloid family members are polymodal ion channels which are stimulated by different

TRPV3 plays essential cellular function and many cytoplasmic proteins regulate these cellular processes. For example, hair morphogenesis and skin barrier formation are two important signaling events mediated via TRPV3 ion channel. TGF-α and EGFR are two regulatory proteins [235], whose "loss-of-function" mutations results in wavy hair phenotype in Mice [108, 109]. Ca^{2+} permeable TRPV3 ion channel forms a signaling complex with TGF-alpha and EGFR. The EGFR activation causes increased activity of TRPV3, which consequently stimulates TGF-alpha release. Transglutaminases are a class of Ca^{2+}-dependent enzymes that play an important role in cornification of keratinocytes. TRPV3 which regulate transglutaminases also have a role in skin barrier formation. It is shown that transglutaminase activity was reduced in TRPV3-KO Mice [107]. Other regulatory proteins include A kinase anchor protein 5 (AKAP-5) [236], Calmodulin [164], TRPV1 [30], TRPC1 and TRPP2. TRPV3 can form functional heteromer with other TRP proteins such as TRPV1 [40], TRPC1 and TRPP2 [229, 237].

1.5.3. Cellular and molecular regulation of TRPV2 and TRPV3:

TRPV2 is present in different cell types where it regulates many physiological functions. In developing DRG and spinal motor neurons, TRPV2 is seen to express during early embryonic days [238]. Expression and distribution of TRPV2 in developing growth cone suggest its possible role in axon outgrowth and TRPV2 activation results in increased Ca^{2+} elevation in developing growth cone [231, 238]. TRPV2 has been implicated to have a role in secretion of insulin from pancreas. Its expression and distribution has been reported in the β type insulinoma cell line and Mouse pancreatic islets but not in α cells. It is also reported as a growth factor activated protein due to its sensitivity for IGF-1. For example, IGF-1 induces TRPV2 translocation from cytoplasm to cell membrane, which in turn regulates insulin secretion and cell growth [110]. Importance of TRPV2 in the immune system has also been reported. Physical stimuli lead to Mast cell degranulation, an effect which is mediated through

repeats at the N-terminus and a consensus 'TRP-box' at the C-terminus [5]. Alignment study shows that Ankyrin repeat 2 and Ankyrin repeat 3 in both TRPV1 and TRPV3 contain sites for two regulatory proteins, ATP, and Calmodulin [164]. Ankyrin repeat of TRPV1 and TRPV3 shows similar conservation pattern. However, very few changes such as insertion or deletions are present in TRPV3, especially in its Ankyrin Repeat Domain [164].

1.5.2. Different interacting proteins of TRPV2 and TRPV3.

Presence of TRPV channel on the membrane with intracellular N- and C-terminus allows many cytoplasmic proteins and membrane components, mainly different lipids and cholesterol to interact with these channels. For example, Stokes et al. in 2002 have reported that in Mast cell, Protein Kinase A (PKA), a Kinase Adaptor protein, Acyl-CoA binding domain protein (ACBD)3 interacts with TRPV2 [170]. Holakovaska et al. have shown that Calmodulin binds to C-terminus of TRPV2 (654-683) [165]. Authors have shown that point mutations at R679 or K681 in TRPV2 reduces Calmodulin binding to TRPV2 by 50%, whereas double mutation at K661/K664 in the same peptide decreases the binding affinity by up to 75% [165]. In Rat Mast cells, TRPV2 interacts transiently with an intracellular localized protein named RGA in a glycosylation dependent manner [23]. Spectrin repeat (SR) protein GSRP-56 (which is a Golgi localized SR- containing protein) also interacts with TRPV2 [26]. For TRPV2 and GSRP-56 interaction two SR domains are essential [26]. TRPV2 has been referred to as a growth factor regulated channel after demonstrating that cell shows Ca^{2+}-influx after treatment with insulin growth factor-1 (IGF-1). Interesting observation about TRPV2 is that it is the only member of Vanilloid group (TRPV1-TRPV4) which shows insensitivity towards ATP and Calmodulin [164, 208, 233, 234]. Another important regulator is PIP_2 which binds to the C-terminus of TRPV2 in the region ranging from 647-715 amino acid. Phospholipase C driven hydrolysis of PIP_2 plays essential role in the regulation of TRPV2 and other TRP channels [192].

knot toxin (RTX/DkTx–TRPV1) where both gates will be open. In both the conditions upper gate of apo-TRPV2 is much wider than apo-TRPV1-Capsaicin and of TRPV1 (RTX/DkTx–TRPV1) **(Fig. 11)**. This study reveals that due to wider pore loop gates of apo-TRPV2 it can accommodate partially hydrated Ca^{2+}, Na^{+} and K^{+} ions, as well as large organic cations in the apo-state.

This study further reveals the interaction of TRPV2 and membrane lipids, such as with cholesterol. Truncated TRPV2 was co-purified along with lipids/cholesterol hemisuccinate. Cholesterol molecule seem to occupys the crevice formed by the S1–S4 helical bundle above the TRP domain. Also, a lipid density was found in the S4, S4-S5 linker and S6 region of truncated TRPV2. The presence of wider pore of Rat-TRPV2 without added lipids suggest that lipid components may promote the desensitization of truncated Rabbit TRPV2 **(Fig. 12)**.

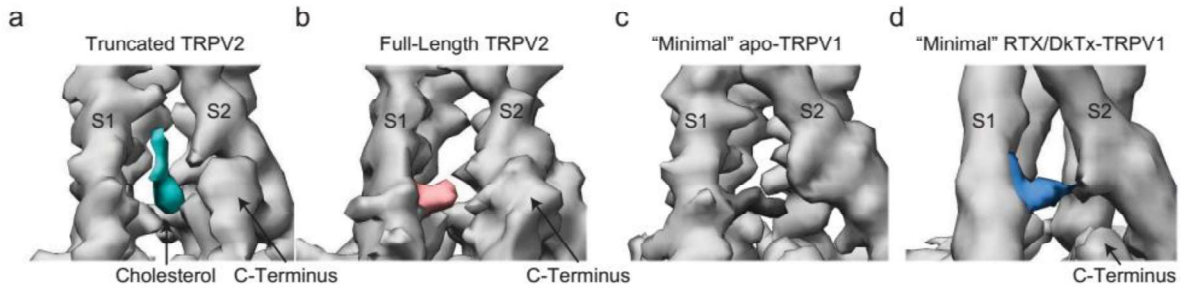

Figure 12. Lipid binding sites in TRPVs: Shown are the cryo EM structure of TRPV1 or TRPV2 with or without agonists. Lipid binding density have been shown in the S1-S4 helices. Figure shows truncated Rabbit TRPV2 (a), full-length Rabbit TRPV2 (b), minimal apo-TRPV1 (c), and minimal RTX/DxTx-TRPV1 (d). Proposed cholesterol density in truncated Rabbit TRPV2 is represented in cyan (a). Salmon, dark grey and blue colour represents similar lipid density in full-length Rat TRPV2, minimal apo-TRPV1 and minimal RTX/DkTx-TRPV1 respectively. Figure taken from [50].

TRPV3 is a 791-amino acid long protein (Human ACA81614.1). It is composed of 18 exons, but due to alternative splicing three forms of TRPV3 is present among Humans which are 90, 791 and 765-amino acid long. However, the most common form present in Human is 791 amino acid long protein. Similar to other Vanilloid family members it also has six Ankyrin

In order to understand the structural basis and agonist/antagonist mediated channel opening/closing, cryo-EM structure of full-length TRPV2 at 5 Å resolution has been solved [50]. Here they have studied apo-TRPV2 (without ligands) and have described that like TRPV1 and TRPA1, it also has two constrictions in the pore loop, one at the selectivity filter (outer side) and the other towards S-6 linker region **(Fig. 10)**.

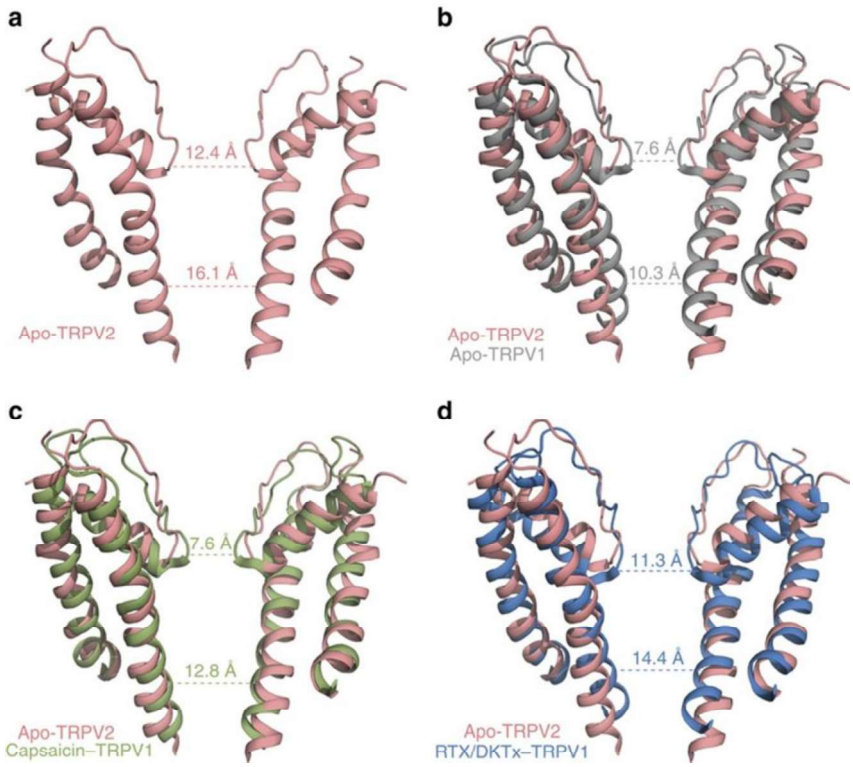

Figure 11. Analysis of the TRPV2 ion permeation pathway: (**a**) Atomic model of the S5–P–S6 region of apo-TRPV2. Two subunits are shown for clarity. The dotted lines show the Cα–Cα distances in the apo-TRPV2 structure, which represent the narrowest points in the upper and lower gates. (**b–d**) Atomic model of the S5–P–S6 region of apo-TRPV2 (salmon) superimposed onto the (**b**) apo-TRPV1 structure (grey, PDB: 3J5P), (**c**) Capsaicin–TRPV1 structure (green, PDB: 3J5R) and (**d**) RTX/DkTx–TRPV1 structure (blue, PDB: 3J5Q). The dotted lines show the Cα–Cα distances at the narrowest points in the upper and lower gates of the TRPV1 structures. Figure taken from [50].

Further analysis has revealed that pore loop of apo-TRPV2 is much wider than apo-TRPV1. Distance measurement of Cα-Cα reveals that apo-TRPV1 possess pore loop of 12.4 Å while apo-TRPV2 possess a pore loop of 16.1 Å. Other than apo-TRPV1 (both the gates are closed) TRPV1 structure was also studied using agonist Resiniferatoxin (RTX) and double-

1.5.1. Structural features and domain structure of TRPV2 and TRPV3:

Similar to other TRPV members, TRPV2 and TRPV3 also have six TM segments, intracellular N- and C-terminus and a pore-loop which is present between 5th and 6th TM segments [6, 229]. The N- and C-terminus of TRPVs interact with different cytosolic proteins and also possess binding sites for different ligands [230]. Vanilloid family members also possess multiple (3-5) Ankyrin repeats at their N-terminal region and a consensus 25 amino acid long 'TRP-box' (a characteristic feature of many TRP channels) at the C-terminal region [5, 52].

Human TRPV2 channel is a 764-amino acid long protein (NP_057197.2). It contains six Ankyrin repeats spanning a region of 70-320 amino acid in the N-terminal. Unlike TRPV1, the ARD of TRPV2 doesn't contain an ATP binding site [164]. The conservation study suggests that both TRPV2 and TRPV1 bind with different sets of regulatory proteins [231]. A consensus motif for N-linked glycosylation of TRPV2 is present between 5th and 6th loop (NXT/S) [185]. This N-linked glycosylation helps trafficking of TRPV2 from intracellular pool to the membrane [25, 38, 232].

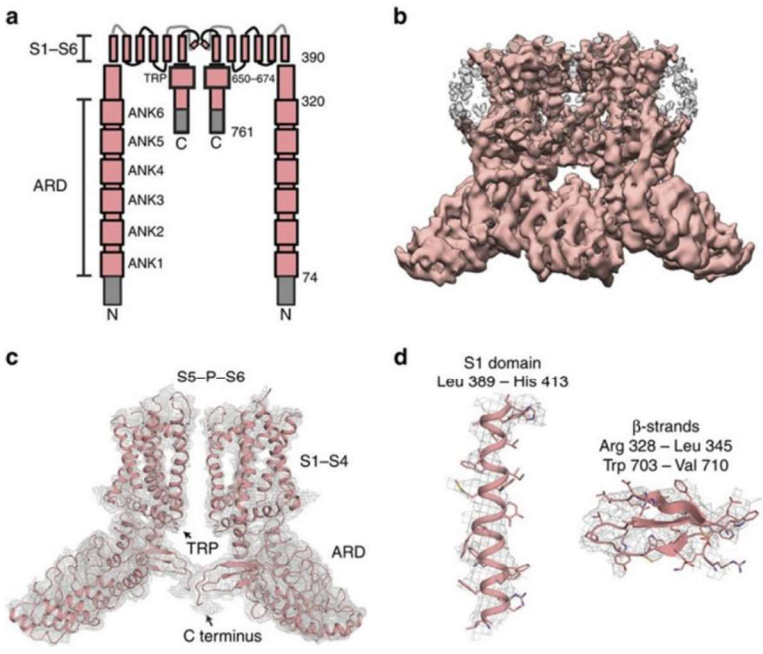

Figure 10. Structural features of TRPV2: (a) Schematic depiction of full-length Rat TRPV2 shown as a dimer with its ankyrin repeat domain (ARD), S1–S4 helices, S5–P–S6 pore domain and C terminus. Missing densities in the corresponding full-length TRPV2 cryo-EM map are depicted in grey. (b) Final full-length TRPV2 cryo-EM map is shown. (c) The TRPV2 atomic model is superimposed onto two subunits of the tetrameric full-length TRPV2 cryo-EM map. (d) Superimposition of representative regions of the full-length TRPV2 cryo-EM map (mesh) with the atomic model (ribbons and sticks), including α helix and β strand. Figure taken from [50].

also present in some non-neuronal cells like Cardiomyocytes, Vascular smooth cells and Macrophage cells where it regulates many physiological functions such as phagocytosis of foreign particles, maintenance of cardiac structure and function etc. Presence of endogenous TRPV2 has been shown as punctate distribution within the soma and axons. It also co-localizes with Rab7, which is a late endosomal marker. Stretch activated TRPV2 is present in the axon and soma and such localizations correlate with the neuronal outgrowth downstream of neurotrophin signaling [171].

Another important member of Vanilloid family is TRPV3, which shows activation threshold at a physiological temperature, i.e. around 28°C and shows 43% sequence identity with TRPV1 [30, 31, 76]. Unlike other Vanilloid members, its expression is very low in the sensory dorsal root ganglion and trigeminal ganglion. In contrast, it's elevated expression has been found in the skin keratinocytes, hair follicle, tongue, testis, cornea, distal part of colon, human larynx and inner ear [31, 65, 72-77]. Among all Vanilloid members, TRPV3 is the only protein which shows relatively very high-temperature flexibility from lower Vertebrate to Mammals, for example, in the Western Clawed Frog *Xenopus tropicalis*, TRPV3 detects cold temperature instead of warm temperature, while in Mammals it is opposite [210]. Among the endogenous modulators that regulate its activity includes PIP_2, ATP, phospholipase C, proton, FPP, and IPP [140, 224-226]. TRPV3 stimulation directly regulates many physiological processes which include inhibition of keratinocyte proliferation, induction of cellular apoptosis, epidermal differentiation, inhibition of hair growth, and cutaneous barrier formation [107-109, 227]. TRPV3 activation also causes some indirect effects which include release of secondary messengers such as ATP, prostaglandin E2, nitric oxide and these messengers in turn initiate many sensory processes like pain and itch [164, 228].

stretch is highly conserved in the non-pit bearing Snakes [116]. Also 21 amino acid are divergent in the pit bearing Snacks but is conserved in the non-pit bearing Snakes. It has been suggested that these amino acids may be important for the infrared detection in the Snakes [116]. Another report from same group have reported that TRPV1 splice variant in Bats (*Desmodus rotundus)* helps in the detection of infra-red. Due to alternate splicing of TRPV1 it results in the channel which have truncated C-terminal domain. This splicing even exclusively takes place in the trigeminal ganglia not in the dorsal root ganglia. In a similar manner, it has been shown that Ultra Violet Radiation (UVR) can activate TRPA1 in Human melanocyte [117]. Further Ca^{2+}-imaging experiments show that the UVR response is mediated by TRPA1 and also involve G-protein and Phospho Lipase C (PLC) signaling pathways [117].

1.5. General overview of TRPV2 and TRPV3 channels:

Among the Vanilloid family members of TRP superfamily, TRPV2 and TRPV3 are least investigated ion channels, and there are ample reasons for that. Even few years before, there were no specific agonist or antagonist available for both these channels. Unlike TRPV1, TRPV2 is insensitive towards Vanilloids, warmth temperature, and protons, but potentiated at noxious temperature 52°C [63, 119, 215, 216]. Higher expression of this channel has been reported in Rat DRG neurons and in spinal cord [217]. Chemical compounds which modulate its activity and act as agonists are 2-APB, Cannabidiol, Cannabinol, Cannabigerol, Cannabidivarin, Cannabigivarin, Diphenylboronic anhydride, Δ9-tetrahydrocannabinol, Tetrahydrocannabinolic acid, Tetrahydrocannabivarin, Lysophosphatidylcholine, Lysophosphatidylinositol, and Probenecid. TRPV2 antagonist includes Ruthenium Red, SKF96365, Tranilast [144, 218-223]. Among DRG neurons, expression and distribution of TRPV2 is mainly restricted in the Aδ-fibers while TRPV1 is mainly present in the c-fiber. Surprisingly expression of TRPV2 is not only restricted to the neuronal cell and tissue but it is

unaffected. Therefore, Birds act as preferred vectors for seed dispersal and effectively in long range distance is covered [213].

Ironically, the sequence as well as function of these TRP channels vary from organism to organism. Yet, in many cases, the functions remain conserved. For example, the mechano-sensory defects observed Osm9 mutant of *C. elegans* can be rescued by Human TRPV4 suggesting that these channels serve as functional homologues across the phylogenetic tree in spite of sequence differences [55]. However, overall, sequences and functions of TRP channels are fairly conserved in animal kingdom since several millions of years. Yet, slight changes in certain sequence can induce changes in functions and regulations. Such subtle changes are critical for imposing "selection pressure" and thus are extremely important for evolutionary perspectives which happens in millions of years.

Many venomous creatures like Snakes, Spiders and Scorpions produce different peptide toxins for defence as well as for predation. These toxins bind to different ion channels (including TRP ion channels) and receptors selectively and modulate them. As a result, these toxins cause shock, paralyse and in some cases death. Interestingly these toxins also bind to some TRP channels including TRPV1 which sensitise the receptor and produce the inflammatory pain [214]. For example, Venom from a Tarantula sp., *Psalmopoeus cambridgei*, has three Inhibitory Cystine Knot (ICK) peptides present in one peptide, and these inhibitory peptides has shown to act on the one of TRP channel which is TRPV1 [214]. Other peptide and venom also binds to some TRP channel such as TRPA1 and TRPM8 [214].

In 2010 Gracheva et al has reported that TRPA1 acts as an "infrared sensor" in the pit organ where function of TRPA1 is essential for the generation of infrared-stimulated signals. TRPA1 detects the radiant heat in the pit organ of Snakes instead of photochemical transduction [59]. TRPA1 (as the infrared sensor in the pit bearing Snakes) have a specific 11 amino acid long sequence that have diverged specially in the pit bearing Snakes while the same

similarly human use TRP for sweet, bitter, and umami test and temperature detection from innoxious hot temperature to noxious hot or noxious cold [12-16]. Indeed, TRP channels also play important role for selection of suitable environmental niche and often are also critical for the prey-predator relationship.

However, the in-depth evolutionary significance of TRP channels in different species has not been studied in great details. However, certain sequences are conserved in certain TRP channels and/or in selected groups but not in all. Such aspects can be correlated with the specific regulation and function of certain TRP channels, especially in species-specific manner [208-211]. For example, in 2009 Matsuura et al has studied conservation and importance of Insect TRP channels [10]. They have studied and compared the presence of different TRP genes in *Drosophila* and few Insect species whose genome has been sequenced [10]. In all the Insect species, they were able to detect the five TRP subfamily members belong to TRPV, TRPN, TRPM, TRPC and TRPML. This signifies that in Insect mechanosensation, phototransduction and lysosomal functions are well conserved [10]. Similarly, tubulin-binding sequences are present in the TRPV1 and such sequences are conserves in all vertebrates since ca 450 million years [152]. Another example is the cholesterol-binding sequences that are present in TRPV4 [57]. Such cholesterol-binding sequences are especially selected in vertebrates, but not in invertebrates [57]. Few other physiological studies also provide information regarding species-specific evolutionary advantage (TRP and ligands) and conservation of specific domains/motifs. For example, Mammals show a very high degree of sensitivity towards Capsaicin, a well-known agonist for TRPV1 while Birds are largely insensitive to Capsaicin [136, 212]. This is mainly due to the point mutation (in Birds) at the TM2-loop-TM3 region that affects the Capsaicin binding [136]. This impose an evolutionary advantage for Plants, because the capsaicin-sensitivity (i.e. strong pungency) repeals Mammals and Birds are

of TRP functional homologues or TRP-like ion channels in the plant kingdom, especially in the lower plants [11]. Very recently one report suggests the presence of TRP channel in *Chlamydomonas* and that TRP channels provide sensory features similar to mammalian TRP channel such as voltage-dependent outward rectification, cationic nonselective permeability, blocking by BCTC, TD-associated modulation, and temperature-dependent gating [17]. In the same study author suggested that similar to mammalian canonical TRP channel, the *Chlamydomonas* TRP1 might be involved in temperature sensation [17]. In 2011 Fujiu et al. in the similar study revealed that *Chlamydomonas* TRP11 is involved in the mechanosensation [18]. Fujiu et al. have also shown that TRP1 expression is up-regulated upon deflagellation linking flagellar localization of TRP1 [18]. Previously mammalian TRPM channel members TRPM1 and TRPM5 were also linked with photosensation in a plant cell [205, 206]. Presence of TRP ion channel in *Chlamydomonas* suggest the long evolutionary conservation of these protein from single-cell organisms to multicellular organisms. Infect there are quite a few reports which suggest that other single-celled organisms including *Dictyostelium*, *Trypanosoma*, *Leishmania*, and *Plasmodium* that also have sequences which code for proteins similar to TRP channels [19].

1.4. The importance of TRP channels in evolution:

TRP channels have been reported from lower and/or single cell organism to the higher and/or multicellular organisms. So far, the TRP channels have not been detected in higher Plants [11]. However, TRP genes have been reported in different unicellular Parasites, Fungus and many other marine organisms [12, 207]. These channels are involved in the detection of different stimuli such as temperature, touch, pain, pheromones, osmolarity, taste, etc. For example, Yeast use TRP channel to detect hypertonicity, male Mice use TRP for pheromone sensing, to differentiate male from female, Nematode uses TRP to detect noxious chemical,

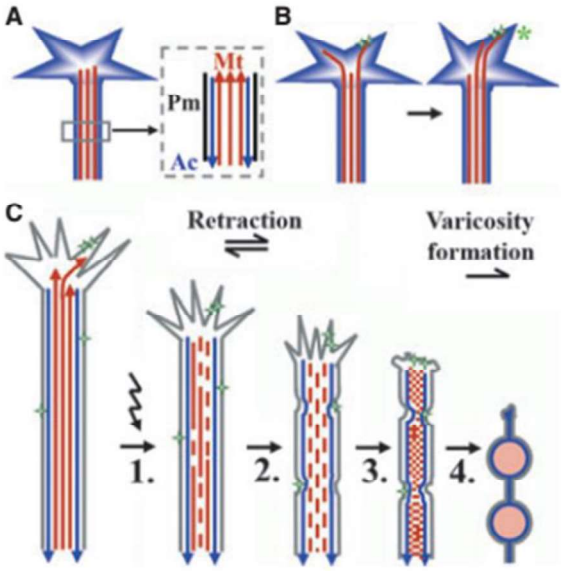

Figure 9. Schematic representation of TRPV1 mediated cytoskeletal reorganisation: (a-b) Image shows role of cytoskeletal components actin and tubulin in growth cone formation. **(c)** shows different steps from growth cone formation to varicosity formation. Taken from [195].

Actin and tubulin both play important role in the many cellular processes such as cell division, motility, cell morphology, and intra cellular transport of molecules. Physical interaction and functional importance of TRP channel have been very well established in past such as some of TRPP and TRPC family members TRPC1, TRPC5 and TRPC6 [86, 200-202]. Previously it has been summarised in a review that how cytoskeletal and scaffolding proteins play important role as structural and functional determinants of TRP channels [203]. In 2014 another review has summarised that the connection between mechanosensitive ion channel and cytoskeleton [204].

1.3. TRP channels in lower organisms, in animals and plants:

Among all organisms starting from bacteria to a multicellular organism including plants; all of them use transmembrane proteins with 6TM segments similar to K^+ channel to sense the external environment and response towards noxious clues [5]. Plants also possess sensory mechanism which helps them to survive in different physiological conditions including touch, osmotic balance, light, and temperature. But so far very few reports suggest the presence

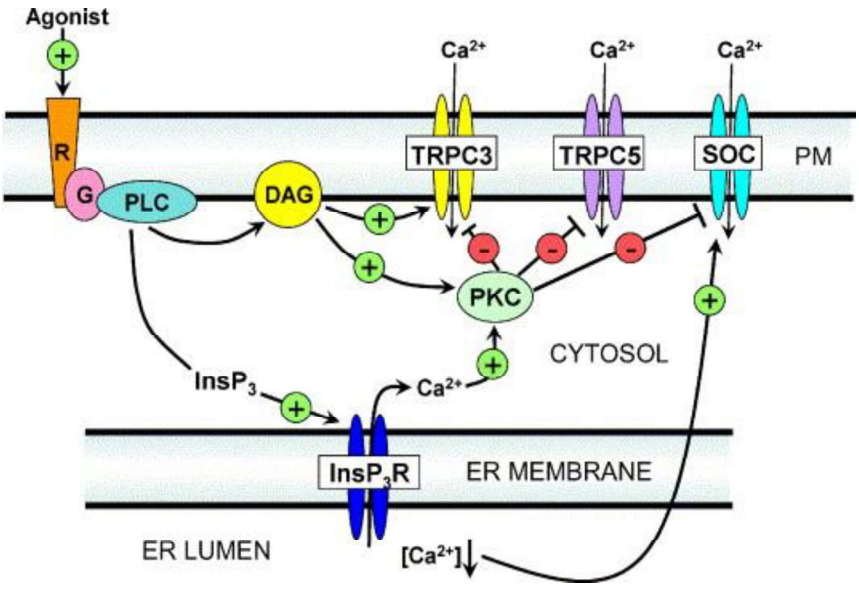

Figure 8. Image shows actions of DAG and PKC on SOCs and TRPC channels: The TRPC channels all appear to be blocked by DAG-induced PKC, but only TRPC3 (and likely TRPC6 and 7) is activated. What accounts for receptor-mediated activation of TRPC5 channels is not known. Figure taken from [180]

1.2.7. Regulation by Cytoskeleton components:

TRP channels are regulated through cytoskeleton elements such as actin and tubulin. Increasing number of evidence suggest that many proteins including cytoskeletal proteins at the plasma membrane form a signaling complex called as "signalplex" [195]. Physical interaction of tubulin and TRPV1 have been shown through biochemically where TRPV1-Ct is sufficient to interact with tubulin [196]. On the other hand, activation of TRPV1 results in the disassembly of microtubule cytoskeleton, while there is no such effect on the actin cytoskeleton [197] **(Fig. 9)**. In 2012 different group also have reported the interaction of intact microtubule and TRPV1 [198]. Another vanilloid family member TRPV4 also have been shown to interact with cytoskeletal elements such as actin and tubulin. Previously it has been shown that C-terminus of TRPV4 is sufficient to interact with both the components. Study also reveals that TRPV4 interacts with polymerised actin and tubulin cytoskeletal proteins and stabilize the microtubule [199].

TRPV1 has also been observed in some of studies where anti TRPV1 antibody shows reactivity at higher size due to glycosylation of TRPV1 at 604 residue (Asn) [185].

1.2.6. By different Ca^{2+}-dependent and Ca^{2+}-independent signaling pathways:

Expression and distribution of TRP ion channel is very much diverse from different tissues to different cell types where they play important role in the Ca^{2+}-dependent and Ca^{2+}-independent signaling events. Two pathways which play important role in Ca^{2+}-signaling are GPCR and tyrosine kinase-mediated activation of PLC. Further this activated PLC acts on PIP_2 and converts into IP3, which acts on the IP3 receptor and cause release of Ca^{2+} from ER [186-190]. There are large number of reports available which explains the association of TRP and PLC pathways, at least in *Drosophila* [191]. TRPV1 interacts with PIP_2 and increased PIP_2 concentration decreases the temperature activation threshold of this receptor [192-194]. There are two opposite mechanisms that has been reported for the action of PIP_2. The PIP_2-mediated sensitisation and desensitisation have been studied [192]. This activation/inhibition dual regulation mechanism might be applicable to some of TRPC and TRPA1 family members [192].

Other Ca^{2+} signaling pathways include store operated Ca^{2+} entry (SOCE) where some of TRP channels may play an important role. Such as TRPC1, TRPC4 and TRPV6 in knockout studies have shown that these channels play essential role in such function [102-106]. Also, it has been shown that increased endothelial permeability due to increased Ca^{2+} concentration cause activation of signaling pathways that result in cytoskeletal reorganization [98]. Study also reveals that this endothelial permeability was a consequence of PKC isoform PKCα [98]. **(Fig. 8)**.

Subsequently Cohen et al. have shown that TRPV2 acts as a substrate for extracellular signal-regulated kinase (ERK) in neurites [171].

1.2.5. By post-translational modifications:

TRP channels are uniquely regulated by different post-translational modifications (PTM). The common PTM events include phosphorylation, dephosphorylation, glycosylation, etc. Kinase-mediated phosphorylation of TRPV1 has been shown to be regulated by different kinase such as PKC, PKA, and CamKII, through which they modulate the activity of TRPV1 [167, 168, 172]. Some phosphatase such as Calcineurin (Ca^{2+} and Calmodulin-dependent serine/threonine phosphatase), dephosphorylates TRPV1 and cause desensitization of TRPV1 [173]. Other kinases such as c-SRC kinase and protein phosphatase also regulates activity of TRPV4. In mast cell, TRPV2 is regulated by PKA [174]. Such regulation needs a kinase adaptor protein, Acyl CoA binding domain protein (ACBD)3 as an interacting partner [170]. TRPV4 ion channel also regulated by phosphorylation at different sites. Such as phosphorylation of TRPV4 at different residue, Ser^{162}, Thr^{175}, and Ser^{189} was enhanced by the activation of PKC activator phorbol 12-myristate 13-acetate or by application of bradykinin and decreased by the PKC inhibition using staurosporine, bisindolylmaleimide I, and rottlerin. They have shown that PKC and PKA mediated phosphorylation of TRPV4 results in increased sensitisation [175]. TRPV4 regulates angiogenesis through modulation of endothelial cell [176]. And this process is regulated through the Rho/Rho kinase pathway [176]. TRPM4 activity is also enhanced through PKC mediated phosphorylation [177]. Other effect includes the inhibitory role of PKC on the TRPC channels such as TRPC3, TRPC4, TRPC5 and TRPC7 are strongly inhibited through PKC activation [178-181]. In addition, uncommon post-translational modifications such as Nitrosylation, Cysteine modifications are also known. For example, some of TRPC and TRPV subfamily members TRPC1, TRPC4, TRPC5, and TRPV1, TRPV3 and TRPV4 gets sensitize upon cysteine S-nitrosylation [182-184]. Glycosylation of

sensor TRPV2 doesn't have this conserved Calmodulin-binding site in its N-terminus [164]. In contrast, study has identified the presence of Calmodulin-binding site on the C-terminus of TRPV2 (654-683) and TRPV5 (587-616). Mutation in the Calmodulin-binding site results in the reduced interaction or complete loss of interaction [165].

Another important regulation of TRP channels is at the level of vesicle fusion. Such as mucolipins (TRPML) are involve in the intra vesicular trafficking. Some of the TRPC family members such as TRPC1, TRPC3-TRPC6 are reported to be present on the rat brain synaptosome [133]. TRPC5 translocation from vesicle to the plasma membrane upon growth factor stimulation has been reported which is termed as 'rapid vesicular insertion of TRP' (RiVIT) [85]. Increasing evidence suggest that TRP channels play important role in the membrane traffic, signal transduction, and vesicular ion homeostasis.

Among other interacting proteins, different kinases are important. Different kinases not only interact but also directly phosphorylates different TRP channels. Such phosphorylation events are hallmark of sensitization steps. For example, Capsaicin Receptor is regulated at the level of phosphorylation by Protein Kinase A (PKA), Protein Kinase C (PKC) and Calmodulin-dependent protein kinase II (CamKII) [166, 167]. PKA-mediated phosphorylation of TRPV1 results in its activation and this further increase its activity [168]. PKC is important regulator of TRPV1 and upon phosphorylation of TRPV1, response against capsaicin, H^+ and another agonist are increased. Various reports suggest that TRPV1 phosphorylation through different PKC isoforms such as PKCα, PKCε and PKCμ increases the activity of TRPV1 [167]. For example, Numazaki et al. have shown that TRPV1 acts as a substrate for PKCε [167]. Olah et al. also demonstrated that PKCα can potentiates TRPV1 activity. PKCβII was shown to interact with TRPV1 and regulates its basal thermal sensitivity [169]. Stokes et al. have reported that TRPV2 and PKA in mast cell interacts with each other [170]. They suggested that PKA-mediated phosphorylation of TRP channel may regulate and modulate their activity [170].

regulates the lateral mobility of TRP ion channels. For example, depletion of membrane cholesterol increases the rate of recovery of TRPV4 as measured by FRAP experiments [57].

Other than specific components present in vertebrate membranes, there are other hydrophobic compounds that acts as specific regulator of TRP channels. For example, Capsaicin, a pungent hydrophobic exogenous plant product activates TRPV1 [32]. Such Capsaicin response can be inhibited by phosphatidylinositol 4,5-bisphosphate (PIP_2) [33]. The cellular level of PIP_2 is determined by the activity of PLC. Therefore, factors affecting PLC activity also in turn regulates TRP channels. In general, PLC activation results in the generation of DAG and free cytoplasmic Ca^{2+}, and this free Ca^{2+} is involved in several subsequent complex signaling events. For example, PLC-mediated hydrolysis of PIP_2 inhibits TRPV1 and increase its thermal sensitivity [32, 136, 138]. TRPC3, TRPC4 and TRPM7 channels also interact with PLCβ and PLCγ [5]. TRPM4 and TRPM5 are also regulated by PLC and subsequent Ca^{2+} signaling events [160, 161].

1.2.4. By interacting proteins:

At the submembranous region, TRP channels interact with different cellular proteins representing cytoskeleton protein, vesicular proteins, different kinases and other enzymes, Ca^{2+}-signaling proteins. Such interactions are critical for channels regulation and functions. Such interactions are critical and unique and/or complex signaling events and physiological functions such as pain sensitization [162]. All these proteins form “signalplex” that are located at the plasma membrane. For example, Ca^{2+}-binding protein Calmodulin interacts with TRPV1, via Calmodulin-binding site present in the C-terminus (35 amino acid) [163]. The N-terminus of TRPV1 (189-222 amino acid) also interact with Calmodulin. Calmodulin interaction is conserved in other thermosensitive members also. Indeed, Calmodulin interacts with TRPV3 and TRPV4 to the same site present on the N-terminus [164]. Surprisingly noxious temperature

Other than complex compounds, there are several metal ions that are known to inhibit the TRP channels activity. Such inhibition is due to the fact that different ions often "misfit" into the actual pore and cause "open-channel-block" a phenomenon that may or may not be reversed [147-149]. For example, TRPV4 channel can be inhibited by ruthenium red, gadolinium and La^{3+} [150].

1.2.3. By cholesterol and different lipids:

Few recent reports suggest that the molecular evolution of TRP channels correlate with the vertebrate evolution [151, 152]. Such analysis strongly indicates that membrane components such as PIP_2, DAG as well as cholesterol and other metabolites which evolved during vertebrate evolution may have strong regulatory role on TRP channels [33, 57, 153, 154]. *In silico* analysis indicate presence of different lipid binding sequence/s in different TRP proteins [57]. Such predictions are further confirmed by biochemical and other experiments which establishes the tight association of TRP proteins with different lipids, PIP_2 and with cholesterol [33, 57, 153]. PIP_2 is an important signaling mediator which is abundant in membrane and it regulates TRP channels [153]. TRPC3 has been reported to act as an inositol-1,4,5-trisphosphate (InsP3) receptor [155, 156]. Another important signaling mediator is DAG, which regulates TRP channels. For example, some family members of TRPC subfamily such as TRPC3, TRPC6 and TRPC7.

In silico analysis identified the presence of (one to many) cholesterol biding motif sequence/s in different TRP proteins and such sequences are well conserved throughout the vertebrates. There are large number of reports that also demonstrate the physical interaction of cholesterol with TRPV1, TRPV3, and TRPV4 [57, 157-159]. Even crystalized truncated Rabbit TRPV2 show the presence of attached cholesterol [50]. All these in general suggest the physical interaction and regulation of TRP channels by cholesterol present in the membrane. Experimental evidence suggests that membrane components such as cholesterol indeed

<25-28°C. TRPV1 can also be activated by low pH. Other than temperature there are large number of reports which suggest that TRP channels can also act as osmosensitive and mechanosensitive sensor in different organism. For example, TRPV4 is activated by mechanical pressure [78, 80, 81, 137]. Infrared and ultraviolet radiation also activate certain TRP channels, such as TRPA1 [59, 117].

1.2.2. By exogenous and endogenous ligands:

TRP channels are known to be activated by different exogenous and endogenous stimuli. Among all, several hydrophobic compounds and different lipids are important. For TRPV1, Capsaicin acts as an exogenous ligand while PIP_2, bradykinin and nerve growth factor (NGF) acts as an endogenous ligand for this receptor [32, 138]. Some other Vanilloid compounds known as "endovanilloids", such as anandamide, arachidonic acid metabolites (such as N-arachidonoyl-dopamine (NADA) can activate TRPV1 [139]. In the same context, 12-hydroperoxyeicosatetraenoic acid, oxidized linoleic acid metabolites, essential oils, Octadecadienoic, also many pungent plant products including Resiniferatoxin, Piperine, Gingerol and Zingerone, Camphor, as well as Eugenol acts as endogenous or exogenous ligand for TRPV1. For TRPV2, Insulin growth factor-1 (IGF-1) acts as an endogenous stimulant [110]. TRPV3 can be activated by endogenous ligands such as FPP, and synthetic ligand such as 2 APB [140-142]. Also, TRPV3 can be inhibited by 17-R- resolving D and 2,2-diphenyltetrahydrofuran (DPTHF) [143, 144]. Similarly, TRPV4 can be activated by 4α-phorbol 12,13-didecanoate (4αPDD), a synthetic ligand at 1μM concentration [145]. Two others structurally similar compounds namely RN1747 and RN1734 act as inhibitor of TRPV4 [146]. In addition, there are natural bioactive compound called Citral which acts as an inhibitor of TRPV4.

lysosomes and in mitochondria [131]. Several TRP channels are present in the cell-cell contact formation sites, synapse and even in isolated Synaptosomes [85, 86, 132]. For example, TRPC3-TRPC6 are shown to be present in rat brain Synaptosomal fraction [133]. TRPV1 is present in synaptosome and also in post-synaptic density (PSD) fraction [134]. Such localizations and trafficking are specifically regulated by interaction of TRP channels with different vesicle regulatory proteins. Indeed, interaction of TRP channels with specific proteins such as with Rabs, VAMP, Snapin and Synaptotagmin have been reported [85, 86, 132]. In a similar manner, TRPML is also involved in intra vesicular trafficking [135].

As biological membranes are largely heterogeneous, different functions of TRP channels are largely dependent on the localization of the respective channels. The membranous compartment and composition of specialized membranes affect channel function at the single molecular level. In addition, there are specific events such as "sensitization and desensitization" that regulate ion channels at the cellular and also at the single channel level. Such regulations are fine-tuned by different mechanisms including different kinase and phosphatase activities. Such regulations essentially alter the opening and closing probability of individual channels. In this section, such mechanisms are discussed in details.

1.2.1. By physical stimuli:

One of the important characteristic feature of TRP channel is their activation by different physical stimuli. Different physical stimuli such as altered temperature, mechanical pressure, osmotic pressure, change in pH etc. can modulate activities of different TRP channels. Several TRP channels act as molecular thermosensor and become activated at different temperature. For example, TRPV1 is activated at high temperature (42°C) and low pH [32, 136]. For example, TRPV2 is activated at 52°C and cell stretch, TRPV3 is activated at >34-39°C, TRPV4 is activated at >27-35°C, TRPA1 is activated <17°C, TRPM8 is activated at

TRPV3	Breast cancer, myasthenic syndrome, non-insulin dependent diabetes mellitus, *Olmsted Syndrome*
TRPV4	Central hypoventilation syndrome, cardiopathy, brachyolmia, spinal muscular atrophy (SMA), hereditary motor and sensory neuropathy type 2 (HMSN2C), spondylometaphyseal dysplasias (SMDK) and metatropic dysplasia
TRPV5	Renal tubular acidosis, cancer
TRPV6	Renal tubular acidosis, cancer
TRPM1	Lymphoma, hypertension
TRPM2	Epilepsy, leukemia, holoprosencephaly HPE1, Knobloch syndrome
TRPM3	Candidate genes for amyotrophic lateral sclerosis with frontotemporal dementia, early-onset pulverulent cataract, hemophagocytic lymphohistiocytosis, infantile nephronophthisis
TRPM4	Diabetes mellitus, prostate cancer, leukemia, lymphoma
TRPM5	Beckwith-Wiedemann syndrome, diabetes mellitus, breast, bladder and lung cancers
TRPM6	Spastic paraplegia, deafness, amyotrophic lateral sclerosis with frontotemporal dementia
TRPM7	Spinocerebellar ataxia, colorectal adenoma, and carcinoma, susceptibility to dyslexia
TRPM8	Chronic obstructive pulmonary disease, Parkinson's disease
TRPP2	Neutropenia, susceptibility to psoriasis
TRPP3	Renal hypoplasia, optic nerve coloboma with renal disease, epilepsy, Alzheimer's disease
TRPP5	Epilepsy, allergy and asthma susceptibility, muscular dystrophy, inflammatory bowel disease
TRPA1	Spastic paraplegia, sensorineural deafness, convulsions
TRPML1	Alzheimer's disease, liposarcoma, mental retardation

1.2. Regulations of TRP channels:

At the molecular level, TRP channels are regulated by different mechanisms. Essentially all these mechanisms collectively affect different steps at the cellular level, i.e. proper vesicular trafficking, localization and recycling of TRP ion channels at the membrane. As transmembrane proteins, TRP channels are synthesized in the ER and subsequently transported to plasma membrane and in other specific subcellular organelles such as in vesicles,

TRPV4-mediated channelopathies has been reported in the human population. Most of the mutation associated with TRPV4 are linked with development of genetic disorder in human population such as Brachyolmia, Spinal Muscular Atrophy (SMA), Hereditary Motor and Sensory Neuropathy type 2 (HMSN2C), Spondylometaphyseal Dysplasias (SMDK) and Metatropic Dysplasia etc. [127-129]. Similarly, TRPV3 is also involved in the pathophysiology of skin disorder (*Olmsted Syndrome*). Mutation associated with this disorder are "gain of function" type and as a result the mutants are constitutively open.

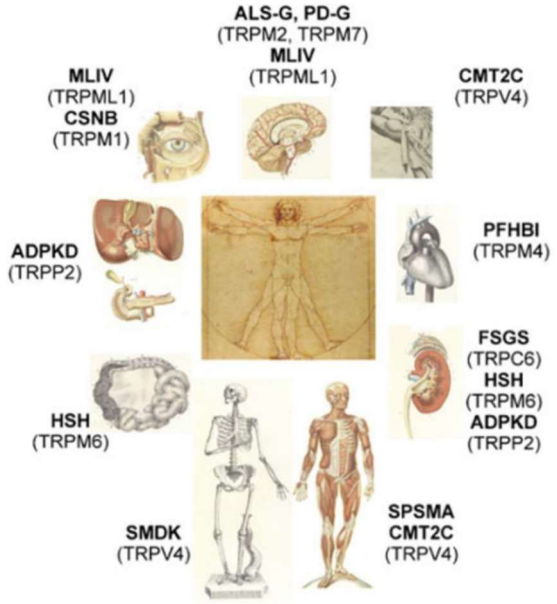

Figure 7. TRP channelopathies: Image represents major target organs in the human body. (Illustrations are from a public domain of US National Library of Medicine, except the Vitruvian Man by Leonardo da Vinci, 1485–1490, Galleria dell' Accademia, Venice, Italy) Figure taken from [130].

Table 2. TRP's and channelopathy Adapted from [53].

Channel	Pathophysiology
TRPC1	Myotonic dystrophy type 2, hypertension, Seckel syndrome
TRPC4	Breast cancer, atopic dermatitis
TRPC5	Coronary heart disease, X-linked mental retardation, migraine
TRPC6	COPD, lung cancer
TRPV1	Breast cancer, myasthenic syndrome, non-insulin dependent diabetes mellitus
TRPV2	Central areolar choroidal dystrophy, myasthenic syndrome, prostate cancer

adipocytes, keratinocytes are important for their physiological function. For example, functional expression of TRP channels in T-cells, macrophages and other immune cells poised these channels as important parameters for immune activation and neuro-immune interactions. Indeed, TRP channels are relevant for release of cytokines and such factors are important stimuli for nociception [27]. Similarly, expression of TRP channels in adipocytes can be relevant for the release of "adepokines" [122, 123]. Presence of some TRP channel in keratinocyte also plays important role in the neuro-keratinocyte interaction as well their important physiological function such as skin barrier formation, morphogenesis and differentiation. Similarly, "endocanabinnoid" system is present in the brain and throughout the central and peripheral nervous system. Hence endocanabinnoid and TRP channel also shows cross talk with each other. Indeed, some of the Canabinnoids also act on TRP channel (example TRPV1) and modulate their activity [124-126].

TRP channel play essential physiological function across the species and these proteins function and sequences are highly conserved across the species. As a result, any change in the sequence due to mutation results in the altered channel function which leads to the different pathophysiological condition **(Fig. 6)**. There are large number of TRP's belong to different sub family such as TRPV, TRPC, TRPP, and TRPML that are associated with many channelopathies **(Fig. 7)**.

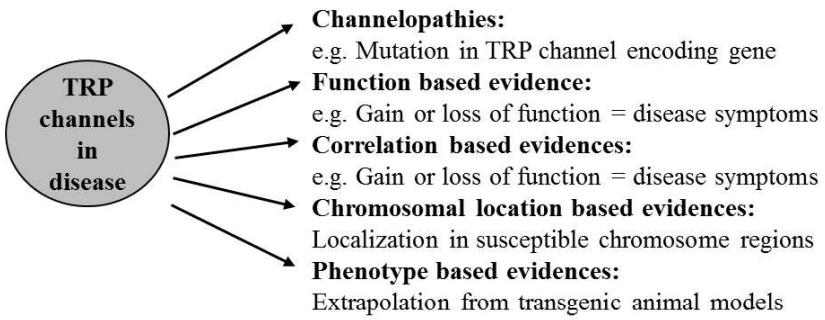

Figure 6. TRPs and disease: Overview of the possible involvement of TRP channels in different forms of pathogenesis. Figure adapted from [53].

abnormal heat evoked current propagation, decreased heat nociception and inflammatory thermal hyperalgesia [119]. TRPV1 and TRPV3 double knockout mice reveals that TRPV1 is a key regulator for sensing noxious heat temperatures and TRPV3 might play supportive role in the absence of TRPV1 [120].

TRPV2 knock out animal reveals that TRPV2 ablation does not change the thermal nociception over a range of temperature [121]. Other study using TRPV3 knockout animals on both C57BL6 and 129S6 backgrounds, as well as animals deficient in both TRPV3 and TRPV4 on a C57BL6 background reveals that both of these proteins do not contribute significantly in the detection of acute heat nociception and inflammatory heat hyperalgesia [119].

Similar study using TRPV3 knockout mice also reveals its importance in the hair morphogenesis. This study reveals that mice lacking TRPV3 results in the wavy hair coat and curly whiskers [107].

1.1.6. TRP channels in sensory functions, pain and other pathophysiology:

Primarily TRP channels play essential role in sensory transduction from single cell to multicellular organism. TRP channels are involved in functions such as osmosensation, thermosensation, detection of noxious stimuli, pheromone sensing, and vision etc. Presence of TRP channel in peripheral nervous system helps in the detection of different painful stimuli caused by temperature (hot or cold), mechanical force, and many noxious chemicals such as Capsaicin. Some of TRP channels such as TRPV1, TRPM8 and TRPA1 detect the temperature induced painful stimuli. Due to the presence and distribution of TRP channels in the peripheral system, these channels play key role in the nociception under physiological and pathological conditions and are also involved in conditions such as inflammation and neuropathy.

TRP channel are present in the both neuronal and non-neuronal system. Among many non-neuronal systems, presence of TRP channels in immune cells, bone cells, pancreatic cells,

stage to the adult stage which requires fine tuning and discrimination between optimal temperature and avoids noxious temperature [113-115].

TRP channels are also involved in detection of complex stimuli. For example, previously it has been reported TRPA1 as an “infrared sensor”, especially in the pit organ of certain snakes where it is essential for the primary transduction of the infrared signal. They demonstrated that TRPA1 detects the radiant heat in the pit organ of snakes instead of photochemical transduction [59]. Further reports show that TRPA1 acts as the infrared sensor in the pit bearing snakes. There is a specific 11 amino acid long sequence which is diverged especially in the pit bearing snakes while the same stretch is highly conserved in the non-pit bearing snakes [116]. It is also possible that these amino acids may be important for the infrared detection in these snakes [116]. In case of Human melanocyte, Ultra Violet radiation (UVR) can activate TRPA1 [117]. Through Ca^{2+}-imaging experiments show that this UVR response is actually mediated through TRPA1 and also involves G protein and phospho lipase C signaling [117].

TRP channels regulate different specific physiological functions such as muscle contraction and vaso-motor control, etc. as these functions are regulated by mechanical changes [12-16]. TRP channels play important role in many physiological and sensory functions, affecting behaviour regulation in general. For example, TRP channels regulate complex functions such as taste, nociception, pheromone signaling, and temperature sensation [12-16]. Also, TRP channels are involve in the detection of osmotic stimuli or cell stretch, mechanotransduction in some single cell as well as in multi cell organisms.

Knock out studies from different groups highlight the importance of TRP channel at cellular level. For example, many independent studies using TRPV1 knockout mice suggest that it plays crucial role in thermal nociception [118, 119]. Similar study using cultured dorsal root ganglion (DRG) neurons from TRPV1 knockout mice shows involvement of TRPV1 in

allow entry of other important ions such as Zn^{2+}, Mg^{2+}, Mn^{2+}, Fe^{2+}, Co^{2+} etc. and therefore is also involved in the maintenance of other ions also. Indeed, TRP channels are involved in homeostasis of metallic ions, such as Ca^{2+} and Mg^{2+} reabsorption and osmoregulation [96]. Notably, in certain cases, TRP channels act as "signalplex" located at the plasma membrane and thus initiate complex signaling events. In many cases, such events are also involved in the Ca^{2+}-independent signaling events [100].

TRP channels are also involved in intracellular Ca^{2+}-buffering and several reports suggest their involvement in Ca^{2+}-release from intracellular organelles. So far, several studies show that TRP's are involved in store-operated Ca^{2+}-entry (SOCE) [101]. Nilius et al. have studied TRPC4$^{-/-}$ mice and demonstrated that TRPC4 is an essential component of SOCE [102]. Another study in Chinese hamster ovary shows that TRPC1 is an essential component of SOCE [103]. Similarly, another study has shown that Ca^{2+} selective TRPV6 could be an essential component of Ca^{2+} release activated current (CRAC) [104-106].

At molecular level, TRP channels act as "cellular receptor" for several chemical and physical stimuli. For example, in *Drosophila*, TRP channels detect and responds to the very minute and large temperature changes. For example, TRPV1 acts as a receptor for Capsaicin and also acts as a nociceptor. TRP channels have been reported to maintain keratinocyte proliferation, differentiation, hair morphogenesis, and skin barrier formation [107-109]. Similarly, TRPV2 also acts as a receptor for insulin growth factor [110]. Cold receptor TRPA1 acts as an infrared sensor in pit bearing snake [59]. In case of T cells, TRP channels play important role during the T cell activation process which involves increased body temperature [27]. Similarly, in case of sperm cells, TRP channels play important role for the chemotactic and thermotactic movement [111]. In *C. elegance,* TRP3 has been shown to be essential for egg and sperm fusion [112]. In mammalian systems, TRP's play a number of developmental and physiological functions. For example, TRP channels also help conversion of the larval

TRPA1	Human: 8q13; mouse: 1 A3	Hair cells, sensory dorsal root and trigeminal ganglia neurons, fbroblasts	Thermo-sensation (noxious cold); the most versatile chemo-sensor; mechano-sensation?; nociception; olfactory responses; cold induced contraction in colon and bladder
TRPML subfamily			
TRPML1	Human: 19p13.3-13.2; mouse: 8 A1.1	Ubiquitous; intracellular ion channel	Essential for endocytosis and endosomal/lysosomal function; regulation of autophagy
TRPML2	Human: 1p22; mouse: 3 H3	Ubiquitous; intracellular ion channel	Endosomal/lysosomal function
TRPML3	Human: 1p22.3; mouse: 3 H3	Hair cells (stria vascularis, stereocilia); intracellular ion channel	Endosomal/lysosomal function; autophagy; hair cell maturation?
TRPP subfamily			
TRPP2	Human: 4q22; mouse: 5 E4	Ubiquitous; mostly in ovary, fetal and adult kidney, testis, and small intestine in both motile and primary cilia	Cardiac, skeletal and renal development; integrity of the vessel wall; negative regulator of endogenous mechano-sensitive channels; mechano-receptor and flow-sensor in endothelium; apoptosis
TRPP3	Human: 10q24-q25; mouse: 19 D1	Adult heart, skeletal muscle, brain, spleen, testis, retina and liver	Renal development; part of putative sour sensor
TRPP5	Human: 5q31; mouse: 18 B3	Testis, brain and kidney	Spermatogenesis?

1.1.5. Different functions of TRP channels:

Although TRP channels are present almost ubiquitously in the cellular system but their functions are much diverse in different organisms and also in different tissues and cells. TRP channels act as non-selective cation channel, which are present on the plasma membrane and also in different intracellular organelles. In spite of differences in the extent of Ca^{2+}-selectivity, activation of TRP channels in general cause Ca^{2+}-influx and therefore initiate complex Ca^{2+}-signaling events [56, 97, 98]. The Ca^{2+} pool induces different signaling processes and physiological processes such as maintenance of Ca^{2+} homeostasis, neurotransmitter release, muscle contraction, cell proliferation, differentiation and often cell death [99]. Being non-selective in nature, these channels also allows influx of ions other than Ca^{2+}. TRP channels

TRPV5	Human: 7q35; mouse: 6 B2	High in kidney; lower in gastro-intestinal tract, pancreas, testis, prostate, placenta, brain and salivary gland	Ca^{2+} (re)absorption channel in kidney and intestines
TRPV6	Human: 7q33-q34; mouse: 6 B2	High in gastro-intestinal tract; lower in kidney, pancreas, testis, prostate, placenta, brain and salivary gland	Ca^{2+} (re)absorption channel in intestines and kidney; key player in Ca^{2+}/1,25-dihydroxyvitamin D3-induced keratinocyte development in the skin
TRPM subfamily			
TRPM1	Human: 15q13-q14; mouse: 7 C	Skin melanocytes, retinal bipolar ganglia	Light response in ON bipolar retinal ganglia cells; tumor repressor in melanoma cells
TRPM2	Human: 21q22.3; mouse: 10 C1	Brain, bone marrow, peripheral blood cells (neutrophils), lung, spleen, eye, heart and liver	Oxidative and nitrosative stress response; activation of granulocytes; pancreas insulin release; critical in apoptosis
TRPM3	Human: 9q21.13; mouse: 19 C1	Primarily in kidney; lower in brain, sensory neurons, testis, ovary, pancreas and spinal cord	Steroid hormone (pregnanolon) sensor; possible regulator in endocrine pancreas, glia cells and cerebellar Purkinje cells
TRPM4	Human: 19q13.32; mouse: 7 B4	Heart, exo- and endocrine pancreas, mast cells, smooth muscle, macula densa, lung and placenta	Mast cell degranulation (histamine release) and migration as a critical Ca-impermeable cation channel regulating Ca^{2+} entry; catecholamine release from chromafn cells; vasopressin release from paraventricular and supraoptic hypothalamic nuclei
TRPM5	Human: 11p15.5; mouse: 7 F5	Tongue (taste bud cells), lungs, testis, digestive system, brain, endocrine pancreas	Taste (sweet, bitter, umami); positive regulator of glucose-induced insulin release; trigeminal nasal chemoreception
TRPM6	Human: 9q21.13; mouse: 19 B	Kidney, colon and intestine	Mg2+ homeostasis and reabsorption in kidney and intestine
TRPM7	Human: 15q21; mouse: 2 F2	Ubiquitous	Mg^{2+} homeostasis and reabsorption in kidney and intestine; cell cycle control; gastrulation; development of thymocytes (thymopoiesis); cell migration; shear stress sensor?; skeletogenesis?
TRPM8	Human: 2q37.1; mouse: 1 C5	Sensory dorsal root and trigeminal ganglia neurons, nodose ganglion cells innervating the upper gut, vascular smooth muscle cells, liver, gastric fundus, bladder (urothelium) and different tissues of the male genital tract; high in tumors from prostate, breast, colon, lung and skin	Thermo-sensation (cold); sperm motility, acrosome reaction
TRPA1 subfamily			

TRPC6	Human: 11q21-q22; mouse: 9 A1	Smooth muscle cells, lung, brain, placenta, kidney (podocyte foot processes), spleen, ovary and small intestine, neutrophils	Vaso-motor regulation; α1 signaling in smooth muscle; smooth muscle proliferation; angiogenesis; endocannabinoid signaling in the brain; promotion of dendrite growth and synapse forming in the developing brain; glomerular flter integrity in the kidney; platelet function; redox sensor; mechano-sensor?
TRPC7	Human: 5q31.2; mouse: 13 B2	Pituitary glands, kidney and CNS (human); heart and lung; weak in CNS and kidney (mouse)	Controls respiratory rhythm activity in pre-Bötzinger complex in the brain
TRPV subfamily			
TRPV1	Human: 17p13.3; mouse: 11 B3	Dorsal root and trigeminal ganglia; spinal and peripheral nerve terminals, brain, skin (cutaneous sensory nerve fibers, mast cells, epidermal keratinocytes, dermal blood vessels, the inner root sheet and the infundibulum of hair follicles, differentiated sebocytes, sweat gland ducts, and the secretory portion of eccrine sweat glands), pancreas, bladder (urothelium, smooth muscle, blood vessels and neurons)	Thermo-sensation (heat); autonomic thermoregulation; nociception; pain management; synaptic plasticity in the brain (long-term depression); endocannabinoid signaling in the brain; food intake regulation; growth cone guidance in the brain; osmosensing in the brain by a particular TRPV1 variant; multiple functions in the gut
TRPV2	Human: 17p11.2; mouse: 11 B2	Dorsal root ganglia and CNS neurons, gastro-intestinal tract, spleen, mast cells, smooth, cardiac and skeletal muscle cells	Thermo-sensation (noxious heat); nociception; axon outgrowth in spinal motor neurons; critical for phagocytosis in macrophages
TRPV3	Human: 17p13.3; mouse: 11 B4	Dorsal root and trigeminal ganglion neurons, brain, keratinocytes, hair follicles, tongue and testis	Thermo-sensation (moderate heat); nociception; skin integrity, wound healing, hair growth and sebocyte function
TRPV4	Human: 12q24.1; mouse: 5 F	CNS (large neurons), trigeminal ganglia, heart, liver, kidney, skin (keratinocytes), osteoblasts, blood vessels (endothelium), bladder (urothelium) and testis, cochlea (inner and outer hair cells, marginal cells of the cochlear stria vascularis), kidney (epithelial cells of tubules and glomeruli)	Thermo-sensation (moderate heat); mechano-sensation; osmo-sensation; nociception; modulation of cell migration; endothelium vaso-motor control and possible shear stress sensor; mechano-receptor in urothelium (important for voiding control); osteogenesis and osteoclast function; important in human bone and neurodegenerative diseases; control adherens junctions in skin; cochlea

and any mutation in these proteins results in the lysosomal storage disorder such as (mucolipidosis type IV).

Table 1. Cellular distribution and physiological function of TRP channel Taken from [96].

Channel subunit	Chromosomal location	Cellular expression	Physiological functions
TRPC subfamily			
TRPC1	Human: 3q22-q24; mouse: 9 E4	Ubiquitous	Generation of the excitatory postsynaptic potential in brain; netrin-1 and brain-derived neurotrophic factor (BDNF)-mediated growth cone guidance; connections to sleep/wakefulness states, alertness and appetite; brain development (together with TRPC5); glutamate signaling in hippocampus; regulation of smooth muscle contraction pulmonary system; platelet function; skeletal muscle differentiation; mechano-sensation?
TRPC2	Human: 11p15.4-p15.3 (pseudogene); mouse: 7 F1	Dendritic tips of the vomeronasal sensory neurons and spermatozoa (mouse)	Pheromone detection that regulates sexual and social behaviors, such as gender recognition and male-male aggression (mouse)
TRPC3	Human: 4q25-q27; mouse: 3 B	Central nervous system (CNS) and smooth and cardiac muscle cells	BDNF-mediated growth cone guidance (TRPC1-independent); spine formation in brain; γ-aminobutyric acid signaling in striatum; astrocyte function; moto-control in cerebellum; cerebral vaso motor control; erythropoietin function; functional coupling to orexin receptor
TRPC4	Human: 13q13.1-q13.2; mouse: 3 D	Placenta, adrenal gland, CNS, endothelium, smooth muscle cells, kidney, intestinal cells of Cajal	Endothelium-dependent vasorelaxation and regulation of transcellular permeation of the endothelial layer; cell-cell adhesion in endothelium through junctional proteins; hypoxia sensing together with TRPC1
TRPC5	Human: Xq23-q24; mouse: X F2	Brain, especially in fetal brain and very weak expression in other tissues	Brain development (together with TRPC1); neurite growth, growth cone guidance and morphology; anxiety, fear and reward processing in nucleus accumbens

Ca^{2+} reabsorption and its expression has been reported in Small intestine, pancreas, placenta, prostate [52].

Expression and distribution of TRPC family member are ubiquitous. TRPC proteins have been widely distributed in different tissue including neuronal and non-neuronal origin such as in heart, brain, testis, ovaries, endothelia, adrenal gland, retina, Lung and Eye. Presence of these proteins in large number of tissues suggest importance of these proteins in different physiological functions such as in acrosome reaction in sperm to different neurological responses such as in male aggression, pheromone response, vasorelaxation, neurotransmitter release, modulating neurite extension etc. [85-87].

TRPM family member are present in eye, brain, kidney, prostate, colon, heart, small intestine, liver, lung, taste receptor cells, trigeminal ganglion and dorsal root ganglion. Where these channels play important role such as redox sensing, taste, hypomagnesemia, hypocalcemia, and detection of cold temperature, etc. [88-90].

TRPA1, the only member of Ankyrin subfamily also shows thermosensitive properties like Vanilloid subfamily members. Its presence and distribution has been reported in the dorsal root ganglion and hair cells [91].

TRPP which is found to be associated in human kidney disease [92]. Members of this subfamily are TRPP2, TRPP3, and TRPP5, all of which abundantly expresses in the kidney and these gene are found to be mutated in autosomal kidney disease. Expression and distribution of these protein were reported in heart, testis, skeletal muscle, brain and cochlea hair cells.

Mucolipin subfamily members are found to associated with lysosomal storage disorder [93-95]. TRPML family members TRPML1, TRPML2, and TRPML3 are widely distributed in the brain, heart, skeletal muscle, and cochlea hair cell. These proteins are modulated by change in pH and Ca^{2+} level. Function of these protein includes hearing, lysosomal trafficking

1.1.4. Tissue-wise distribution of TRP channels:

Expression of TRP channel varies largely in different individuals, tissues and cells. Most of the expression studies have used RT-PCR, immunostaining and/or western blot-based approach to determine the presence of TRP channels at RNA and/or protein levels. Due to the use of such approaches and technical limitations; expression data is highly variable and difficult to reach to some conclusion. Presence of TRP channels in different sensory receptors (cells and tissue) enables many sensory functions including thermosensation, mechanosensation, osmosensation, etc. TRPV1 is mainly present in primary afferent nociceptor [60, 61]. There are large number of evidence which suggest that TRPV1 is present in unmyelinated C-fibers which contributes to major portion of somatosensory neuron in rodent's sensory ganglia [62, 63]. Other than this it is also present in the trigeminal ganglion (TG) and dorsal root ganglion (DRG). Presence of this receptor in specific subset of neurons correlate with their function.

TRPV2 which is present in central and peripheral nervous system including medium and large diameter primary afferent (myelinated A and C- fibers) which are devoid of capsaicin receptor [64-69]. Unlike TRPV1 and TRPV2, TRPV3 is very less abundant in DRG and TG ganglion [70]. However, abundant expression of TRPV3 is reported in skin keratinocyte and hair cells [71]. Apart from neuronal (DRG and TG) its high expression was also reported in tongue, testis, cornea, the distal colon, human larynx and inner ear [31, 65, 72-77].

TRPV4 which is reported to be potentiated by hypotonicity-induced cell swelling [78-81], and its presence has been reported in lung, spleen, kidney, testis, brain, cochlea, skin, smooth muscle, liver, and vascular endothelium [80-84].

TRPV5 plays important role in Ca^{2+} reabsorption in the kidney, and its presence has been reported in the Kidney, duodenum, jejunum, placenta, pancreas where it plays essential role [52]. Another close homologue of this group is TRPV6 which also plays important role in

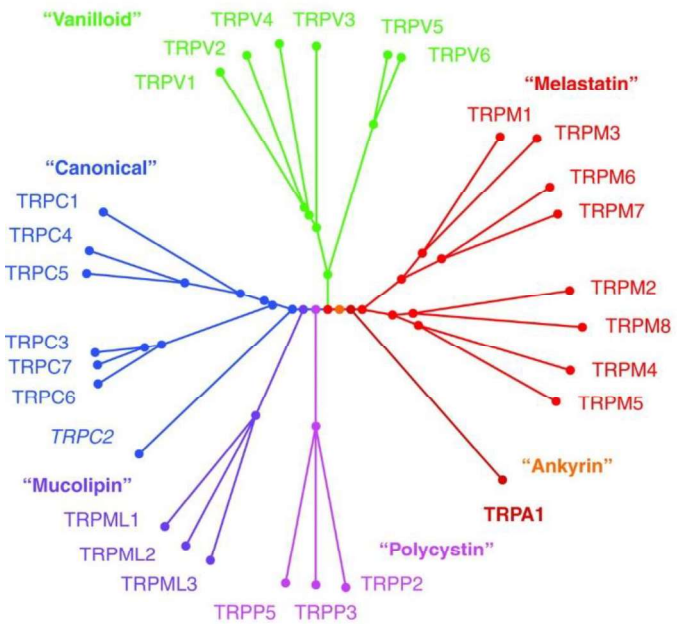

Figure 5. The phylogenetic tree represents the (human) transient receptor potential (TRP) ion channel superfamily: TRP channels are divided into six subfamilies including TRPC (canonical), TRPM (melastatin), TRPV (vanilloid), TRPA (ankyrin), TRPP (polycystin), and TRPML (mucolipin). Figure taken from [56].

In the same context, it is also important to note that due to the advancement of gene sequencing, a lot of new sequences have been identified which suggest presence of different genes in different species that are "homologues" of TRPs. In addition, there are several cases of gene-duplication, gene multiplication and gene-loss in certain species and such events strongly correlate with the behaviour, physiology, sensory functions and other aspects of bio-diversity. For example, in *Xenopus*, TRPV4 has 5 homologues [57]. In Zebra fish, TRPM8 gene is lost and such gene loss may have implication in terms of adaptation in low temperature and non-seasonal breading behaviours [27, 58]. In addition, there are minor changes in the gene sequences which cause gain or loss of substitution of one or more amino acids. Such changes often alter the structure – function relationship of the channels. For example, a 21-amino acid long sequence present in TRPA1 of pit bearing snakes have been linked with the unusual properties of infra-red sensing in such snakes [59].

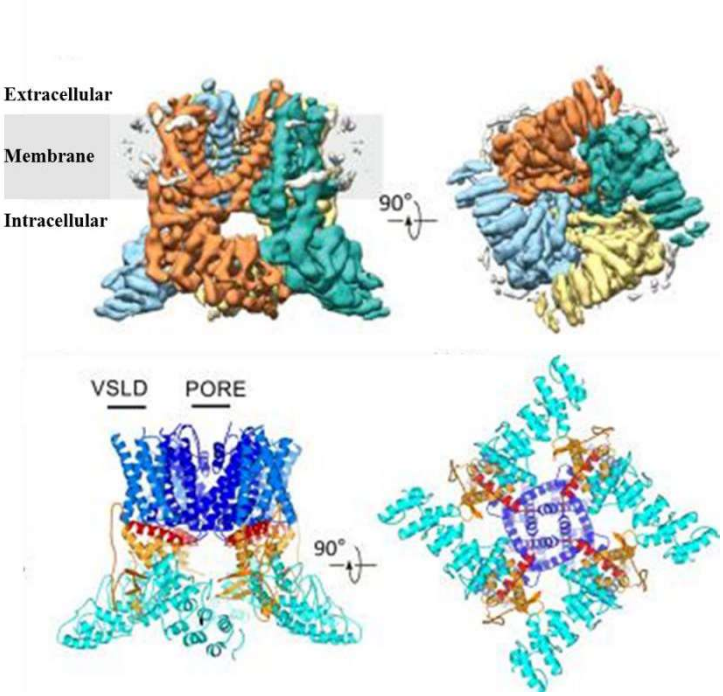

Figure 4. Representation of 3D reconstituted image of TRPV2: Upper panel shows cryo EM structure of Rabbit homotetramer reconstruction with four-fold symmetry and each protomer is coloured differently. Lower panel shows atomic model of TRPV2 built from the EM density, with the domain architecture delineated by different colours Figure taken from [49].

1.1.3. Classification of TRP channels:

TRP channels have been classified based on their sequence similarity and homology with other members. Based on the sequence similarity, TRP's have been classified into 6 subfamilies', namely TRPV (Vanilloids), TRPC (Canonical) TRPM (Melastatin), TRPML (Mucolipins), TRPA (Ankyrin), and TRPP (Polycystins) [5] **(Fig. 5)**. However, this classification is not actually based on the structure or functions. It is important to note that often the functions of TRP ion channels are well conserved from protists, worms, and flies to human [51-54]. For example, human TRPV4 can rescue the mechanosensitive defects observed in OSM9 mutant of *C. elegans* [55]. Such conservation in function may suggest for a similar structure function relationship, though sequences may not be similar.

from the tetrameric structure of TRPV5 and TRPV6 that they may form homomeric and heteromeric ion channel and upon formation of tetramer they from a selectivity filter with D^{541} and D^{542} [42, 48]. This "selectivity-filter" allows only Ca^{2+} to pass through the membrane **(Fig. 3)**. However, it is also known that selectivity filter does not impose directionality on the transported ions.

In 2016, cryoelectron microscopic structure of Rabbit TRPV2 have been reported which describes the structure of TRPV2 at the resolution of 4Å [49]. This study indicates that TM6 shows a different confirmation then reported for TRPV1, which is important for gating of channel. This also reveals that ankyrin repeat domain plays important role in the pore opening along with TRP domain [49] **(Fig. 4)**. Similar study also has reported the full-length TRPV2 structure at the resolution of 5 Å solved by cryo EM [50]. This study reveals that TRPV2 is similar to TRPV1 in terms of pore forming, especially at the upper and lower gates. They have also studied the full-length agonist free TRPV2 and compared the closed and agonist-activated TRPV1 structure. This study also suggests that agonist-free TRPV2 has much wider pore loop structure compare to closed or activated TRPV1 [50].

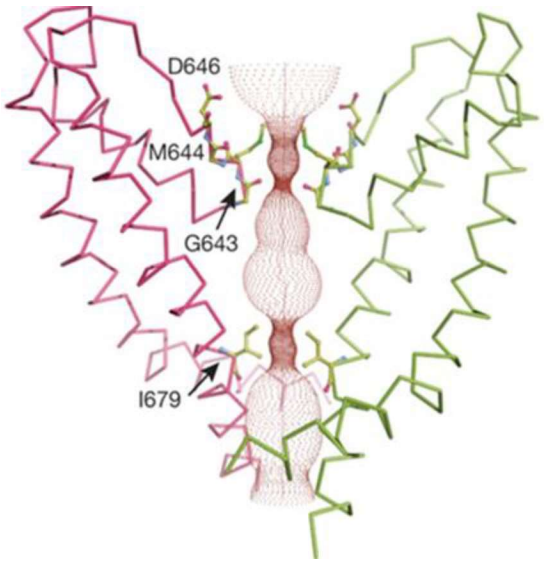

Figure 3. Representation of the ionic selectivity filter of TRPV1: Image shown here represents TRPV1 ion channel and specific amino acid residues which form the selective filter in order to allow the movement of divalent cations. Figure taken from [46].

Figure 1. Schematic representation of mammalian TRP monomer: Contain six TM segments, intracellular N- and C-terminus at the cytoplasmic side. The N-terminus contains ligand binding sites and multiple Ankyrin repeats, while C-terminus contains a conserved TRP-box motif just after the end of TM6 domain. Figure taken from [44].

Till date very few TRP channel have been analysed for high-resolution structure and these TRP channels were studied through single particle cryoelectron microscopy. For the 1st time in 2008 a 19Å structure of TRPV1 reveals two distinct regions. Large open basket-like structure region represents cytoplasmic N and C terminus, while compact structure represents the transmembrane region [45]. Structure also reveals that majority of portion is hanging towards cytoplasmic side while only 1/3 portion is present in the membrane **(Fig. 2)**.

In 2013, open and close structure of TRPV1 at the resolution of 3.4Å through single cryoelectron microscopy reveals the activation mechanism [46]. These structures also reveal the channel opening and closing mechanism along with the importance of selectivity filter. Most of the TRP's channels are "non-selective" in nature, i.e. these channels allow conductivity of different ions such as Na^{+}, K^{+}, and Ca^{2+}, Fe^{2+}, Sr^{2+}, Zn^{2+}, Mg^{2+}, Mn^{2+}, Hg^{2+} upon activation [47].

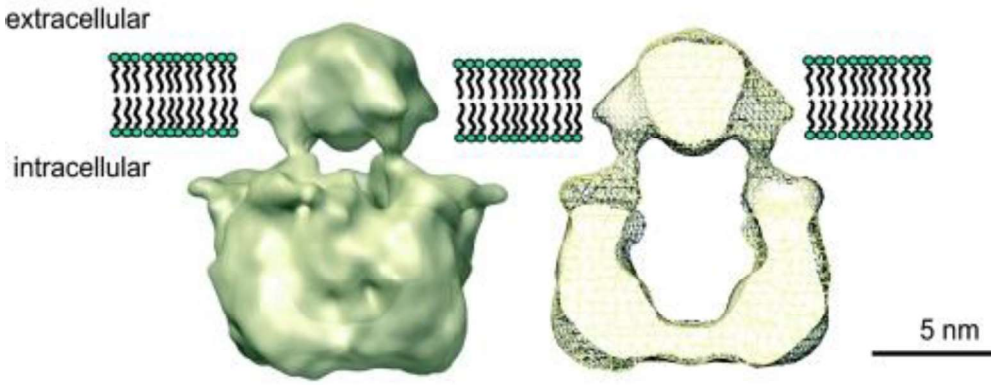

Figure 2. Representation of the 3D structure of TRPV1 in the plasma membrane: A vertical cut-away view shows the internal mass distribution of the protein Figure taken from [45].

However, TRPV5 and TRPV6 are two distant members of TRPV subfamily that are much more selective for Ca^{2+} ions. The charged residues present in the TM regions form the "selectivity-filter" that allows the ions to pass-over during the open-conformation. It is revealed

transmembrane segment. The intracellular N-terminus contains multiple ankyrin repeat motifs. Intracellular N- and C-terminus domains, extracellular loops contain different ligand binding sites. Similarly, the transmembrane region and unstructured loops also have binding sites for different lipids, membranous components (such as cholesterol, PIP_2) **(Fig. 1)** [33-39]. These ligands in general modulate channel's conformation upon binding and thus regulate channel activities. The C-terminal region of TRP channels often have the 'TRP-box', a motif sequence which contains "EWKFAR" sequence. The TRP-box is functionally relevant and are present in all Canonical members but less conserved in Vanilloid and Melastatin families. Similarly, ankyrin repeats are mainly present in the N-terminal portion of members belong to TRPC, TRPV and TRPA family.

TRP channels are known to form tetramers. Though TRP channels mainly form homo-tetramers, there are several reports that suggest the formation of hetero-tetramers as well [40, 41]. For example, TRPV1 and TRPV3 receptors have shown to form the functional hetero tetramer in dorsal root ganglion and trigeminal ganglion in human [40]. Other Vanilloid members include TRPV5 and TRPV6 which also form the functional heterotetramer [42]. Similarly, Transient Receptor Potential Channels, namely TRPP2 and TRPC1 assemble to form heterotetramer [43].

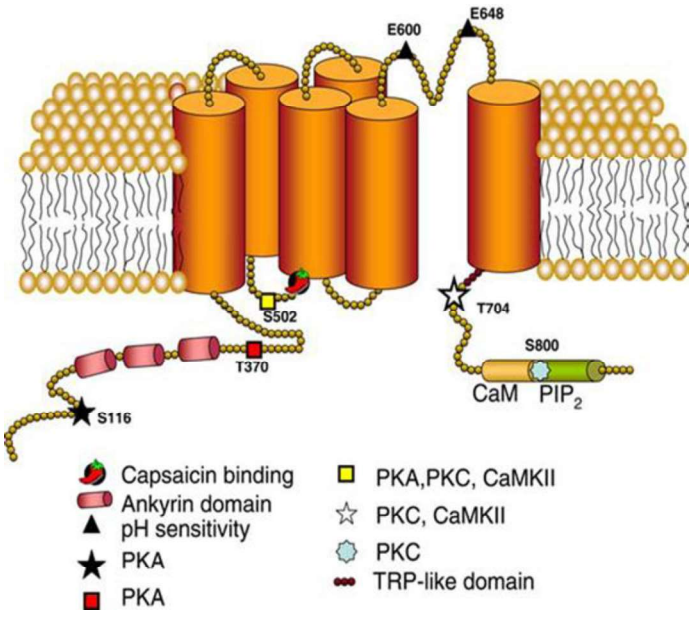

etc. were also reported (Montell C. 2011, Tominaga M. 2016, Jie Geng 2011). During 1969, Cosenns et al for the 1st time have isolated and characterized the *Drosophila* TRP mutants where this mutant shows transient response against the continuous light stimuli. This mutant behaves like blind animal in response to continuous light, and such effects can be rescued by giving the dark pulse [4]. In 1989 Montell et al. for the 1st time have reported that the product of TRP gene is a 143 kDa protein with multiple transmembrane segments [2]. They proposed that TRP gene codes for an integral membrane protein, which shares common features of other membrane proteins, such as the absence of a hydrophobic N-terminal signal sequence (responsible for translocation of membrane protein), and presence of even number of transmembrane domains (suggesting a topology of both N- and C-terminal portion to be in the same side of the plasma membrane). They have also provided a model representing general architecture of TRP protein where it was proposed that TRP protein has actual six transmembrane segments, and both N- and C-terminus regions are located towards the cytoplasm. Subsequently, it was proposed that TRP proteins could actually act as an ion channel which shares the common features with other integral membrane proteins (such as $GABA_A$, glycine, and Nicotinic acetylcholine ligand-gated receptors) and TRP protein was also shown to be involve in the signal transduction (Barnard et al. 1987). Identification of TRPV1 as the "Capsaicin Receptor" was the next milestone discovery in this filed [32]. As a result of that, other TRPV members were identified in next few years and characterization of the same begin.

1.1.2. Structural features of TRP channels:

The diverse functions of different TRP channels are due to their different sequences. Yet there are specific features that are common in TRP channels. In general, TRP channels are represented by six transmembrane segments, intracellular N- and C-terminus in the cytoplasmic site. The "pore" is formed by sequence present between fifth and sixth

mechanical stimuli [8-11]. Such as in Yeast, TRP channel is involved in sensing hypertonicity [12, 13]. Similarly, in Nematode and in Worm, TRP channels are involved in sensory functions that are crucial for avoiding noxious chemicals [14]. Insects use these channels for vision [10]. Mice use TRP channels for pheromone sensing [15]. In Human, TRP channels are involved in different functions like taste, thermosensation, etc. [16]. TRP channels have not been identified in advanced plants so far, however, ion channels with completely different sequence that can sense temperature has been identified [17-19].

Among all TRP superfamily, Vanilloid family is recognized as a thermosensitive family which has six members (TRPV1-6). Among all six members, only four (TRPV1-4) are thermosensitive in nature and these channels can be activated at different temperature ranging from 27°C to 52°C [2]. Expression and functional significance of TRPV1 and TRPV4 are well established [20-22]. The other two members (TRPV5 and TRPV6) are not thermosensitive but highly Ca^{2+}-selective in nature [2]. In contrast, Transient Receptor Potential Vanilloid subtype 2 and 3 are relatively less explored ion channels that are present within this family. TRPV2 can be activated at 52°C and this channel is reported to be present in many cell types of neuronal and non-neuronal origin. Such as it is present in Brain, dorsal root ganglion, cardiac tissue, T cells, macrophage, HEK293T and F11 cell line, etc. [23-28]. TRPV3 is an innocuous/warmth receptor and it is activated at 30-33°C and reported to be present in hair, skin and relatively less expressed in brain and other neuronal tissues [29-31].

1.1. General overview about the TRP Channels

1.1.1. Brief history of TRP channel research:

After the discovery of Rhodopsin as photoreceptor later on it was found that Transient receptor potential (TRP) ion channel also plays role in photo transduction process. Later on, their other sensory functions such as thermosensation, mechanosensation, infrared sensation,

1. Introduction:

TRP channels were first discovered in the *Drosophila* eye, where *Drosophila* photoreceptor lacking TRP gene shows transient voltage in response to continuous light stimuli [1]. This is one of the major reason that these proteins were termed as transient receptor potential (TRP) channels [2]. These mutants were first reported by Brauch Minke [1, 3, 4]. Subsequently, several TRP channels have been identified and characterized. TRP ion channels have been classified based on their homology and sequence similarity. TRP channels are mainly present in the unicellular as well as in multicellular organism (except plants). There are no reports which shows their presence in higher plants. In all cases, these channels perform diverse functions. Broadly TRP channels have been classified into 6 subfamilies based on their homology and sequence similarity. These sub groups are namely: TRPV (Vanilloids), TRPC (Canonical), TRPM (Melastatin), TRPML (Mucolipins), TRPA (Ankyrin), and TRPP (Polycystins) [5]. The structural features of these ion channels are typically represented by intracellular N- and C-terminal domains, six transmembrane segments, and the functional pore which is formed by the 5^{th} and 6^{th} transmembrane regions [6]. The N-terminus contains Ankyrin repeat motifs that are mostly found in TRPA, TRPV and TRPC family members [5]. In many cases, the C-terminus contains a consensus stretch of amino acid sequence commonly known as 'TRP-box' and such sequence is present in many TRP members belong to TRPV, TRPC and TRPM family [5].

All TRP channels assemble to form a tetramer (homomer or heteromer) and such tetramer is the actual form of functional channels [7]. The tetrameric form of these channels can conduct influx of different cations. TRP channels are also present in lower eukaryotes such as in Choanoflagellates, Protists, Chlorophyte, Algae, Yeast, and Fungi where these channels perform different functions that are largely related to sensing different chemo, thermal and

Chapter 1

Introduction

Burmese Python	XP_007438955.1	818

Common Cuckoo	XP_009556781.1	787
Anna's Hummingbird	XP_008493324.1	788
Red-Legged Seriema	XP_009699809.1	787
Sunbittern	XP_010153216.1	786
Barn Owl	XP_009970996.1	787
Hoatzin	XP_009944089.1	787
Red-Throated Loon	XP_009816957.1	787
Dog	XP_005625015.1	791
Domestic Cat	XP_006940018.1	791
Water Buffalo	XP_006079771.1	798
Wild Yak	XP_005906744.1	791
American Buffalo	XP_010845784.1	791
Sheep	XP_004012614.1	790
Sperm Whale	XP_007125526.1	791
Pig	XP_005669174.1	791
European Shrew	XP_004605021.1	791
Bat	XP_006761558.1	791
Black Flying Fox	XP_006922255.1	791
Golden Snub-Nosed Monkey	XP_010380522.1	791
Small Madagascar Hedgehog	XP_004716220.1	791
Yellow-Throated Sandgrouse	XP_010081996.1	791
Killer Whale	XP_004267084.1	787
Horse	XP_005597720.1	791
Green Sea Turtle	XP_007057812.1	800
American Alligator	XP_006275259.1	773
Chinese Alligator	XP_006033191.1	784
Western Clawed Frog	NP_001243218.1	773
Elephant Shark	XP_007894728.1	751
Western Painted Turtle	XP_008167187.1	828

Table 7. List of TRPV3 sequences used in this study:

Species	Accession No.	Length
Human	ACA81614.1	791
Mouse	NP_659567.2	791
Pygmy Chimpanzee	XP_008960843.1	791
Rat	NP_001020928.2	791
Thirteen-Lined Ground Squirrel	XP_005337351.1	792
Chicken	XP_004946732.1	787
Blind Mole Rat	XP_008853834.1	791
Bactrian Camel	XP_010948530.1	791
Prairie Vole	XP_005349656.1	797
Prairie Deer Mouse	XP_006992285.1	791
Golden Hamster	XP_005067481.1	791
Lesser Egyptian Jerboa	XP_004672442.1	791
Degu	XP_004638337.1	791
Naked Mole-Rat	XP_004857266.1	791
Aardvark	XP_007935665.1	791
Cape Golden Mole	XP_006863324.1	792
Cape Elephant Shrew	XP_006899806.1	791
Platypus	XP_001508712.2	792
Northern Fulmar	XP_009577964.1	787
Adelie Penguin	XP_009326905.1	787
Emperor Penguin	XP_009276461.1	787
Great Cormorant	XP_009501827.1	787
Little Egret	XP_009632246.1	787
Dalmatian Pelican	XP_009477903.1	787
Crested Ibis	XP_009462803.1	787
Golden-Collared Manakin	XP_008928724.1	787
Downy Woodpecker	XP_009901562.1	787

Table 6. Description of different domains, motifs and regions of TRPV3 considered in this study:

Domains/Motifs	Amino acid positions	Species	Reference
Transmembrane1	436-463	Human	[31]
Loop1	464-482	Human	[31]
Transmembrane2	483-511	Human	[31]
Loop2	512-519	Human	[31]
Transmembrane3	520-544	Human	[31]
Loop3	545-546	Human	[31]
Transmembrane4	547-570	Human	[31]
Loop4	571-586	Human	[31]
Transmembrane5	587-609	Human	[31]
Loop5	610-620	Human	[31]
Pore loop	621-642	Human	[31]
Loop6	643-649	Human	[31]
Transmembrane6	650-677	Human	[31]
C Terminal	678-791	Human	[31]
N Terminal	1-213	Human	[31]

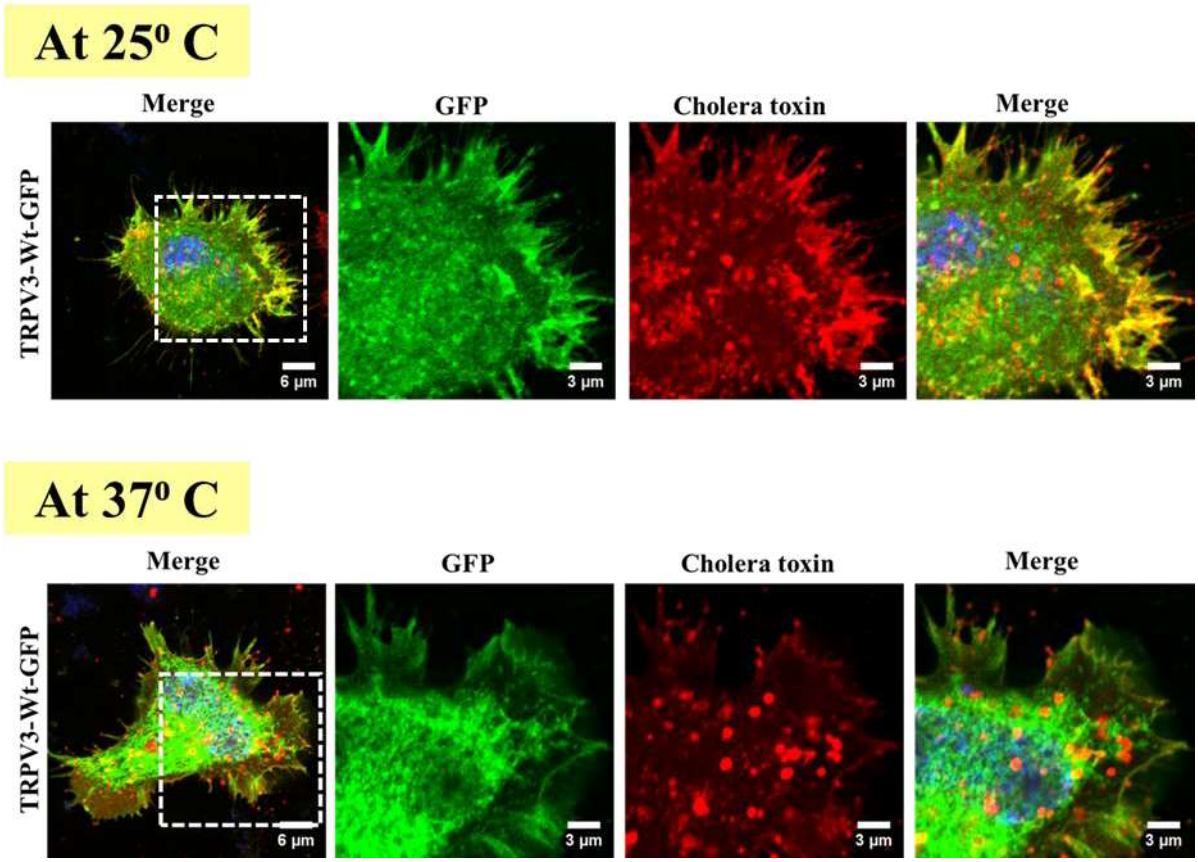

Figure 84b. TRPV3-Wt colocalizes with cholera toxin. F11 cells transfected with TRPV3-Wt and after fixation followed by staining with Cholera toxin 594. Representative images indicate that cholera toxin shows more colocalization at 25ºC with compare to 37ºC. (Right side image shows the zoom up).

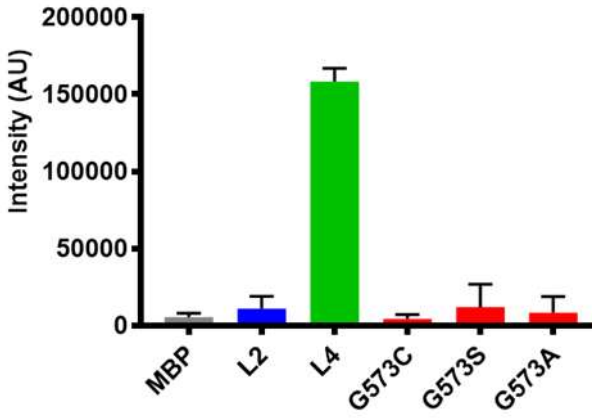

Figure 84a. OS mutants have decreased binding affinity for cholesterol. Dot blot experiment with different fragments of MBP-TRPV3-Wt and OS mutants reveals that Loop4-G573C, G573S, and G573A doesn't interacts with cholesterol while Wt-Loop4 interacts with cholesterol. MBP has taken as negative control (n=3).

2.4.14. TRPV3-Wt shows temperature dependent colocalization with Cholera toxin: To further characterise the TRPV3 and cholesterol interaction, we did a temperature dependent experiment. Since 37ºC is near activation temperature for TRPV3 and if cholesterol have any role in the sensitization or desensitization of TRPV3 we should see difference in the colocalization. After 24 hrs of transfection with TRPV3-Wt culture plates were placed in an incubator set at different temperature 25ºC and 37ºC for two hrs. Followed by fixation with 4% PFA. We have stained the cells with Cholera toxin and did a confocal imaging. Result indicates that TRPV3-Wt shows more colocalization with Cholera toxin at 25ºC with compare at 37ºC. This suggest that more colocalization at 25ºC could be because tight cholesterol interaction helps in the channel closing. Whereas 37ºC is near activation temperature and channel opening probability is more that's why we see less colocalization at this temperature **(Fig. 84b)**.

snorkeling residues (Arg and Tyr) present at the LWI of TRPV3 from different phyla are shown. These AA (mean value) vary differently from fishes to mammals and there is a clear indication that these snorkeling residues are selected under very specific and stringent conditions, such as level of membrane cholesterol. Total content of snorkeling AA in the LWI of TRPV3 is also less in cold-blooded than in warm-blooded animals, but is statistically non-significant. **b.** The percent Arg content (mean value) in the LWI does vary between cold and warm animals, and also across the phylum. This difference remains statistically significant (***). In cold-blooded animals, the percent Tyr content decreased steadily during the Piscean to reptilian evolution in each phylum, indicating that in case of low body temperature, the level of membrane cholesterol has influence on the selection of Tyr residues in the LWI. **c.** The total percentage (mean value) of Tyr at the LWI of TRPV3 in all cold-blooded animals, decreased slowly during the transition of cold to warm animals and then remain same within all warm animals (with a lower value). **d.** Total percentage of Ser in the warm blooded and cold-blooded animals does not show any significant changes. However, mammals, birds, reptiles, and amphibian show steady increase in the percentage of Ser. This suggests that core-body temperature has a strong influence on the selection of Arg residues. Total Arg content in LWI of TRPV3 is more in cold-blooded than in warm-blooded animals, but this difference is non-significant. (* = $p<0.05$, **=$p<0.01$).

2.4.13. Biochemical dot blot experiment reveals that TM-loop4-TM-OS mutants shows reduced binding to cholesterol with compare to Wt:

In order to further confirm the *in silico* experiments and to find weather there is any difference in the binding of cholesterol with wt and OS mutant. We have cloned the TRPV3-Wt-TM-Loop2-TM, TRPV3-Wt-TM-Loop4-TM, TRPV3-G573C-TM-Loop4-TM, TRPV3-G573S-TM-Loop4-TM, TRPV3-G573A-TM-Loop4-TM in pMalC5x an MBP expression vector. After purification of different protein fragments, we have performed a spotting experiments with cholesterol. Results shows that loop4 of TRPV3-Wt shows strong interaction with cholesterol, while OS mutants do not show reduced affinity with cholesterol **(Fig. 84a)**.

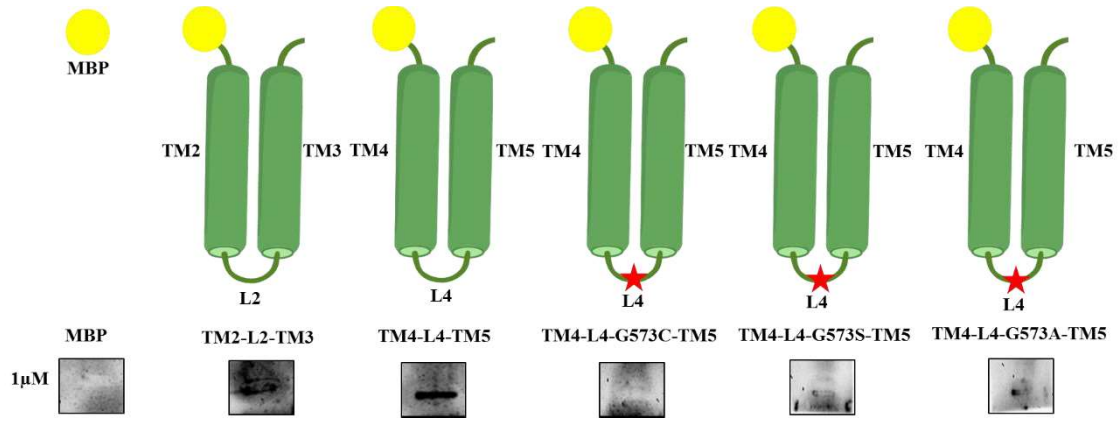

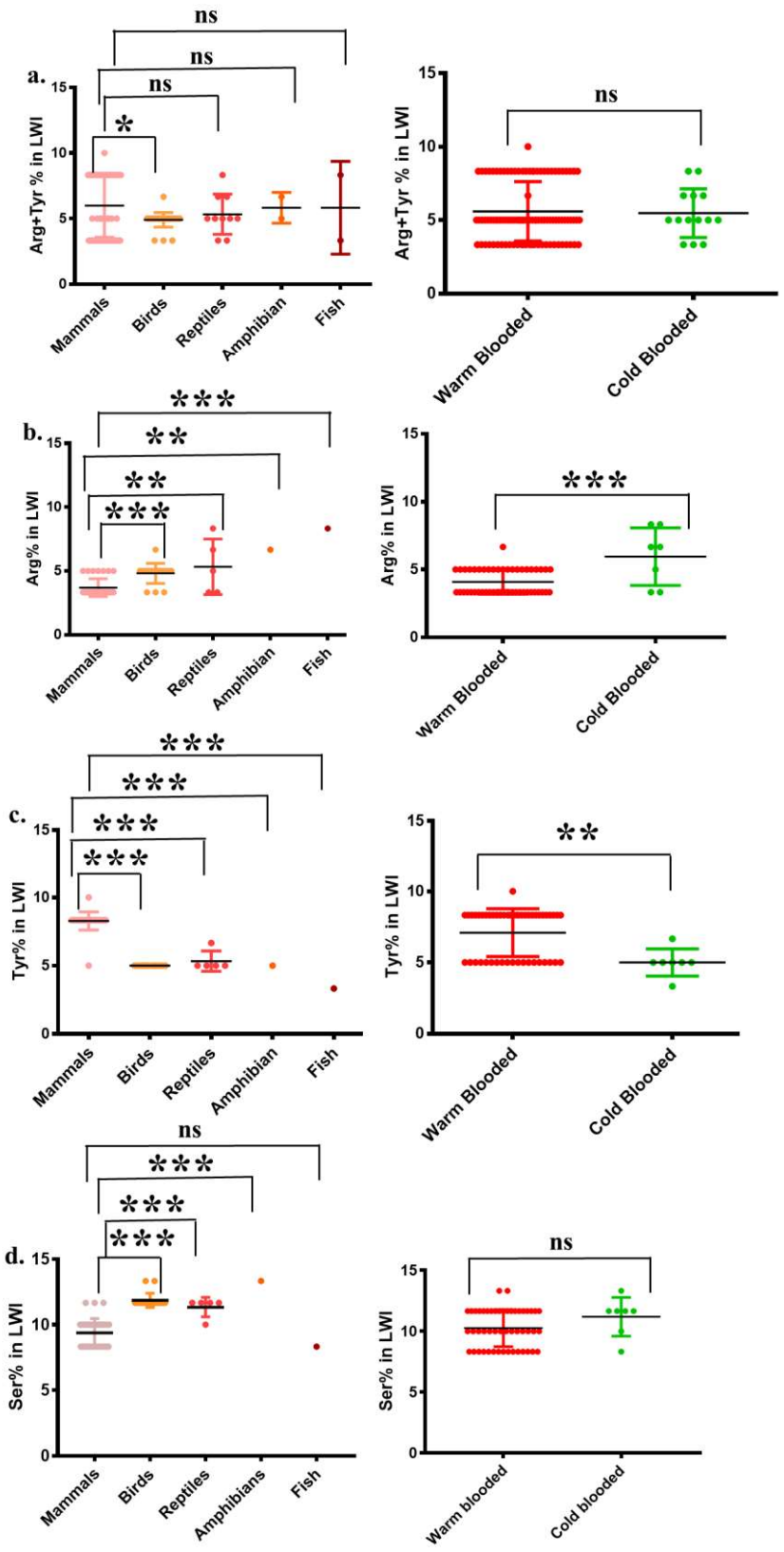

Figure 83. Frequency of amino acid present in the lipid water interface of TRPV3. Total 60 AA representing all 12 LWI regions of TRPV3 sequences from 56 species were considered and percentage of only Arg, Tyr and Ser was analysed in individual phyla or in cold-blooded and warm-blooded animals. **a.** The total percent of

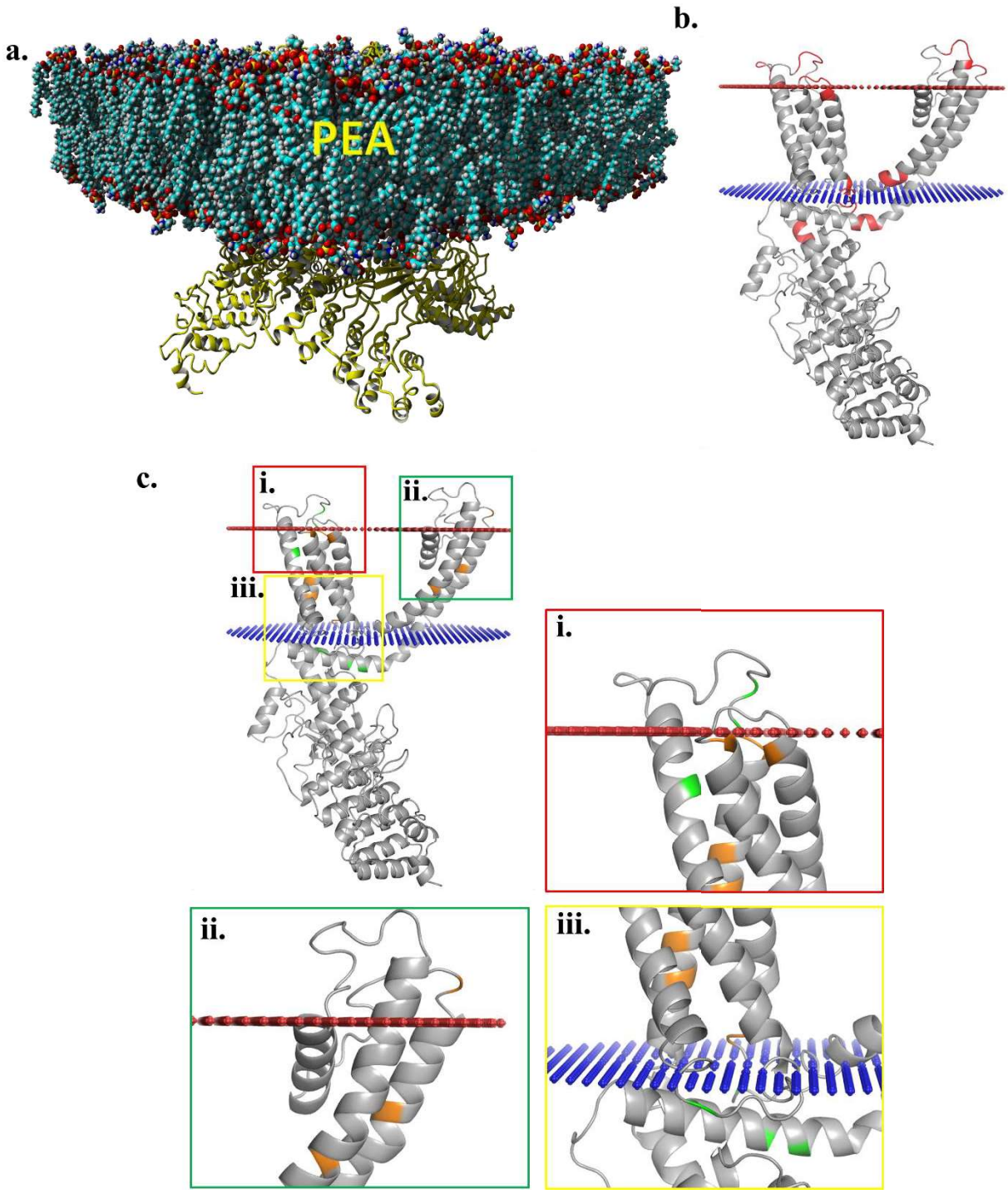

Figure 82. Unlike TRPV1, TRPV3 does not have enriched amount of Arg or Tyr in its LWI region. Arg and Tyr residues are not enriched in the lipid-water interface of hTRPV3. **a.** Side view of a 3D structure of Human TRPV3 tetramer embedded in a lipid bilayer made of PEA respectively. The hTRPV3 closed conformation was used and the entire system is stabilized in the lipid bilayer after a short equilibration of 250 ps simulation. The interface residues are marked in red colour. **b.** Residues marking the lipid-water interface are coloured red. **c.** Arginine (Green) and Tyrosine (Orange) residues are present in the core of the lipid bilayer regions and the magnified images of specific lipid-water interface regions are shown in right side (**i, ii, iii**).

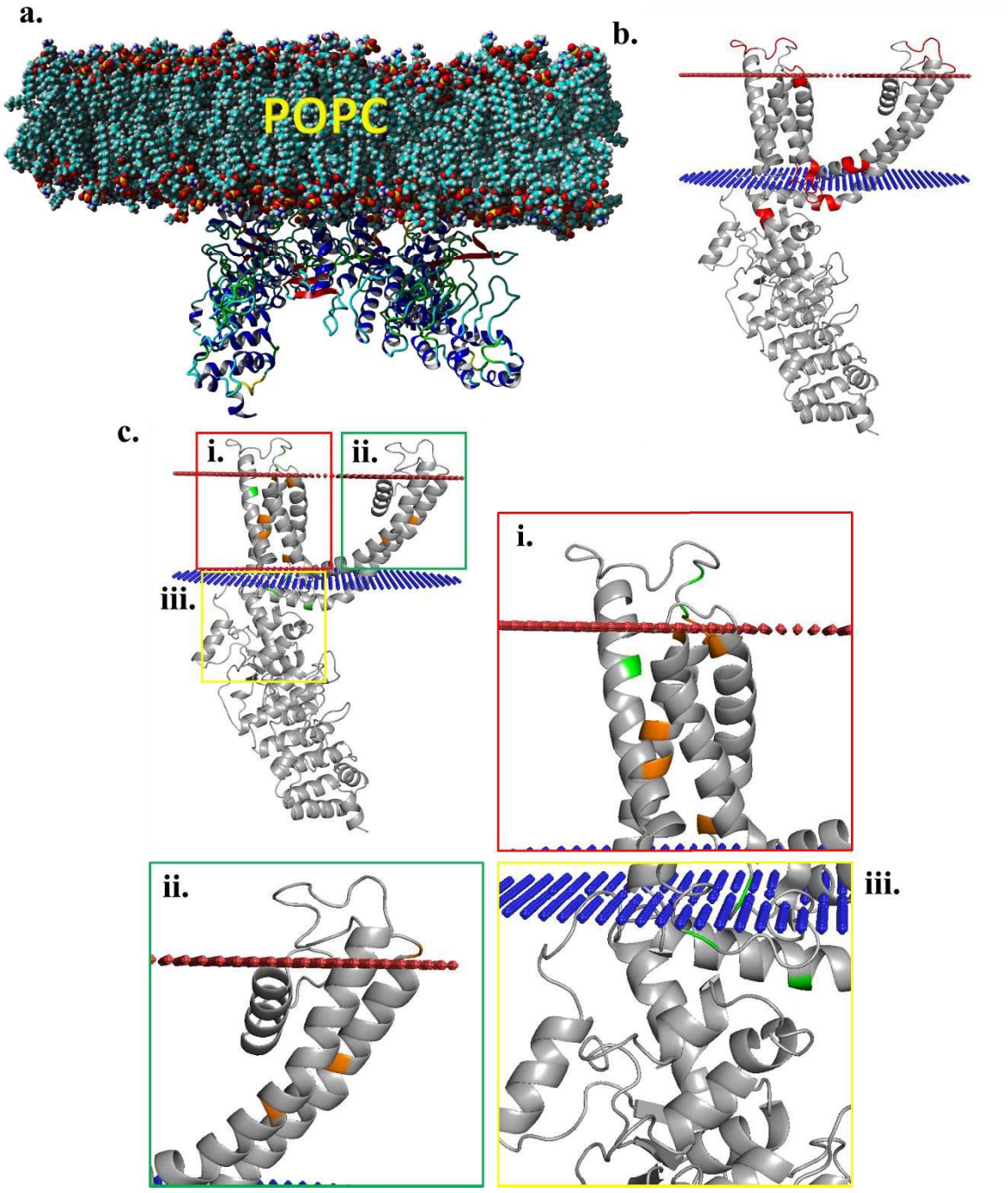

Figure 81. Unlike TRPV1, TRPV3 does not have enriched amount of Arg or Tyr in its LWI region. Arg and Tyr residues are not enriched in the lipid-water interface of hTRPV3. **a.** Side view of a 3D structure of Human TRPV3 tetramer embedded in a lipid bilayer made of POPC. The hTRPV3 closed conformation was used and the entire system is stabilized in the lipid bilayer after a short equilibration of 250 ps simulation. The interface residues are marked in red colour. **b.** Residues marking the lipid-water interface are coloured red. c. All Arginine (Green) and Tyrosine (Orange) residues are highlighted. Most of Arg and Tyr residues are present at the core of the lipid bilayer. The magnified images of specific lipid-water interface regions are shown in right side as (**i, ii, iii**).

Table 5. Amino acid frequency at lipid water interface.

Amino Acid	Mammal (Human)	Bird (Chicken)	Reptile (Python)	Amphibian (Western Clawed Frog)	Fish (Shark)
(Gly)	1.66	3.33	6.66	6.66	1.66
(Pro)	1.66	0	5	1.66	1.66
(Ala)	8.33	5	5	1.66	10
(Val)	1.66	1.66	1.66	8.33	6.66
(Leu)	10	10	10	10	11.66
(Ile)	5	5	6.66	1.66	3.33
(Met)	1.66	1.66	1.66	1.66	0
(Cys)	1.66	1.66	1.66	1.66	1.66
(Phe)	1.66	1.66	3.33	5	1.66
(Tyr)	8.33	5	5	6.66	3.33
(Trp)	0	0	0	0	0
(His)	5	1.66	5	0	3.33
(Lys)	13.33	8.33	10	6.66	6.66
(Arg)	3.33	5	3.33	3.33	8.33
(Gln)	5	6.66	3.33	5	5
(Asn)	1.66	6.66	1.66	5	1.66
(Glu)	13.33	11.66	5	10	8.33
(Asp)	5	5	8.33	13.33	6.66
(Ser)	8.33	13.33	10	8.33	8.33
(Thr)	3.33	5	6.66	1.66	8.33

at LWI of TRPV3 **(Tab. 5)**. In some cases, Tyr and Arg gets replaced by positively charged amino acid Histidine. Presence of Histidine residue (which needs specific pH for protonation) in LWI provides useful information about the microenvironment needed for TRPV3 function. Analysis was performed to understand the frequency distribution of all 20 amino acids in the LWI region across the vertebrate species for TRPV3. Analysis shows that distribution of Ser which acts as proton donor and acceptor for H- bond formation was preferred during the course of evolution in vertebrate **(Fig. 83d)**. Considering full-length TRPV3 (all vertebrates), % of Arg was significantly high in cold blooded animals as compare to warm blooded animals **(Fig. 83b)**. While other amino acid Tyr shows opposite pattern, i.e. Tyr is more in the warm-blooded animals in compare to cold blooded **(Fig. 83c)**. However, Ser does not show significant difference in warm and cold-blooded animals, suggesting that certain percentage of Ser is critical for TRPV3 function and selection / retention of Ser is irrespective of changes in body temperature **(Fig. 83d)**.

mutants, we calculated the average binding energies from global docking experiments and from multiple hits. Comparison reveals that there is no significant difference in the binding energies in TRPV3-Wt (open, close) as well as in case of OS mutants **(Fig. 80a-b)**. This suggests three aspects: First, TM-loop4-TM of TRPV3 is highly important for TRPV3 interaction with cholesterol (Earlier similar region, i.e. TM-loop4-TM have been implicated in the interaction of cholesterol with TRPV4). Second, cholesterol interaction is critical for TRPV3 functions as both wild type and OS-mutants retain interaction with reasonably high binding energies. Third, the minute differences in binding energies and modes may be extremely relevant for TRPV3 functions. In order words, subtle or minute differences in cholesterol interaction (both in terms of binding energies and modes) may be sufficient for TRPV3 channel opening. However, further experiments are needed for that.

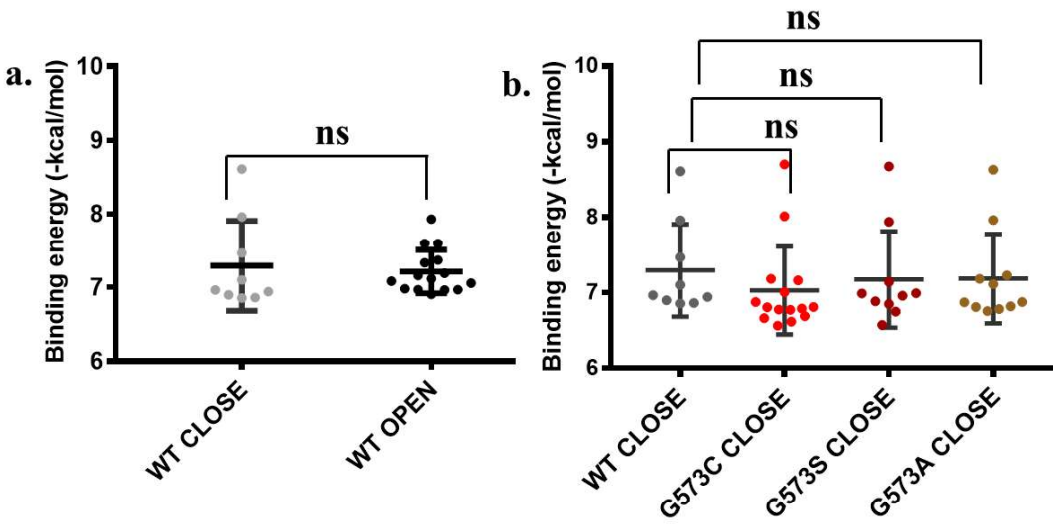

Figure 80. Cholesterol and TRPV3 interaction energies do not vary much in different conformations or even in different mutants. Graph represents various hits from global docking in TRPV3 (Close and Open conformation) and with OS mutants.

2.4.12. Leu, Lys, Glu and Ser residues are preferred in the LWI of TRPV3:

Further single amino acid conservation of 5-amino acid and their distribution in lipid water interface reveals that charged amino acid such as Leu and Glu show comparatively more selection and conservation in LWI of TRPV3. Also, Leu and Ser was found to be more frequent

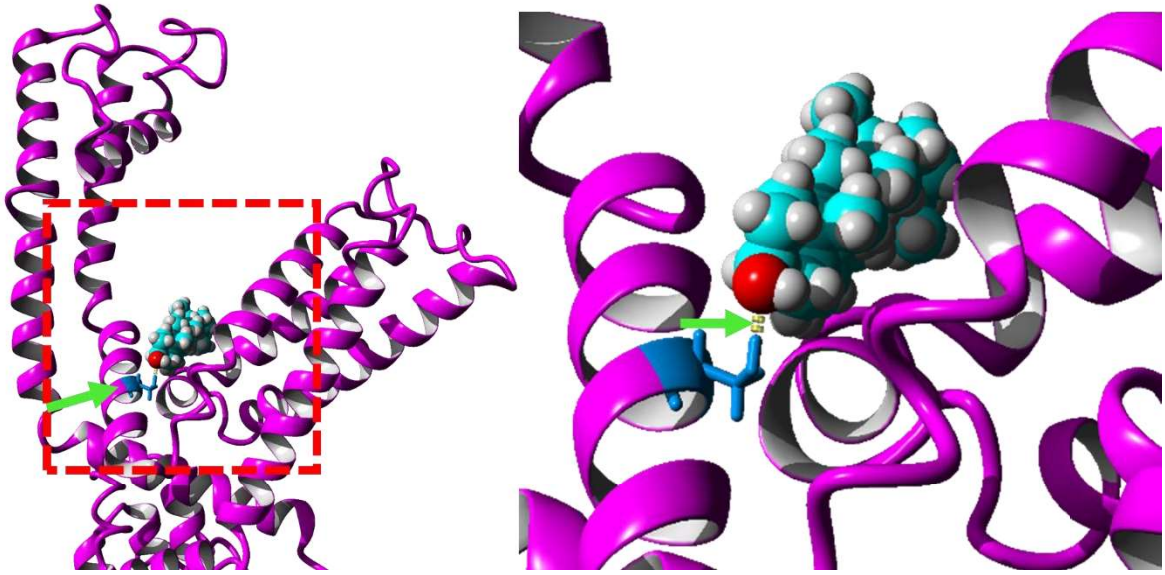

Figure 78. OS mutant G573S retain interaction with cholesterol in its closed state. The cholesterol binds with TRPV3-G573C with an energy value of -7.94 kcal/mol through the Ser-576 present in Loop4 region. Ser-576 forms an H-bond with the OH- group of Cholesterol at this position. This interaction is similar to what has been observed in case of Wild type TRPV3. Right side image shows the zoomed image.

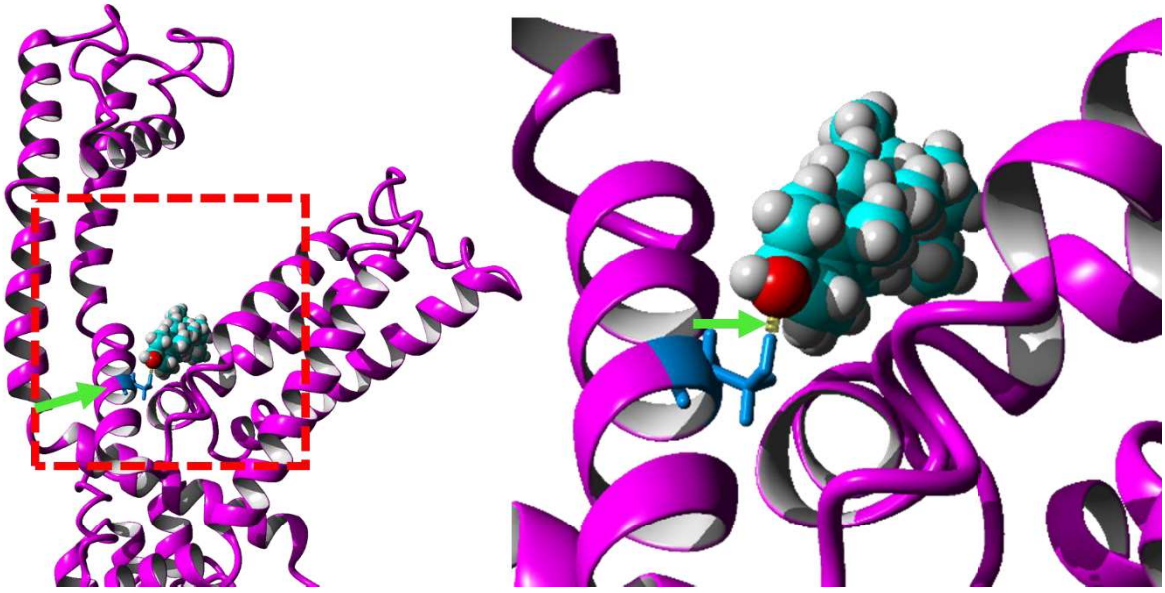

Figure 79. OS mutant G573A retain interaction with cholesterol in its closed state. The cholesterol binds with TRPV3-G573C with an energy value of -7.96 kcal/mol through the Ser-576 present in Loop4 region. Ser-576 forms an H-bond with the OH- group of Cholesterol at this position. This interaction is similar to what has been observed in case of Wild type TRPV3. Right side image shows the zoomed image.

2.4.11. Cholesterol-binding energy from global docking reveals no significant difference in open, close and OS mutants:

In order to confirm the differences or no differences in terms binding energies, particularly in case of open and closed conformation as well as between the wild type and

respectively, that are comparable to the binding energy of TRPV3-Wt (-8.02 kcal/mol) **(Fig. 77-79)**. This result suggest that cholesterol may play important role in the regulation of TRPV3 at different level such as (trafficking, membrane localization and constitutive opening of OS mutants). However further experiments needed to established all cholesterol mediated regulation.

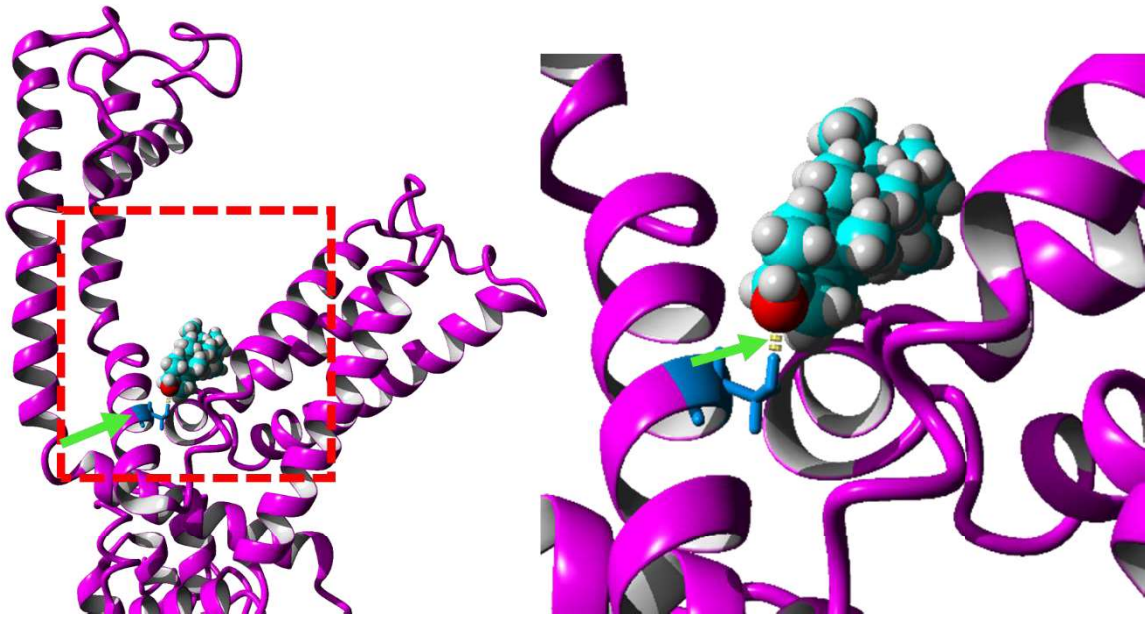

Figure 77. OS mutant G573C retain interaction with cholesterol in its closed state. The cholesterol binds with TRPV3-G573C with an energy value of -8.01 kCal/mol through the Ser-576 present in Loop4 region. Ser-576 forms a H-bond with the OH- group of Cholesterol at this position. This interaction is similar to what has been observed in case of Wild type TRPV3. Right side image shows the zoomed image.

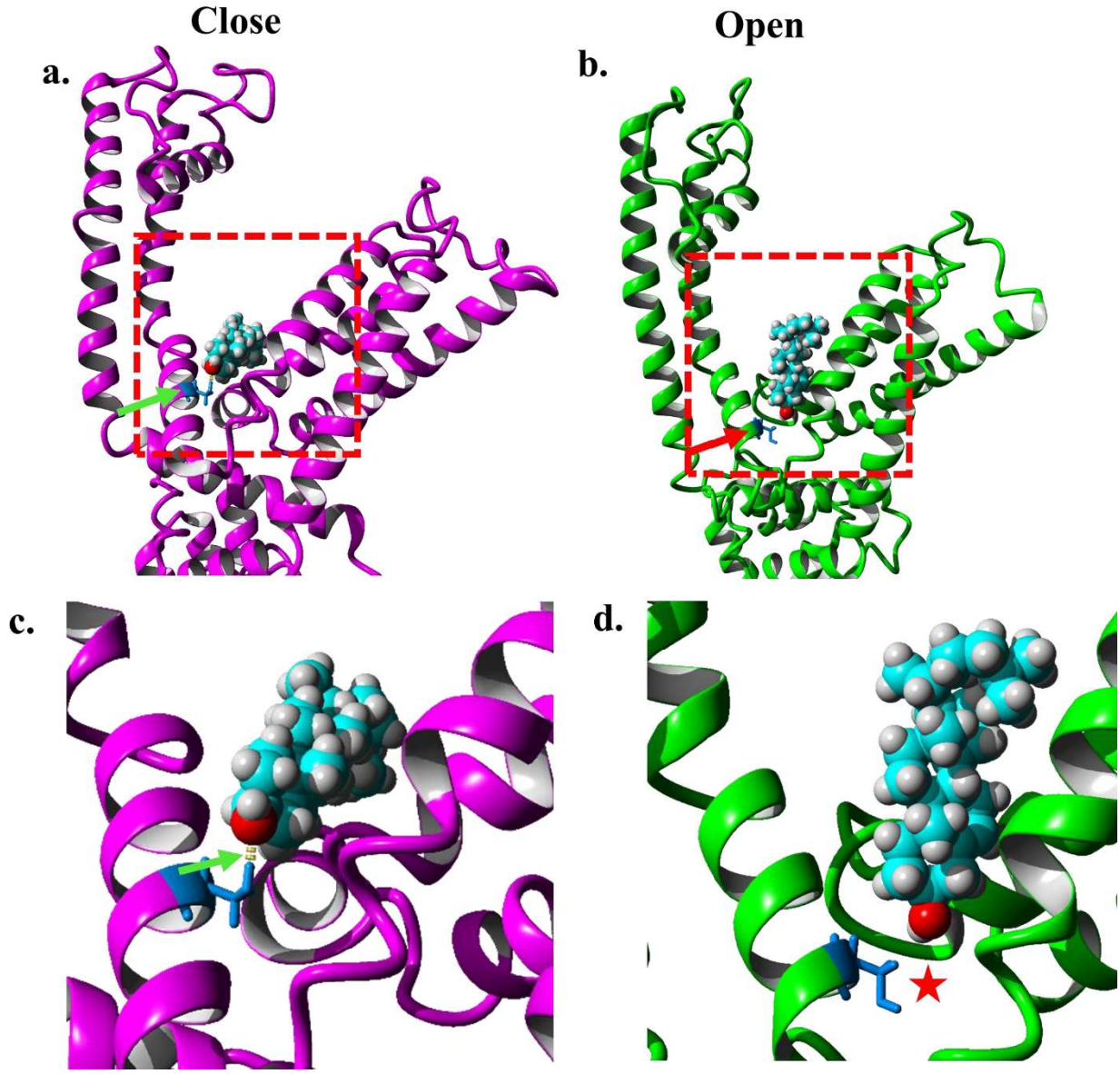

Figure 76. Cholesterol binds to TRPV3-Wt-Loop4 in close conformation with high binding energy. **a.** Image shows docking of TRPV3-Wt in close conformation with H-bond at Ser-576 position. **b.** In open conformation this binding energy is reduced (from -8.61 to -6.90 kcal/mol.). **b & d.** Enlarged images show interaction of cholesterol with TRPV3 in closed and open confirmation respectively. (Green represents open and Magenta represents close conformation).

2.4.10. TRPV3-OS mutants shows reduced binding to cholesterol with compare to Wt:

In order to further characterize if there is any difference in binding energy of cholesterol interaction with TRPV3-Wt or TRPV3-OS mutants, we have performed global docking of cholesterol on the Wt and TRPV3 mutants. Results show that OS mutants (G573C, G573S, and G573A) interacts with binding energies (-8.01 kCal/mol, -7.94 kCal/mol, -7.96 kCal/mol)

Figure 74. hTRPV3 has conserved cholesterol-binding sequences at the lipid-water interface region. Sequence alignment of the different segments of hTRPV3 (aa 319-326 and 376-385) and (aa 357-363 and 563-567) containing conserved CARC, CRAC motif of vertebrates is shown. Also Critical amino acids defining this motif L/V-$X_{(1-5)}$-Y-$X_{(1-5)}$-R/K are indicated by asterisk (*).

2.4.9. TRPV3 interacts with cholesterol in close conformation with higher binding energy in some conformation:

In order to further validate the TRPV3 and cholesterol relationship we have performed a global docking with cholesterol in both open and close conformation. Docking experiments reveals that in close conformation cholesterol interacts with higher binding energies (-8.61 kcal/mol) and forms H- bond with Ser-576 position **(Fig. 75a-b)**. While in open confirmation we could not detect such H- bond and the binding energy is low (-6.90 kcal/mol) **(Fig. 75b)**. This suggest that TRPV3 might shows strong interaction with Cholesterol in close conformation through loop 4 and such interaction is week in open conformation, at-least when these modes or conformations are considered.

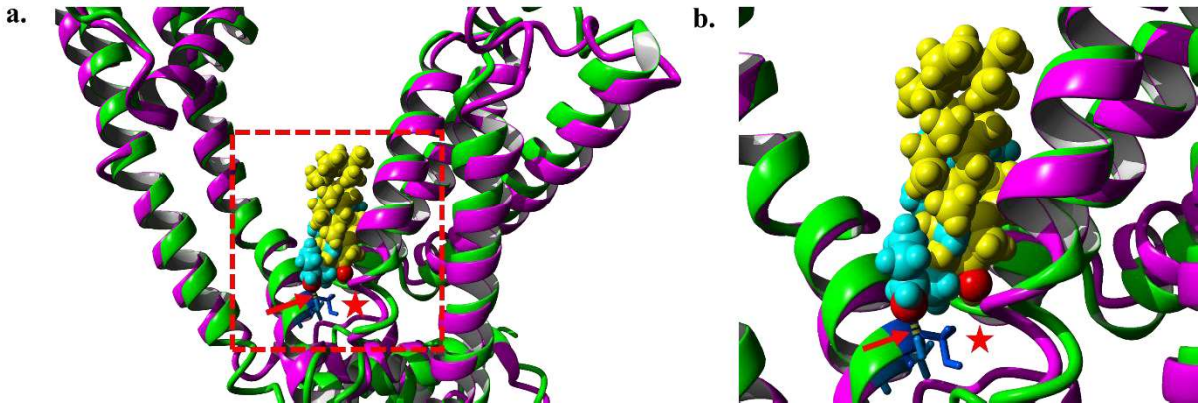

Figure 75. Overlap of TRPV3 with cholesterol in closed and open confirmation. a. Image shows docking of TRPV3-Wt in close and open conformation with cholesterol. H-bond found only in close confirmation at Ser-576 position. b. Zoom up image highlighted H-bond with arrow head and no H-bond with asterisk. (Green represents open and Magenta represents close conformation).

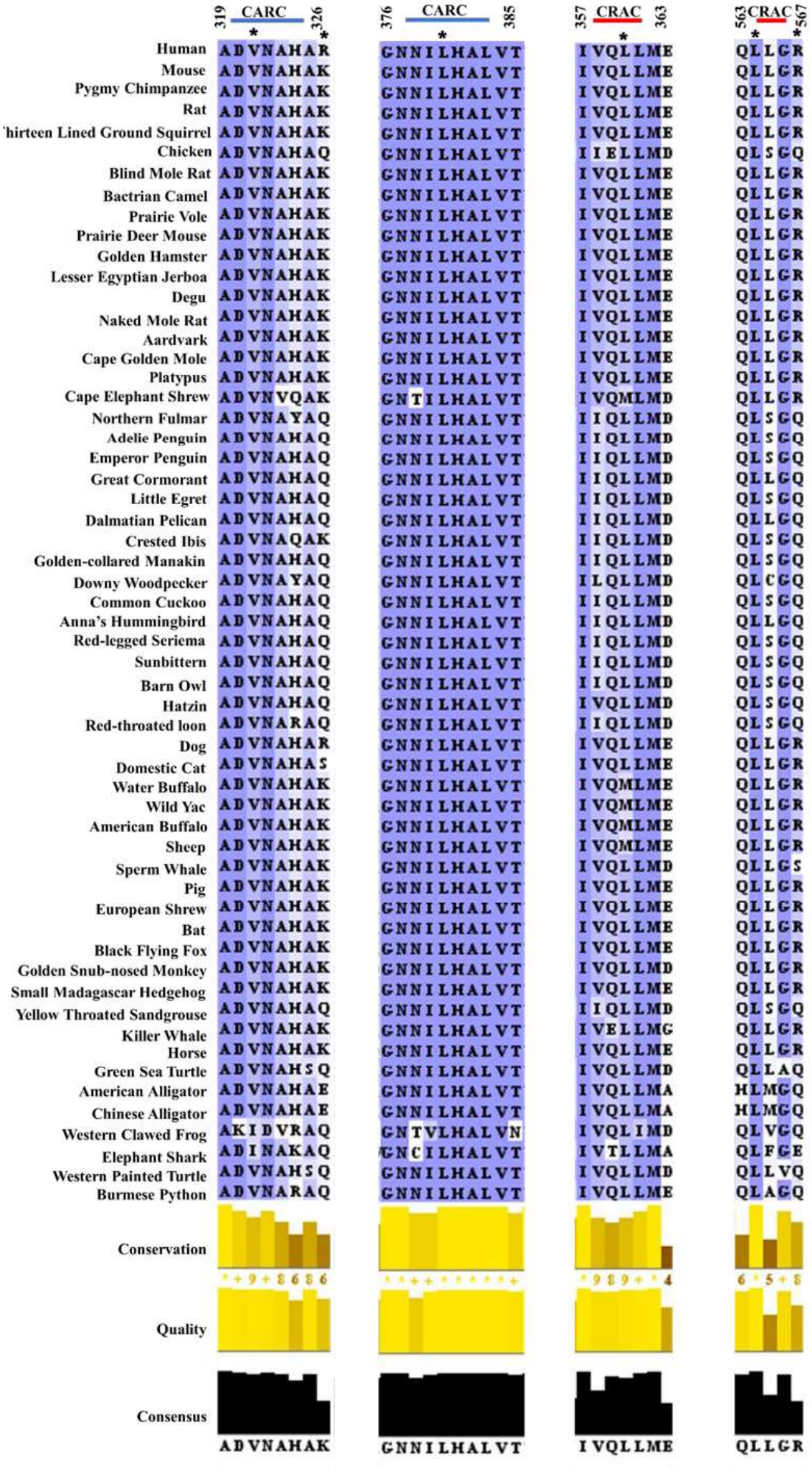
319 CARC 326
376 CARC 385
357 CRAC 363
563 CRAC 567
Human ADVNAHAR GNNILHALVT IVQLLME QLLGR
Mouse ADVNAHAK GNNILHALVT IVQLLME QLLGR
Pygmy Chimpanzee ADVNAHAK GNNILHALVT IVQLLME QLLGR
Rat ADVNAHAK GNNILHALVT IVQLLME QLLGR
hirteen Lined Ground Squirrel ADVNAHAK GNNILHALVT IVQLLME QLLGR
Chicken ADVNAHAQ GNNILHALVT IIELLMD QLSGQ
Blind Mole Rat ADVNAHAK GNNILHALVT IVQLLME QLLGR
Bactrian Camel ADVNAHAK GNNILHALVT IVQLLME QLLGR
Prairie Vole ADVNAHAK GNNILHALVT IVQLLME QLLGR
Prairie Deer Mouse ADVNAHAK GNNILHALVT IVQLLME QLLGR
Golden Hamster ADVNAHAK GNNILHALVT IVQLLME QLLGR
Lesser Egyptian Jerboa ADVNAHAK GNNILHALVT IVQLLME QLLGR
Degu ADVNAHAK GNNILHALVT IVQLLME QLLGR
Naked Mole Rat ADVNAHAK GNNILHALVT IVQLLME QLLGR
Aardvark ADVNAHAK GNNILHALVT IVQLLME QLLGR
Cape Golden Mole ADVNAHAK GNNILHALVT IVQLLME QLLGR
Platypus ADVNAHAK GNNILHALVT IVQLLME QLLGR
Cape Elephant Shrew ADVNVQAK GNTILHALVT IVQMLMD QLLGR
Northern Fulmar ADVNAYAQ GNNILHALVT IIQLLMD QLSGQ
Adelie Penguin ADVNAHAQ GNNILHALVT IIQLLMD QLSGQ
Emperor Penguin ADVNAHAQ GNNILHALVT IIQLLMD QLSGQ
Great Cormorant ADVNAHAQ GNNILHALVT IIQLLMD QLLGQ
Little Egret ADVNAHAQ GNNILHALVT IIQLLMD QLSGQ
Dalmatian Pelican ADVNAHAQ GNNILHALVT IIQLLMD QLLGQ
Crested Ibis ADVNAQAK GNNILHALVT IIQLLMD QLSGQ
Golden-collared Manakin ADVNAHAQ GNNILHALVT IIQLLMD QLSGQ
Downy Woodpecker ADVNAYAQ GNNILHALVT ILQLLMD QLCGQ
Common Cuckoo ADVNAHAQ GNNILHALVT IIQLLMD QLSGQ
Anna's Hummingbird ADVNAHAQ GNNILHALVT IIQLLMD QLLGQ
Red-legged Seriema ADVNAHAQ GNNILHALVT IIQLLMD QLSGQ
Sunbittern ADVNAHAQ GNNILHALVT IIQLLMD QLSGQ
Barn Owl ADVNAHAQ GNNILHALVT IIQLLMD QLSGQ
Hatzin ADVNAHAQ GNNILHALVT IVQLLMD QLSGQ
Red-throated loon ADVNARAQ GNNILHALVT IIQLLMD QLSGQ
Dog ADVNAHAR GNNILHALVT IVQLLME QLLGR
Domestic Cat ADVNAHAS GNNILHALVT IVQLLME QLLGR
Water Buffalo ADVNAHAK GNNILHALVT IVQMLME QLLGR
Wild Yac ADVNAHAK GNNILHALVT IVQMLME QLLGR
American Buffalo ADVNAHAK GNNILHALVT IVQMLME QLLGR
Sheep ADVNAHAK GNNILHALVT IVQMLME QLLGR
Sperm Whale ADVNAHAK GNNILHALVT IVQLLMD QLLGS
Pig ADVNAHAK GNNILHALVT IVQLLME QLLGR
European Shrew ADVNAHAK GNNILHALVT IVQLLME QLLGR
Bat ADVNAHAK GNNILHALVT IVQLLME QLLGR
Black Flying Fox ADVNAHAK GNNILHALVT IVQLLME QLLGR
Golden Snub-nosed Monkey ADVNAHAK GNNILHALVT IVQLLMD QLLGR
Small Madagascar Hedgehog ADVNAHAK GNNILHALVT IVQLLME QLLGR
Yellow Throated Sandgrouse ADVNAHAQ GNNILHALVT IIQLLMD QLSGQ
Killer Whale ADVNAHAK GNNILHALVT IVELLMG QLLGR
Horse ADVNAHAK GNNILHALVT IVQLLME QLLGR
Green Sea Turtle ADVNAHSQ GNNILHALVT IVQLLMD QLLAQ
American Alligator ADVNAHAE GNNILHALVT IVQLLMA HLMGQ
Chinese Alligator ADVNAHAE GNNILHALVT IVQLLMA HLMGQ
Western Clawed Frog AKIDVRAQ GNTVLHALVN IVQLIMD QLVGQ
Elephant Shark ADINAKAQ GNCILHALVT IVTLLMA QLFGE
Western Painted Turtle ADVNAHSQ GNNILHALVT IVQLLMD QLLVQ
Burmese Python ADVNARAQ GNNILHALVT IVQLLME QLAGQ
Conservation
Quality
Consensus
ADVNAHAK GNNILHALVT IVQLLME QLLGR

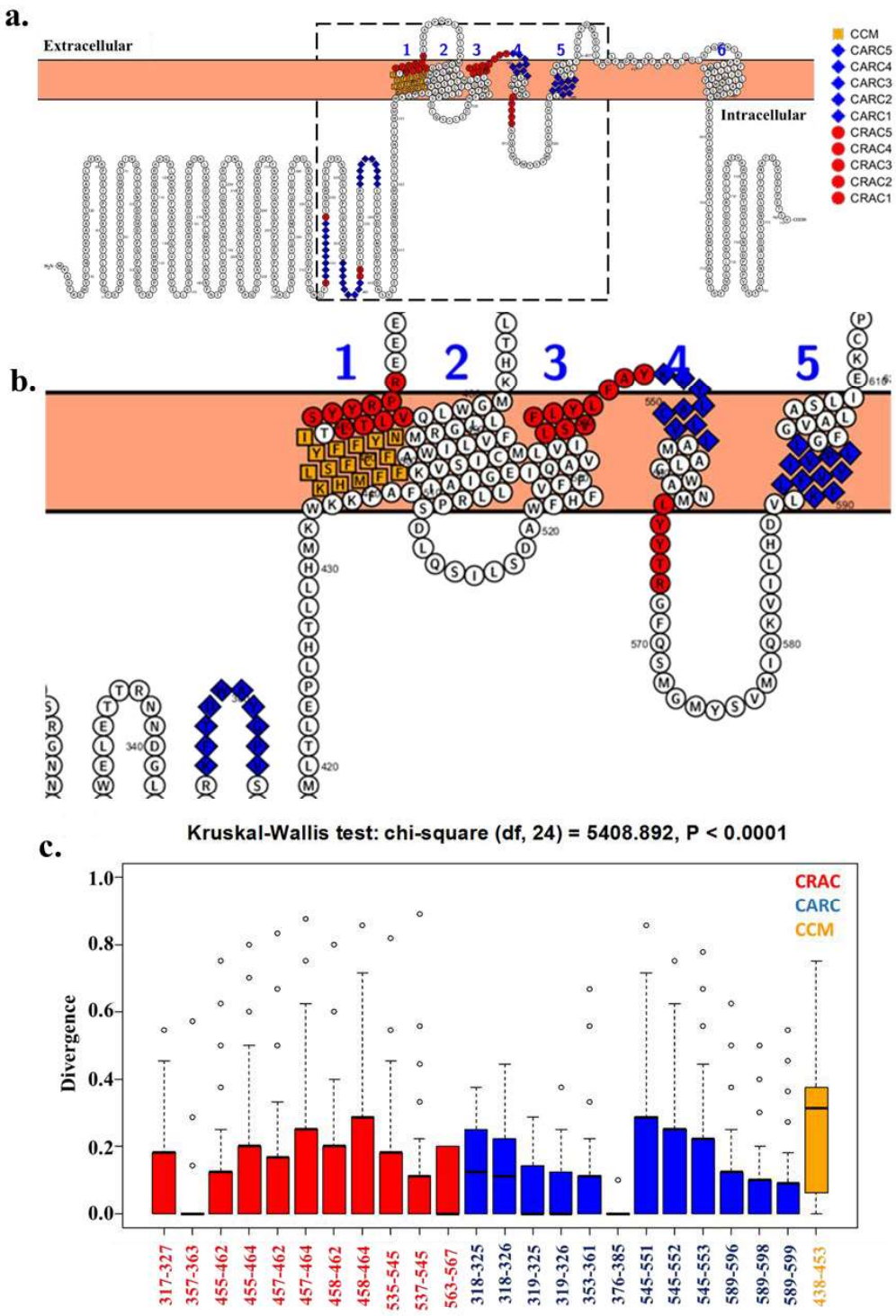

Figure 73. TRPV3 has conserved cholesterol-binding sequences at the lipid-water interface region. a. Eleven possible cholesterol binding sites, namely CRAC (Red) or CARC (orange) motifs are identified in hTRPV3 and one Cholesterol consensus motif (CCM) is present. **b.** Enlarged image representing CRAC (Red) or CARC (Orange) motifs. c. Box plot depicting the conservation of individual CRAC, CARC and CCM motifs are shown. **c.** The amino acid numbers are indicated below and the CRAC motif (aa 357-363 and 563-567) and CARC motif (aa 319-325, 310-326 and 376-385) is the most conserved among all these cholesterol-binding motifs.

2.4.8. Identification of possible cholesterol-recognition motifs within TRPV3:

After identification of different snorkeling amino acids in the lipid water interface region of TRPV3, we have further looked if there is any presence of cholesterol recognition motif sequences, particularly in the highly conserved regions. This is logical as cholesterol serves as one of the main component of membrane and provides unique microenvironment to the transmembrane proteins present there. Regulation of TRPV3 through cholesterol is reported but the actual binding site and mechanism is not reported [159]. In this context, we have analysed Cholesterol recognition amino acid consensus (CRAC) motifs (L/V-X¬(1-5)-Y-X(1-5)-R/K) and observed that such motifs are conserved in TRPV3 in all vertebrates **(Fig. 73)**. We have identified 11 CRAC motifs and 12 CARC (Inverted CRAC) motifs in hTRPV3 out of that three CARC (319-325, 310-326 and 376-385) and two CRAC (357-363 and 563-567) are highly conserved throughout the vertebrate evolution **(Fig. 73c)**. We have also found a CCM motif [RK]-X(7,10)-[WY]-X(4)-[IVL] (438-453) in hTRPV3. However, box plot analysis reveals that CCM motif is comparatively less conserve in TRPV3 **(Fig. 73c)**.

After finding the presence of cholesterol binding motif in TRPV3 we have looked at the conservation of pattern in all vertebrate species. For that we have align the sequence in mega software. Different conserved CRAC (aa 357-363 and 563-567) and CARC motif (aa 319-325, 310-326 and 376-385) have been shown in the **(Fig. 74)**.

compare to the residue present in the outside (represented as all outside). This analysis reveals that amino acids present on inner side of lipid bilayer are functionally more relevant on the structure -function relationship of TRPV3 **(Fig. 71-72a)**. Our finding suggests this differential conservation of inner and outer (LWI) residue could be due to the fact that differential composition of membrane could play important role in determining the LWI residue. Also, residue which are present inside could play important role in the different intracellular signaling such as protein phosphorylation. Result also indicates that residue present towards inner leaflet may play important role in the determining polarity, which helps in the interaction of membrane protein with lipids and their precise orientation at the membrane.

2.4.7. The LWI-residues have undergone different selection pressure throughout vertebrate evolution due to N- and C-terminal peptide directionality:

To further understand the molecular evolution of TRPV3, we have analysed the conservation of N and C-terminus of different transmembrane helices in relation to the lipid bilayer. If there is no difference due to the N- and C-terminus orientation, then uniform selection pressure is expected in both N- and C-terminal sequences. However, our analysis suggests that N-terminus of TM regions (represented as all N-ter) shows more conservation then the residue present on C-terminus of TM region (represented as all C-ter). Out of 6 N-terminus and 6 C-terminus stretches, TM3N and TM6N are highly conserved while in case of C-terminus, the TM2C, TM4C and TM6C are highly conserved **(Fig. 71-72a)**. With all these observation, conservation of N-terminus over C-terminus and all inside vs. all outside provides a topological uniqueness of TRPV3 in different lipid bilayer.

present in the LWI. Snorkeling amino acids such as Arginine, histidine and glutamic acid are found to be present in the LWI of TRPV3 in POPC membrane.

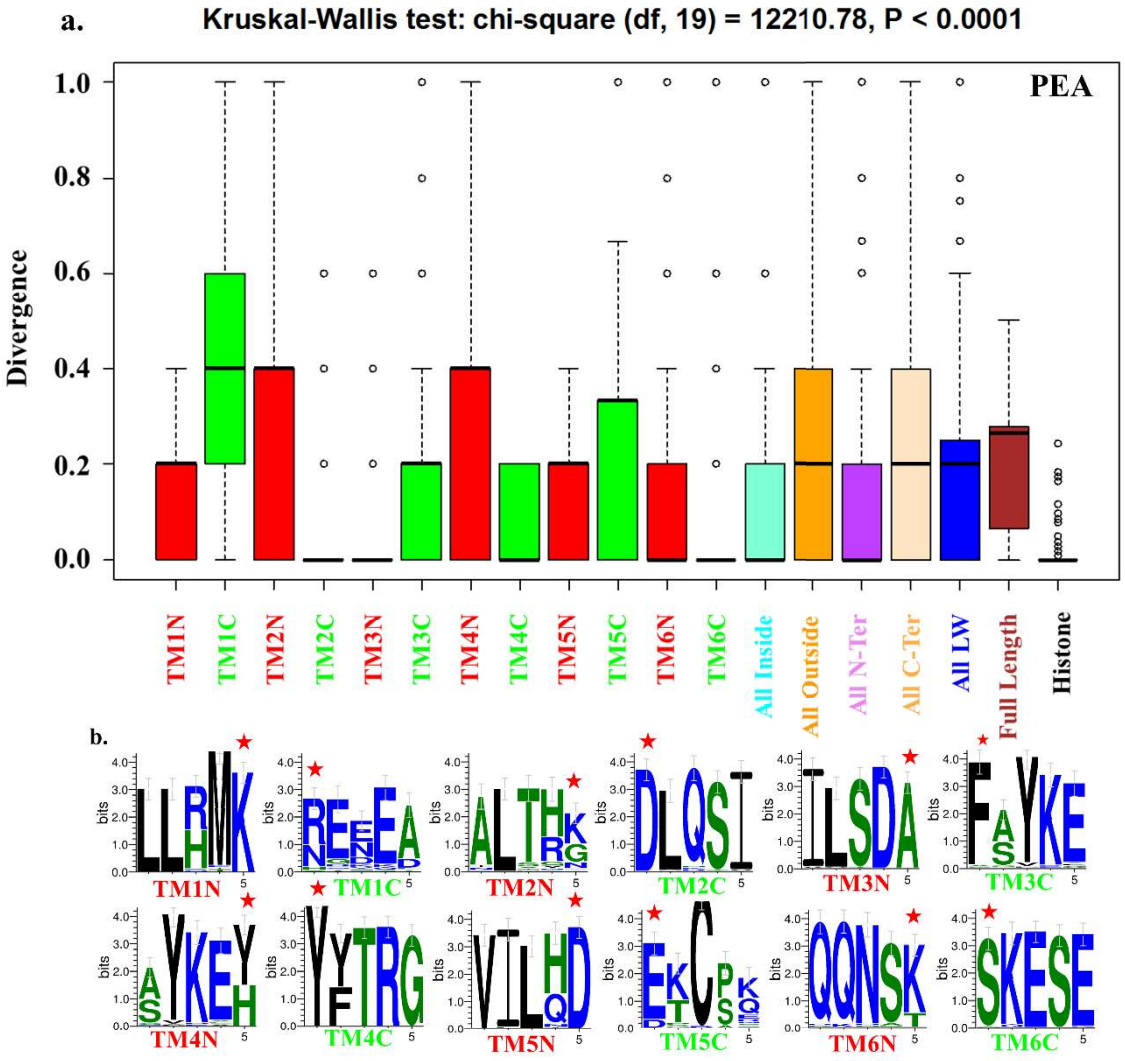

Figure 72. Conservation and selection of amino acids located at the lipid-water interface of TRPV3 throughout vertebrate evolution. a. Box plot showing conservation of 5 amino acid stretch sequences (marking the amino acids present in LWI) in each side of the TM of TRPV3 in PEA. The LWI residues present in the inner leaflet of the membrane are highly conserved in vertebrates**. b.** Conservation analysis of each residue present in the LWI. Snorkeling amino acids are present in the LWI of TRPV3 in PEA membrane.

2.4.6. Amino Acids present at the inner leaflet evolved under more stringent selection pressure:

Plasma membrane composition is non-homogeneous and non-identical on outer and inner side. To understand the effect of lipid membrane composition on evolution of TRPV3 we have calculated the 5-amino acid stretch from both side of membrane. Results show that residue present in the inner side of the membrane are more conserved (represented as all inside) with

2.4.5. Amino Acids present in the lipid-water interface are highly conserved:

After determining the set of amino acid present in the LWI, we explored the conservation pattern of these amino acids. Analysis suggest that these residues are mostly conserved. Out of 6 N-terminal (TMN) and 6 C-terminal (TMC), N-terminus TM3N and TM6N are highly conserved **(Fig. 71-72a)**. Similarly, the C-terminus TM2C, TM4C, and TM6C are highly conserved **(Fig. 71-72a)**. Further characterization at single amino acid level shows that charged amino acids (Arg, Glu, and Asp) and aromatic amino acids (Tyr, Phe) are distinctly conserved in these specific positions **(Fig. 71-72b)**. Often such amino acids are selected over other amino acids at the exact border position which demark the TM helices with the LWI region.

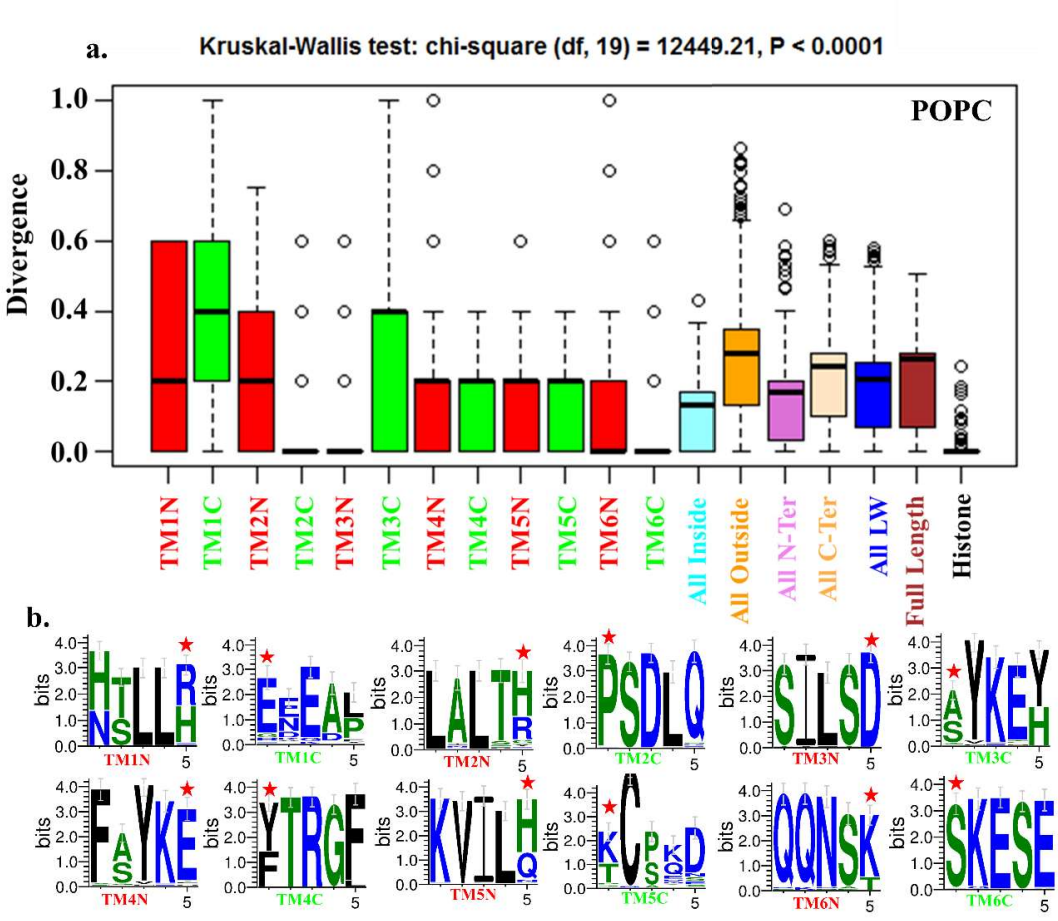

Figure 71. Conservation and selection of amino acids located at the lipid-water interface of TRPV3 throughout vertebrate evolution. a. Box plot showing conservation of 5 amino acid stretch sequences (marking the amino acids present in LWI) in each side of the TM of TRPV3 in POPC membrane. The LWI residues present in the inner leaflet of the membrane are highly conserved in vertebrates**. b.** Conservation analysis of each residue

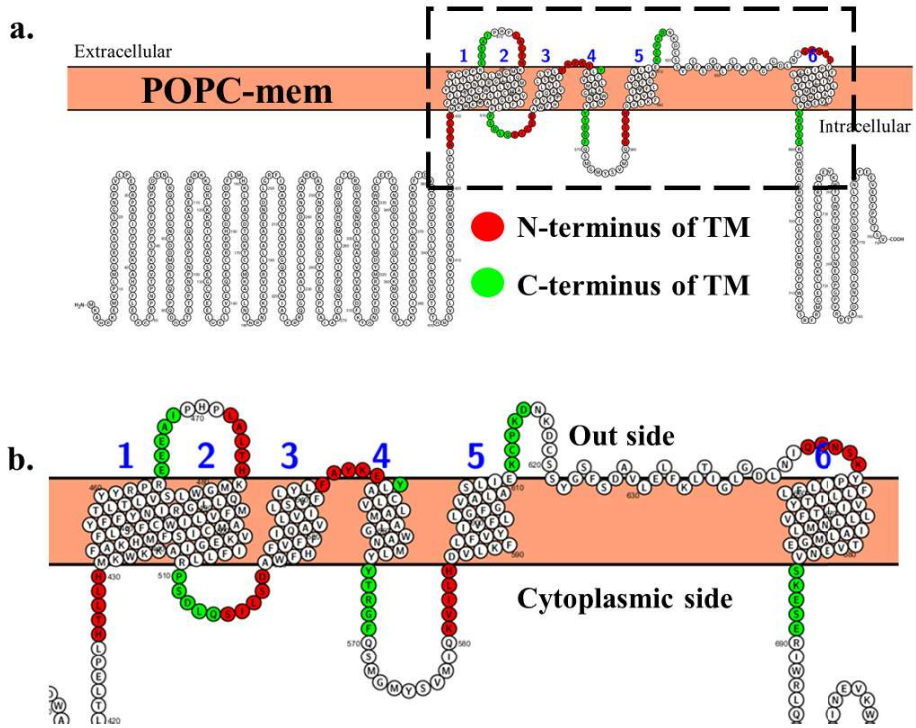

Figure 69. Distribution of amino acids at the lipid-water interface of TRPV3. a-b. Schematic representation of hTRPV3 sequence in lipid bilayer made of POPC is shown. Residues located at the lipid-water interface are highlighted (red and green indicate the residues at the N-terminal and C-terminal of each TM helices respectively). (Some of residue are overlapping in TM3C and TM4N which are 543-546).

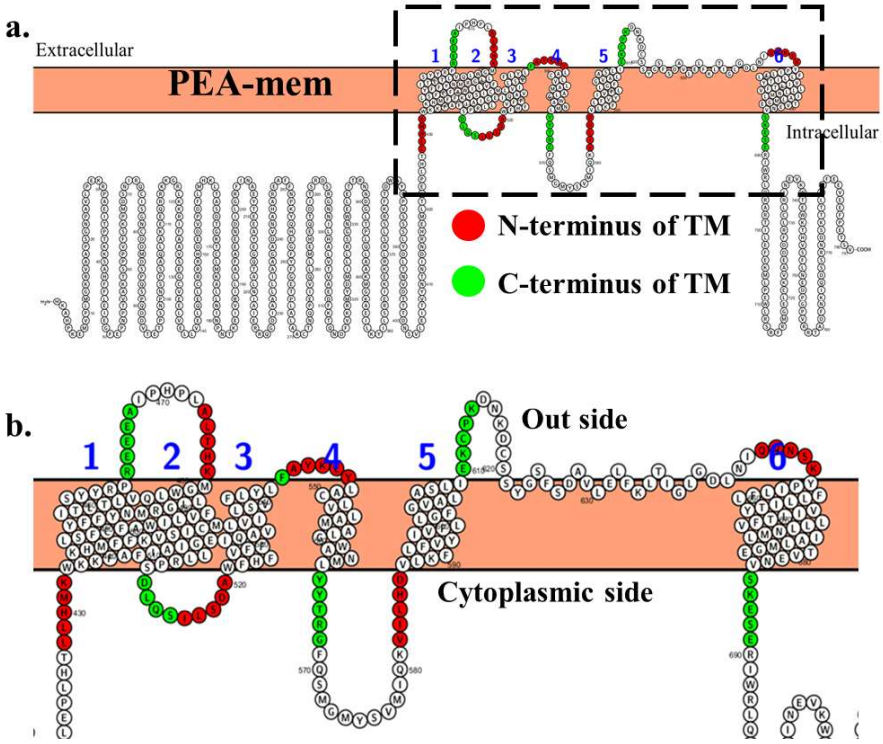

Figure 70. Distribution of amino acids at the lipid-water interface of TRPV3. a-b. Schematic representation of hTRPV3 sequence in lipid bilayer made of PEA is shown. Residues located at the lipid-water interface are highlighted (red and green indicate the residues at the N-terminal and C-terminal of each TM helices respectively). (Amino acid residue 516 is overlapping between TN2C and TM3N. Similarly, amino acid 543-546 are overlapping between TM3C and TM4N.

2.4.4. Determination of the lipid-water interface (LWI) amino acids of TRPV3:

It is well known that the core of the lipid bilayer is mostly represent water-free environment. Lipid Water Interface (LWI) region is represented by a special physio-chemical microenvironment present in both side of a biological membrane system where availability of free water is very less. This poses a special microenvironment where behaviour of different amino acids, such as protonation, de-protonation, solubility, pKa values etc. are different. Such aspects can be very crucial for amino acid side chain structures and thus for the proteins functions.

In this work we have analysed the conservation of amino-acid residues which are present in lipid water interface (LWI) of TRPV3. For this study, we have selected 5 amino acid sequences of each side of TM helices which covers approximately 6Å to 10Å length in linear direction. These 5 amino acids are present at the end of N- and C-terminal helices. Snorkeling amino acids which are present at the LWI region shows interactions with lipids. Such interactions define lipid – peptide interactions and are crucial for biological functions of proteins. For this study we have selected two different lipids bilayer, namely POPC and PEA membrane **(Fig. 69-70)**.

2.4.2. Different domains and motifs of TRPV3 has been selected through different selection pressure:

In order to find out the conservation of different regions in TRPV3, we have performed statistical for the conservation of different regions across the vertebrate species. This analysis shows that loop2, TM4, loop4, and TM5 are relatively more conserved with comparison to another domain of TRPV3. This suggest that these domains, which show more conservation are under high selection pressure **(Fig. 68)**.

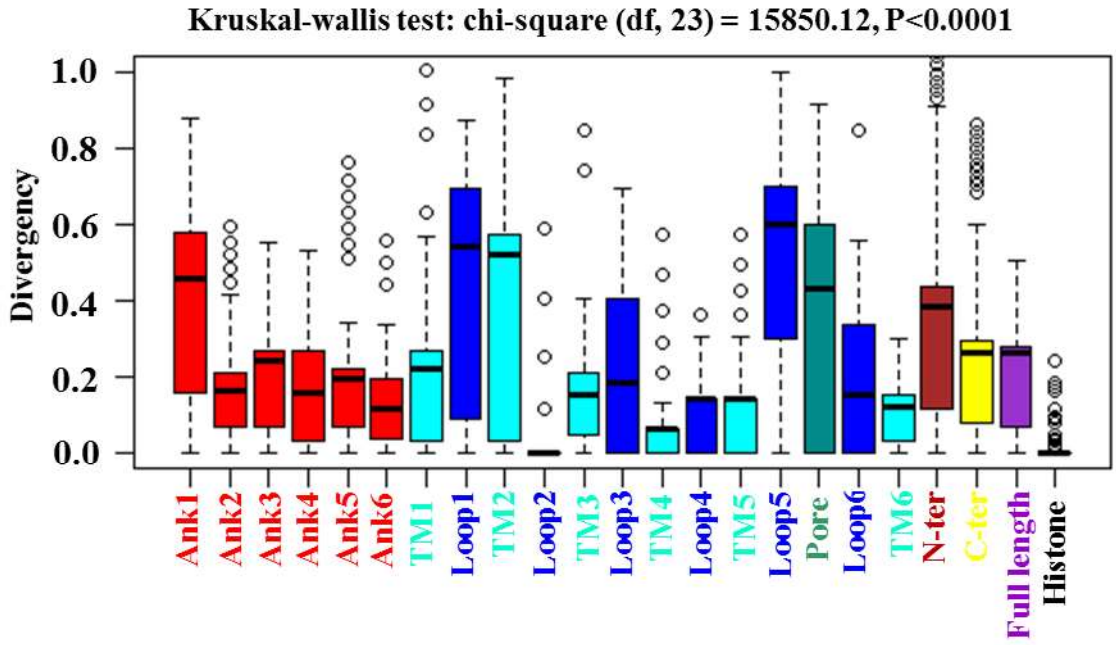

Figure 68. Box plot shows conservation of different domain of TRPV3 across vertebrate. Figure shows that different regions of TRPV3 have evolved under stringent selection pressure. Intracellular loop2, loop4 are highly conserved along with TM4 and TM5. For this analysis we have taken histone as control. In box plot analysis higher, the value less conserve the domain and lesser value shows more conservation.

2.4.3. Homology modelling of TRPV3:

Recently the high-resolution structure of TRPV1, both in closed conformation and in open conformation has been solved [46, 273]. This offers great opportunity to analyse the structure-function analysis of TRPV3. For this analysis rTRPV1 structure 3J5P was used as closed conformation and 3J5R was used as open conformation. Using both of these structure as template we have prepared a homology model of hTRPV3, both in open and closed confirmation by using default programme in Yasara software.

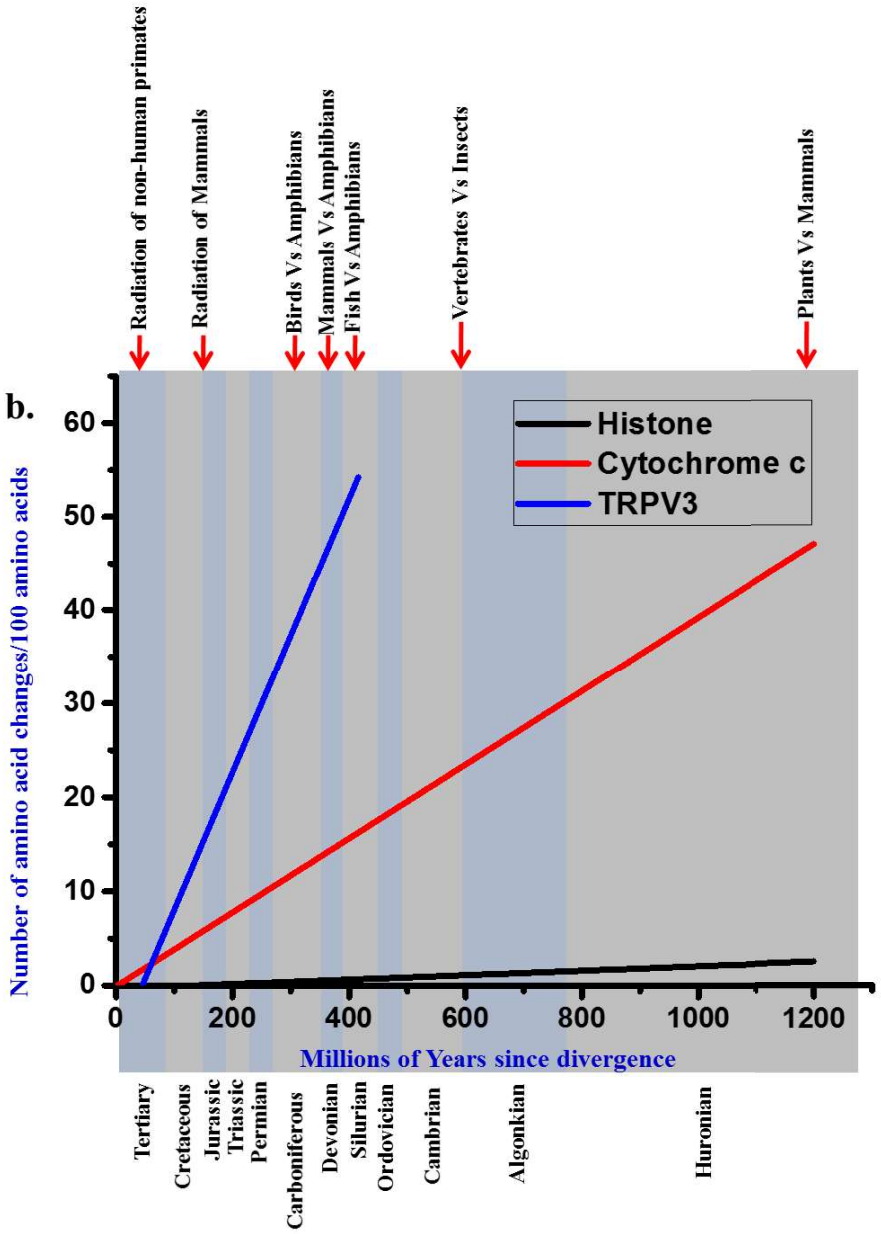

Figure 67. Phylogenetic analysis of TRPV3. a. TRPV3 gene is present in vertebrates only. The phylogenetic tree of TRPV3 from fish, amphibians, reptiles, birds and mammals. Elephant shark serves as out group reference control. **b.** Conservation of TRPV3 is shown. For this analysis Histone and Cytochrome C have been taken as reference control.

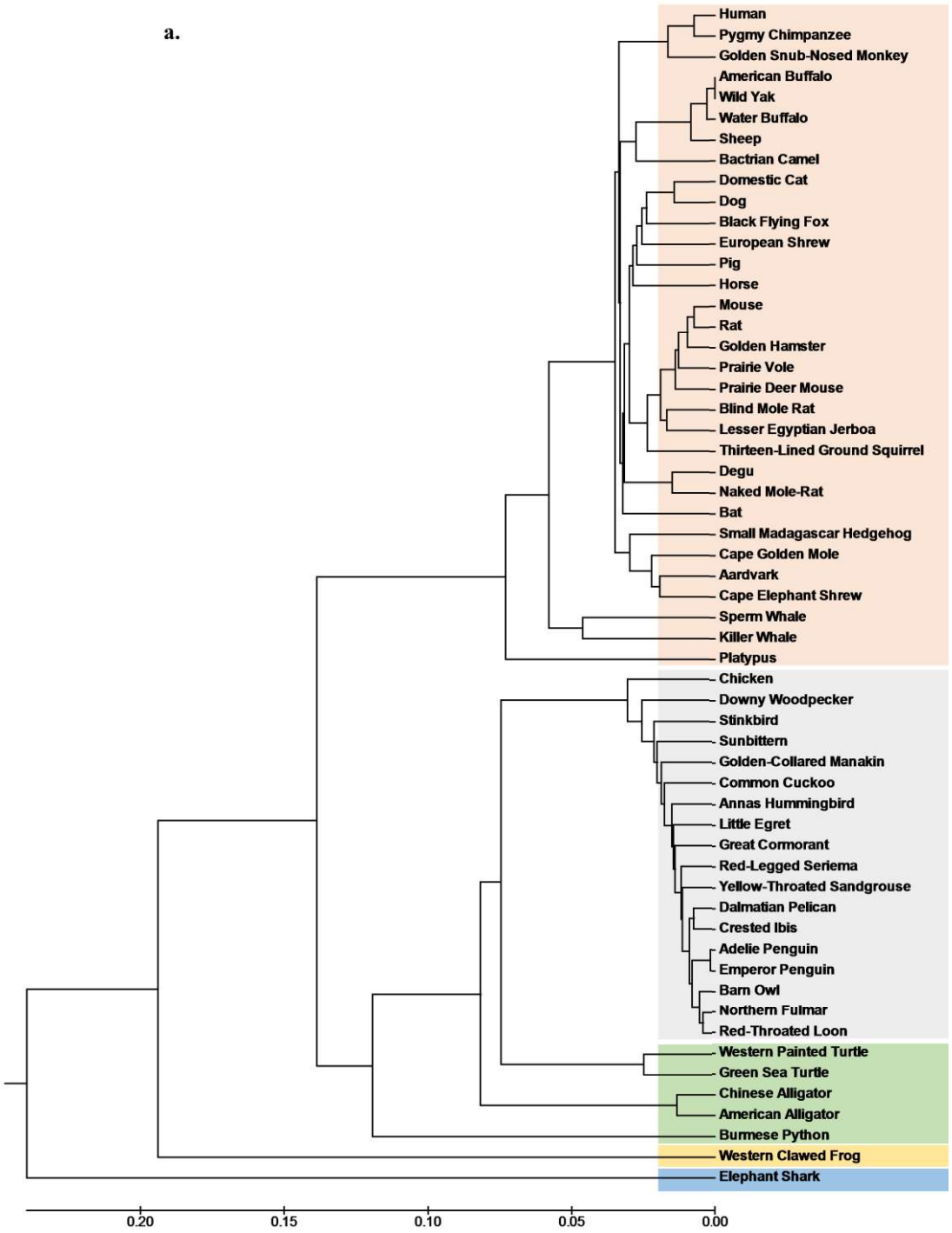
a.
Human
Pygmy Chimpanzee
Golden Snub-Nosed Monkey
American Buffalo
Wild Yak
Water Buffalo
Sheep
Bactrian Camel
Domestic Cat
Dog
Black Flying Fox
European Shrew
Pig
Horse
Mouse
Rat
Golden Hamster
Prairie Vole
Prairie Deer Mouse
Blind Mole Rat
Lesser Egyptian Jerboa
Thirteen-Lined Ground Squirrel
Degu
Naked Mole-Rat
Bat
Small Madagascar Hedgehog
Cape Golden Mole
Aardvark
Cape Elephant Shrew
Sperm Whale
Killer Whale
Platypus
Chicken
Downy Woodpecker
Stinkbird
Sunbittern
Golden-Collared Manakin
Common Cuckoo
Annas Hummingbird
Little Egret
Great Cormorant
Red-Legged Seriema
Yellow-Throated Sandgrouse
Dalmatian Pelican
Crested Ibis
Adelie Penguin
Emperor Penguin
Barn Owl
Northern Fulmar
Red-Throated Loon
Western Painted Turtle
Green Sea Turtle
Chinese Alligator
American Alligator
Burmese Python
Western Clawed Frog
Elephant Shark
0.20
0.15
0.10
0.05
0.00

Chapter 2.4: Importance of cholesterol in regulation of TRPV3:

(This chapter is under preparation as a manuscript: Yadav M, Goswami C. (2018) Conservation analysis of TRPV3 in Lipid water interface and cholesterol mediated regulation.

TRP channels show diverse cellular functions and are potentiated by different mechanisms. Also, their surrounding microenvironments within lipid bilayer too modulate their activities. Unlike other transmembrane proteins, the TRP proteins are surrounded by different lipids and cholesterol. Some of the TRP's are known to interact with different lipids and these interactions regulate their functions and different signaling events. The TRP ion channels are polymodal in nature and one of their unique gating mechanism is their activation by temperature. These channels have relatively high Q10 values and a little change in temperature can results in the conformational change which in turn ultimately results in the channel activation. Although there are species specific differences in TRP's regulation and function, however, activation by hot or cold temperature, i.e. by temperature change is conserved throughout the species. This suggest that thermosensitive nature of these TRP's are conserved during the course of evolution. The work described in this chapter analysed the TRPV3 sequences from different species and extract useful information regarding its structure and function.

2.4.1. TRPV3 is a vertebrate-specific ion channel:

In order to explore the molecular evolution of TRPV3, the phylogenetic tree of TRPVv3 was analysed. The TRPV3 sequence is available in fish, amphibian reptiles, birds and mammals. The tree reveals that it is present in vertebrate only and is missing in invertebrates **(Fig. 67a)**. Also, the comparative sequence analysis reveals that TRPV3 emerged in vertebrates **(Fig. 67b)**, approximately around 450-500 million year ago. Analysis also suggest that probably it is emerged during transition from Devonian to Silurian era **(Fig. 67b)**.

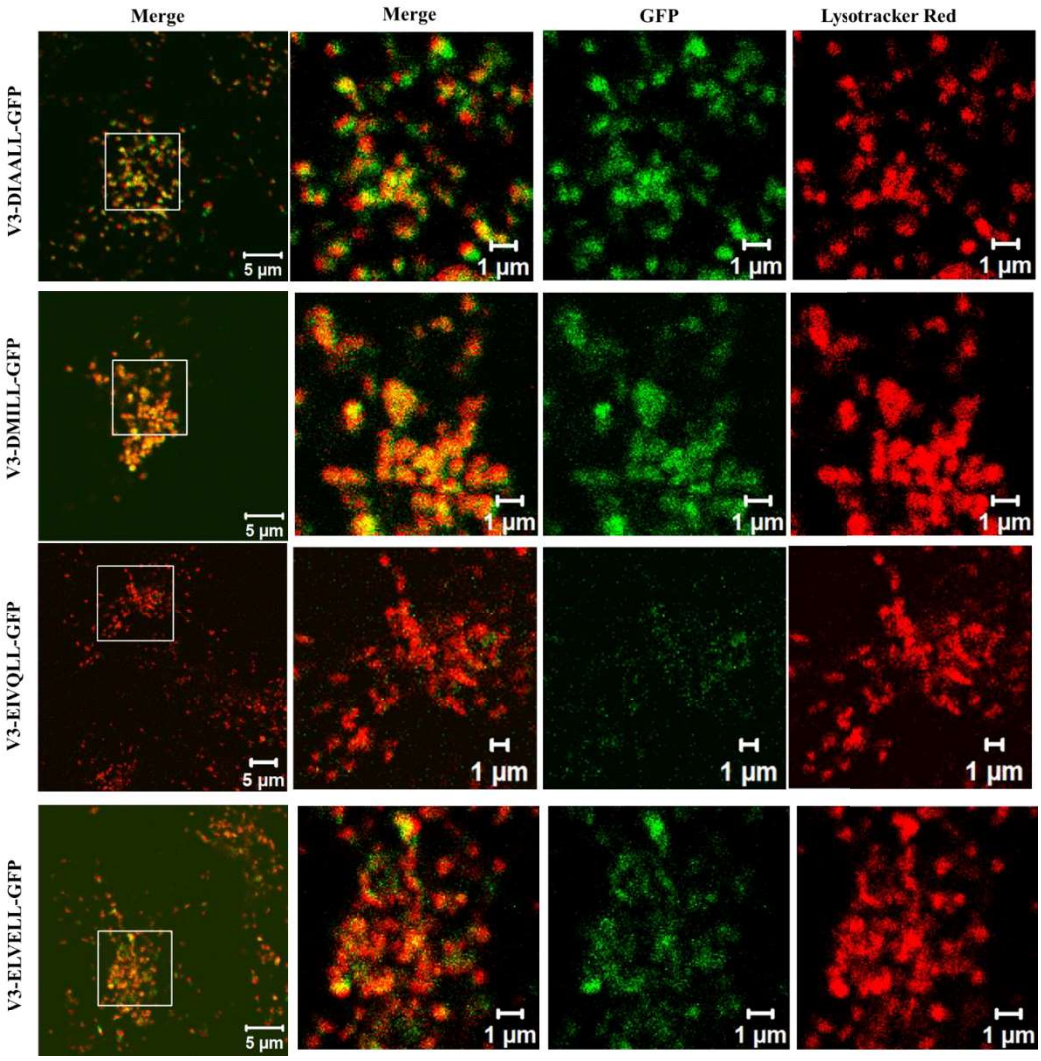

Figure 66. Lysosomal targeting sequence (LTS) present in TRPV3 co localize with LysoTracker Red: Live cell imaging of HaCaT cells transfected with TRPV3-LTS-GFP, (ELVELL, DIAALL, EIVQLL, DMILL) after 24 hours of transfection cells were stained with LysoTracker Red (100nM) for 30 min. Except EIVQLL, all (ELVELL, DIAALL, DMILL) shows significant co localization with LysoTracker Red.

sequences among all vertebrates, the LTS sequences were aligned. Such analysis reveals that DMILL is highly conserved through all vertebrates **(Fig. 65)**.

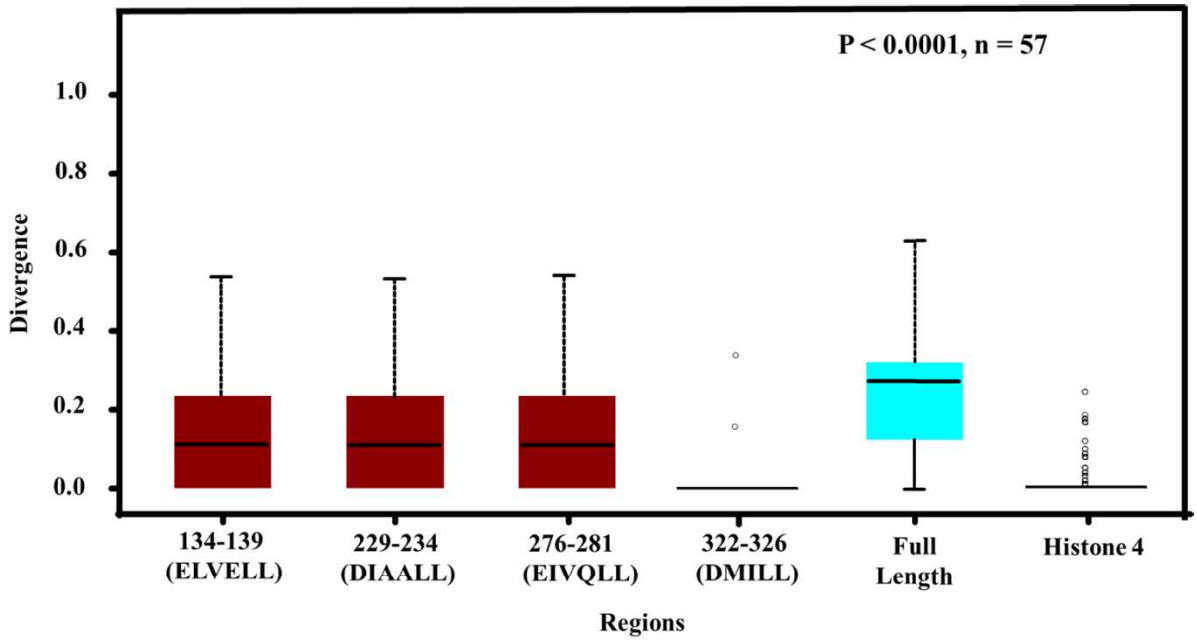

Figure 65. Lysosomal targeting sequence (LTS) is present in TRPV3: Box plot depicting the conservation of four stretch sequences (ELVELL, DIAALL, EIVQLL, DMILL) present in the N terminus of TRPV3. Among them DMILL is highly conserved in all vertebrates**.** (Lower the value more it is conserve). In this analysis, lower value represents more conservation of the protein and *vise versa*. (Kruskal-Wallis test: chi-square P<0.00001 and n=57).

2.3.9. Lysosomal targeting sequence (LTS) present in N terminus of TRPV3 co localizes with LysoTracker Red:

After biochemical and insilico analysis that TRPV3 is present in lysosome, to revalidate we have clone the four stretch of LTS in GFP vactor. After transfection with four TRPV3-LTS-GFP we have labelled HaCaT cells with LysoTracker Red (100nM for 30 min) and imaged with confocal microscope. Surprisengly we have noted that all (ELVELL, DIAALL, EIVQLL, DMILL) LTS except EIVQLL co localizes with LysoTracker Red. Presence of these small fragments of TRPV3 with lysosome marker i.e. with LysoTracker Red confirms that TRPV3 is a lysosomal protein **(Fig. 66)**.

of these lysosomes to get labelled with LysoTracker Red dye. **b.** Kymograph analysis of the lysosomal movement in HaCaT cells expressing TRPV3-Wt or G573C or G573S mutants as GFP-tagged proteins after stable selection are shown. TRPV3 co-migrates with lysosomes in cells expressing TRPV3-Wt [272].

2.3.7. TRPV3 is present in the lysosomal fraction isolated from goat brain extract:

To further confirm if TRPV3 is present in the lysosomal fraction, we have purified the lysosomal fraction from goat brain and probed with TRPV3 specific antibody. We could detect the reactivity for TRPV3 in both lysosomal and mitochondrial fractions **(Fig. 64b)**. Further we have also checked the enrichment for lysosomal marker Lamp1 in the same fraction **(Fig. 64a)**.

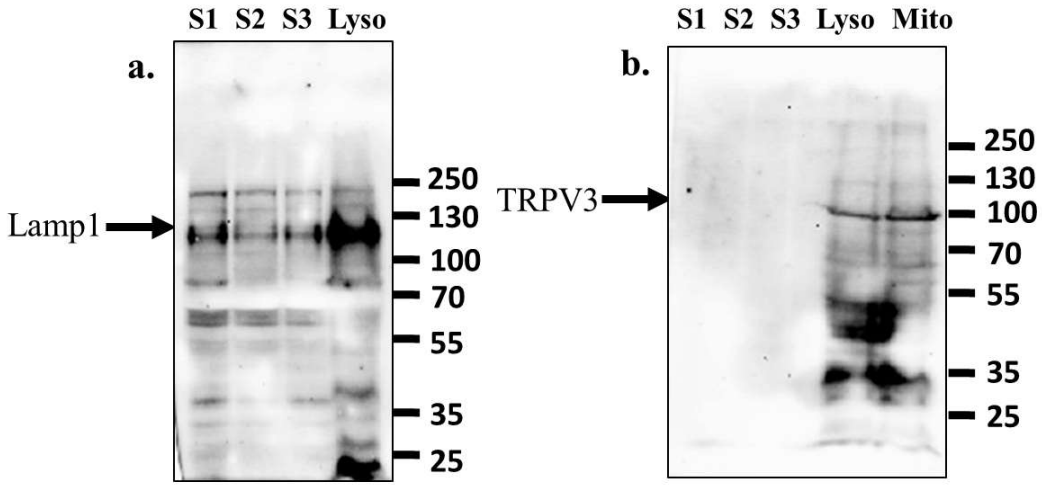

Figure 64. TRPV3 is present in the lysosomes: a. Western blot analysis of SI (Lane 1), S2 (Lane 2), S3 (Lane 3) and lysosomal fraction (Lane 4) isolated from goat brain and probed with anti-TRPV3 (right side) and anti-Lamp1 (left side). Enriched amount of TRPV3 (indicated by arrow) is detected in the lysosomal fraction. **b.** Western blot analysis of purified lysosomal and mitochondrial fraction isolated from goat brain shows the presence of endogenous TRPV3 (indicated by arrow) [272].

2.3.8 Lysosomal Targeting Sequences (LTS) are present in N terminus of TRPV3:

To further confirm the presence of TRPV3 in lysosome, we have performed *in silico* analysis with all verterbrates species sequences. We could detect four LTS streach (ELVELL, DIAALL, EIVQLL, DMILL) sequences in the N-termins. To find out the conservation of LTS

frame respectively. **b-c.** TRPV3 activation by FPP doesn't show any changes in overall calcium level (except very mildly in cells expressing TRPV3-Wt). In contrast, inhibition of TRPV3 cause sharp rise in the intracellular Ca^{2+}-levels (in arbitrary units). Though different OS-mutants respond differently against DPTHF, all mutants reveal much larger Ca^{2+}-levels compared to the TRPV3-Wt. **d.** Time required to reach maxima intensity after DPTHF treatment. OS-mutants take equal or longer time to reach maxima as compare to TRPV3-Wt suggesting that cells expressing OS-mutants have defective Ca^{2+}-buffering activity (n=20). (P-values are as follows *** <0.001, ** <0.01, * <0.05, n = 20 cells in each case).

2.3.6. OS mutants localizes in Lysosome:

Effect of OS mutants on different cell organelles gives a hint about the presence of TRPV3 in intracellular compartment/s. In order to find out if TRPV3 is present in lysosome, we performed live cell imaging of stable cells expressing Wt and OS mutants labelled with LysoTracker Red and found that TRPV3-Wt along with OS mutants (at least TRPV3-G573C and TRPV3-G573S) colocalize with Lysotracker Red. **(Fig. 63a)**.

Kymograph analysis reveal that both TRPV3-Wt as well as OS-mutants colocalize and comigrates with LysoTracker Red labelled organelles **(Fig. 63b)**.

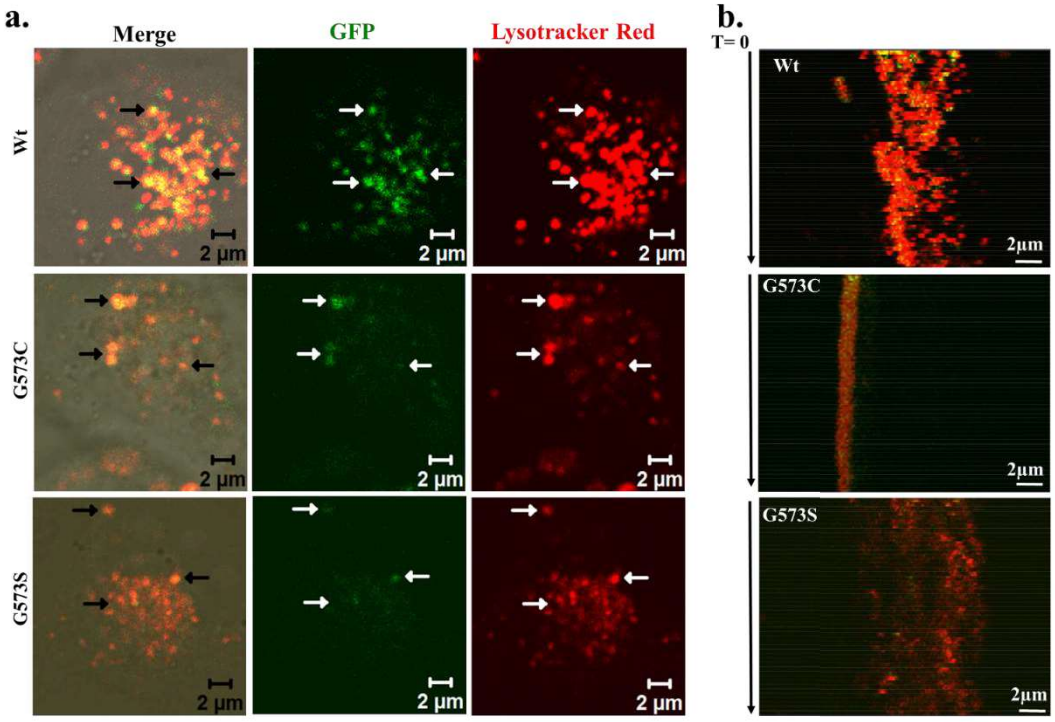

Figure 63. TRPV3-Wt or OS-mutants colocalise with Lystracker Red: a. Both TRPV3-Wt as well as OS-mutants localize in lysosomes in live cells. Shown are the confocal images of HaCaT cells expressing TRPV3-Wt or TRPV3-G573C or TRPV3-G573S mutants as GFP-tagged proteins after stable selection. Points of colocalizations are indicated by white arrows. Experiments aiming to probe two other mutants, namely G573A and W692G in lysosomes failed mainly due to the presence of very low number of lysosomes and/or inefficiency

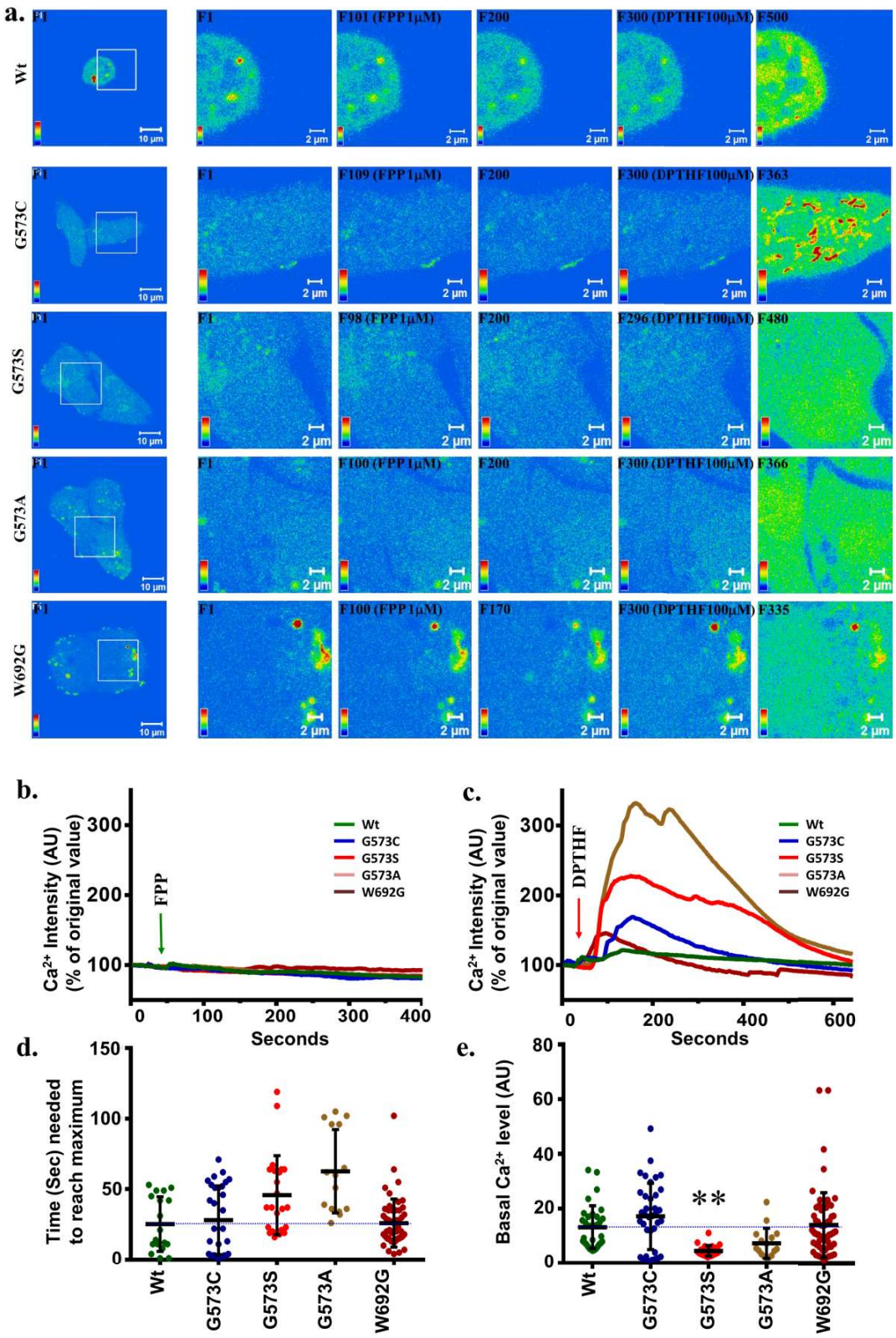

Figure 62. Inhibition of TRPV3 leads to increased intracellular Ca^{2+}-levels and mutants affect intracellular Ca^{2+}-buffering activity: a. Shown are the live cell time series images depicting the changes in intracellular Ca^{2+}-levels in cells expressing TRPV3-Wt or OS-mutants. The white square represents the area of the cell shown in details. TRPV3 activator (FPP, 1µM) and inhibitor (DPTHF, 100µM) were added at 100th frame and at 300th

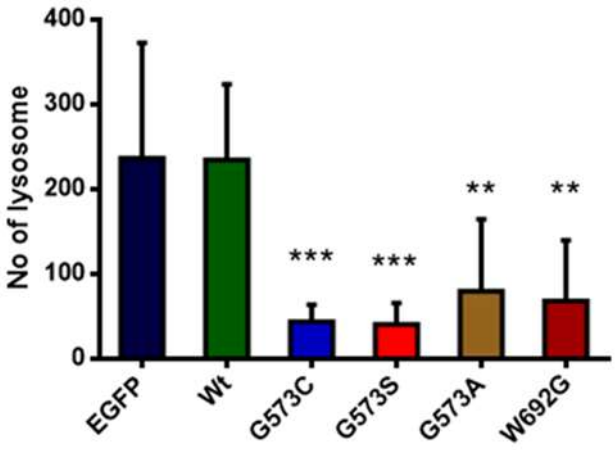

Figure 61. OS-mutants have low number of lysosomes: HaCaT cells stably expressing either TRPV3-Wt or OS-mutants were labelled with LysoTracker Red and number of lysosomes per cell were quantified. The cells expressing OS-mutants show significantly lower number of lysosomes than the cells expressing TRPV3-Wt (P-values are as follows *** <0.001, ** <0.01, n = 20 cells in each case) [272].

Unlike other TRPVs, TRPV3 is known to have unique property of not being desensitized in response to Ca^{2+}. Therefore, we calculated the time required to reach the maximum Ca^{2+} level after inhibition and we found that OS mutant takes longer time to reach the maxima (namely G573S and G573A) whereas the TRPV3-Wt cells takes smaller time to reach maxima **(Fig. 62d)**. The basal Ca^{2+} without activation or inhibition in stable cells expressing TRPV3-Wt or OS-mutants were analysed. No significant difference in the basal Ca^{2+} level G573C and W692Gwas observed **(Fig. 62e)**. However, the G573S or G573A mutant expressing cells show lesser amount of basal Ca^{2+}-level.

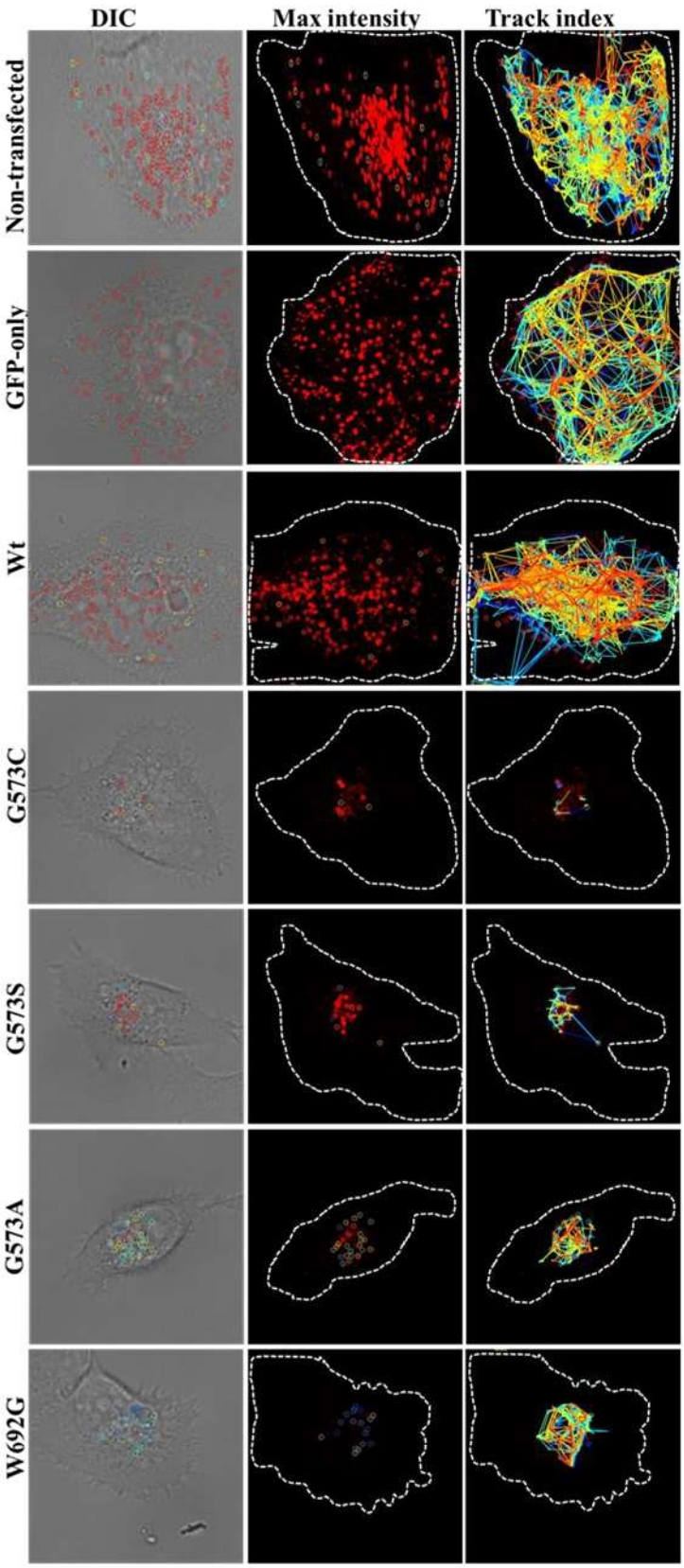

Figure 60. OS-mutants have low number of lysosomes and reduced lysosomal movement: Live HaCaT cells stably expressing TRPV3-Wt or OS-mutants were labelled with LysoTracker-Red and time series images were acquired. Left panel images show the DIC images super imposed with the LysoTracker-Red labelled Lysosomes (red circles). The white dotted lines show the periphery of the cells. The track index of respective Lysosomal movements is indicated by lines (Right panel). All images were processed in FIJI software plugin track mate.

expressing cells show very high calcium flux, and OS-mutants show even larger levels of Ca^{2+}-influx when compared to TRPV3-Wt cells **(Fig. 62a-c)**.

movement. Cells were incubated with LysoTracker Red 100nM for 30 min reveals that un transfected, TRPV3-Wt and EGFP control cells shows very high number of lysosome and high movement while the OS mutant expressing cells shows very less or restricted movement and significantly reduced labelling of LysoTracker Red. **(Fig. 60)**

Movement of lysosome was measured with the help of Track Mate software where we have shown the intensity of lysosome and movement of each particle. DIC image shows the reduced number of lysosome in case of OS mutant expressing cells. **(Fig. 60)**

Calculation of lysosome number in stable cell expressing TRPV3-Wt and OS mutant reveals that EGFP control and TRPV3-Wt expressing cells have equal number of lysosome while OS mutant expressing cells have significantly reduced number of lysosome with compare to Wt and EGFP control. **(Fig. 61)**

2.3.5. OS mutant affects intracellular calcium homeostasis:

Ca^{2+}-ion is an important factor involved in maintenance of ionic balance and pH homeostasis. As OS mutants affect the localization and function of different subcellular organelles like mitochondria and lysosome, we explored if activation or inhibition of TRPV3 leads to any change in the Ca^{2+}- dynamics in the stable cells expressing TRPV3-Wt and OS mutants.

For this we labelled the cells with Fluo4 for 1 hour and subsequently performed live cell imaging and tested the effect of specific activator and inhibitor of TRPV3. We noted that TRPV3 activation with FPP have little or no effect on the TRPV3-Wt or the OS mutant expressing cells. This is in agreement with the fact that all the OS-mutant's mutants are constitutively active in nature and further activation doesn't show any effect **(Fig. 62a-c)**. However, upon inhibiting TRPV3 by pharmacological means (DPTHF), the TRPV3-Wt

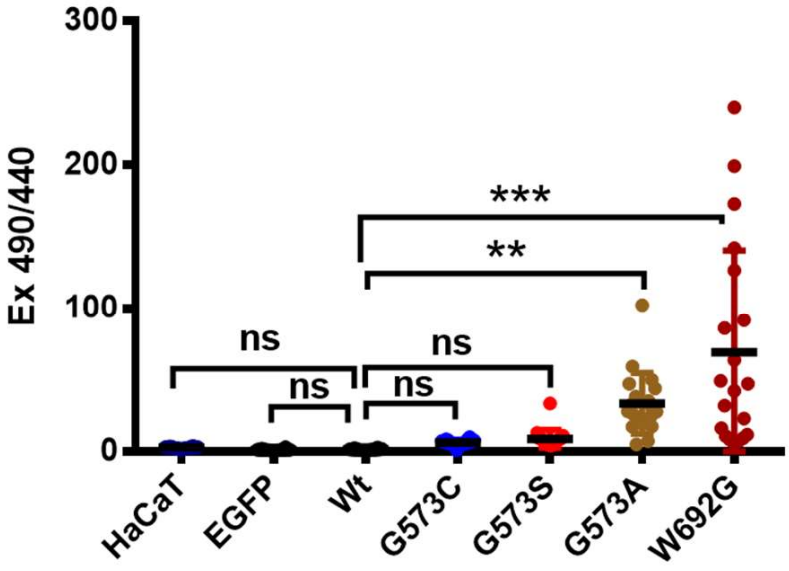

Figure 59a. OS-mutants have altered cytoplasmic pH: Quantification of the ratio of BCECF fluorescence intensity (in arbitrary unit) in HaCaT cells stably expressing either TRPV3-Wt or OS-mutants. The cells expressing OS-mutants have significantly higher pH than the cells expressing TRPV3-Wt or GFP and non-transfected cells (P-value <0.001, n = 20 cells) Upper bar graph shows calibration of BCECF.

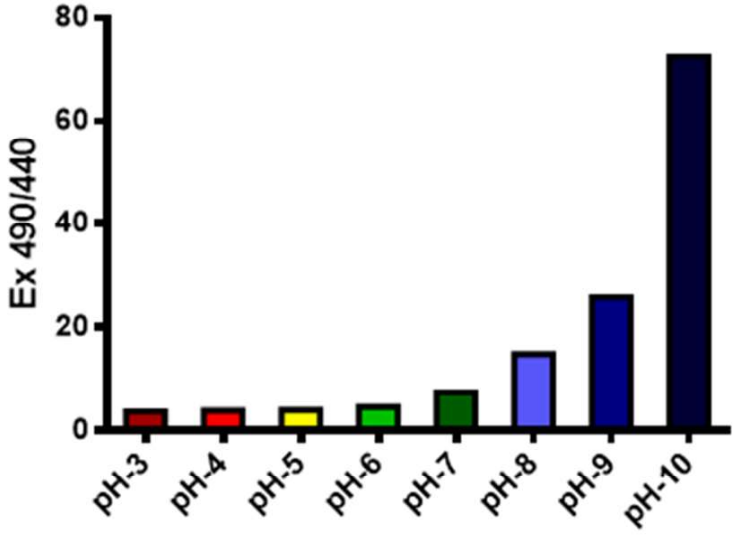

Figure 59b. Calibration plot of BCECF: Graph shows the calibration of BCECF in tris buffer of varying pH. Calibration experiment was done using the fluorescence spectrophotometer.

2.3.4. Stable cell expressing OS-mutants shows reduced lysosome number and movement:

Stable cell expressing TRPV3-Wt and OS mutants in HaCaT cells labelled with lysosomal dye LysoTracker Red shows significant less number of lysosome and reduced

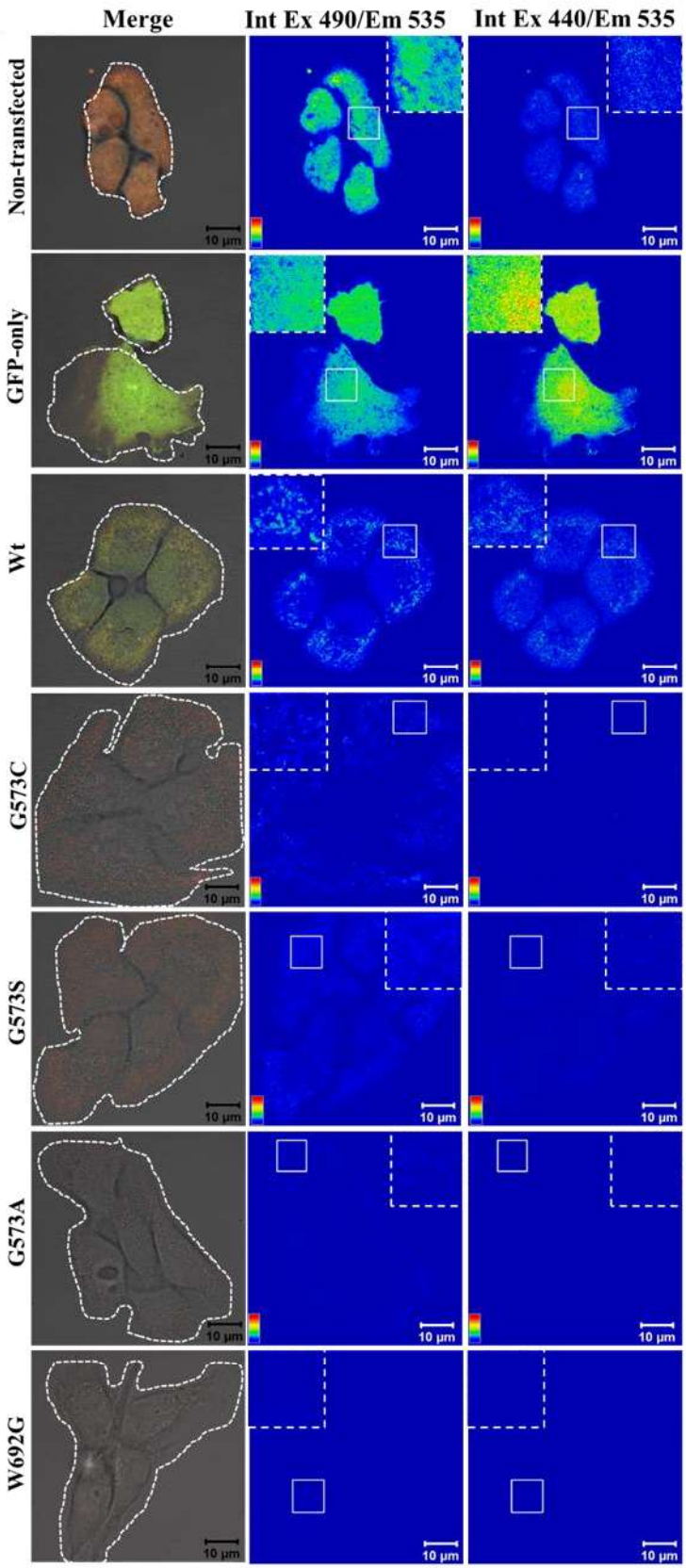

Figure 58. OS-mutants have altered cytoplasmic pH: Stable cell lines expressing TRPV3-Wt or OS-mutants were labelled with BCECF and merged images are provided in left side and fluorescence intensity profiles of individual images acquired with single emission and dual excitation (at 490nm and 440nm) are provided in the middle and right panel respectively. An enlarged view of the cell is provided *in set*.

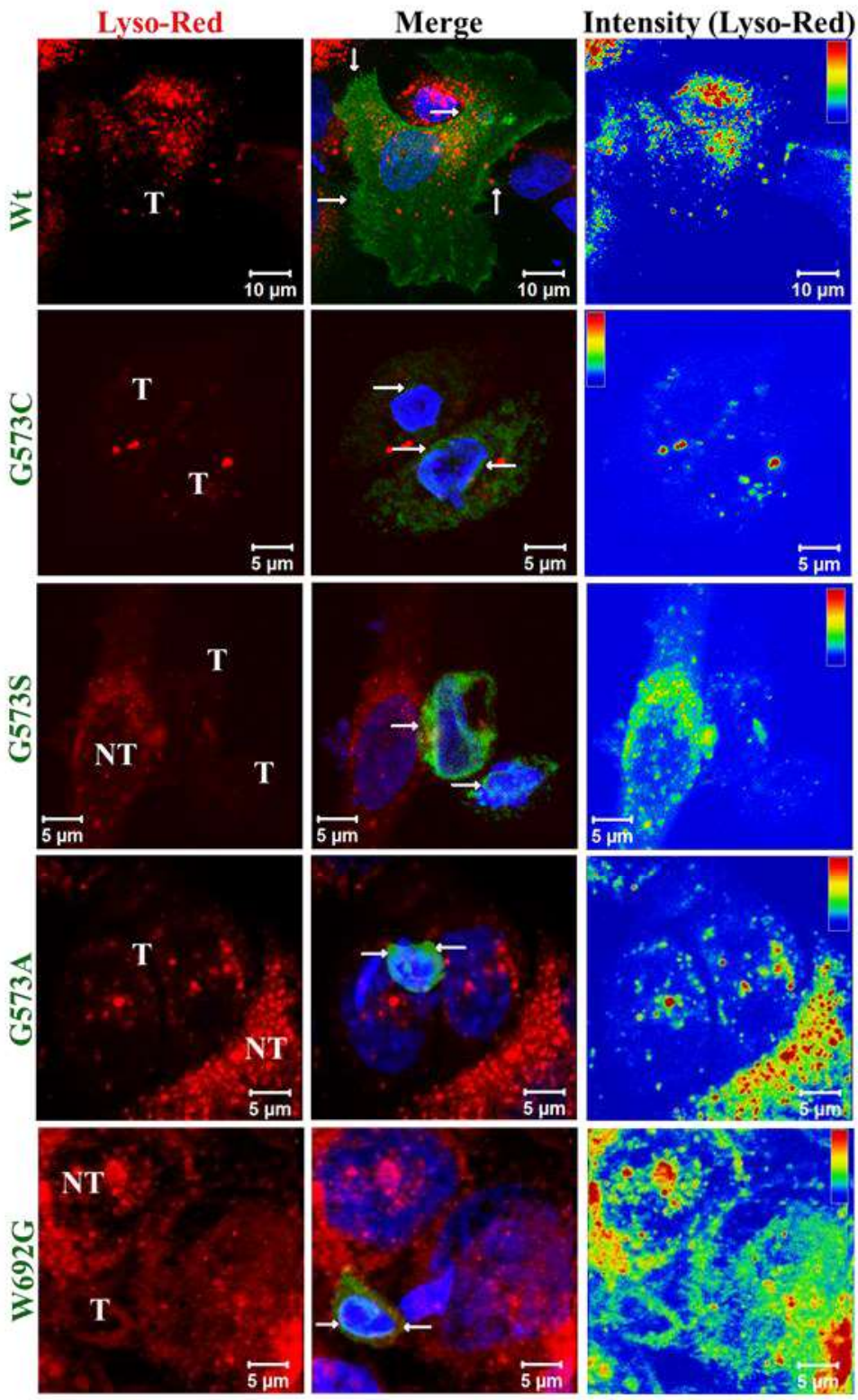

Figure 57. OS-mutants induce impaired Lysosomal distribution and function: Confocal images of transfected HaCaT cells (T) expressing TRPV3-Wt or OS-mutants (green) labelled with LysoTracker Red (Red). Cells expressing OS-mutants reveal either no or very less LysoTracker Red staining. Intensity profiles of LysoTracker Red staining are provided in right panel.

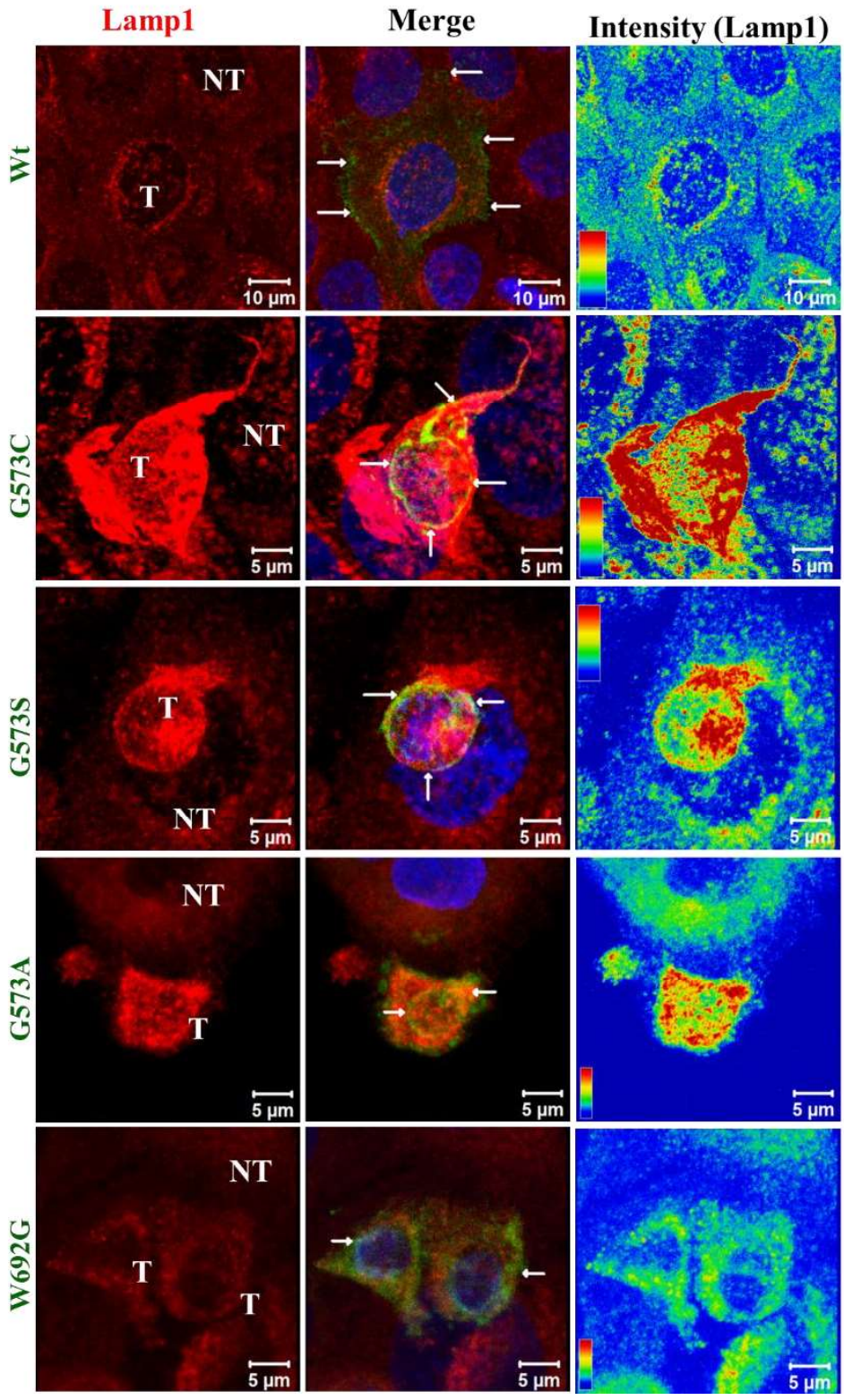

Figure 56. OS-mutants induce impaired Lysosomal distribution and function: Shown are the confocal images of transfected (indicated by T) HaCaT cells expressing TRPV3-Wt or OS-mutants (green) for 36 hours and stained with anti-Lamp1 antibody (Red) and DAPI (blue). Nearby non-transfected cells are indicated by NT. Anti-Lamp1 staining appears as aggregated clusters in OS-mutants expressing cells. Intensity profile of anti-Lamp1 staining is provided in right panel.

2.3.2. OS-mutants shows impaired lysosomal distribution:

HaCaT cells transiently expressing TRPV3-Wt or OS mutant were fixed with 4% PFA and stained with anti-Lamp1 antibody. This experiment reveals that untransfected and TRPV3-Wt cells have normal distribution of lysosomes (Lamp1 staining) while cells expressing OS mutants have aggregation of lysosome and very less labelling of anti Lamp1 antibody. TRPV3-G573C, G573S, G573A transfected cells shows high level of aggregation of lysosome, while TRPV3-W692G expressing cells shows very less labelling of Lamp1 (T and NT represents transfected and non-transfected respectively) **(Fig. 56)**.

We have checked the lysosomal activity with LysoTracker Red dye which labels the lysosome if it has acidic pH. Changes in the pH of lysosome leads to reduced signal for LysoTracker Red. HaCaT cells transiently expressing TRPV3-Wt or OS mutants were labelled with Lysotracker Red. TRPV3-Wt cells show the normal LysoTracker Red labelling, while the mutant cells show reduced LysoTracker Red labelling (G573C), while other mutants such as G573S, G573A, W692G show aggregation of lysosome **(Fig. 57)**.

2.3.3. Stable cells expressing OS-mutants cause impaired cytoplasmic pH:

Change in lysosome distribution and activity could be a cause of altered lysosome pH, the molecular reason or a consequence observed in case of OS mutants. To find if altered lysosomal distribution leads to change in lysosomal function, we used the stable lines expressing TRPV3-Wt or OS mutants and did live cell imaging using a pH sensitive dye BCECF. It has a duel excitation (Ex-490 Em-535) and single emission (Ex-440 Em-535) which offers different fluorescence emissions as pH changes. Quantification of live cell images with calibration of BCECF has been shown in **(Fig. 59a)**. The results show that TRPV3-Wt and EGFP control and un-transfected control cells have nearly same pH while the cells expressing OS mutants shows reduced signal for Ex-440 Em-535. Quantification of these live cell images show that cytoplasmic pH shifts toward basic in OS mutant expressing cells **(Fig. 59a)**.

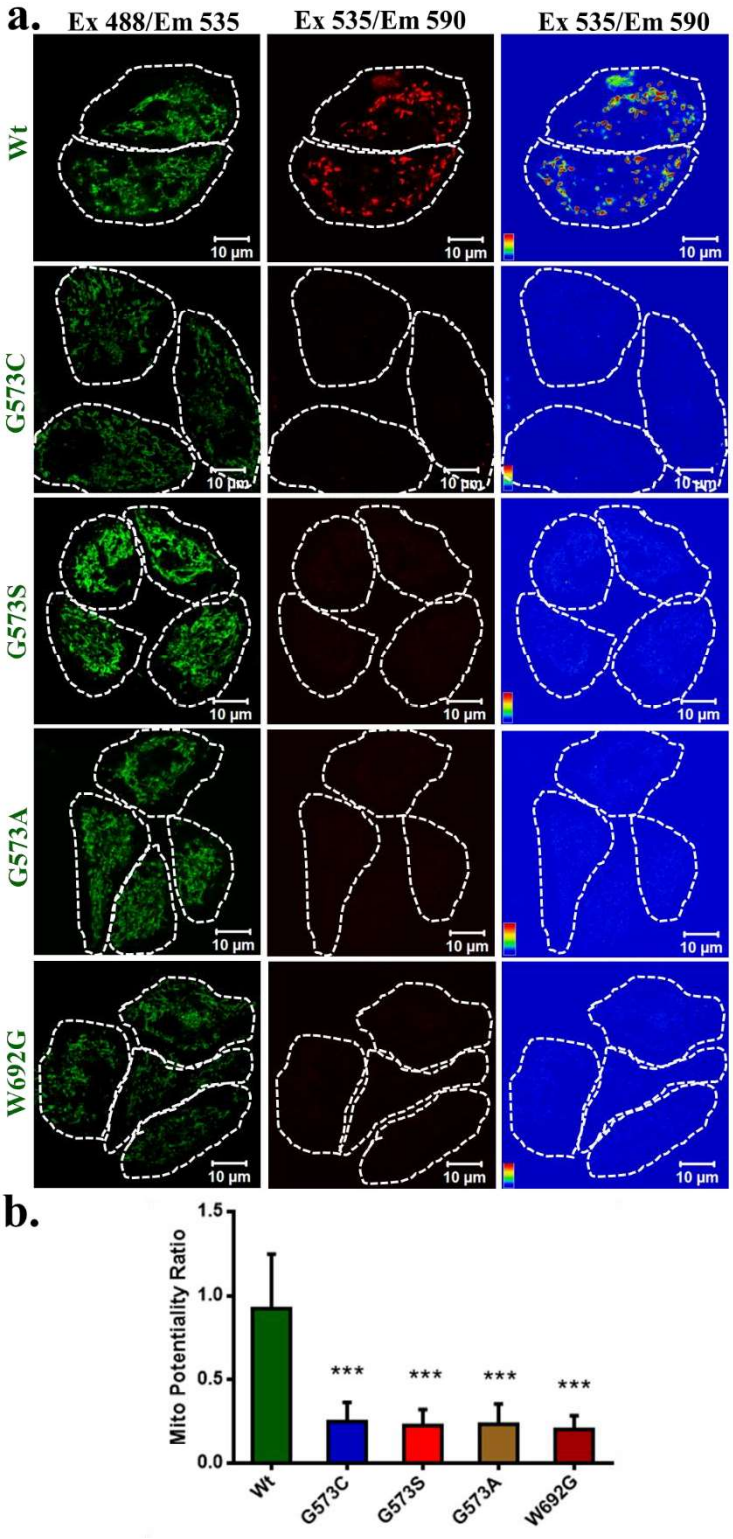

Figure 55. OS-mutants cause lower mitochondrial potentiality: a. Live cell images of stable HaCaT cells expressing TRPV3-Wt or OS-mutants labelled with mitochondrial potentiality indicator dye JC1. Left panel images show the fluorescence as observed by excitation at 488 nm and emission at 535 nm. The middle panel images show the fluorescence as observed by excitation at 535 nm and emission at 590 nm. Corresponding fluorescence intensity is provided in the right panel images. **b.** Quantification of the fluorescence intensities as observed by live cell imaging as described in figure a. All these OS-mutants reveal reduced mitochondrial potentiality while wild type expressing cells show the normal mitochondrial potentiality (P-value <0.001; n = 15 cells in each case). In all the set dye concentration and incubation time (1µM for 1hr) is same.

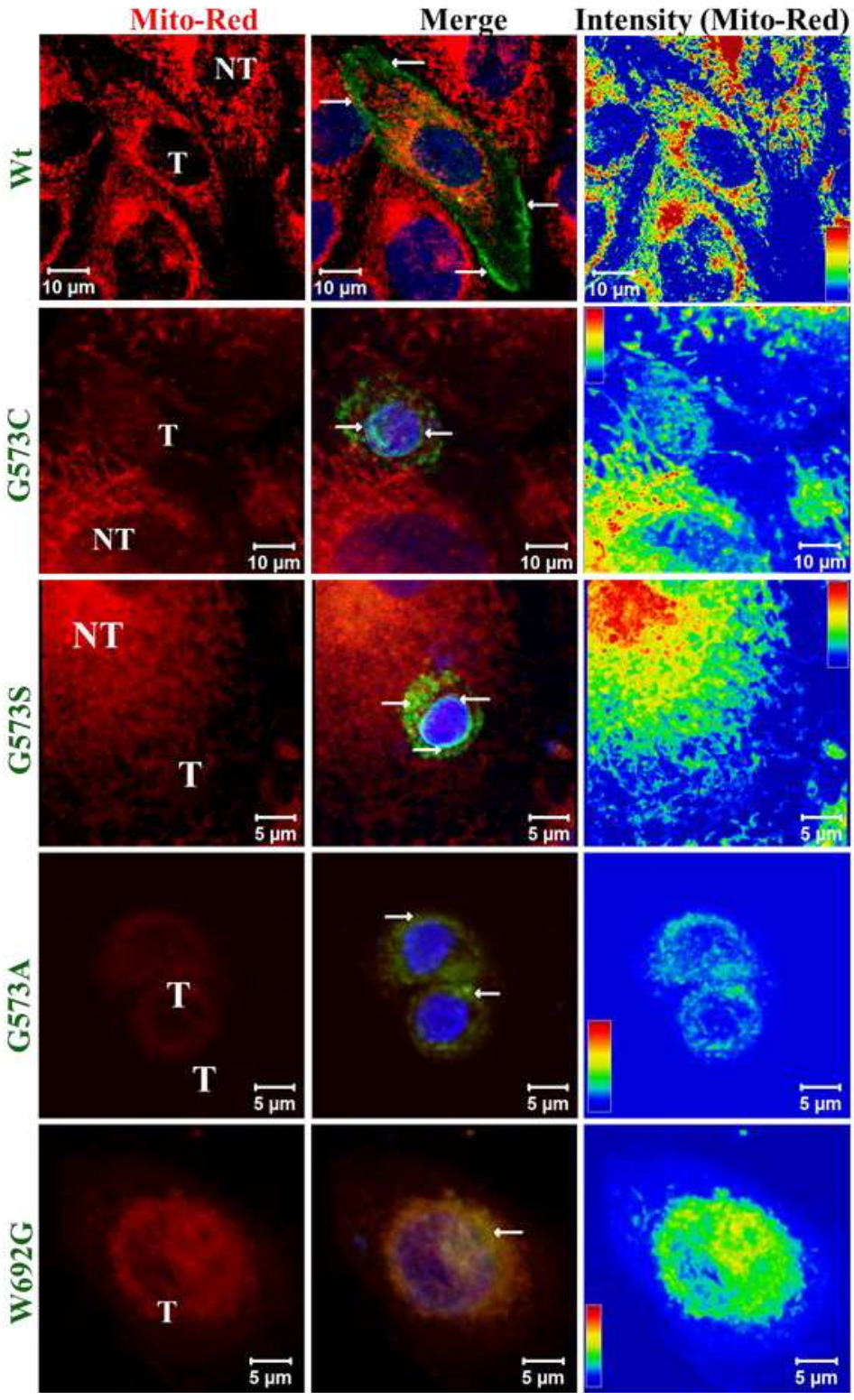

Figure 54. OS-mutants induce impaired mitochondrial distribution: Confocal images of transfected HaCaT cells (T) expressing TRPV3-Wt or OS-mutants (green) labelled with MitoTracker Red (Red). OS-mutant expressing cells reveal either no MitoTracker Red staining or the staining appears as aggregated clusters. Intensity profiles of MitoTracker Red staining are provided in right panel.

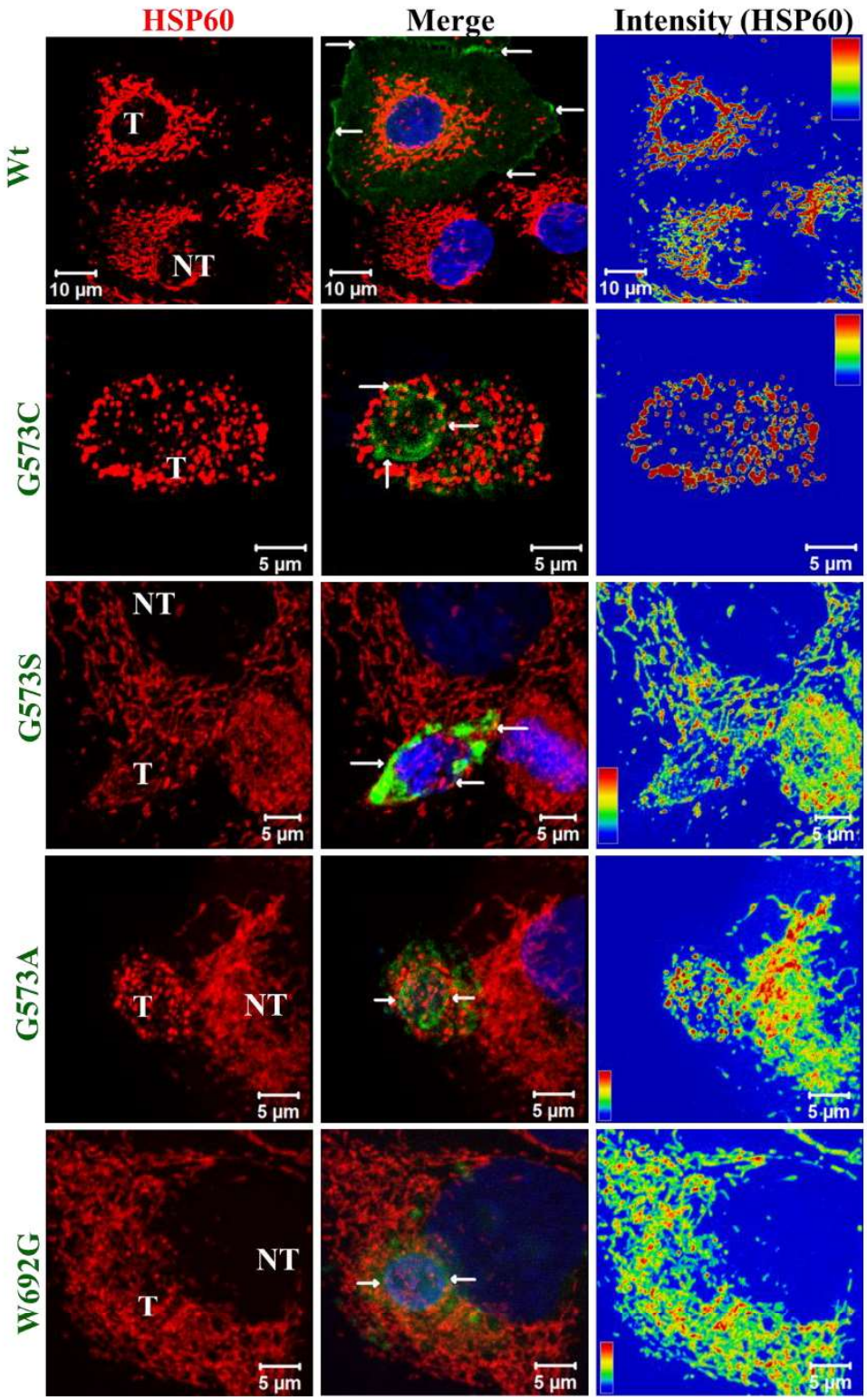

Figure 53. OS-mutants induce impaired mitochondrial distribution: Shown are the confocal images of transfected HaCaT cells (T) expressing TRPV3-Wt or OS-mutants (green) for 36 hours and stained with anti-HSP60 antibody (Red) and DAPI (blue). Non-transfected cells are indicated by NT. Anti-HSP60 staining appears as aggregated clusters in OS-mutant expressing cells. Intensity profile of anti-HSP60 staining is provided in right panel.

mutants, we have prepared the stable line expressing OS mutants and performed functional assays for mitochondria and lysosomes.

We expressed the TRPV3-Wt and OS mutants in HaCaT cells and stained with mitochondrial antibody HSP60 and found that cells expressing OS mutants show aggregated and round shaped mitochondria while cells expressing TRPV3-Wt show normal distribution **(Fig. 53)**. Addition of mitochondrial staining dye MitoTracker Red also labels only few mitochonria in cells expressing OS mutant expressing while TRPV3-Wt expressing cells shows normal distribution and labelling of mitochondria **(Fig. 54)**.

Stable cells expressing TRPV3-Wt or OS mutants were checked for the potentiality of mitochondria through mitochondrial potentiality dye JC1. OS mutant expressing cells show reduced mitochondrial potentiality when compared to Wt expressing cells. Live cell imaging of JC1 reveals that cells expressing TRPV3-Wt have emission in both green (Ex 488/Em 535) and red (Ex 535/Em 590), while mutant expressing cells failed to shows emission in the red region. This confirms that cells expressing OS mutants have mitochondria with reduced mitochondrial potentiality **(Fig. 55a)**. Quantification of stable cells expressing TRPV3-Wt or OS mutants labelled with JC1 show that TRPV3-Wt cells show normal mitochondrial potentiality while mutant expressing cells show significantly reduced mitochondria potentiality **(Fig. 55b)**.

Chapter 2.3: Importance of TRPV3 in Lysosomal functions:

Lysosomal non-functionality has been associated with many pathophysiological disorders. Changes in lysosomal number and shape or altered pH of lysosome leads to the imbalance in the pH of cell. This results in the inhibition of essential physiological processes. Balance of lysosomal and cellular pH is a complex mechanism which is mediated by several ion transporters and pump. Several monovalent and divalent ions like Na^+, Ca^{2+}, K^+, H^+, Cl^- plays crucial role in the regulation of endolysosomal pH regulation. Ion channels, transporters, antiporters and pumps (such as H^+-pump or v-ATPase, CIC-7 antiporter, $H^+/K^+/Na^+$ antiporter, Na^+ channel, K^+ channel, and Ca^{2+} leak channels) act together in order to maintain the cellular pH (Ishida et al., 2013). Other Ca^{2+} channels, namely TPCs are present in the endolysosomal compartments and play a role in endosomal pH regulation.

TRPV3 has importance in the skin morphogenesis and hair growth. Knockout studies show that TRPV3 $^{-/-}$mouse have severe defects in the skin and hair growth. In this chapter, we have tried to explore the presence of TRPV3 in specific subcellular compartment of cell, such as in lysosome and in mitochondria. Presence of TRPV3 in the lysosome provides an indication of its function in the maintenance of lysosomal pH which directly affects the cytoplasmic pH of cell. The findings that TRPV3 is present in lysosomal fraction and mitochondrial fraction from goat brain is therefore important enough. To validate this further, we have identified and characterized the lysosomal targeting sequences of TRPV3. The conserved and functional lysosomal target sequences also reveal the importance of TRPV3 in lysosomal functions.

2.3.1. OS-mutants have altered mitochondrial distribution and function:

Expression of OS mutants lead to the altered distribution of different cell organelles like mitochondria, lysosome golgi and ER. To further validate and explore the effect of OS

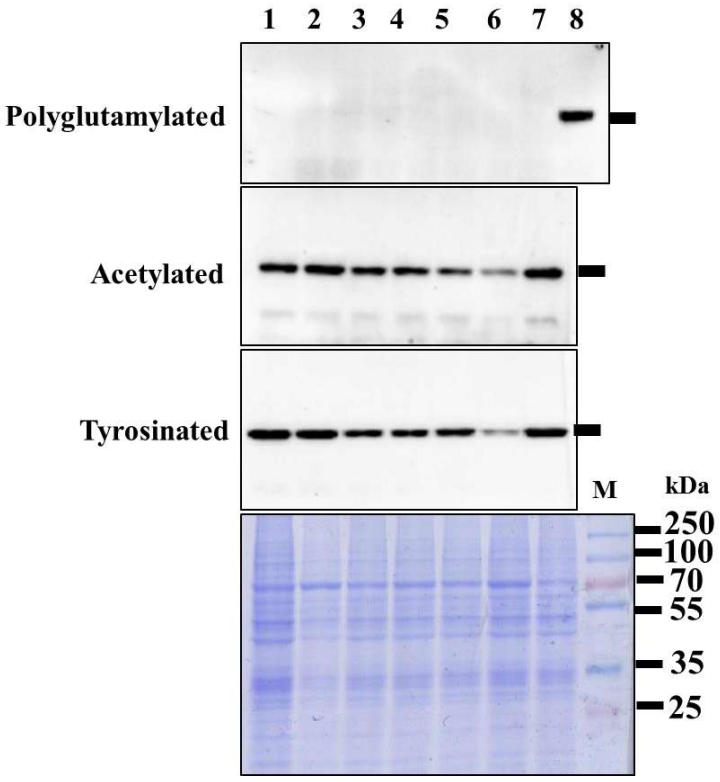

Figure 52. Level of modified tubulin in stable cells expressing OS mutant and Wt: HaCaT cells expressing different OS mutant and Wt were probed with modified tubulin antibodies (acetylated, polyglutamylated, and Tyrosinated). Cells expressing OS mutants show low accumulation compared to nontransfected HaCaT and Wt expressing cells. Lane from (1-8) represents HaCaT control, TRPV3-Wt, TRPV3-G573C, TRPV3-G573S, TRPV3-G573A, TRPV3-W692G, EGFP control and Brain extract respectively.

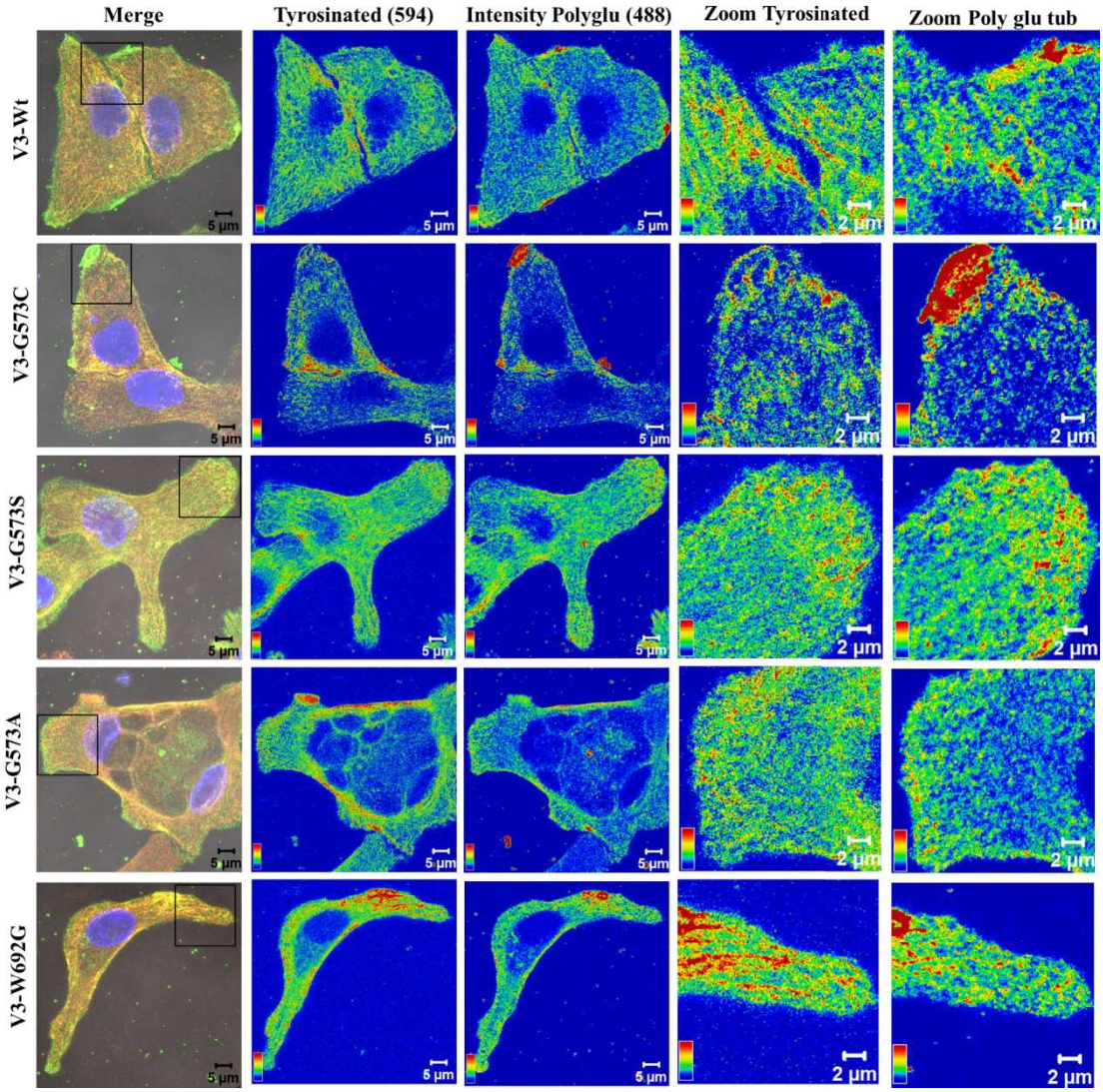

Figure 51. Localization and distribution of modified tubulin in OS mutant and Wt expressing cells: Stable cells expressing TRPV3-Wt or OS mutants were fixed and immunostained for polyglutamylated tubulin (green), tyrosinated tubulin (red) and DAPI imaged with confocal microscope and found that their OS mutant expressing cells shows differential labelling as compared to Wt expressing cells (OS mutant expressing cells show differential labelling of tyrosinated and polyglutamylated tubulin).

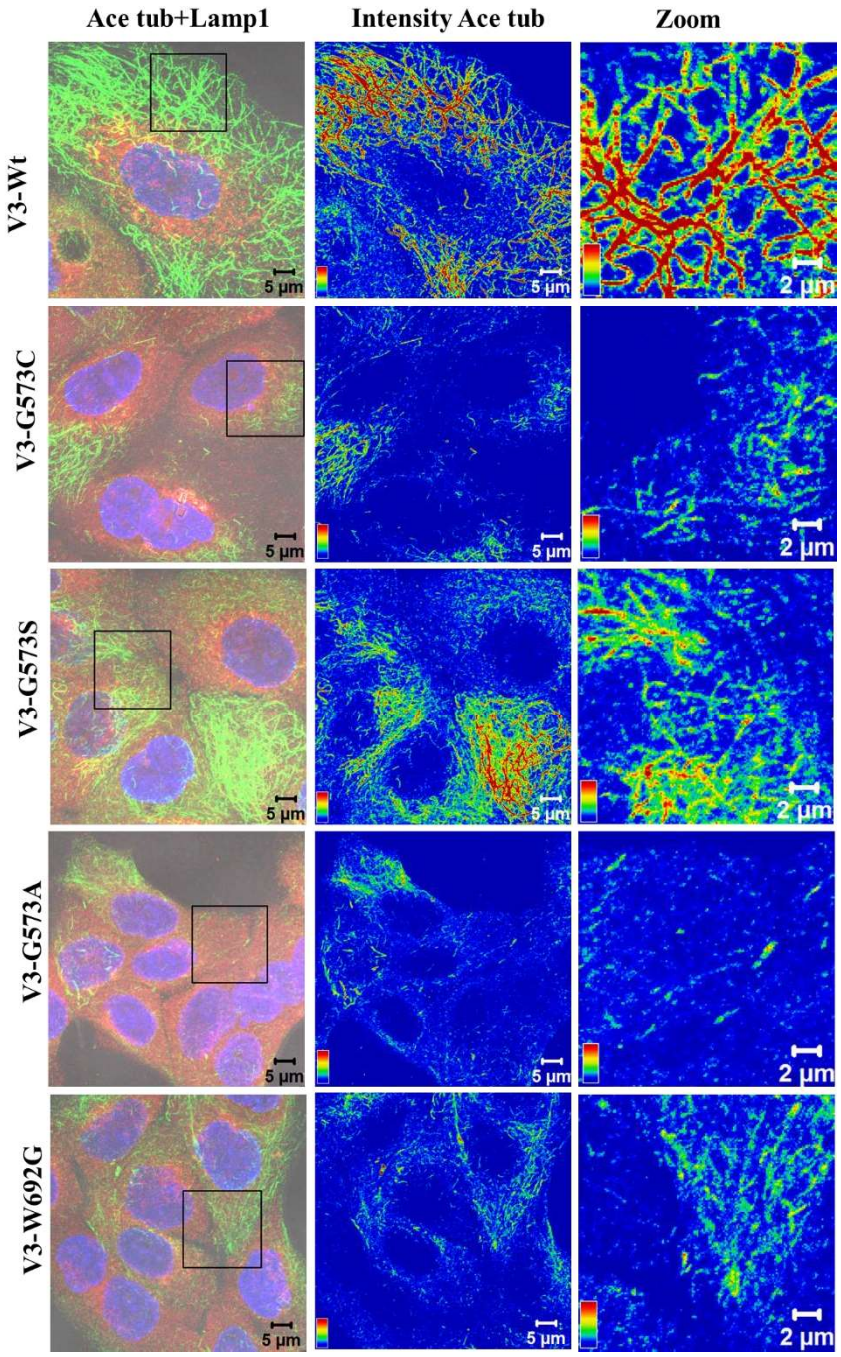

Figure 50. Localization and distribution of modified tubulin in OS mutant and Wt expressing cells: Stable cells expressing TRPV3-Wt or OS mutants were fixed and immunostained for acetylated tubulin and imaged with confocal microscope and found that their OS mutant expressing cells shows differential labelling as compared to Wt expressing cells (OS mutant expressing cells show reduced level of acetylated tubulin).

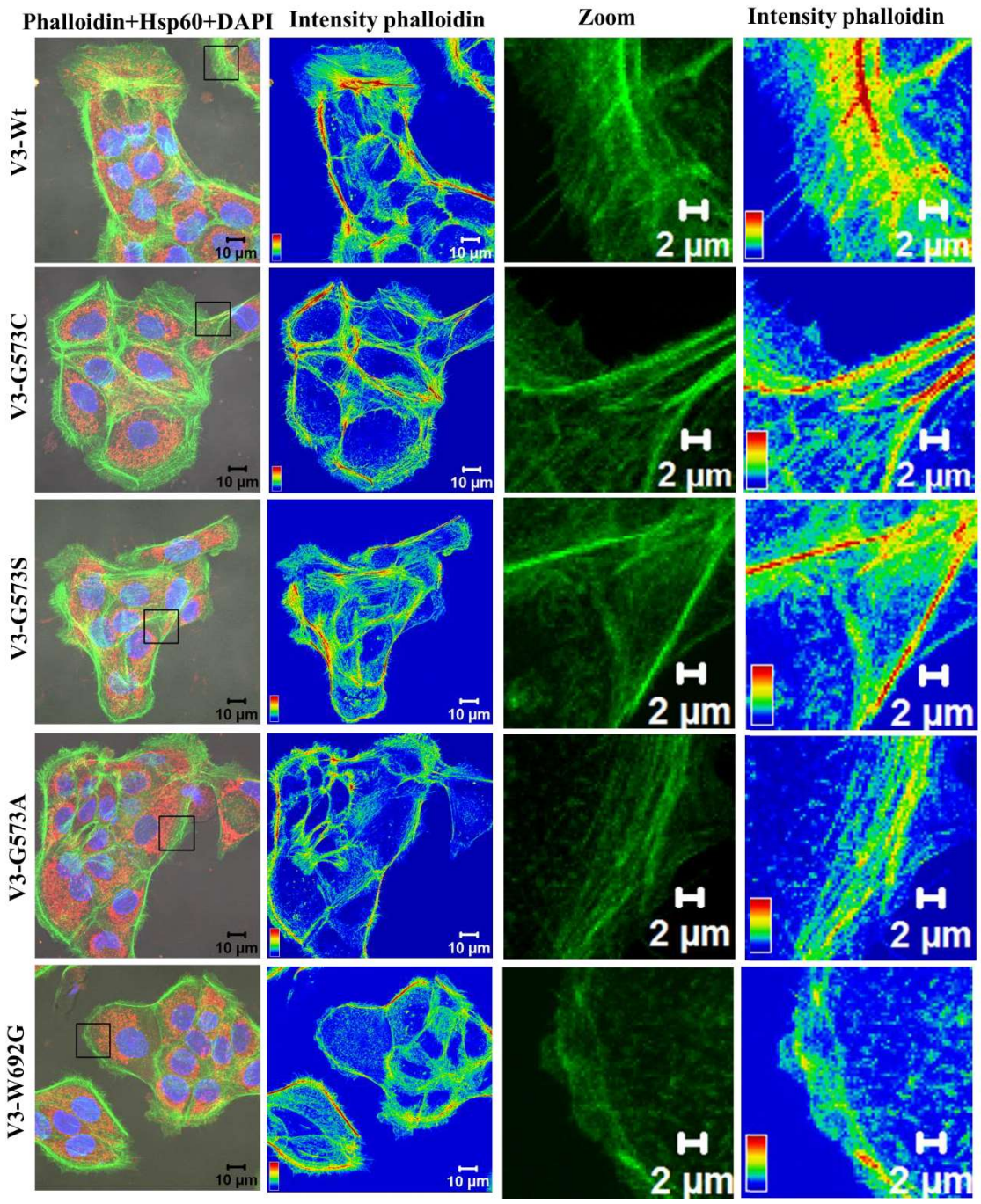

Figure 49. Localization and distribution of actin in OS mutant and Wt expressing cells: Images shown are the fixed stable cells expressing TRPV3-Wt and OS mutants immunostained with Phalloidin (green). Hsp60 (red), and DAPI (blue) Images were acquired with confocal microscope. No significant differences in the labelling and distribution of actin was observed between these stable cells.

In OS conditions, the keratinocyte functions are directly affected. Therefore, through immunofluorescence and western blotting analysis we checked the level and distribution of different modified tubulins in stable cells expressing TRPV3-Wt or different OS mutants. Surprisingly, cells expressing OS mutants show different distribution of tubulin as compared to TRPV3-Wt expressing cells. The immunofluorescence images of Tyrosinated, polyglutamylated, and acetylated tubulin **(Fig. 50-51)** confirm this.

Cell extracts obtained from stable cells expressing TRPV3-Wt or OS mutants were analysed by Western blot analysis with antibodies specific for Tyrosinated, polyglutamylated, and acetylated tubulin. OS mutant expressing cells have differential levels of modified tubulin when compared to TRPV3-Wt expressing cells or nontransfected control cells **(Fig. 52)**.

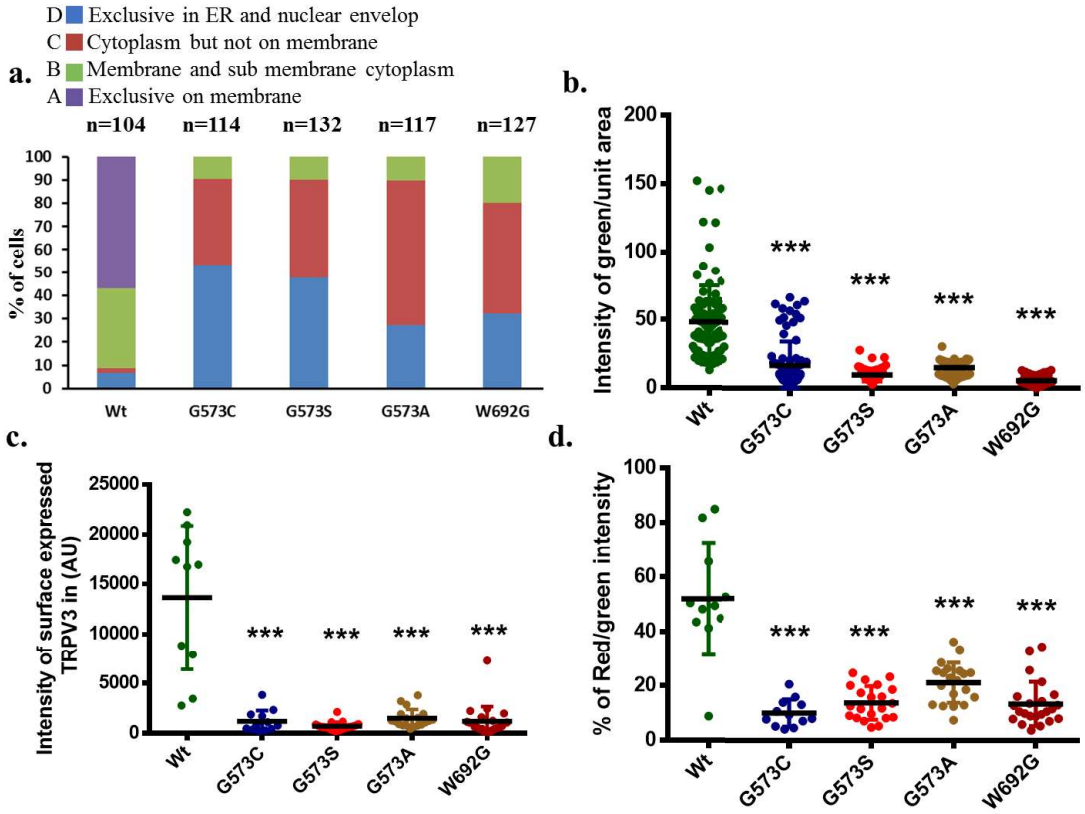

Figure 48. OS mutants reveal reduced surface expression: a. Percentage scoring of cells expressing TRPV3-Wt or OS-mutants are shown. Cells were classified according to the localization of TRPV3, i.e.: exclusively on the membrane (A-type), in membrane and in the sub-membranous region (B-type), in cytoplasm but not on the membrane (C-type), and exclusively in the ER and in nuclear envelop (D-type). TRPV3-Wt is primarily localized on membrane and sub membranous region, while OS mutants are mainly restricted in the ER and in the nuclear envelop. **b.** Shown are the quantification of the amount of TRPV3 present in plasma membrane per unit surface area. Minimum 10 or more region-of-interests (ROI) in the membrane region from individual cells in each group was considered and plotted. **c.** Quantification of the total surface expression of TRPV3 is shown. Amount of TRPV3 present in the surface is quantified by calculating total intensity of TRPV3 in un-permeabilized cells detected by extracellular loop-specific antibody raised against TRPV3. Microscopic images of similar experiments are represented in Fig 1D. **d.** Percentage expression of TRPV3 at the surface is estimated by quantifying the total TRPV3-GFP present in individual cell (considered as 100%) and the amount of TRPV3 that can be labelled by extracellular-loop specific antibody. In each case p value <0.001 is considered as significant [272].

2.2.8. Analysis of distribution and levels of different cytoskeleton components in stable cells expressing TRPV3-Wt or OS mutants:

In order to characterize the levels and distribution of cytoskeleton components in stable cells expressing TRPV3-Wt or OS mutants, we have stained HaCaT cells with Phalloidin. OS mutants expressing cells do not shows any drastic difference in Phalloidin staining when compared to TRPV3-Wt cells **(Fig. 49)**.

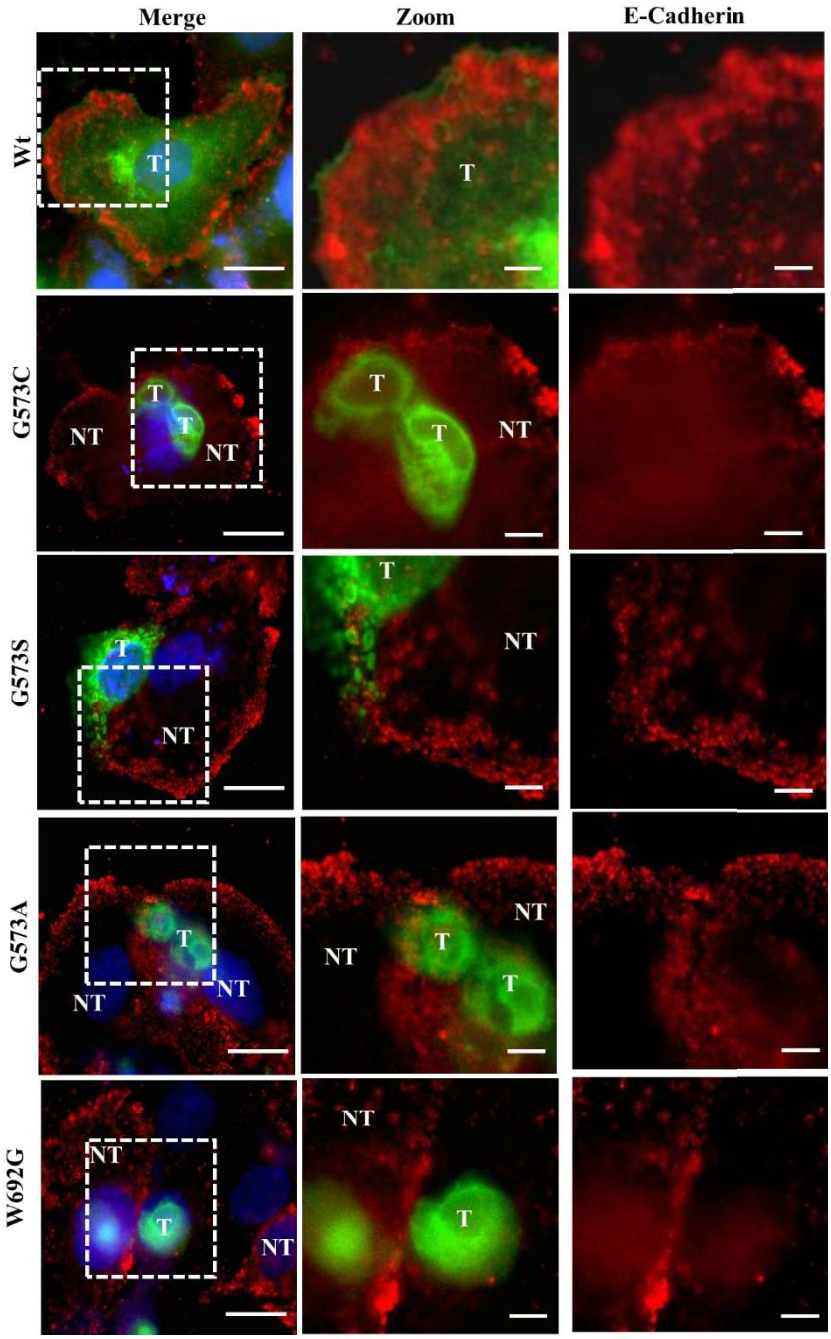

Figure 47. OS-mutants do not localize on membrane: Shown are the fluorescence images of HaCaT cells transiently expressing TRPV3-Wt or OS-mutants. Cells were fixed within 36 hours after transfection and were immunostained for anti E Cadherin without permeabilization. TRPV3-Wt localizes on the membrane and shows E-Cadherin, while OS mutants do not localize on membrane [272].

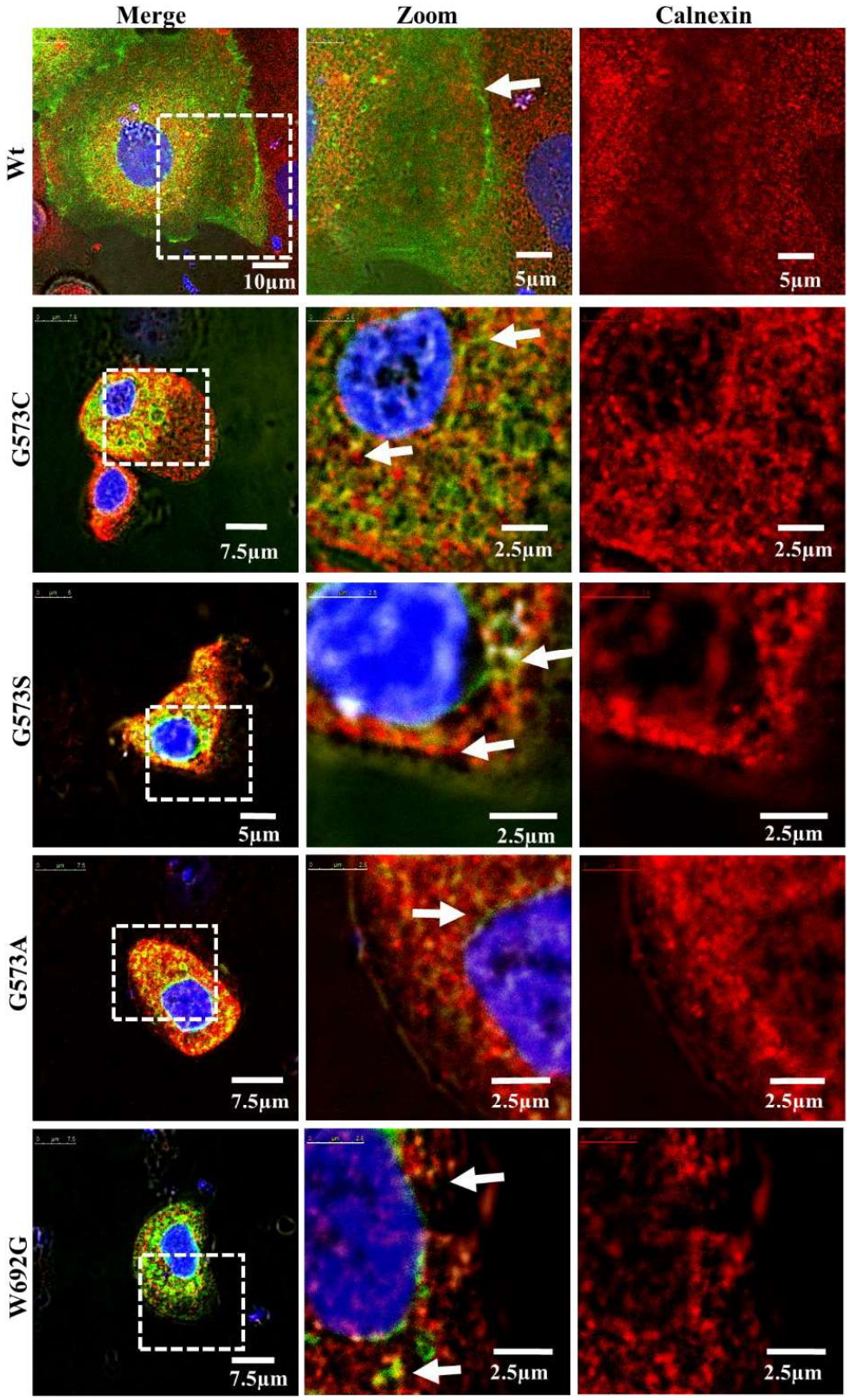

Figure 46. OS-mutants co localize with Calnexin: Shown are the confocal images of HaCaT cells transiently expressing TRPV3-Wt or OS-mutants. Cells were fixed within 36 hours after transfection and the cells were stained for anti-Calnexin antibody. TRPV3-Wt shows discrete ER labelling and TRPV3-Wt localizes on membrane, while OS mutants show colocalization with ER (Merge image) which suggest that OS mutants have reduced surface expression and are mainly retained in ER [272].

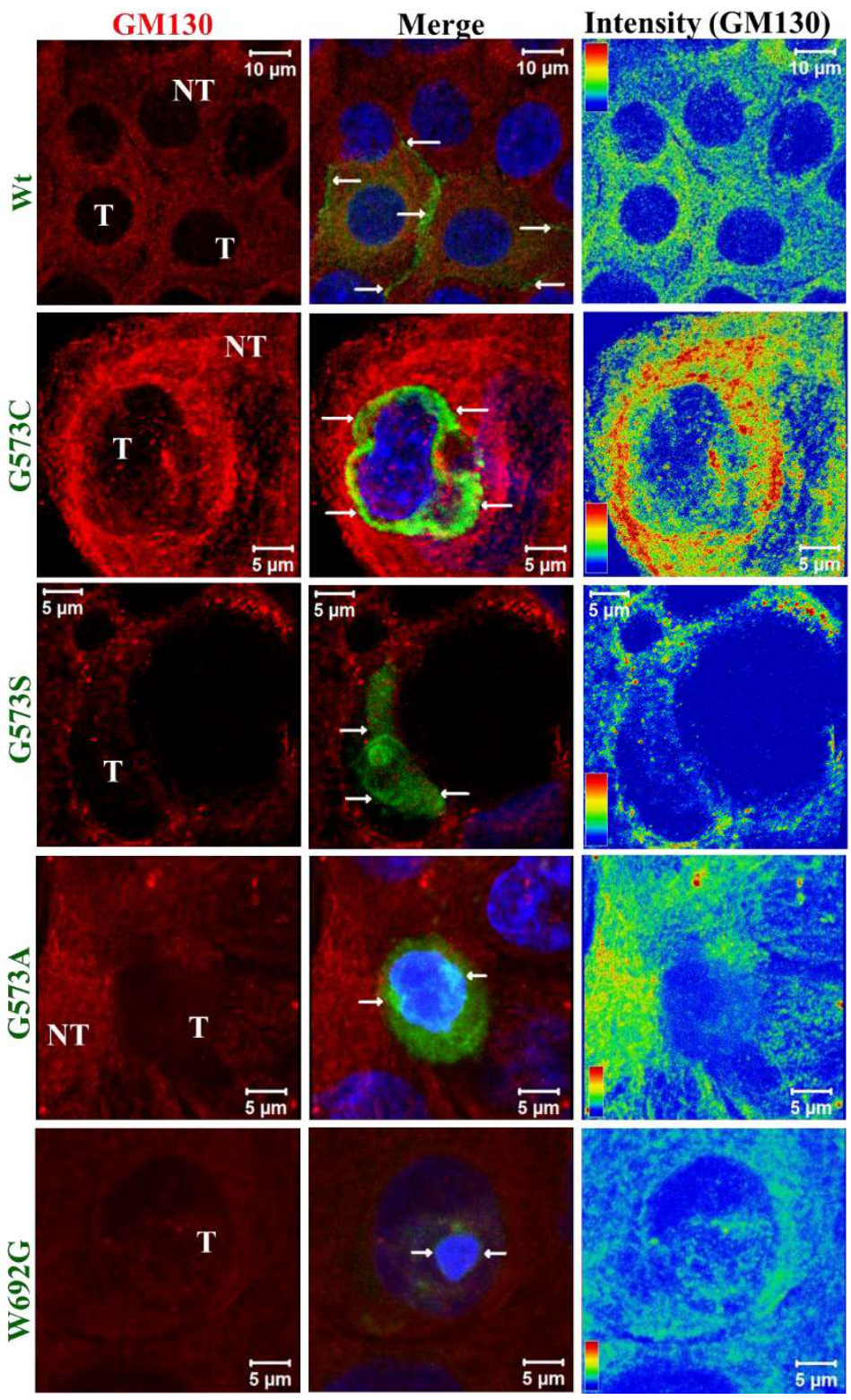

Figure 45. OS-mutants induce impaired Golgi distribution: Confocal images of transfected HaCaT cells (T) expressing TRPV3-Wt or OS-mutants (green) stained with anti-GM130 antibody (a marker for Golgi complex; Red) and DAPI (blue). Anti-GM130 staining either appears as aggregated clusters or no staining at all in OS-mutant expressing cells. Intensity profile of anti-GM130 staining is provided in right panel [272].

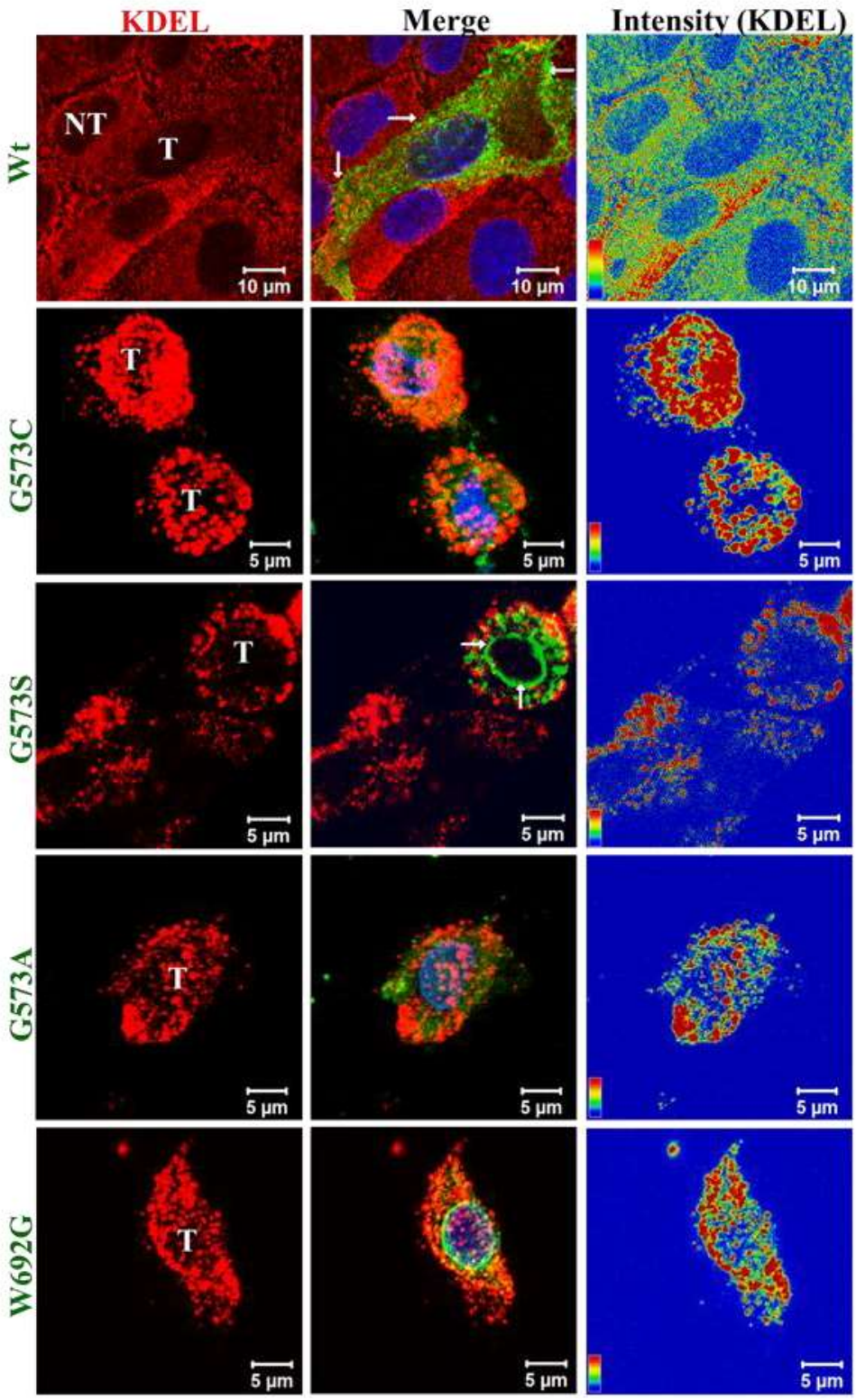

Figure 44. OS-mutants induce impaired ER distribution: Shown are the confocal images of transfected HaCaT cells (T) expressing TRPV3-Wt or OS-mutants (green) for 36 hours and stained with anti-KDEL antibody (a marker for ER-targeted proteins; Red) and DAPI (blue). Anti-KDEL staining appears as aggregated clusters in OS-mutant expressing cells. Intensity profile of anti-KDEL staining is provided in right panel [272].

immunostaining, and the localization of TRPV3 strongly suggest that OS-mutants induce mislocalization of ER-targeted proteins in general and development of aggregated ER.

As OS-mutants are largely accumulated in the ER regions, we explored the vesicular distribution in these cases. We labelled cells with antibody specific for Golgi complex (GM130). We noted that well distributed Golgi bodies in cells expressing TRPV3-Wt **(Fig. 45)**. In contrast, cells expressing OS-mutants show either much reduced levels or clustered Golgi bodies suggesting a general vesicular trafficking problem.

2.2.7. OS-mutants are retained in ER:

To further validate we used an antibody (Calnexin) specific for ER and stained the transfected cells which expressing TRPV3-Wt and OS mutants. The results reveal that TRPV3-Wt expressing cells have discrete staining for ER and TRPV3-Wt localizes on membrane. But all the OS mutants, show co localization with Calnexin in the ER or in fragmented ER which suggest that these mutants are unable to reach plasma membrane **(Fig. 46)**.

We used an antibody as a marker for membrane protein (E cadherin) and demonstrate that TRPV3-Wt is present on plasma membrane while different OS mutant expressing cells do not have GFP signal on their membrane. This confirms that cell expressing OS mutants have altered/reduced membrane trafficking **(Fig. 47)**.

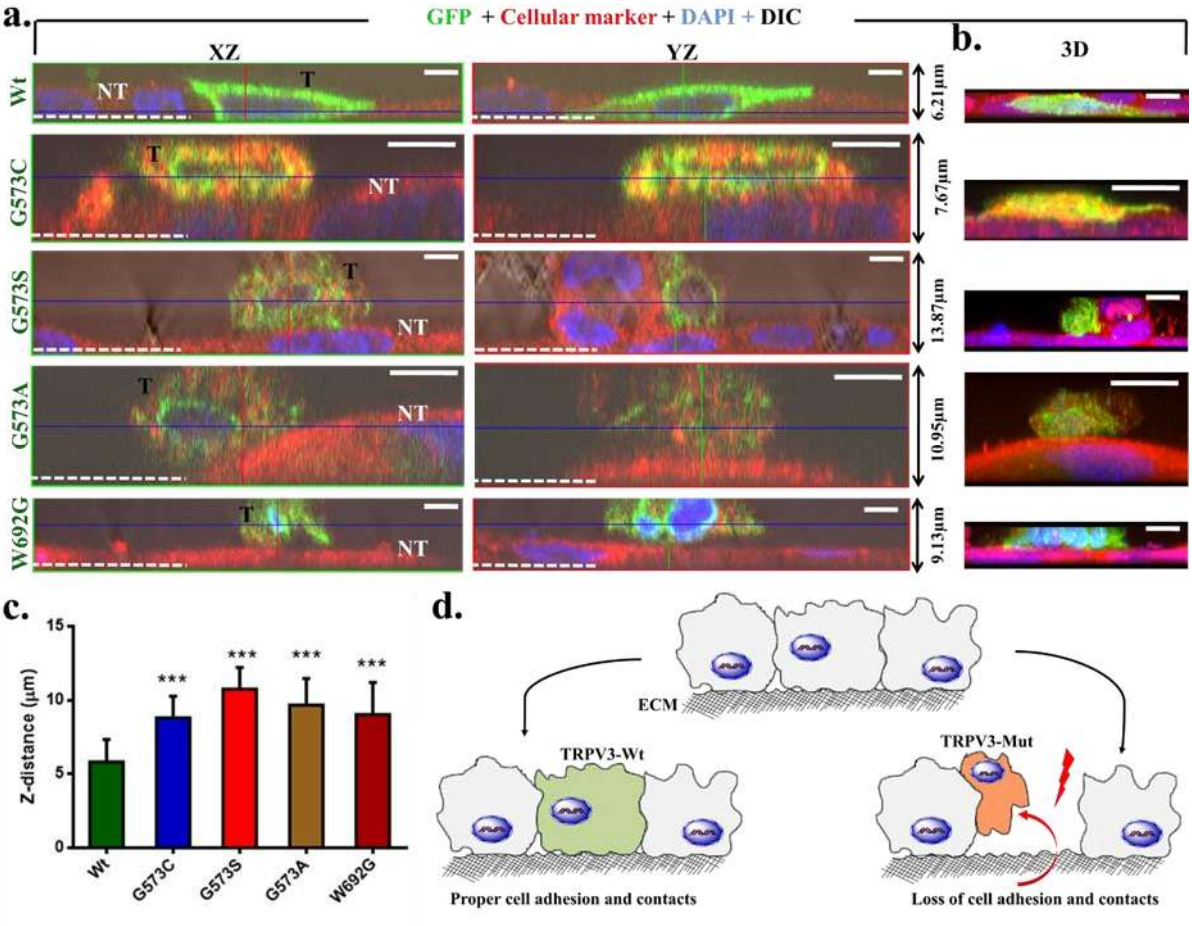

Figure 43. Expression of OS-mutants induce impaired cell adhesion: a. Shown are the XZ, YZ plane and 3D (right panel) confocal images of representative HaCaT cells that express transiently either TRPV3-Wt or OS-mutants. The GFP fluorescence (green) distinguishes the transfected cells (T) from non-transfected (NT) cells (red) and the white dotted line indicate the Z-position of the uncoated glass coverslip. While cells expressing TRPV3-Wt are flat and tightly adhere to the glass surface, the cells expressing OS-mutants are much spherical in shape and are loosely attached to the glass surface and mostly grow on other non-transfected cells. The continuous white line indicates the scale bar (5 µm). **c.** OS-mutants reveal significant increment in Z-distance than the cells that express TRPV3-Wt (n = 20 cells in each case, P-value <0.001). **d.** A schematic diagram demonstrating the loss of cell adhesion and cell-to-cell contacts due to expression of OS-mutants [272].

2.2.6. Expression of OS-mutants alter distribution of ER and Golgi bodies:

As expression of OS-mutants reveal reduced surface localization and are mainly restricted in the perinuclear region, we tested if these mutants cause abnormalities in the ER distribution and functions. For that purpose, we expressed TRPV3-Wt as well as OS-mutants transiently in HaCaT cells and immunostained with KDEL antibody, a marker for ER-targeted proteins. We noted that cells expressing OS-mutants reveal aggregated KDEL staining while cells expressing TRPV3-Wt reveal normal distribution of KDEL staining **(Fig. 44)**. The KDEL

expressing cells. For statistical text we have measured the Z-distance of at least 20 cells. Results indicate that mutant expressing cells have higher Z-distance **(Fig. 43c)**.

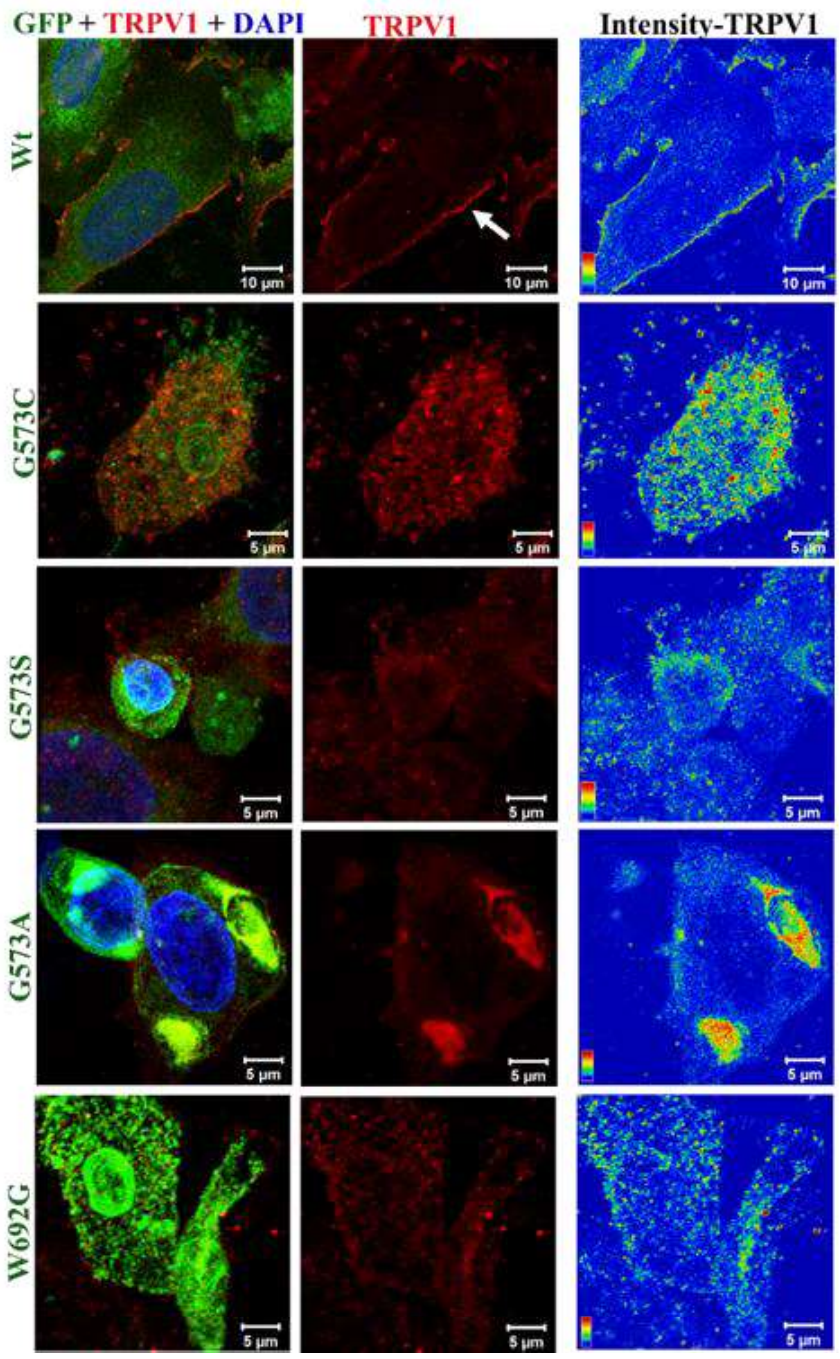

Figure 42. OS-mutants show impaired trafficking for membrane proteins: Shown are the confocal images of HaCaT cells transiently expressing TRPV1 along with either TRPV3-Wt or OS-mutants. Cells were fixed within 36 hours after transfection and the un-permeabilized cells were stained for TRPV1 using an antibody that is raised against extracellular loop of TRPV1. This antibody detects TRPV1 at the surface (red) only in cells expressing TRPV3-Wt but much less or not at all in cells expressing OS-mutants. GFP fluorescence of TRPV3-Wt or OS-mutants is indicated in green and the intensity of the TRPV1 surface expression is indicated in the right panel [272].

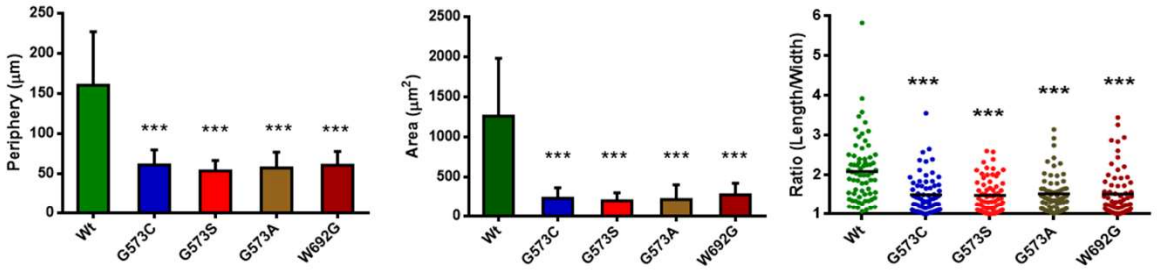

Figure 41. HaCaT cells expressing OS mutants show altered morphology: Cells expressing OS-mutants have much reduced cell periphery, area and are more round in shape (in each case n = 70 cells and p value <0.001 is considered as significant) [272].

2.2.4. OS-mutants affect surface expression of other proteins:

Further characterization of OS inducing mutants reveals that not only TRPV3 mutants have reduced surface expression but these mutants also hamper the surface expression of other proteins as well. To conform that we have co-expressed wild-type TRPV1 along with TRPV3 (Wild type or OS-mutants). We used 5:1 ratio (molar) of plasmid DNA in order to express more TRPV1 and less TRPV3. We noted that after cotransfection of TRPV1 along with TRPV3-GFP, only TRPV3-Wt expressing cells show TRPV1 localization on membrane while OS mutant expressing cells show no surface expression of TRPV1 (TRPV1 is retained mainly in the intracellular regions) **(Fig. 42)**.

2.2.5. OS-mutants affect cell adhesion:

As a consequence of disease, OS patients continue to loose keratin layer from their skin. In this context, we further measured the Z-distance from the glass surface on which cells were grown to the top distance of the cell. We found that TRPV3-Wt cells were flatten in shape and with perfect morphology while OS mutant expressing cells were not attached on the glass surface or loosely attached on the top of non-transfected cells **(Fig. 43a-b)**. As a result, we found that OS mutant expressing cells were having higher Z-distance as compared to the Wt

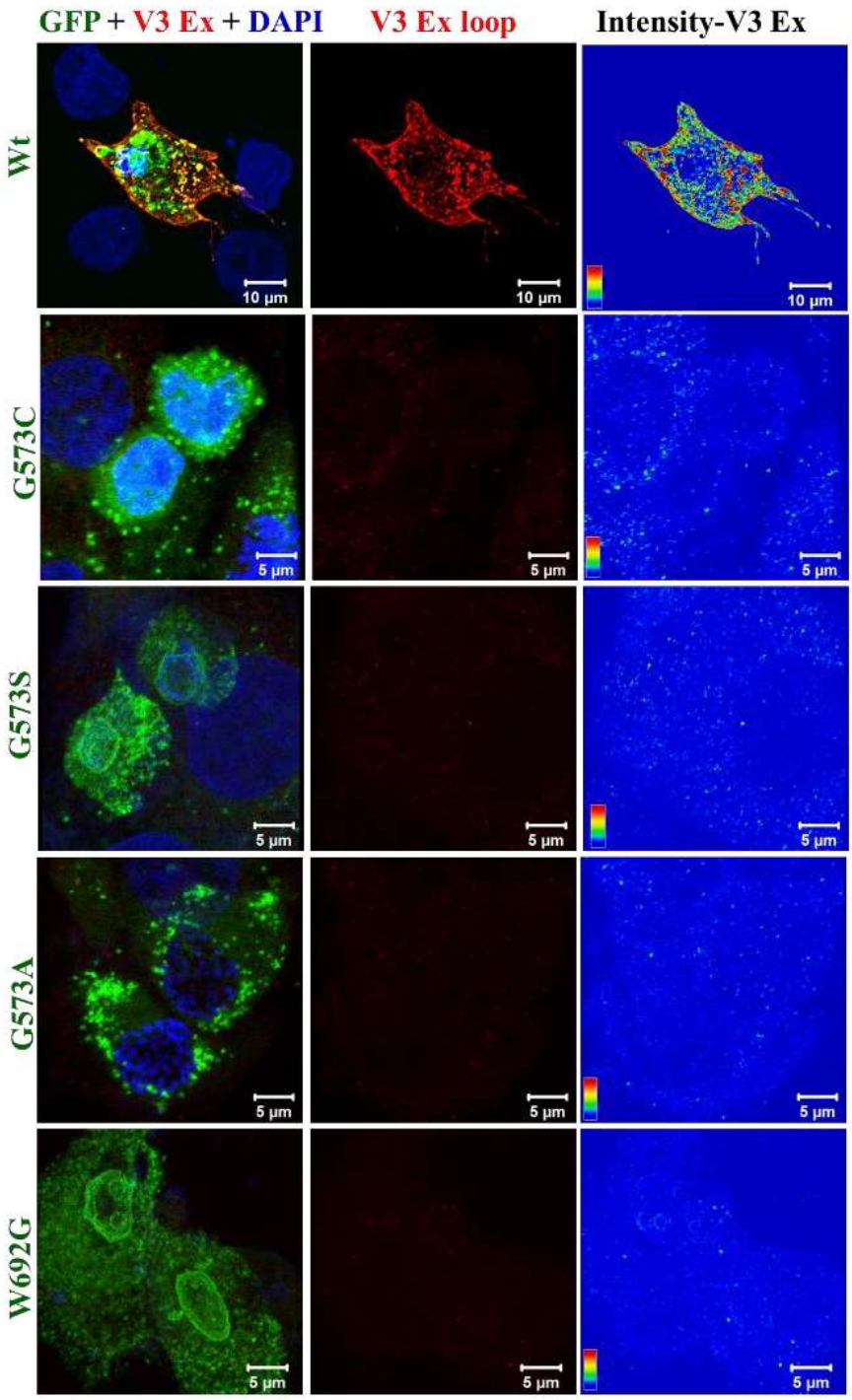

Figure 40. OS-mutants but not TRPV3-Wt have reduced surface expression: Antibody raised against extracellular loop detects TRPV3 available at the cell surface (red) only in un-permeabilized cells. Cells expressing TRPV3-Wt but not OS-mutants reveal presence of TRPV3 at the cell surface. Intensity of TRPV3 stained by this antibody is provided (in Rainbow scale) in the right side [272].

To explore that the surface expression of OS-mutants is indeed reduced, we used an antibody specific for the extracellular loop region of TRPV3 and thus were able to detect the TRPV3 present in the plasma membrane without permeabilizing the cells using an antibody that recognizes the amino acid sequence 464-478 located at the 1st extracellular loop region of TRPV3 (Alomone Lab). This antibody readily detects TRPV3 at the surface of non-permeabilized HaCaT cells transiently expressing TRPV3-Wt-GFP but not in cells expressing the other OS mutants, namely TRPV3-G573S, TRPV3-G573C, TRPV3-G573A and TRPV3-W692G. This antibody did not detect the non-transfected HaCaT cells either, most likely due to no expression or undetectable level of expression of endogenous TRPV3. This result strongly suggests that only TRPV3-Wt-GFP but not the OS-causing mutants are present in the surface (**Fig. 40**).

2.2.3. OS-mutants affects cell size and morphology:

It was observed that OS mutant expressing cells show altered cellular morphology. In order to confirm this changes in cell shape, cell periphery and area of OS mutant expressing cells were calculated. After transfection cells became smaller in size, while TRPV3-Wt expressing cells were flat and normal in shape and size **(Fig. 41)**. This in general suggest problems in terms of vesicular recycling and other cellular functions.

also expressed in HaCaT cells as GFP-tagged proteins (collectively termed as OS-mutants). Unlike the wild type TRPV3, we noted that OS-mutants have much altered cellular distribution and are localized in the perinuclear regions, mainly restricted to the ER and in the nuclear envelope **(Fig. 39)**.

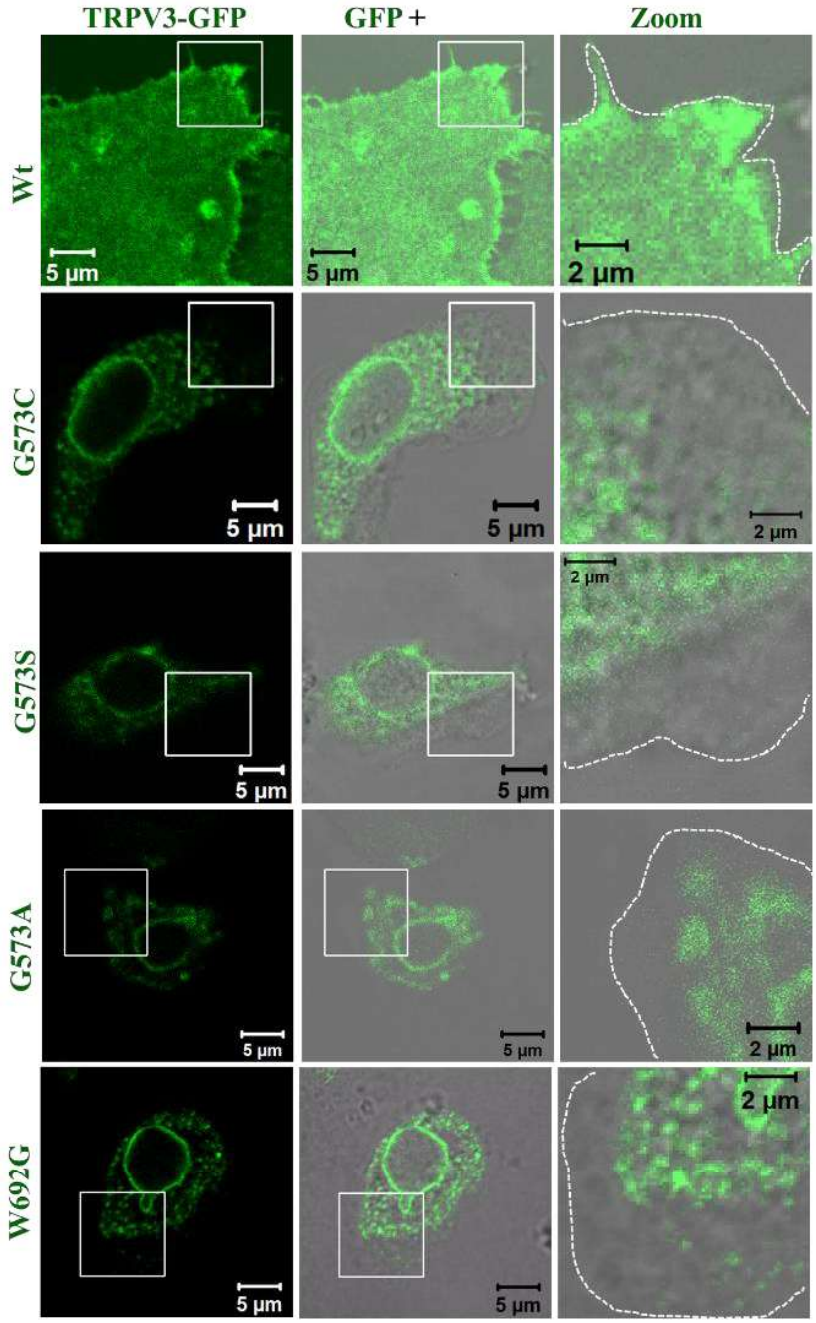

Figure 39. OS-mutants but not TRPV3-Wt have reduced surface expression: Shown are the confocal images of HaCaT cells transiently expressing TRPV3-Wt and different OS-mutants. The GFP fluorescence (green) alone or merged with DIC are shown. These OS-mutants show no localization at the cell surface and accumulate at the ER. Dotted lines show the boundary of the transfected cells [272].

view. All these mutants are constitutive active as a result they allow continuous flux of ions across the membrane.

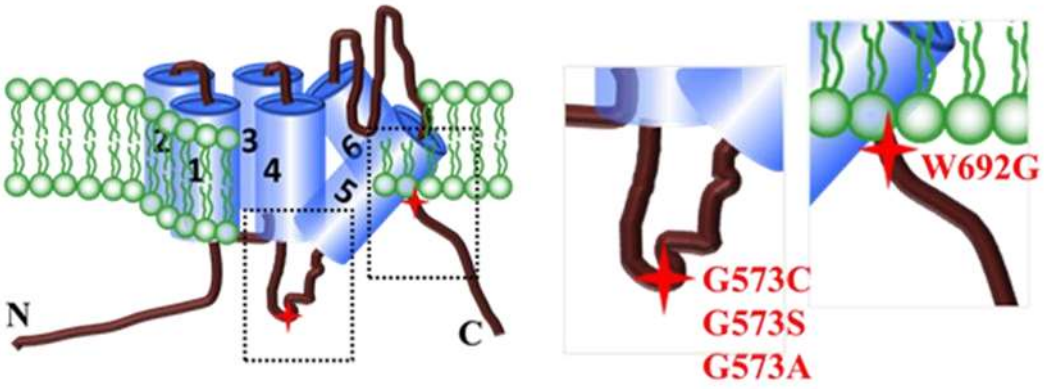

Figure 37. Schematic representation of TRPV3 protein and *Olmsted Syndrome* point mutation: Cartoon representation of TRPV3 protein in the membrane and enlarge view shows four-point mutations, namely G573A, G573S, G573C and W692G [272].

2.2.1. Wild type TRPV3 is localizes at cell-cell contact sites in keratinocytes:

To characterize the hTRPV3-Wt in relation to keratinocyte function we transfected GFP tagged hTRPV3 in keratinocyte derived cell line HaCaT and found that TRPV3-Wt is enriched at cell-cell contact sites and plasma membrane **(Fig. 38)**.

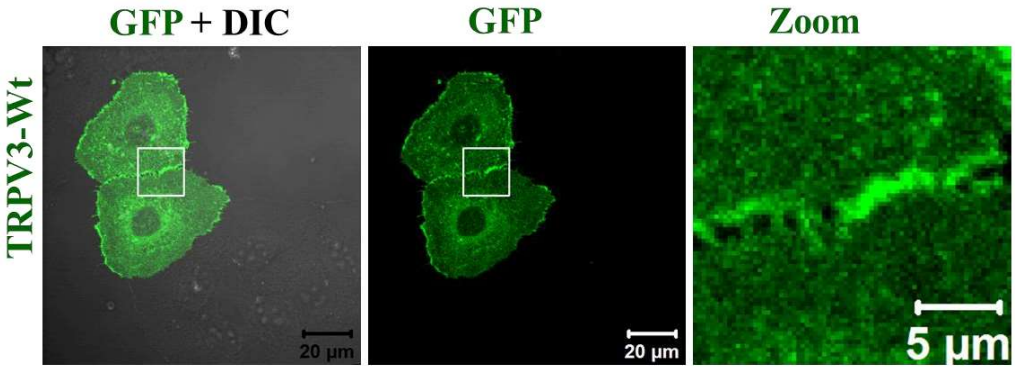

Figure 38. TRPV3-GFP localize on membrane and cell-cell contact sites: Shown are the 3D-reconstituted confocal images of HaCaT cells transiently expressing TRPV3-GFP, the enlarged image demonstrates the presence of TRPV3 at cell-cell contact sites [272].

2.2.2. OS-mutants have reduced surface expression:

To explore the localization pattern of these TRPV3 mutants, full-length TRPV3 carrying the following point mutations individually: G573S, G573C, G573A and W692G were

Chapter 2.2: Characterization of TRPV3 mutants leading to OS:

(This chapter has been published as a manuscript: Yadav M, Goswami C. (2016) TRPV3 mutants causing *Olmsted Syndrome* induce impaired cell adhesion and nonfunctional lysosomes. *Channels (Austin)*. 18:1-13.**)**

Importance of TRPV3 protein in skin and hair morphogenesis is well established. Recently there are several reports which suggest that TRPV3 is essential for normal functioning of the cells and any point mutation in TRPV3 leads to severe pathophysiological conditions known as *Olmsted Syndrome*. Previously apart from TRPV3 gene several other gene have been associated with *Olmsted Syndrome*, LOR gene has been implicated in the pathogenesis of several hereditary diseases with mutilating *Palmoplantar Keratoderma* (PPK), a disorder which has certain similarity with *Olmsted Syndrome*. Notably, LOR gene codes for loricrin which is main component of the cornified cell envelop present in terminally differentiated epidermis, and it is also associated with inherited skin diseases such as with *Vohwinkel's Syndrome* and progressive symmetric erythrokeratoderma. However, specific screening studies have failed to detect any mutations in LOR gene in *Olmsted Syndrome* patients. No mutations have been detected in three other important genes namely KRT1 (Keratin 1), GJB2 (Gap junction protein beta 2) and SLURP1 (Secreted Ly-6/uPAR-related protein 1); which are otherwise involved in other skin related problems. However, it has been demonstrated that a missense mutation in membrane bound transcription factor protease site 2 (MBTPS2) is involved in the development of *Olmsted Syndrome*, though the exact molecular mechanisms remain uncharacterized. In this regard, involvement of TRPV3, which acts as a non-selective cation channel is highly significant. Though involvement of other candidate's genes in the *Olmsted Syndrome* pathophysiology cannot not ruled out at this stage.

In **(Fig. 37)** shows the schematic representation of TRPV3 protein with six transmembrane segments in membrane with intracellular N and C terminus. Olmsted mutants present in loop four (G573C, G573S, G573A) and TRP box (W692G) are depicted in enlarge

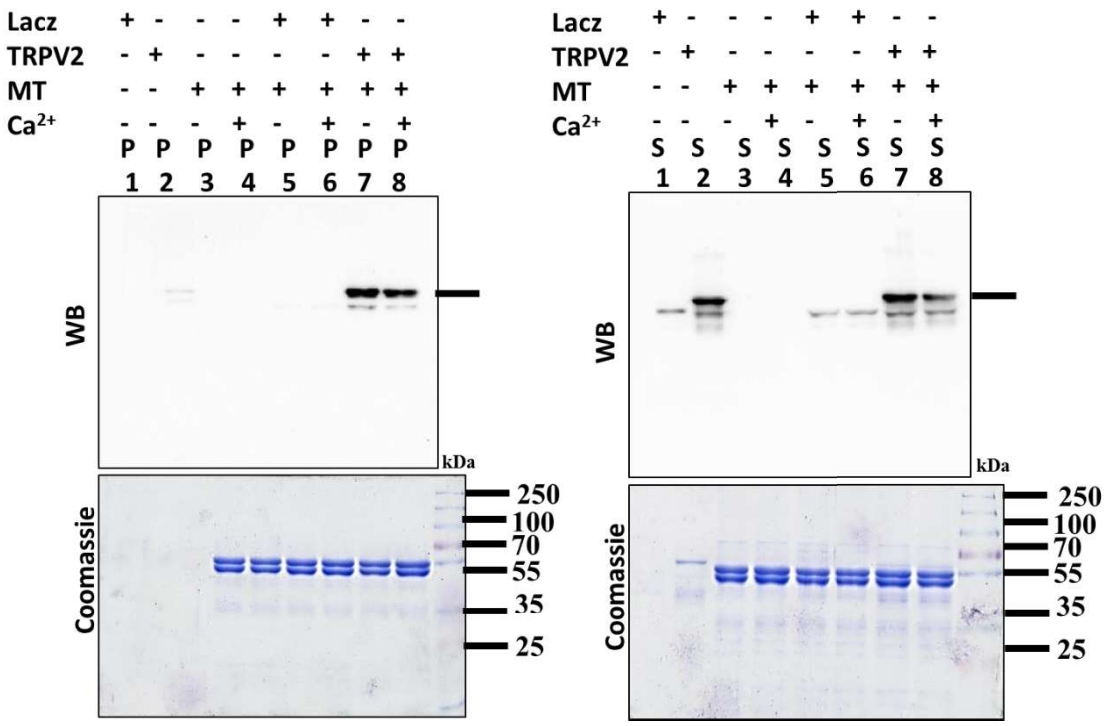

Figure 36. TRPV2-Ct co-sediments with microtubule: Tubulin dimers were incubated with GTP for polymerization. During this incubation, 2µg of MBP-LacZ or TRPV2-Ct were added in presence and absence of Ca^{2+} (1mM). Supernatant (**S**) and pellet (**P**) were separated by centrifugation and analysed by 10% SDS-PAGE. Proteins presence has been checked by Coomassie brilliant blue. Upper panel represents the Western blot and lower panel represents Coomassie brilliant blue staining. MBP-TRPV2-Ct co-sediments with polymerised microtubule. Western blot with anti-MBP antibody detects the MBP-tagged proteins mainly in the pellet fractions.

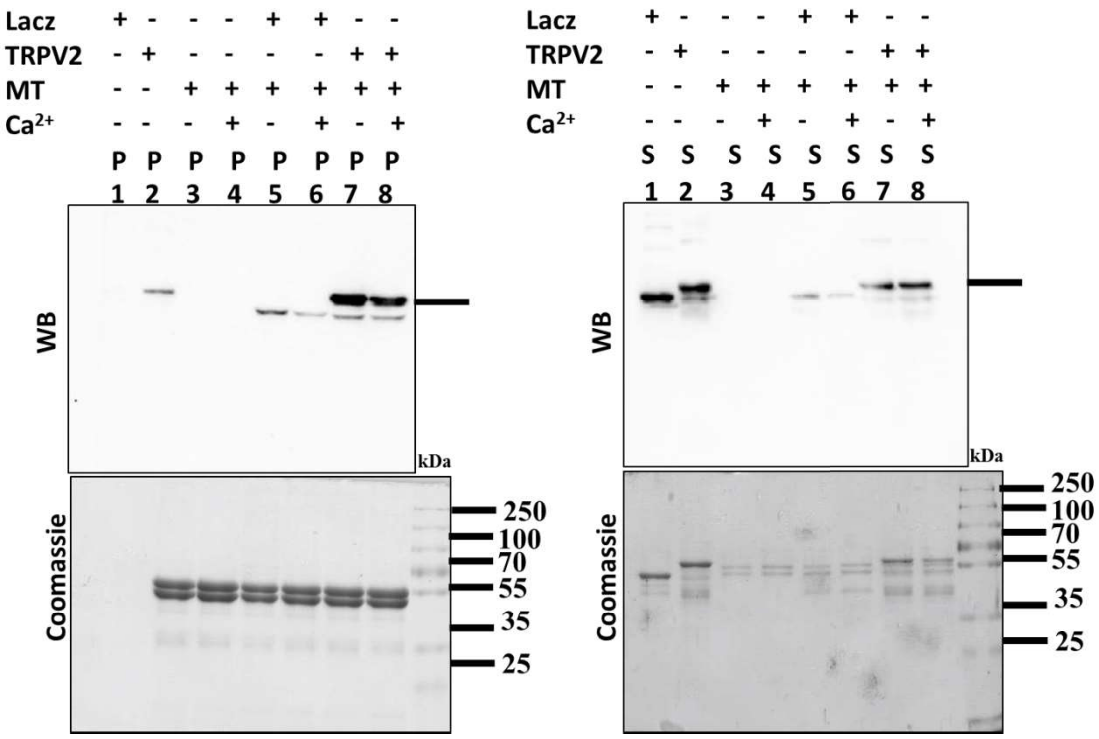

Figure 35. TRPV2-Ct co-sediments with Taxol-stabilized and polymerized microtubule: Microtubule dimers were incubated with Taxol and GTP for polymerization. Followed by incubated with 2µg of proteins MBP-LacZ and TRPV2-Ct in presence and absence of Ca^{2+} (1mM). Supernatant (**S**) and pellet (**P**) were separated by centrifugation and analysed by 10% SDS-PAGE. Proteins presence has been checked by Coomassie brilliant blue (CBB). Upper panel represents the Western blot suggest that TRPV2-Ct co-sediments with polymerised microtubule. Western blot with anti-MBP antibody detects in pellet fraction.

To further confirm TRPV2-Ct and microtubule interaction we perform another co-sedimentation experiment during polymerization of microtubule. Microtubule formation was initiated by adding GTP in absence of Taxol in the soluble tubulin dimers (90 µg). This was followed by adding MBP-LacZ and MBP-TRPV2-Ct (10 µg) on the same time on tubulin dimers, in presence and absence of Ca^{2+}. Polymerized microtubule along with bound proteins were separated through centrifugation. Centrifuged (supernatant and pellet) fractions were separated and analyzed through SDS-PAGE and by Western blot. For detection of the proteins, anti-MBP antibody was used. Western blot analysis reveals that MBP-TRPV2-Ct is mainly present in the pellet fraction along with polymerized microtubule. While we could detect very less MBP reactivity in the supernatant fraction. This data suggests that TRPV2-Ct interact directly with the polymerized microtubules, at least in this experimental condition **(Fig. 36)**.

MBP antibody. Western blot analysis reveals that MBP-TRPV2-Ct was majorly present in the pellet fraction (around 70%) along with polymerized microtubule. While we could also detect MBP reactivity in the supernatant fraction. This data suggests that TRPV2-Ct interacts with polymerized form of tubulins **(Fig. 35)**.

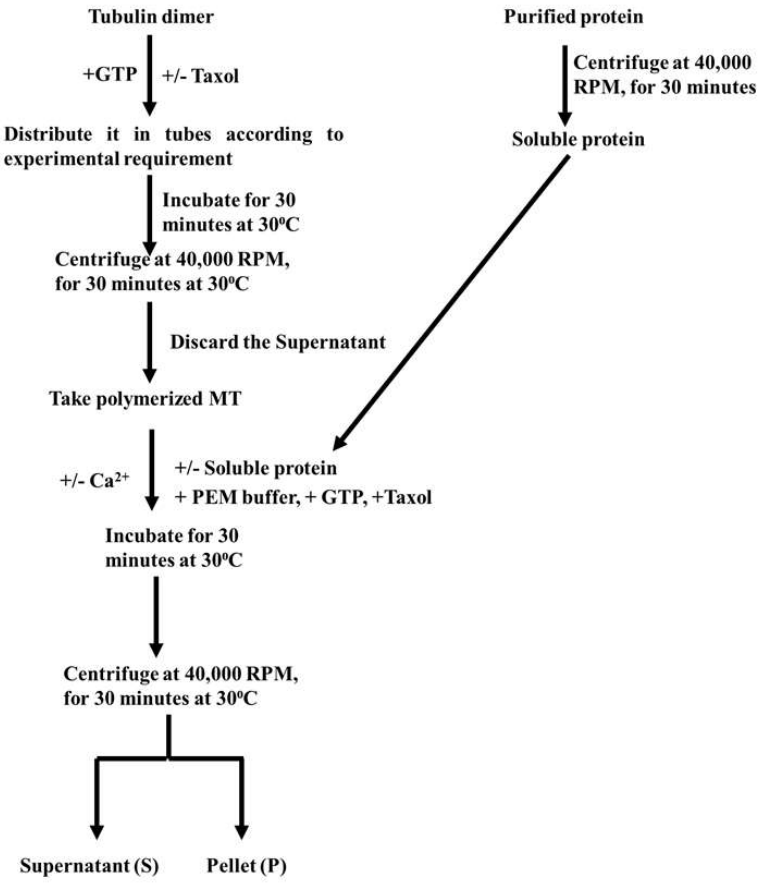

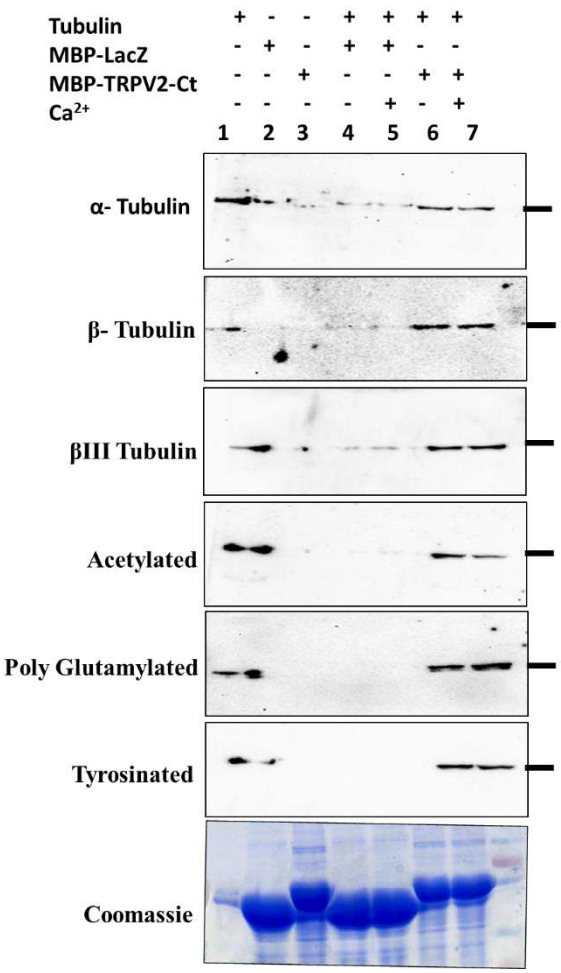

Figure 34. Direct pull down of TRPV2-Ct with purified tubulin: MBP-TRPV2-Ct immobilized on amylose beads are incubated with purified tubulin in presence or absence of Ca^{2+} (1 mM). All bound proteins were eluted with 20 mM maltose, subjected to 10% SDS-PAGE, and probed for different modified tubulins with specific antibodies. Lower image Coomassie brilliant blue shows loading control.

2.1.20. TRPV2-Ct co-sediment with Taxol-stabilized and polymerized microtubule:

In order to further confirm the interaction of TRPV2-Ct and tubulin we performed a co-sedimentation assay. Microtubule formation was initiated by adding GTP in presence of Taxol in the soluble tubulin dimers. Followed by adding the MBP-LacZ and MBP-TRPV2-Ct on the polymerized microtubules in presence and absence of Ca^{2+}. Polymerized microtubule along with bound proteins were separated through centrifuge. Centrifuged (supernatant and pellet) fractions were separated through SDS-PAGE and analyzed through western blot by using anti

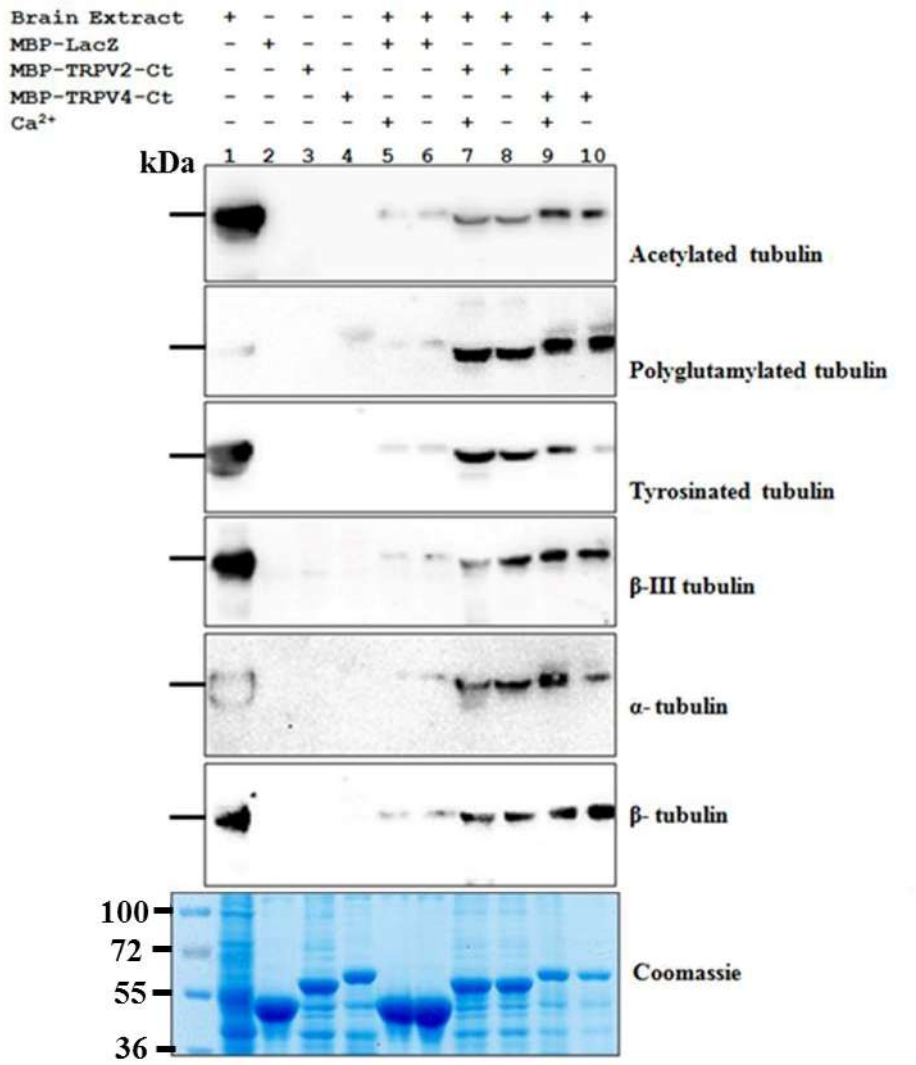

Figure 33. C-terminal cytoplasmic domain of TRPV2 interacts with different tubulins: MBP-TRPV2-Ct immobilized on amylose beads are incubated with goat brain extract in presence or absence of Ca^{2+} (1 mM). All bound proteins were eluted with 20 mM maltose, subjected to 10% SDS-PAGE, and probed for different modified tubulins with specific antibodies. Lower image Coomassie brilliant blue shows loading control. MBP-TRPV4-Ct is used as a positive control.

2.1.19. TRPV2-Ct directly interacts with tubulin and other modified tubulin:

Pull down assay from goat brain reveals that TRPV2-Ct interacts with tubulin and different form of modified tubulin. In order to find out if it is a direct interaction, we did a pull-down assay with purified tubulin dimer and TRPV2-Ct. samples were probed with different modified tubulin antibody for western blot analysis. Our results reveal that α- tubulin, β-tubulin, acetylated tubulin, polyglutamylated tubulin and Tyrosinated tubulin and β-III tubulin was successfully pull down along with TRPV2-Ct. **(Fig. 34)**.

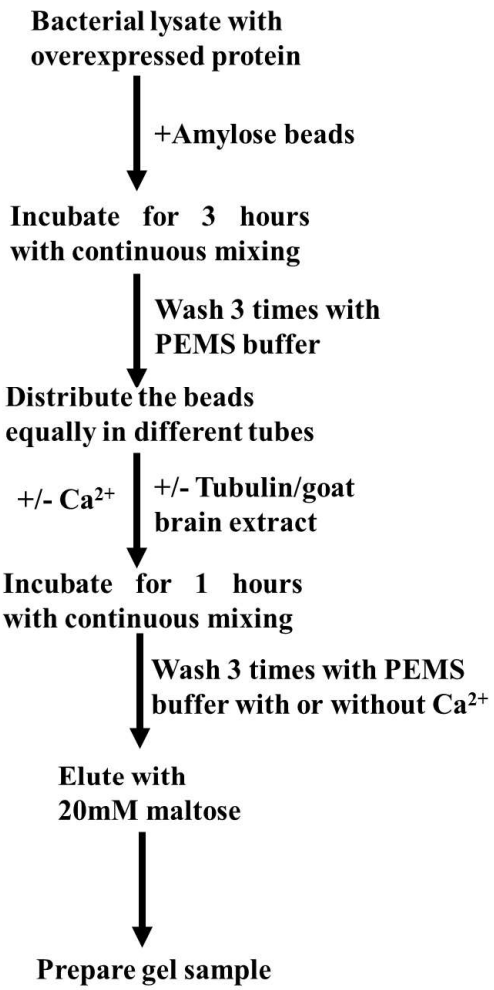
Bacterial lysate with overexpressed protein
+Amylose beads
Incubate for 3 hours with continuous mixing
Wash 3 times with PEMS buffer
Distribute the beads equally in different tubes
+/- Ca2+
+/- Tubulin/goat brain extract
Incubate for 1 hours with continuous mixing
Wash 3 times with PEMS buffer with or without Ca2+
Elute with 20mM maltose
Prepare gel sample

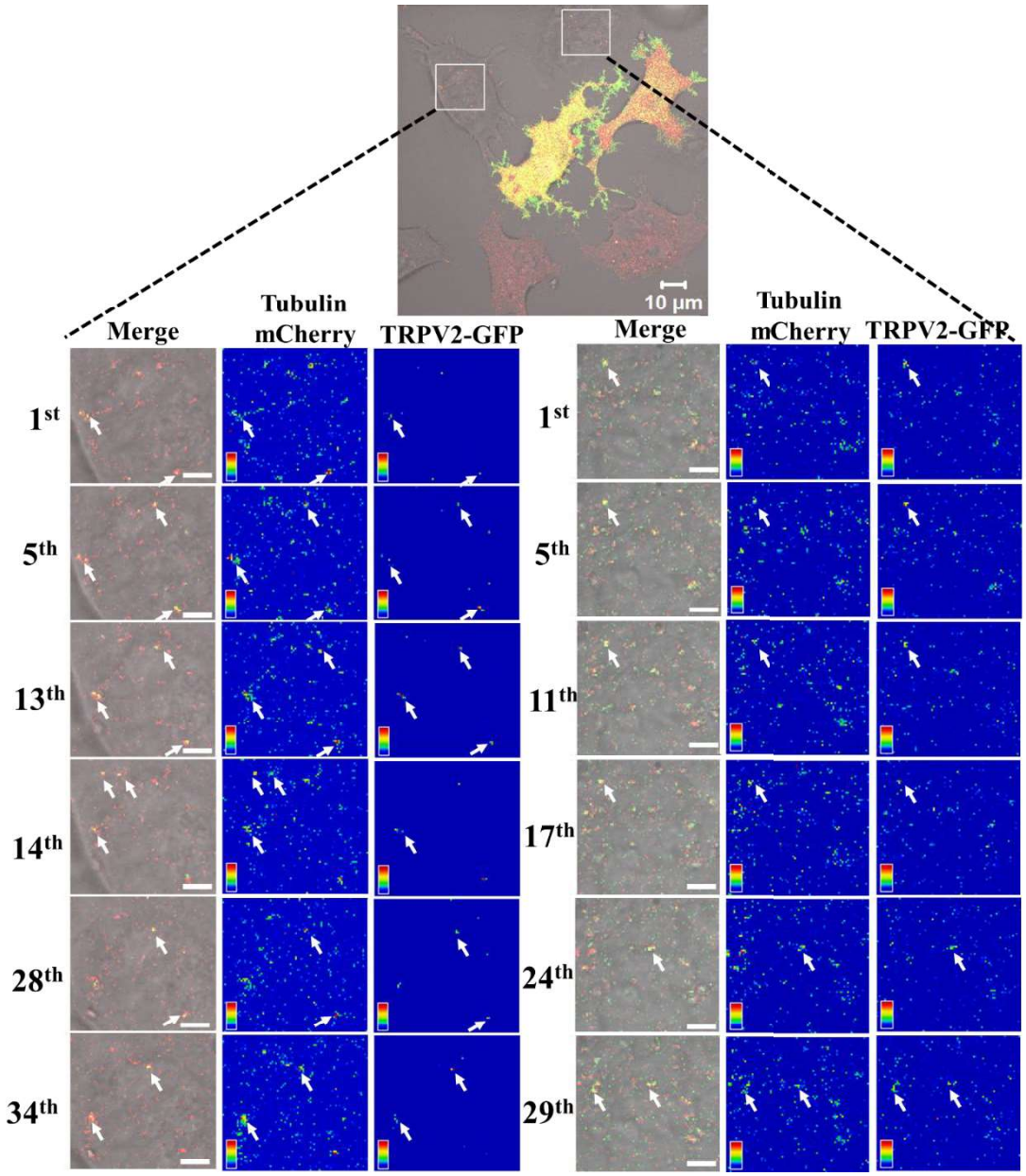

Figure 32. TRPV2-GFP colocalizes and comigrates with tubulin-mCherry: Representative confocal images of live F11 cells transfected with TRPV2-GFP (green) and tubulin-mCherry (red). Time series image shows that both tubulin-mCherry and TRPV2-GFP colocalizes. Both proteins colocalizes in small particle-sized structures and comigrates together even in cells that express both proteins in low levels. Lower panel shows the zoomed image. (Scale bar 2µm).

2.1.17. Co-migration of TRPV2 with tubulin-mCherry in F11 cells:

In order to explore further TRPV2 and tubulin crosstalk, we performed live cell imaging in F11 cells after expressing both TRPV2-GFP and tubulin-mCherry. Live cell imaging experiments show colocalization of TRPV2-GFP and tubulin. To rule out the possibilities if possible artefact of over expression, we analyzed cells with very low level of expression. In low expressing cells too, we found both TRPV2 and tubulin colocalize in small vesicle-like structures and both proteins comigrate along with such entities in spatiotemporal manner **(Fig. 32)**.

2.1.18. TRPV2-Ct interacts with tubulin and different modified tubulin:

Immunofluorescence images and live cell experiment suggest that TRPV2 and cytoskeleton element (tubulin) may interact physically with each other. In order to find out whether TRPV2 interacts with tubulin or not we expressed MBP-TRPV2-Ct and did a pull-down assay with goat brain extract for possible interacting partner **(Fig. 33)**.

Samples were probed for different tubulin antibodies. It was found that TRPV2-Ct interacts with α tubulin, β tubulin, and neuronal marker β III tubulin, both in presence and absence of Ca^{2+}. Apart from this several modified tubulins, such as Acetylated tubulin, Polyglutamylated tubulin, and Tyrosinated tubulin interact with MBP-TRPV2-Ct in both Ca^{2+} dependent and independent manor **(Fig. 33)**.

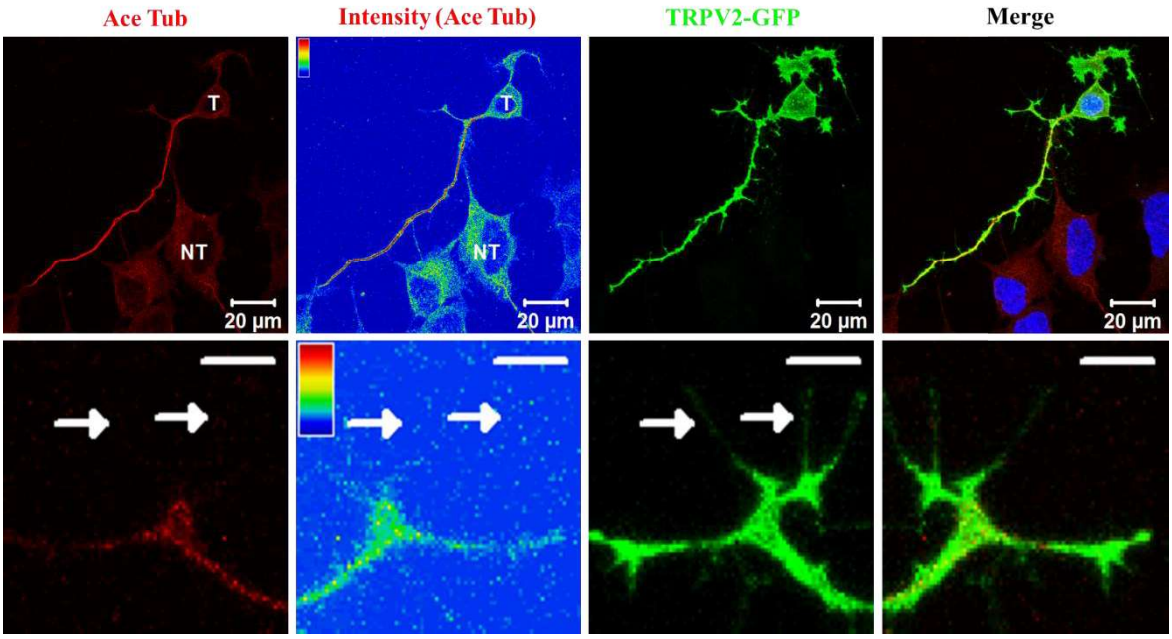

Figure 30. Acetylated tubulin is not present in filopodial tip: Representative confocal images of F11 cells transfected with TRPV2-GFP and stained with acetylated tubulin. Intensity profile shows enrichment of acetylated tubulin in neurites but not in the filopodial tip. Lower panel shows the zoomed image. (T and NT represents the transfected and non-transfected cells respectively). Scale bar 2µm.

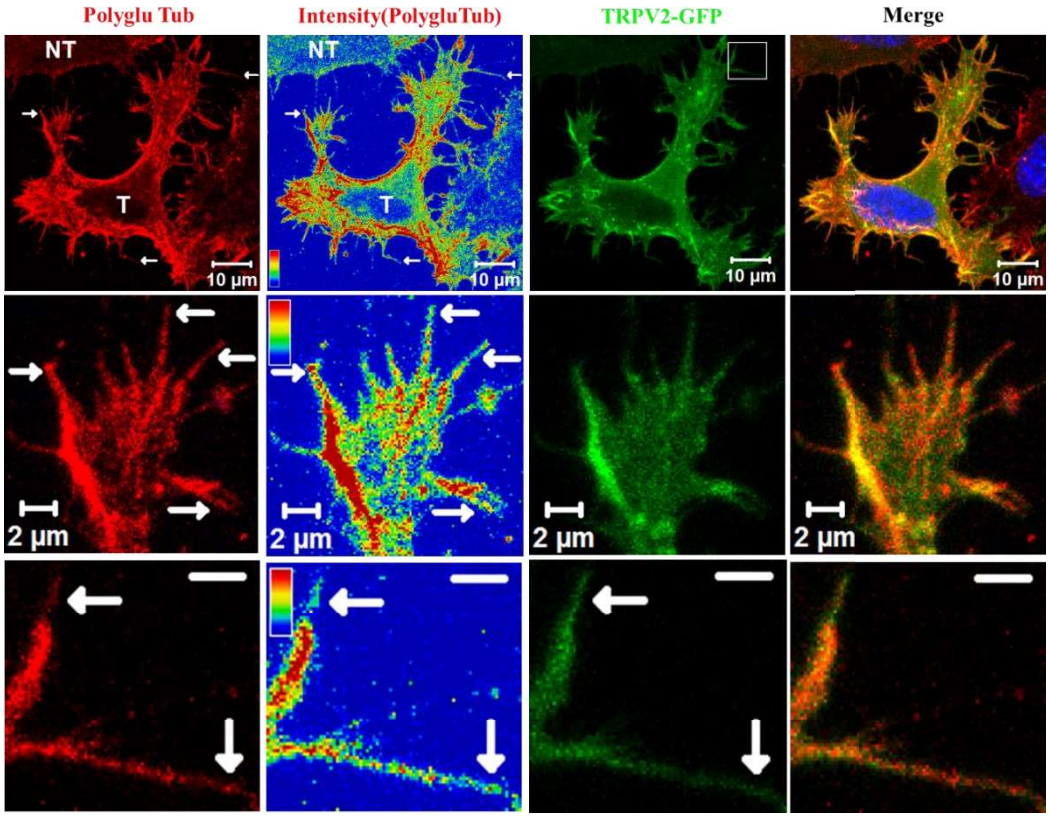

Figure 31. Polyglutamylated tubulin is present in filopodial tip and growth cone. Representative confocal images of F11 cells transfected with TRPV2-GFP and stained Polyglutamylated tubulin. Intensity profile shows enrichment of Polyglutamylated tubulin in filopodia and growth cone structures. Lower panel shows the zoomed image. (T and NT represents the transfected and non-transfected cells respectively). Scale bar 2µm.

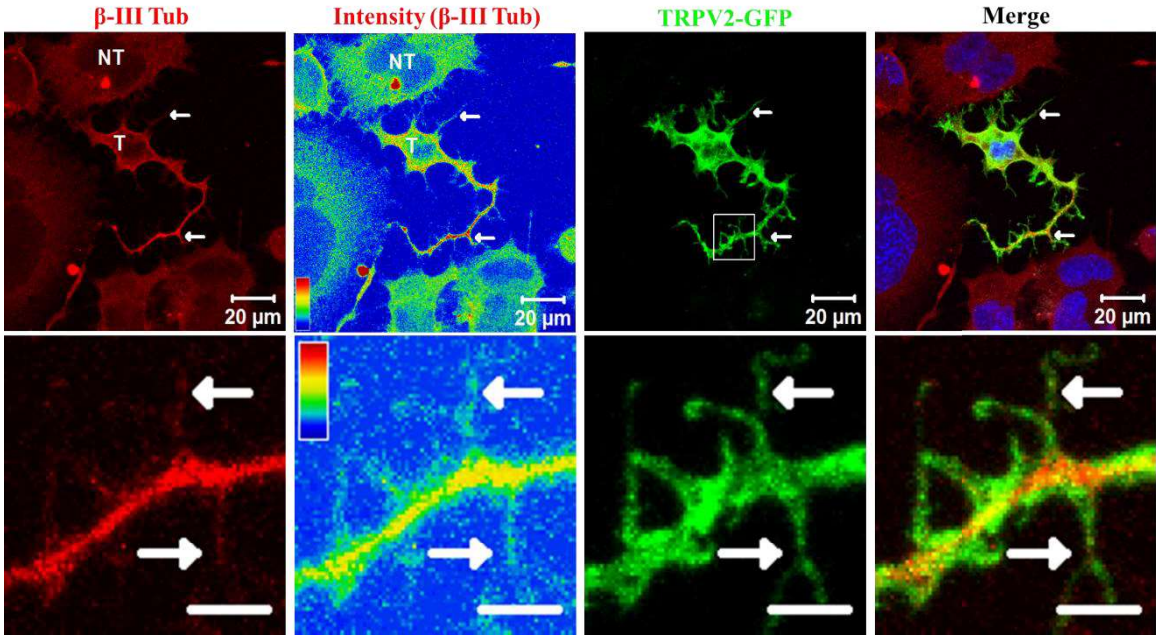

Figure 28. β-III tubulin is present in filopodial and neurite tip: Representative confocal images of F11 cells transfected with TRPV2-GFP and stained with neuronal marker β-III tubulin. Intensity profile shows enrichment of β-III tubulin in neurites. Lower panel shows the zoomed image. (T and NT represents the transfected and non-transfected cells respectively). Scale bar 2µm.

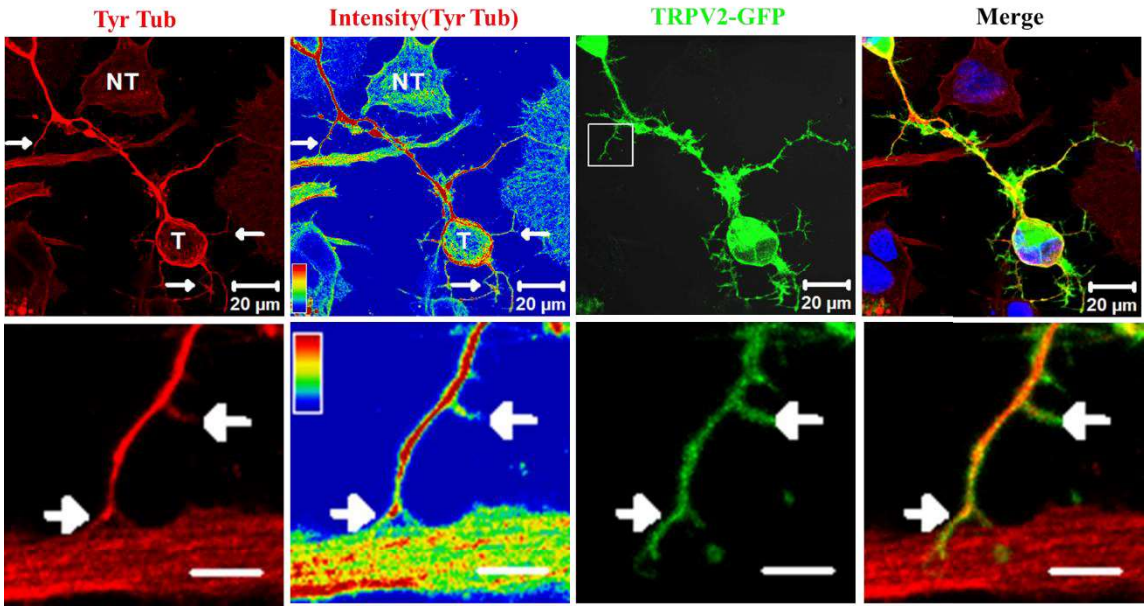

Figure 29. Tyrosinated tubulin is present in filopodial and neurite tip: Representative confocal images of F11 cells transfected with TRPV2-GFP and stained with Tyrosinated tubulin. Intensity profile shows enrichment of Tyrosinated tubulin in neurites. Lower panel shows the zoomed image. (T and NT represents the transfected and non-transfected cells respectively). Scale bar 2µm.

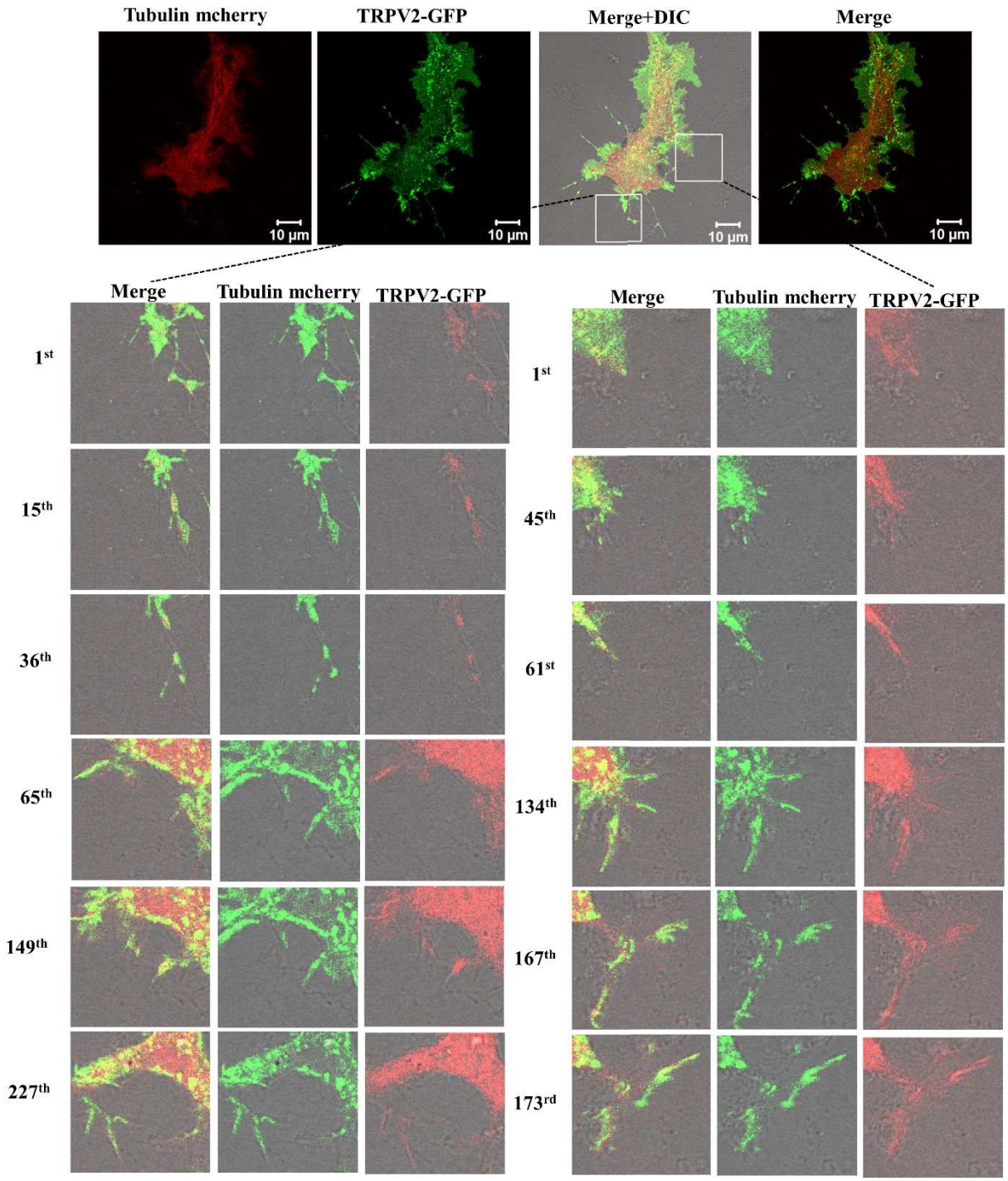

Figure 27. Tubulin mCherry is present in the TRPV2-GFP containing filopodia and both colocalizes in live cell imaging: Time series images shows after co transfection with TRPV2-GFP and tubulin mCherry. Lower two panel shows the zoom up of image, arrow head indicated the presence of tubulin and TRPV2 in specific position such as, filopodia, neurite, and membrane. Scale bar represents (2µm).

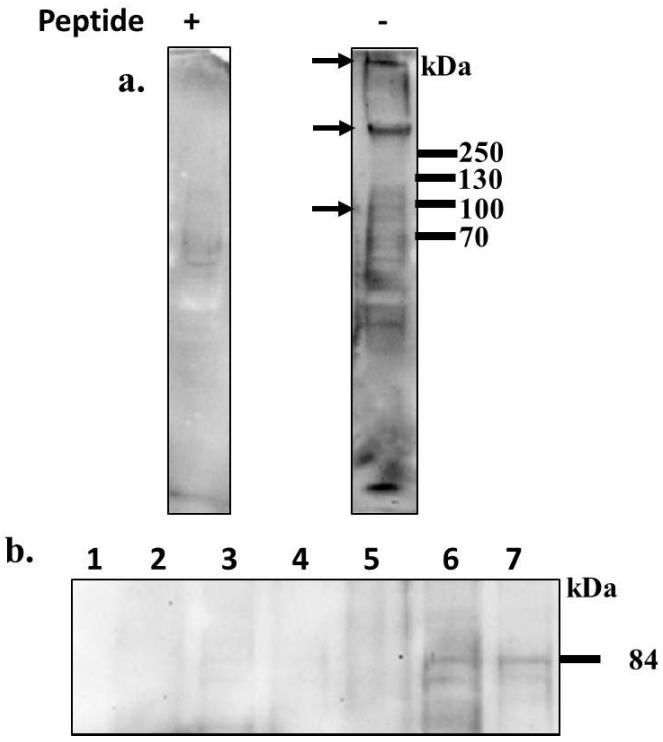

Figure 26. TRPV2 is present in rat brain fractions: a. Represents the Synaptosome fraction from rat brain shows reactivity for TRPV2 antibody (bands at higher size were detected along the size of TRPV2), and this signal diminish in the presence of blocking peptide. **b.** Represents western blot analysis of lane 1 (Cytosolic protein), 2 (Microsomes), 3 (Light membrane), 4 (Crud membrane), 5 (Myelin), 6 (Synaptosome) and 7 (Synaptic junction protein). These sample were probed with anti TRPV2 antibody. Presence of TRPV2 has been detected in Synaptosome and synaptic junction protein fractions.

2.1.16. TRPV2 positive filopodia contains different modified tubulins:

After detecting that TRPV2 regulates morphology and cell size of F11 cell and it is functionally present in this neuronal cell, we have further characterised the physical presence of stable and dynamic microtubule in the specific region of neuronal cells such as filopodia, growth cone, neurites and lamellipodia. To characterise this F11 cells were transfected with TRPV2-GFP and stained with different modified tubulins such as (β-III tubulin, Tyrosinated tubulin, acetylated tubulin and polyglutamylated tubulin). Representative confocal images show the presence of TRPV2 in filopodial structure and neurites along with β-III tubulin, Tyrosinated tubulin, and polyglutamylated tubulin **(Fig. 28-31)**.

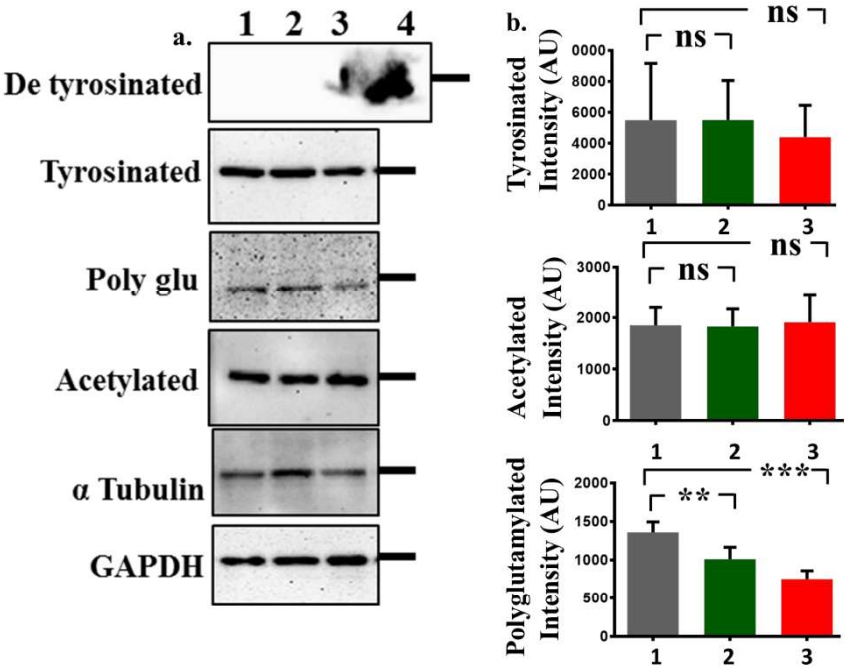

Figure 25. Pharmacological modulation of TRPV2 alters in the level of selected post-translationally modified tubulin: a. F11 cells were activated (by Probenecid 10µm) or inhibited (by Tranilast 75µm) for 12 hours followed by gel sample preparation and probed for different modified tubulins markers. De tyrosinated tubulin level was very low. P values that are ≥ 0.1, ≤ 0.01 and ≤ 0.001 are considered as non-significant (ns), ** and *** respectively. n = 4.

2.1.15. Tubulin mCherry is present in the TRPV2-GFP positive filopodia and neurite:

After finding that TRPV2 is present in Synaptosome fraction, a live cell imaging experiment was performed where TRPV2-GFP and tubulin m-Cherry were co transfected. Time series representative images shows that TRPV2-GFP containing filopodia and neurite are also positive for tubulin mCherry **(Fig. 27)**. This indicates specific role of TRPV2 in processes such as neuritogenesis cell morphology and cell shape.

Figure 24. Activation of TRPV2 induce rapid translocation in leading edges but not on the filopodial tips: a. Shown are the live cell image of F11 cell expressing TRPV2-GFP (green) and actin-RFP (red) merged with DIC images. Activation of TRPV2-GFP by 2APB also causes changes in sub-membranous actin cytoskeleton and results in rapid translocation of TRPV2-GFP to the leading edges, merging of actin-ribs in the lamellipodium boundary. Intensity profile of the TRPV2-GFP and actin-RFP are provided in below. b. Shown are the enlarged portion of the leading edge of a F11 cell expressing TRPV2-GFP and actin-RFP before and after activation with 2APB. The filopodial tips are marked with white arrows. TRPV2-GFP is mainly present in the filopodial base but not in the filopodial tips.

2.1.13. Effect of TRPV2 activation and inhibition on tubulin modification:

F11 cells express TRPV2 endogenously. Therefore, if activation or inhibition of TRPV2 can alter the level of different modified tubulin that was explored. TRPV2 was activated by (Probenecid 10μM) or inhibited by (Tranilast 75μM) with specific activator or inhibitor for 12 hours. Subsequently, total cell extracts were prepared and the analyzed by SDS-PAGE as well as by Western blot and probed for different modified tubulins (Acetylated, Polyglutamylated, Tyrosinated) **(Fig. 25a)**. Experiments shows that the level of acetylated and Tyrosinated tubulin remain mostly unaltered. However, level of polyglutamylated tubulin become reduced upon TRPV2 modulation. Both activation or inhibition of TRPV2 reduces the level of polyglutamylated tubulin **(Fig. 25b)**. Level of de tyrosinated tubulin was very low in our experimental conditions, since it is already reported in F11 cells [197] **(Fig. 25a)**.

2.1.14. TRPV2 is present in Synaptosome fraction from rat:

TRPV2 is present at specific structures such filopodial tips, neurites and growth cone, suggesting that TRPV2 might be present in neuron-neuron contact sites as all these specialized structures are possible sites for neurochemical communications. Therefore, presence of TRPV2 was tested in the synaptic fraction isolated from Rat brain. Different fractions representing cytosolic fraction, microsomes, light membrane, crude membrane, Myelin fraction, Synaptosome and Synaptic junction fractions were probed with TRPV2 specific antibody. TRPV2 level is enriched in Synaptosome and PSD fractions **(Fig26a-b)**. Also, TRPV2 signal was diminished in the presence of blocking peptide **(Fig. 26a)**.

can also be reproduced by application of 2APB (10µM), another activator of TRPV2 **(Fig. 24a)**. In all cases, such changes are accompanied by rapid translocation of TRPV2 in the membrane, alteration in the actin filaments. Activation of TRPV2 induce rapid translocation in leading edges but not on the filopodial tips **(Fig. 24b)**. Taken together, our results suggest that TRPV2 play important role in regulation of neurites and such functions involve Tyrosine phosphorylation and regulation of sub membranous actin cytoskeleton.

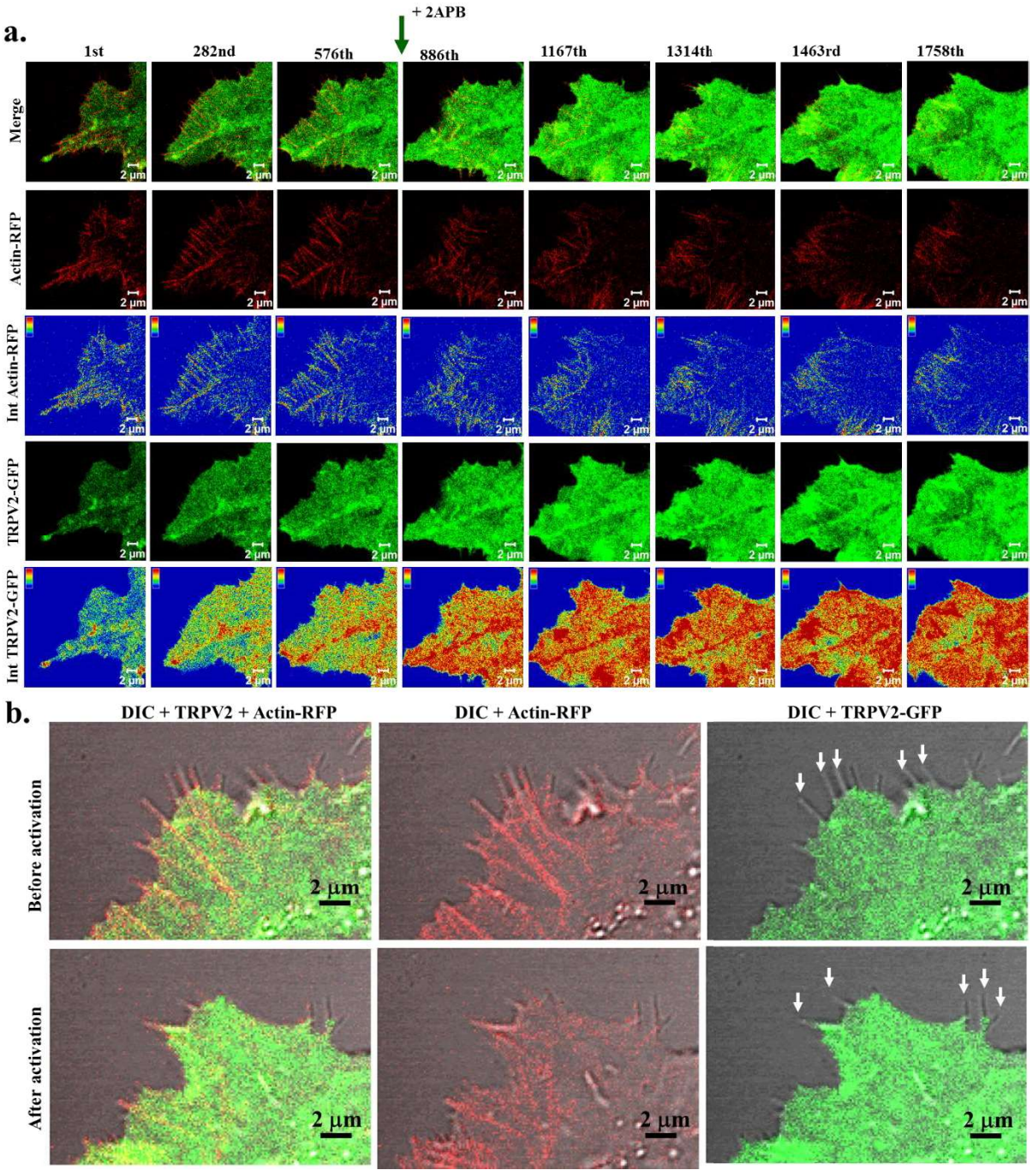

Figure 22. TRPV2 colocalizes with sub-membranous actin cytoskeleton and TRPV2 activation causes membrane remodeling: a. Live cell image of a F11 cell co-expressing TRPV2-GFP (green) and actin-RFP (red) demonstrating colocalization of TRPV2-GFP and actin-RFP in specific cellular regions such as in neurites and in filopodia. **b.** Live cell image of F11 cell co transfected with TRPV2-GFP and actin-RFP shows that activation of TRPV2 by Probenecid alters actin cytoskeleton dynamics leading to changes in cell morphology, such as extension of cell membrane (upper panel), formation of massive lamellipodium (middle panel) and merging of lamellipodium (lower panel).

2.1.11. TRPV2 interacts with actin through its C-terminal region:

Next, we tested if TRPV2 interacts with actin. For that purpose, we expressed the C-terminus of TRPV2 as a MBP-tagged protein and performed pull-down experiment with soluble extract obtained from goat brain. The pull-down samples were probed for the presence of actin by western blot analysis. Results suggest that Actin-interacts with MBP-TRPV2-Ct but not with MBP-LacZ **(Fig. 23a-b)**.

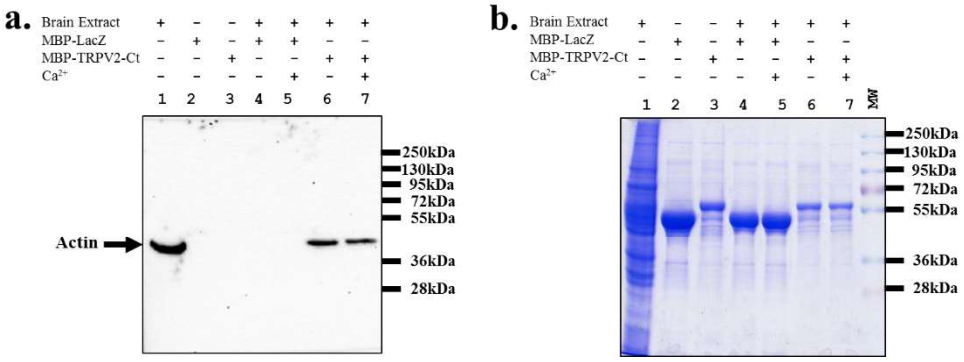

Figure 23. The C-terminus of TRPV2 interacts with actin: a. Soluble brain extract supernatant (lane 1) was pulled-down with purified MBP-LacZ (lane 4-5), MBP-TRPV2-Ct (lane 6-7) and probed for bound actin by Western blot analysis. **b.** The corresponding Coomassie gel is shown in right side.

2.1.12. Activation of TRPV2 causes membrane remodeling:

Next, we explored if TRPV2 activation and inhibition can cause rapid changes in the cell morphology and if such changes accompany remodeling of sub-membranous actin cytoskeleton. For that purpose, we co-expressed TRPV2-GFP and actin-RFP and performed live cell times series imaging. Activation of TRPV2 by Probenecid leads to rapid changes in actin cytoskeleton causing to changes in cell morphology, such as extension of cell membrane, formation of massive lamellipodium and merging of lamellipodium **(Fig. 22b)**. Such effects

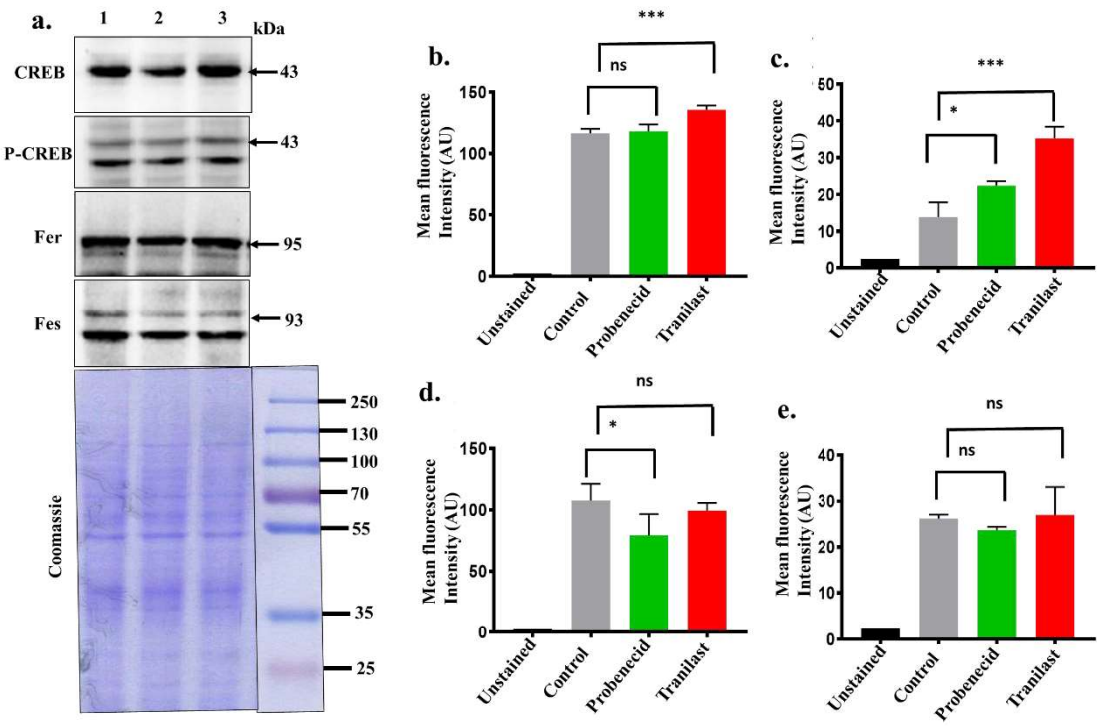

Figure 21. Pharmacological modulation of TRPV2 results in change of cytoplasmic tyrosine kinase: a. Represents western blot analysis of F11 cell extracts after long term activation and inhibition. 1, 2 and 3 represents the control, probenecid and tranilast treatment respectively. Lower image Coomassie represents the loading control for experiment. b-e. represents the FACS analysis of F11 cell after long term treatment with probenecid and tranilast. b-e. are CREB, P-CREB, FER and FES level respectively. The P values ≤ 0.001, 0.01, 0.5, 0.1 are considered as ***, **, *, and ns respectively.

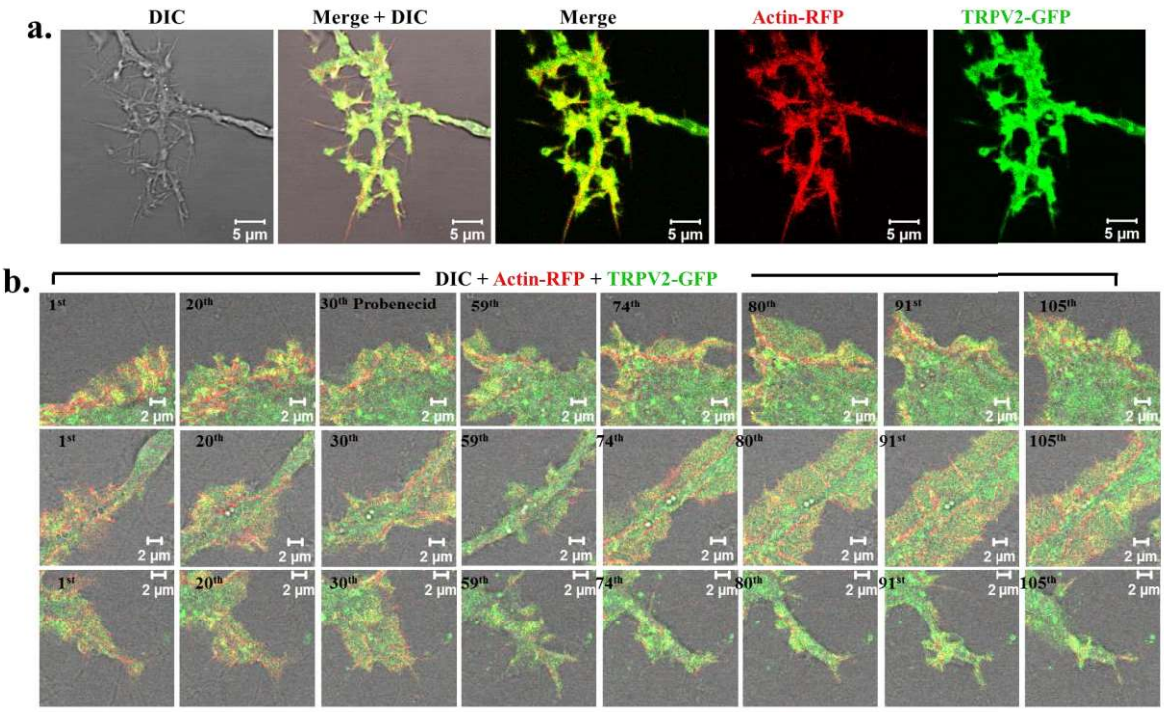

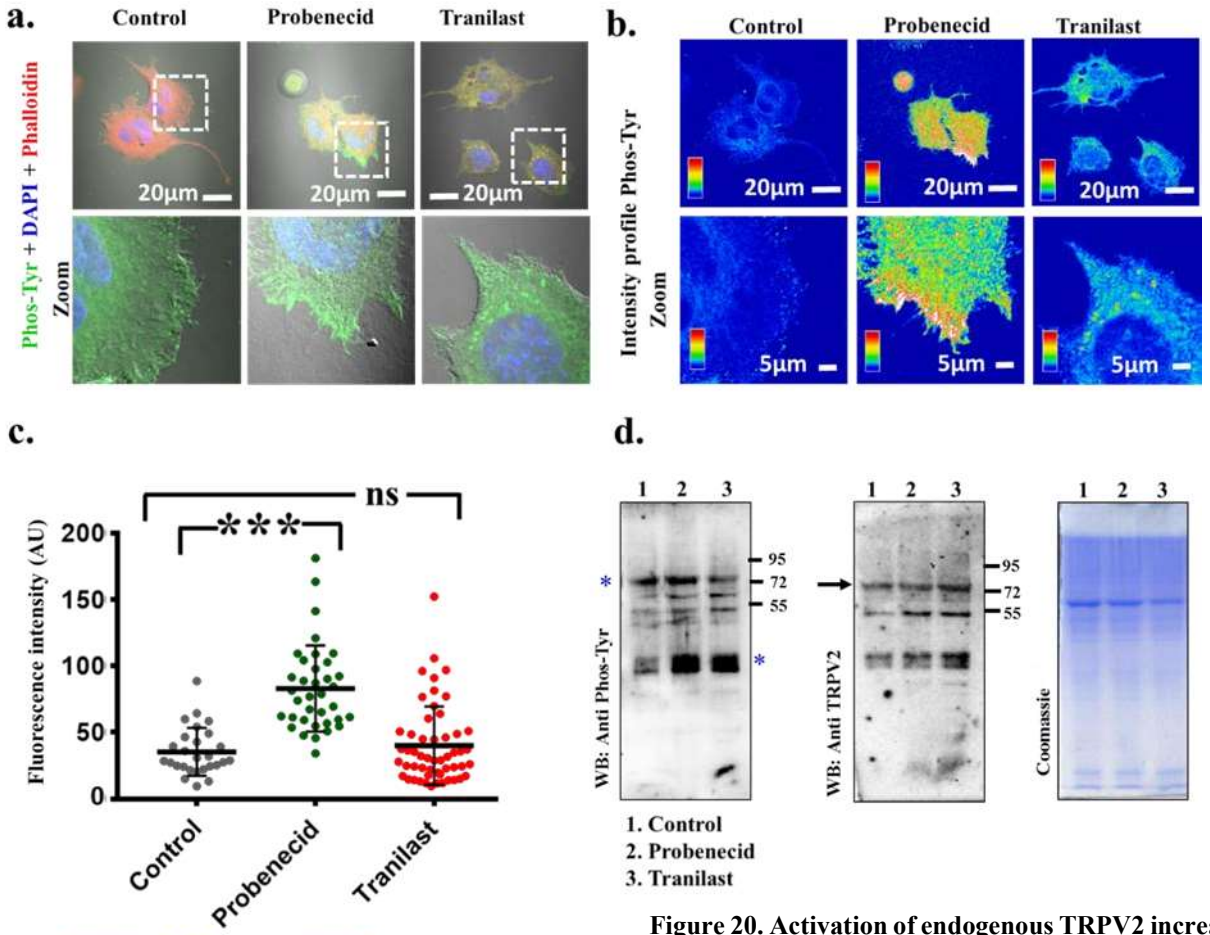

Figure 20. Activation of endogenous TRPV2 increases both level of Phospho-Tyrosination and TRPV2 in F11 cells: **a-b.** Confocal images demonstrating the F11 cells or their enlarged peripheral portions (lower panel) stained for Phospho-Tyrosination (green), Phalloidin (red) and DAPI (blue). Cells were grown in resting condition or in the presence of TRPV2 activator or inhibitor. Activation of F11 cell by Probenecid induces enhanced Phospho-Tyrosination staining in the cell membrane and sub-membranous regions. Intensity profile of the Phospho-Tyrosination staining is provided in right side (b). **c.** Quantification of Phospho-Tyrosination staining of each cell grown in different conditions of activation and inhibition is provided. P values that are ≥ 0.1 and ≤ 0.001 are considered as non-significant (ns) and *** respectively. **d.** Shown are the western blot analysis of the total cell extracts derived from F11 cell grown in resting condition or in the presence of TRPV2 activator or inhibitor. Blots were developed by anti-Phospho-Tyrosine antibody and by anti-TRPV2 antibody. Activation of TRPV2 results in more Phospho-Tyrosination of proteins. Coomassie-stained gel is used as a loading control. **e.** Microscopic images demonstrating the expression level of TRPV2 in F11 cells grown in control condition or in different conditions of activation and inhibition. Activation of F11 cell by Probenecid enhanced the endogenous level of TRPV2, especially in the cell body. Intensity profile of the TRPV2 immunoreactivity is provided in right side.

This Phospho-Tyrosination pattern remain unaltered upon pharmacological inhibition of TRPV2 (Fig. 20c). Western blot analysis also suggests changes in the Phospho-Tyrosination pattern also **(Fig. 20d)**. The expression level of endogenous TRPV2 remain unaltered in case of pharmacological activation or inhibition of TRPV2 **(Fig. 20d)**. However, in case of pharmacological activation, the level of TRPV2 become significantly high **(Fig. 20e)**.

2.1.9. TRPV2 modulation results in change of cytoplasmic tyrosine kinase level:

To further confirm the Phospho-Tyrosine signaling after pharmacological modulation of TRPV2. We have also checked the level of two cytoplasmic tyrosine kinase level through western blotting and FACS analysis **(Fig. 21a-e)**. FACS analysis reveals that cAMP binding transcription factor CREB level increase after TRPV2 inhibition while activation does not show any change **(Fig. 21b)**. Also, activated form of this transcription factor (P-CREB) shows increase upon activation, while inhibition further increases its level **(Fig. 21c)**. Cytoplasmic tyrosine kinase FER level decreases after activation while inhibition does not change its level **(Fig. 21d)**. While another kinase FES does not show any change with compare to control **(Fig. 21e)**.

2.1.10. TRPV2 colocalizes with actin cytoskeleton:

As TRPV2 is present in typical structures that are enriched with actin cytoskeleton, we explored if both TRPV2 and actin colocalizes. For that purpose, we expressed TRPV2-GFP and actin-RFP in F11 cells and performed co-localization experiments. We noted colocalization of TRPV2-GFP with actin-RFP in live cells in specific areas, such as in filopodial regions, neurites and in thin lamellipodial regions and also in actin-rib projections **(Fig. 22a)**. Further pharmacological activation of TRPV2 during live cell imaging results in change in the actin cytoskeleton and which results in altered cell morphology **(Fig. 22b)**.

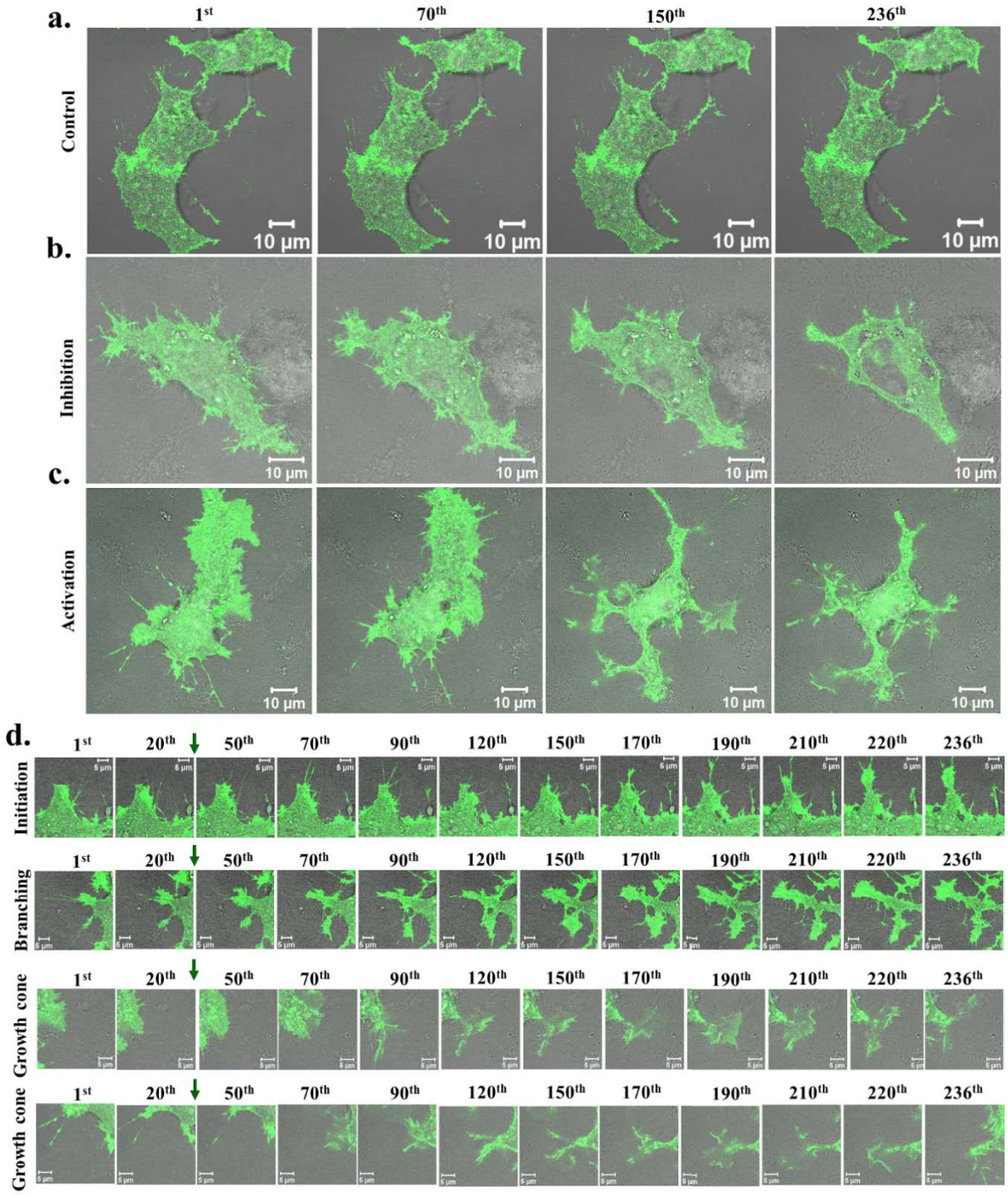

Figure 19. Activation of endogenous TRPV2 leads to immediate membrane ruffling and alters filopodial and growth cone dynamics: a-c. Representative live cell imaging of F11 cells expressing TRPV2-GFP (green) merged with DIC are shown. When cells were left un-treated (a), there is not much change in the morphology. Inhibition of TRPV2 activity by Tranilast (b) leads to quick reduction of cell size suggesting that TRPV2 activity contributes to the maintenances of cell morphology. Activation of TRPV2 with Probenecid (c) results in rapid membrane-ruffling leading to changes in cell morphology. **d.** Shown are the time-series images of enlarged sections of a F11 cell that have been treated with Probenecid (indicated by a green arrow) (added just before 50th frame). Activation of TRPV2 results in different events controlled by sub-membranous actin cytoskeleton leading to changes in membrane ruffling. The time gap between each image frame 0.04 Sec.

Activation of TRPV2 increases the distance (of primary neurite) between cell body to the first point where secondary neurite originates. The mean/average distance is unaltered when grown in presence of inhibitor Tranilast. The values were plotted in ascending order (e). The P values ≤ 0.001, 0.01, 0.5, 0.1 are considered as ***, **, *, and ns respectively. **f.** Shown is a simplified model demonstrating the changes in cell morphology and development of complex neurites due to activation of TRPV2.

2.1.7. Inhibition but not the activation of TRPV2-GFP results in cell retraction:

Importance of TRPV1 in the context of growth cone dynamics is well established [266, 269]. Therefore, we tested if TRPV2 also act in the same processes. Time series images from TRPV2-GFP expressing live F11 cells were acquired to monitor the effect of TRPV2 activation or inhibition. For this purpose, cells that express moderate amount of TRPV2-GFP and flatten in morphology were used. In resting conditions, these cells do not change their morphology over time drastically **(Fig. 19a)**. However, upon inhibition of TRPV2 activity by pharmacological means results in retraction of cells suggesting that TRPV2 activity helps in maintenance of cell morphology **(Fig. 19b)**. However, activation of TRPV2 by Probenecid results in rapid membrane ruffling, changes in lamellipodial and filopodial dynamics **(Fig. 19c)**. Such events often result in initiation of neurites, branching of neurites and growth cone formation and growth cone splitting **(Fig. 19d)**.

2.1.8. Activation of TRPV2 results in increased Phospho-Tyrosination at leading edges:

Tyrosine kinase activity is important for the regulation of the leading edges affecting cell adhesion and cell spreading [270, 271]. Therefore, we tested the effect of TRPV2 activation and inhibition on the level of Phospho-Tyrosination. Immunofluorescence analysis confirmed that TRPV2 activation leads to increased overall Phospho-Tyrosination and especially at the cell edges **(Fig. 20a-b)**. Quantification of fluorescence intensities of total Phospho-Tyrosination from multiple cells also indicate that activation of TRPV2 leads to increased Phospho-Tyrosination **(Fig. 20c)**.

2.1.6. TRPV2 affects neurite branching:

The changes in number as well as length of primary and secondary neurites in general suggest that TRPV2 is involved in initiation of new neurites. Therefore, we tried to explore the importance of TRPV2 in neurite branching process. In order to explore this, we have measured the distance between cell body and the origin of the first secondary neurite **(Fig. 18d-e)**. Such analysis indicates that activation of TRPV2 significantly increases the primary neurite length between cell body and the origin of the first secondary neurite. In the same notion, inhibition of TRPV2 also reduces this distance. This result establishes a correlation between TRPV2 activities with the initiation of new neurites.

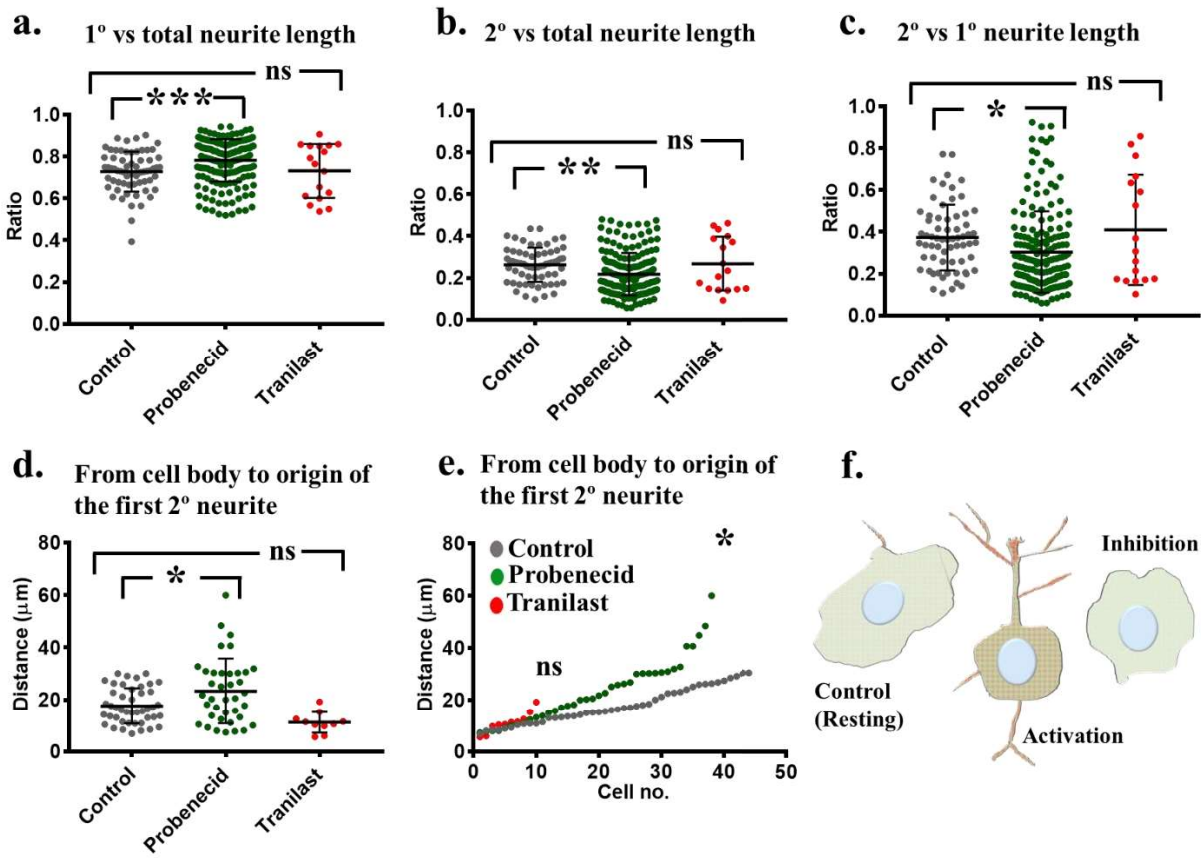

Figure 18. Activation of endogenous TRPV2 affects primary neurites more than secondary neurites: a-c. Ratio of primary neurite length to total cell length (a), or secondary neurite length to total cell length (b) or secondary neurite to primary neurite length were quantified for cells grown in different conditions. This ratio is significantly higher when cells are grown in presence of TRPV2 activator Probenecid (10μM for 12 hours) and mean is unaltered when grown in presence of inhibitor Tranilast 75μM for 12 hours (n =109 for control, 89 for Probenecid-treated conditions and n = 143 for Tranilast-treated conditions). **d-e.** Cells were grown in different conditions and the distance between cell body to the origin of first secondary neurite developed was quantified.

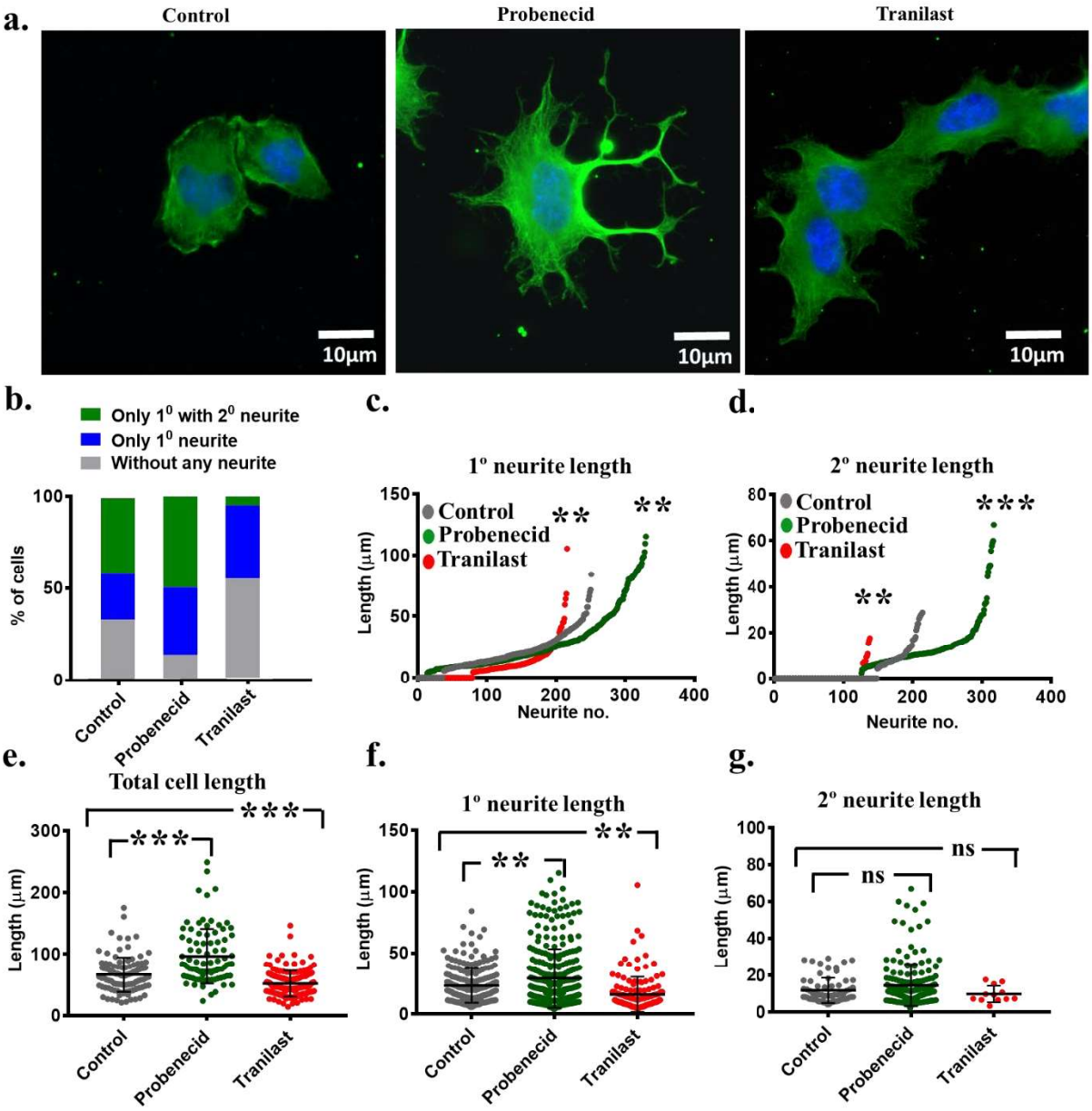

Figure 17. Endogenous TRPV2 activation increases cell size and enhances neuritogenesis: a. Representative fluorescence microscopic images of F11 cells grown in control condition, activated with Probenecid (10µM for 12 hours) or inhibited with Tranilast (75µM for 12 hours) and stained with anti-tubulin are shown. Activation of endogenous TRPV2 with Probenecid results in altered cell morphology and formation of more neurites. In contrast, inhibition of TRPV2 (treated with Tranilast) results in smaller sized cells as compared to the control cells. **b.** Activation of TRPV2 induces more neurites. F11 cell were grown in control condition or treated with Probenecid or Tranilast and were quantified and percentage of cells without any neurite, with at-least one primary (1°) neurite, and with at-least one secondary (2°) neurite originated from primary neurite are plotted. **c.** Length of the 1° neurites (n =109 for control, 89 for Probenecid-treated conditions and 143 for Tranilast-treated conditions are plotted in ascending orders. For cells without any 1° neurite, the length of the 1° neurite is considered as zero. **d.** Length of the 2° neurites (n =109 for control, 89 for Probenecid-treated conditions and 143 for Tranilast-treated conditions) are plotted in ascending orders. For 1° neurite without any 2° neurite, the length of the 2° neurite is considered as zero. **e-g.** Length of the total cell (e), 1° neurite (f) and 2° neurite (g) from cells grown in control condition, activated with Probenecid or inhibited with Tranilast are plotted. The average length of the 2° neurites are non-significantly (ns) different when cells were grown in different conditions. P values ≤ 0.001, 0.01, 0.5, 0.1 are considered as ***, **, *, and ns respectively.

establishes a direct correlation between TRPV2 function with the initiation of neurites from cell body or even from the primary neurite. In addition, the length of the primary neurites is significantly longer in cells that were treated with TRPV2 activator and significantly shorter in cells that are treated with TRPV2 inhibitor **(Fig 17c and Fig 17f)**. However, analysis of the length of secondary neurites indicates that there is no significant difference between cells that are pharmacologically modulated (activated or inhibited) with the cells that are grown in control conditions **(Fig 17d and Fig 17g)**. These results may also suggest that endogenous TRPV2 activity is involved in the formation of cell polarity, at least in F11 cell. This result suggests that though activation of endogenous TRPV2 induce more secondary neurites, their lengths are independent of TRPV2 function and therefore suggest the involvement of TRPV2 in complex signaling events. To establish the importance of TRPV2 in neuritogenesis further, we analyzed the ratio between primary, secondary and total neurite lengths. We noted that the ratio of primary neurite length with total neurite length is significantly higher when cells were treated with TRPV2 activator and remain unchanged when cells were treated with inhibitors **(Fig. 18a)**. In the same notion, ratio of secondary neurite length with total neurites length is significantly lower when cells were treated with TRPV2 activator and remain unchanged when cells were treated with inhibitors **(Fig. 18b)**. Similar trend in ratio between the lengths of secondary neurite with primary neurite is observed **(Fig. 18c)**. This result suggests that endogenous TRPV2 affects primary neurites more than the secondary neurites in terms of length.

2.1.5. Endogenous TRPV2 in F11 cells is involved in neuritogenesis:

We explored if endogenous TRPV2 also involved in the neuritogenesis and if pharmacological activation or inhibition of TRPV2 alters this. Therefore, we have activated endogenous TRPV2 with specific activator (Probenecid) at sub-optimal concentration (10μM) for 12 hours. Similarly, endogenous TRPV2 activity was also inhibited by using (Tranilast) at (75μM) concentration (more than optimal concentration to ensure the complete blockade of TRPV2 activity) for 12 hours. Subsequently cells were fixed without disturbing the media and the cells were immunostained with tubulin antibody to analyze their morphology and length of the neurites as well. Our results suggest that activation of TRPV2 leads to elongation of cell sizes very much whereas pharmacological inhibition of TRPV2 reduces the cell length significantly compared to the control cells **(Fig. 17a)**. We also measured several parameters related to neuritogenesis events such as percentage of cells having no-neurite, or percentage of cells having at least a single 1° neurite or more than one 1° neurites (originated from cell body). We also measured other parameters such as length of total cell, length of primary neurites and length of secondary neurites and their comparative ratios. In control condition, there are around 30% cells which are without any neurite while TRPV2 activated (Probenecid-treated) conditions only 5-7% of cells are without any neurite **(Fig. 17b)**. In case of TRPV2-inhibited (Tranilast-treated cells) conditions, around 60% cells remain without any neurite, suggesting that activation of endogenous TRPV2 enhances the neuritogenesis process as a whole (enhances the % of cells with neurites) while inhibition of TRPV2 reduces the % of cells with neurites). In the similar manner, percentage of cells with a single primary neurite is increased when TRPV2 is activated (35%) compared to cells that ware grown in resting conditions (20%). Similarly, percentage of cells with at least a secondary neurite (originated from primary neurite) is increased after activation of endogenous TRPV2 (55%) compared to cells that are in resting condition (40%) or grown in inhibited conditions (3-4%). This result also strongly

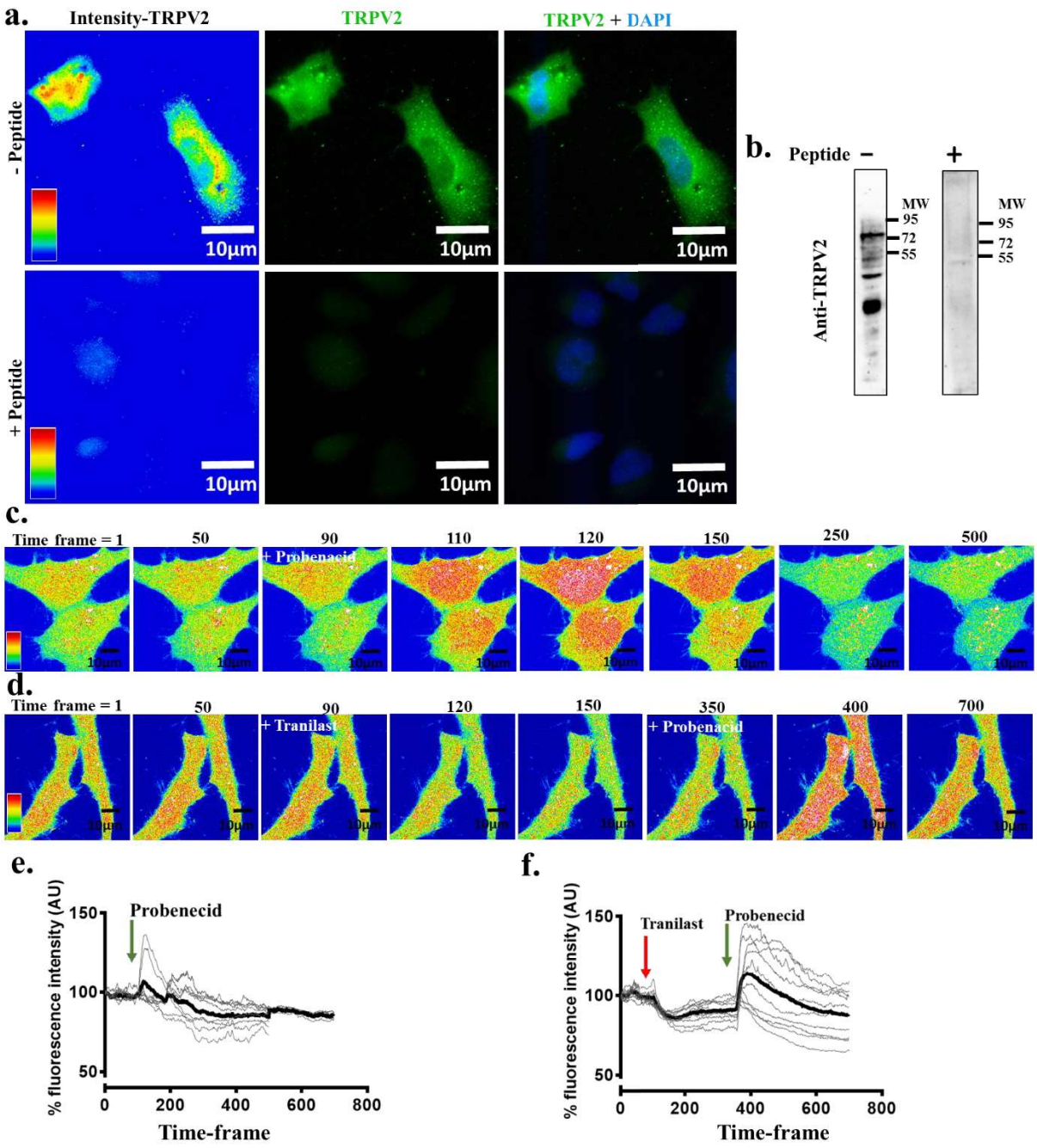

Figure 16. F11 cells endogenously express functional TRPV2: a. Immunofluorescence images of F11 cells stained with anti-TRPV2 antibody in absence (lower panel) or presence (upper panel) of specific blocking peptide are shown. **b.** Western blot analysis of F11 cell extract probed with anti-TRPV2 antibody are shown. Presence of specific blocking peptide diminished the TRPV2-specific immunoreactivity completely. **c.** Live cell imaging of F11 cells loaded with Fluo-4 demonstrating the transient and sharp increase in the intracellular Ca^{2+}-level immediately after treating the cells with specific activator (Probenecid, 250µM). The interval between each time frame is 0.5 sec. **d.** Similar Ca^{2+}-imaging of F11 cells shows immediate drop in intracellular Ca^{2+}-level followed by application of specific inhibitor (Tranilast, 75µM). Further application of specific activator (Probenecid, 250µM) cause again sudden increase in Ca^{2+}-level. **e-f.** Quantification of intracellular Ca^{2+}-levels as shown above (c-d) are represented. In each case fluorescence intensity (in arbitrary unit) from multiple cells (n =10) are shown. The average value is shown as a thick black line. The interval between each time frame is 0.5 sec.

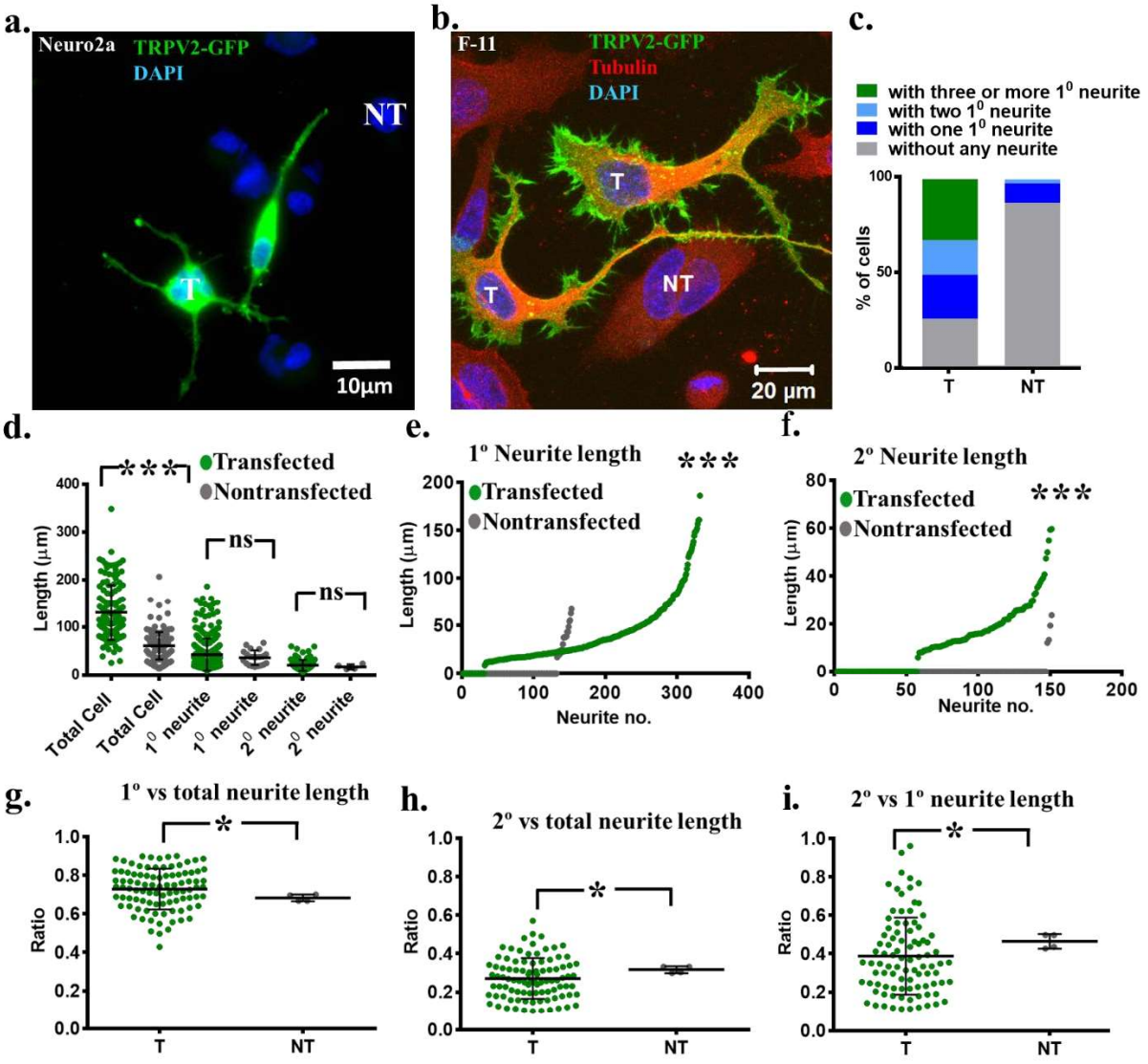

Figure 15. Exogenous expression of TRPV2 induces neuritogenesis and enhances cell elongation: a-b. Representative fluorescence microscopic images demonstrating Neuro2A (a) and F11 (b) cells expressing TRPV2-GFP. Transfected cells (T) become much elongated and have higher number of neurites with complex branches compared to non-transfected (NT) cells. **c.** Expression of TRPV2-GFP enhances neuritogenesis. Percentage of F11 cells having at-least one primary neurite, two primary neurites, more than 2 primary neurites or no neurites were quantified (n =149 for non-transfected cells and n =131 for transfected cells). d. Quantification of the length of the entire cell (n = 149), primary (1°) neurite (n = 100) and secondary (2°) neurites (n = 80) originated from F11 cells over expressing TRPV2-GFP are shown. The mean cell length become significantly different (p value) while the mean length of the 1° and 2° neurites are not-significantly different. **e-f.** Length of the 1° neurites (n =131 for transfected and n = 149 for non-transfected cells) and 2° neurites (n =131 for transfected and n = 149 for non-transfected cells) present in transfected (n = 99) and non-transfected (n = 48) F11 cells are plotted in ascending orders. For cells without any 1° neurite, the length of the 1° neurite is considered as zero (e). Similarly, for 1° neurites without any 2° neurite, the length of the 2° neurite is considered as zero (f). **g-i.** Ratio (of length) of 1° neurites to total cell (g), 2° neurite to total cell (h) and 1° to 2° neurite (i) are plotted for each cell. Marginal differences in these ratios between transfected and non-transfected cells are observed. P values ≤ 0.001, 0.01, 0.5, 0.1 are considered as ***, **, *, and ns respectively.

2.1.4. Functional TRPV2 is expressed endogenously in F11 cells:

F11 cell is known to express TRPV2 endogenously [25]. We tried to confirm the expression of TRPV2 in F11 cells in our culture conditions. We explored the endogenous expression of TRPV2 by immunofluorescence and western blot analysis. These we performed both in presence and absence of a TRPV2-specific blocking peptide **(Fig. 16a-b)**. These results suggest the endogenous expression of TRPV2 in F11 cells. In order to conform this endogenous expression further, we loaded cells with Fluo-4, a Ca^{2+}-sensor dye and treated these cells with TRPV2 specific agonists and performed live cell imaging to acquire the changes in the Ca^{2+}-level. Activation of TRPV2 by specific agonist (Probenecid) causes significant increase in the Ca^{2+}-level. This rise in Ca^{2+}-level is transient in nature and the increased level fades off quickly. Similarly, inhibition of TRPV2 by Tranilast causes a drop in intracellular Ca^{2+}-level. Further application of Probenecid causes increases in intracellular Ca^{2+}-level **(Fig. 16c-d)**. Quantification of multiple cells for the fluorescence intensity also confirms the same **(Fig. 16e-f)**. Taken together results suggest that functional TRPV2 is expressed endogenously in F11 cells.

To explore if TRPV2 overexpression can indeed enhance neuritogenesis, we quantified the percentage of cells that show the presence of at least a single primary (1°) neurite, or at least two primary neuritis (both originated from cell body) or even more number of primary neuritis (all originated from cell body). Approximately 70% of TRPV2-GFP expressing F11 cells develop at least a single neurite within 24 hours. In contrast, only ~25% non-transfected F11 cells develop neurites within the same time points. The percentage of cells with at least two or more than 2 primary neurites are much higher in cells that are expressing TRPV2-GFP than that of the nontransfected F11 cells **(Fig. 15c)**. Subsequently we analyzed for the length of the primary and secondary neurites. TRPV2-GFP expressing cells have more number of primary (1°) as well as secondary (2°) neurites **(Fig. 15d-f)**. However, we noted that the average length of the 1° or 2° neurites are almost same (and the difference are non-significant) between cells expressing TRPV2-GFP or that are non-transfected **(Fig. 15d)**. Further analysis reveals that the length of the 1° neurites consist majority of the length of the total neurites and the value is marginally more for TRPV2-GFP expressing cells (average value is ~70%) than nontransfected cells **(Fig. 15g)**. Ratio of 2° vs. total neurite length also suggest that 2° neurites contribute ~25% of the total neurites length and such value is marginally less for TRPV2-GFP expressing cells than that of the non-transfected cells **(Fig. 15h)**. Similarly, ratio of 2° vs. 1° neurites also indicate that the average value is slightly less for TRPV2-GFP expressing cells than that of the non-transfected cells. This data strongly suggests that over-expression of TRPV2-GFP induces more number of neurites per cell (and mainly from the cell body), but does not affect average length of the individual neurites per se. Alternatively, this data suggest that over-expression of TRPV2 inducers signaling events that cause initiation of more neuritis from cell body, but once the neurites are formed, their lengths are independent of the level of TRPV2 expression *per se* (discussed later).

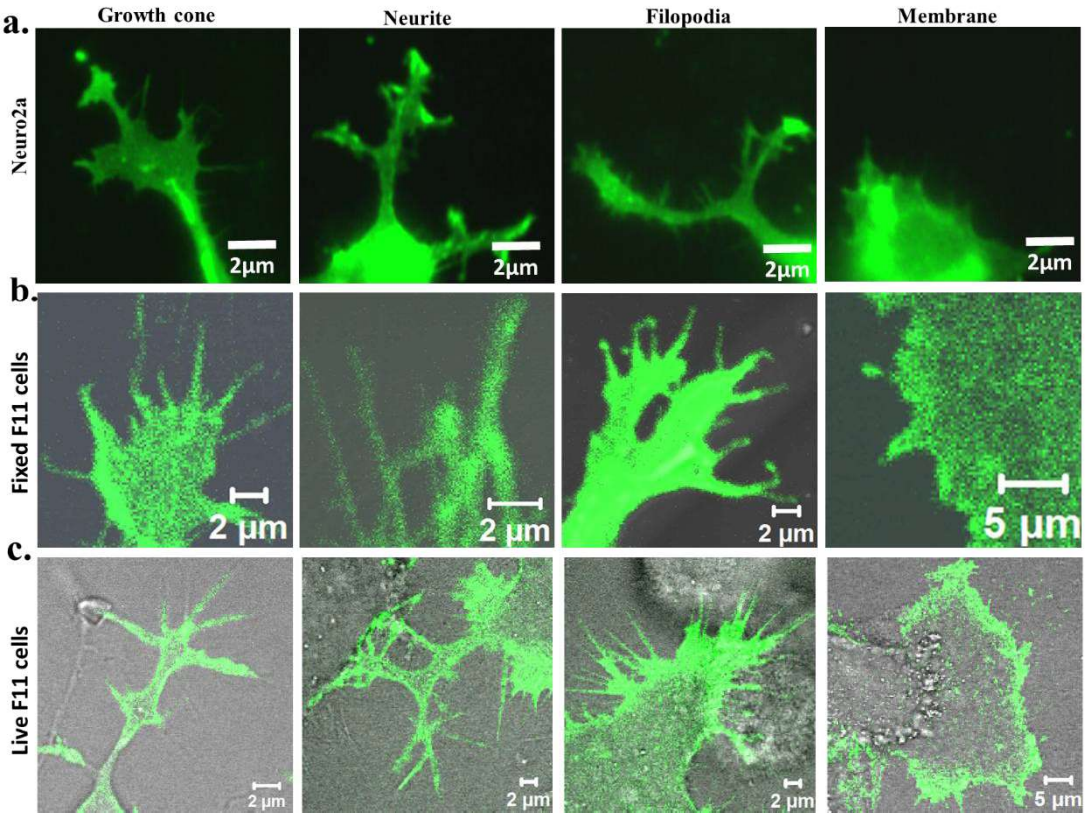

Figure 14.i. TRPV2-GFP is present in membrane, growth cone, filopodia, and neurite: a. TRPV2-GFP localizes in the specialized cellular structures such as at growth cone, neurite and filopodia when expressed in Neuro2A (neuronal) cells. **b-c.** TRPV2-GFP localizes in the similar specialized cellular structures such as at growth cone, neurite, filopodia in fixed (b) as well as in live (c) F11 (neuronal) cells. However, such phenotype is not observed in the only GFP-control expressing cells.

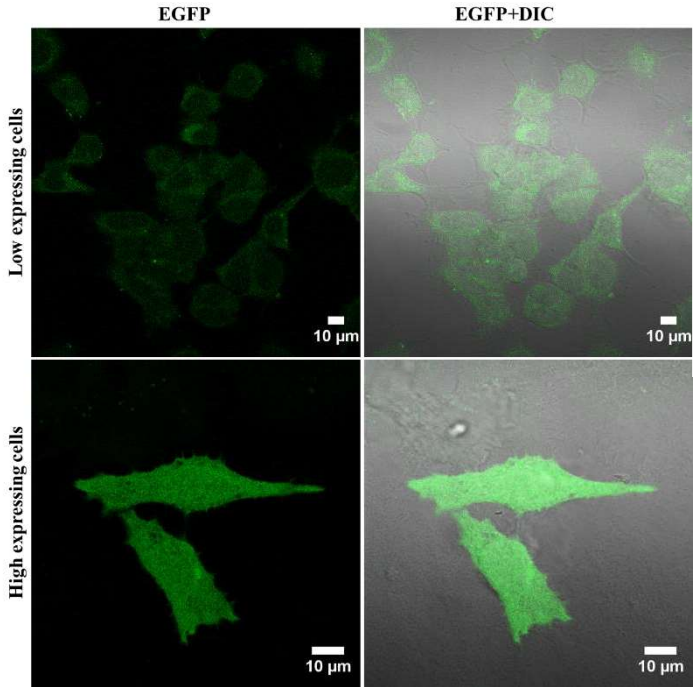

Figure 14.ii. Confocal images of EGFP overexpressing cells. F11 cell transfected with EGFP and after fixation with 4% PFA. Representative images do not show any affect shown by TRPV2-GFP.

in specific membranous regions such as in growth cones and also in filopodial structures **(Fig. 14.i.b)**. Such localizations were also observed in live F11 cells suggesting that these specific localizations are of special interest **(Fig. 14.i.c)**. To conform these localizations, we have used another neuronal cell line and expressed TRPV2-GFP there. Similar localizations were also observed in fixed Neuro2A cells confirming that TRPV2 is localized in these specific structures **(Fig 14.i.a)**. Growth cones are specialized structure presents at the nerve endings and are involve in neurite extension, neurite bending, cell to cell contact formation and also in synapse formation. Filopodial structures are actin-rich membranous projections and are involved in sensing different environment and chemical stimulus [267, 268]. Presence of TRPV2 in such localizations strongly suggest that TRPV2 might have importance in all these functions and may be involved in complex signaling events regulating cellular processes mediated through these structures. This results also suggest that TRPV2 may be present in cell to cell contact sites as well as in synapse and may be relevant for synaptic functions. However, to exclude the GFP overexpression artefact we have transfected the EGFP in F11 cells, which do not show any such effect shown by TRPV2-GFP **(Fig 14.ii)**.

2.1.3. Exogenous expression of TRPV2 causes change in cell morphology and induces neuritogenesis:

To explore the importance of TRPV2 in functions related to neurite formation and further extension, we transfected TRPV2-GFP in F11 cells and analyzed the different properties of neuritis originated from non-transfected F11 cells or F11 cells transiently expressing TRPV2-GFP. Cells overexpressing TRPV2-GFP become much elongated compared to non-transfected cells and drastic difference in the cell length is visible **(Fig. 15b)**.

tubulin, different post-translationally modified tubulin and regulation of submembranous cytoskeleton has been tested.

2.1.1. Exogenous expression of TRPV2 in non-neuronal cell results in change of cell shape:

Though the expression of TRPV2 was initially thought to be restricted in neuronal cells only, later report confirmed the expression of TRPV2 in different non-neuronal cells also [96]. In order to explore the effect of TRPV2 in cell morphology, we expressed TRPV2-GFP in different non-neuronal cell lines. In particular, we expressed TRPV2 in ChoKI (Chinese Hamster Ovary derived cell line), HaCat (Keratinocyte cell line), HEK (Human Embryonic Kidney cell line), and in Saos-2 (primary human osteosarcoma). In all these cases, we noted a drastic change in the cell morphology and the TRPV2 expressing cells become much flat in morphology and much bigger in sizes **(Fig. 13)**. This indicates that TRPV2 may play important role in regulation of sub-membranous actin cytoskeleton influencing different cellular functions such as cell adhesion and cell spreading.

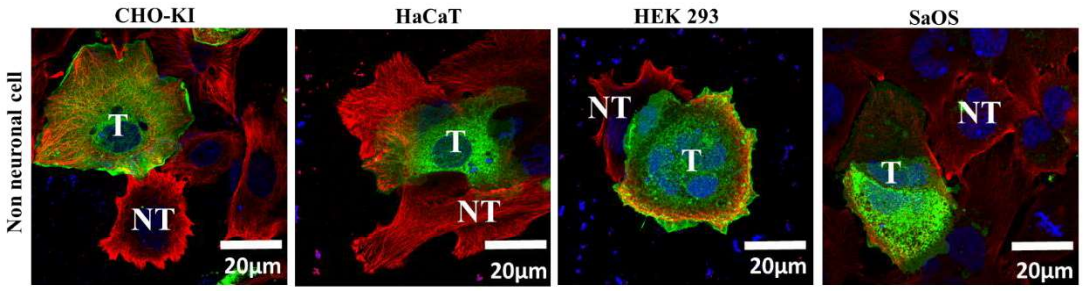

Figure 13. Ectopic expression of TRPV2 alters cell morphology: Shown are the confocal images of different cells expressing TRPV2-GFP. Different non-neuronal cells (CHO-K1, HaCaT, HEK293, and Saos-2) become enlarged after expressing TRPV2-GFP (green) while non-transfected cells remain normal in sizes. (T and NT represents transfected and non-transfected cells respectively).

2.1.2. TRPV2 localize at membrane, filopodia, growth cone and neurite in F11 cell and Neuro2a:

In order to understand the localization of TRPV2 in peripheral neurons, we have expressed TRPV2-GFP in F11 cells, fixed after 48 hours and noted that TRPV2-GFP localizes

Chapter 2.1: Importance of TRPV2-cytoskeleton cross talk in the context of neuronal functions:

(This chapter is under communication as a manuscript: Yadav M, Goswami C. (2018). Activation of TRPV2 induces neurite initiation and branching.

Cytoskeleton proteins (such as Actin, Tubulin) are abundantly present in the cytoplasm and have broad implication in cell shape, cell adhesion, cell migration, polarity development, etc. For neuronal cells, these components regulate key functions such as growth cone formation, growth cone turning, filopodial dynamics, neuronal guidance, neurite growth, etc. Interestingly, such functions are regulated by different signaling events as well as complex spatiotemporal Ca^{2+}-dynamics [111, 258-261]. Abnormalities in either cytoskeleton regulation or signaling events or Ca^{2+}-dynamics results in development of serious pathophysiological conditions. Such functions typically involve alteration of sub-membranous cytoskeleton, a very specialized entity located just beneath the plasma membrane [262, 263]. The sub-membranous cytoskeleton is physically connected or linked with the plasma membrane. The physical and dynamic interaction between cytoskeleton and plasma membrane is mediated by selected and specific transmembrane proteins representing specific receptors and ion channels. While information about submembranous actin cytoskeleton is well-studied, the importance of submembranous microtubule cytoskeleton is underexplored. Therefore, understanding the molecular partners involved in interaction and regulation of submembranous microtubule cytoskeleton is of fundamental interest.

There are several reports which suggest that ion channels present in the plasma membrane interact with cytoskeleton components [264, 265]. Members belong to TRP subfamily, especially TRPV1 and TRPV4 are reported to interact with soluble tubulin, polymerized microtubules [196, 199]. These channels also regulate microtubule dynamics [162, 195, 197, 266]. Therefore, these channels play critical role in the regulation of submembranous cytoskeleton. In this chapter, the possibilities TRPV2 interaction with soluble

Ion channels represent specialized membrane proteins that are critical for several cellular functions including ionic homeostasis. Ion channels are also regulated by several feed-back mechanisms. Components present in the lipid bilayer, the microenvironments at the membrane and submembranous regions, and the submembranous cytoskeleton are important factors that are regulated by ion channels and also impose strong feedback on the ion channels, especially their localizations, functions and regulations. In this thesis work, importance of TRPV2 in the regulation of submembranous microtubule cytoskeleton and possible physical interaction with the microtubule components were characterized (Chapter 2.1). In the next chapter, importance of TRPV3 and different point mutants causing *Olmsted Syndrome* in the context of structure-function relationship of different sub-organelles was characterized (Chapter 2.2). Importance of TRPV3 in the regulation of cellular pH, Ca^{2+} and lysosomal function is described (Chapter 2.3). In the last section, importance of membrane Cholesterol in the structure function of TRPV3 is described (Chapter 2.4).

Chapter 2

Results

suggested that cholesterol molecules may form an annular belt like structure with transmembrane helices to provide them different conformations [438, 439]. This cholesterol and TRPV3 interaction may have strong pathophysiological implication since the TRPV3 mutant's results in the development of many skin related abnormalities such as pruritus and hyperkeratosis. Understanding the molecular mechanism of TRPV3 regulation may be helpful in the pharmacological targeting of this ion channel, however further experiments are needed in order to understand this complex relationship.

cholesterol supplemented condition [159]. Above findings suggest that cholesterol mediated potentiation might be important for activation of TRPV3 channel.

3.4.6. Cholesterol interaction with TRPV3-Wt and OS mutants:

In silico analysis study shows the presence of cholesterol recognition amino acid consensus motif in the loop 4 of TRPV3. Further analysis and global docking experiments suggest that TRPV3 might interact with cholesterol in the intracellular loop 4. Cholesterol interaction with TRPV3 might have broad implication in the downstream signaling events such as PIP_2, phosopholipase C and EGF-mediated signaling cascades. For example, TRPV3 is regulated through EGF signaling and EGF signaling is regulated through plasma membrane cholesterol level [107, 437]. Two important TRPV3 regulators are phospholipase C and PIP_2, both shows antagonistic properties. Phospholipase C potentiates TRPV3 while PIP_2 inhibits its activity. Also, phospholipase C activity is increased by cholesterol supplementation which decreases the plasma membrane PIP_2 levels that is how cholesterol mediated potentiation of TRPV3 happens. Docking results where TRPV3 close structure interact with cholesterol but not the open structure, suggest that cholesterol might play important role in the closing of channel. Further constitutive active OS mutant also shows lower binding energy with compare to TRPV3-Wt which again suggest that cholesterol tight association is required to keep it in close state. Further biochemical characterization by using purified TM-Loop2-TM, TM-Loo4-TM, TM-Loo4-G573C-TM, TM-Loo4-G573S-TM, TM-Loo4-G573A-TM proteins tagged with MBP shows that Wt TM-Loop-4-TM binds strongly with cholesterol while the other mutants show almost no binding or reduced binding. This suggests that TRPV3-Wt in the plasma membrane may have strong interaction with cholesterol and this interaction may be helpful to keep the channel in close confirmation. However, it is possible that in the case of OS mutants, the interaction with TRPV3 might be weak and as a result these mutants have better opening probabilities and therefore are constitutively active in nature. Earlier it has been

charged (Arg, Glu, and Asp) and aromatic amino acid (Tyr, Phe and Trp) are conserved in the lipid water interface. These specific amino acids play essential role in the regulation of ion channel. LWI analysis of TRPV3 channel reveals that distribution of specific snorkeling amino acid (Arg and Tyr) share a complex relationship with body temperature. This analysis reveals that these snorkeling residues were selected under stringent selection pressure and membrane cholesterol content. Total Arg and Tyr content was found to be high in the warm-blooded animal as compare to the cold-blooded animals. Also, percent Tyr content in the LWI also varies between cold and warm animals. However, the total percentage of Arg at the LWI of TRPV3 increases in warm to cold blooded transition. Another amino acid which is Tyr shows high percent in warm blooded while it is lower in cold blooded animals. All these observations suggest that cholesterol and lipid play important role in the regulation of TRPV3.

3.4.5. Cholesterol-mediated regulation of TRPV3 channel functions:

Transmembrane proteins are tightly regulated through lipid and cholesterol content in the membrane [434-436]. This tightly regulated interaction mostly keeps these proteins in the thermodynamically ground state in normal physiological conditions. For ion channels these interactions mostly correlate with the closed state. Any alteration in the cholesterol content and /or in the interaction may result in the opening of these channels and may allow the influx of different ion across the membrane. This work establishes the interaction of cholesterol with TRPV3, especially in the closed state. This finding is also in agreement with the fact that sensitization of TRPV3 is dependent on the membrane cholesterol [159]. In 2014 Klein et al. have shown the cholesterol-mediated sensitization of TRPV3. Through changes in the plasma membrane cholesterol content they have found that in cholesterol supplement condition, TRPV3 is sensitized and thus prone to activation by lower concentration of agonists. Also, temperature-dependent activation of TRPV3 is shifted towards lower temperature in

3.4.3. Cholesterol binding motif sequences in TRPV3:

TRPV3 is present in DRG neurons and many of these cells are also positive for TRPV1 [30]. Increasing evidence suggest that this two-close homologues can also form heteromeric channels in neuronal system [40]. However, TRPV3 expresses abundantly in the epithelial keratinocyte and hair follicles where it is reported to be regulated by cholesterol [159]. Cholesterol content in the membrane affects TRPV3 activity. One study reveals that cholesterol supplementation in membrane sensitizes TRPV3 to lower temperature and lowers the concentration of agonists required for activation. This study suggests that there might be some consensus cholesterol-binding motifs present in the TRPV3 which potentiates its activity, by means of activation of downstream signaling cascades Also, they have reported that this increased channel activity is not because of the increased plasma membrane targeting of protein. Our *in silico* analysis reveals the presence of cholesterol recognition amino acid consensus (CRAC) motifs (L/V-X¬(1-5)-Y-X(1-5)-R/K) and some of these motifs are conserved in all vertebrates. We have identified 6 CRAC- and 4 CARC-motifs (inverted CRAC) in complete TRPV3 sequence. Among them, (CRAC 357-363, 563-567) and (CARC 319-326, 376-385) were found highly conserved in all vertebrates. Sequence alignment from different vertebrate species shows that (CRAC 558-572) motif present in the loop4 is with highest level of conservation in all vertebrate species. These suggests that cholesterol might regulate TRPV3 through binding in the loop 4.

3.4.4. Importance of important amino acids in Lipid-water interface:

Lipid-water interface (LWI) plays a key role in the regulation of transmembrane protein [434-436]. Earlier from our lab LWI analysis of TRPV1 reveals that small stretch of amino acids are conserved with compare to full length. Which suggest that these residues are under positive selection pressure. Further single amino acid analysis from TRPV1 reveals that few

Figure 99. The evolutionary changes of TRPV3 channels in the vertebrate lineages. The major evolutionary events are indicated on the respective branches. The amino acid sequences of the N- and C-terminal regions of the TRPV3 channels were conserved among amniote species, while the N- and C-terminal regions of TRPV3 in the western clawed frog were highly diversified from those regions of TRPV3 in other terrestrial vertebrate species. The ancestral states of the terminal regions are ambiguous since teleost fishes have lost the TRPV3 gene. Western clawed frog and mammals acquired opposite temperature sensitivities of TRPV3 channels; however, the timing of the shift is not clearly determined since the temperature sensitivities of TRPV3 channels of birds and reptiles have not been reported. Taken from [210].

3.4.2. TRPV3 as a vertebrate-specific ion channel:

Warm temperature/near body temperature sensation through TRPV3 is essential physiological process in the higher vertebrates. More specifically homeothermic vertebrates shows higher level of cholesterol Importance of warm sensing TRPV3 is more in the homeothermic vertebrates with compare to the ectothermic vertebrate **(Fig. 100)**. It shows evolutionary flexibility among vertebrates which is a direct consequence of change in the amino acid sequence. Such essential role of TRPV3 in the mouse and western clawed frog is opposite warm and cold sensation respectively. Another TRP member, TRPM8 also shows similar characteristic feature of TRPV3. It detects the cold temperature in the western and African clawed frog (noxious) while in rat and chicken it detects slightly cold.

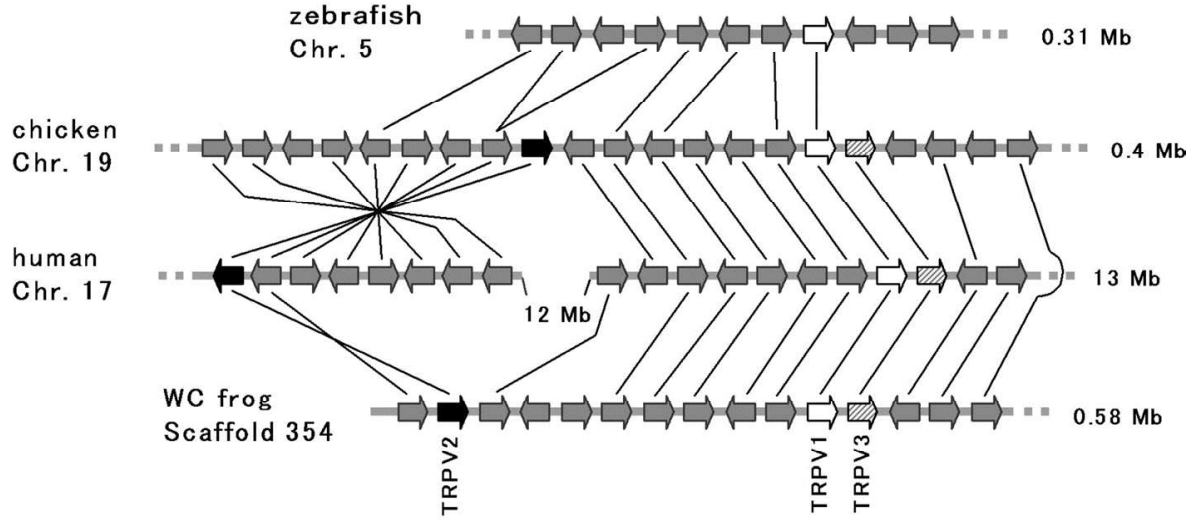

Figure 100. Gene orders surrounding TRPV1, TRPV2, and TRPV3 of 4 species belonging to different vertebrate classes. The lengths of the genomic regions are shown on the right. The arrow indicates the gene with the direction. The orthologous genes are connected by the lines. The open, filled, and striped arrows indicate TRPV1, TRPV2, and TRPV3 genes, respectively. Chr, chromosome Taken from [211].

3.4. Regulation of TRPV3 by cholesterol:

3.4.1. Evolution of TRPV3:

TRPV3 from fish, amphibian to vertebrate shows maximum evolutionary flexibility. Saito et al in 2011 shows the conservation of TRPV3 in different species where they have found that N- and C-terminal of TRPV3 from western clawed frog are more diversified in comparison to regions of TRPV3 in other terrestrial vertebrate species. Further detailed analysis reveals that TRPV3 channel property are largely different in western clawed frog and mammals. For example, chemical modulators which potentiate mammalian TRPV3 failed to show any effect on the western clawed frog. Also, their thermal properties are very much contrasting such as mammalian TRPV3 can be activated by warmth temperature while western clawed frog TRPV3 is activated by cold temperature. Further analysis reveals that teleost fish lineages have lost TRPV3 gene with time while all mammals have retained TRPV3. The unique presence and distribution of TRPV3 in skin correlates very well with its property during the evolution of vertebrates (from western clawed frog and mammals) [210] **(Fig. 99)**.

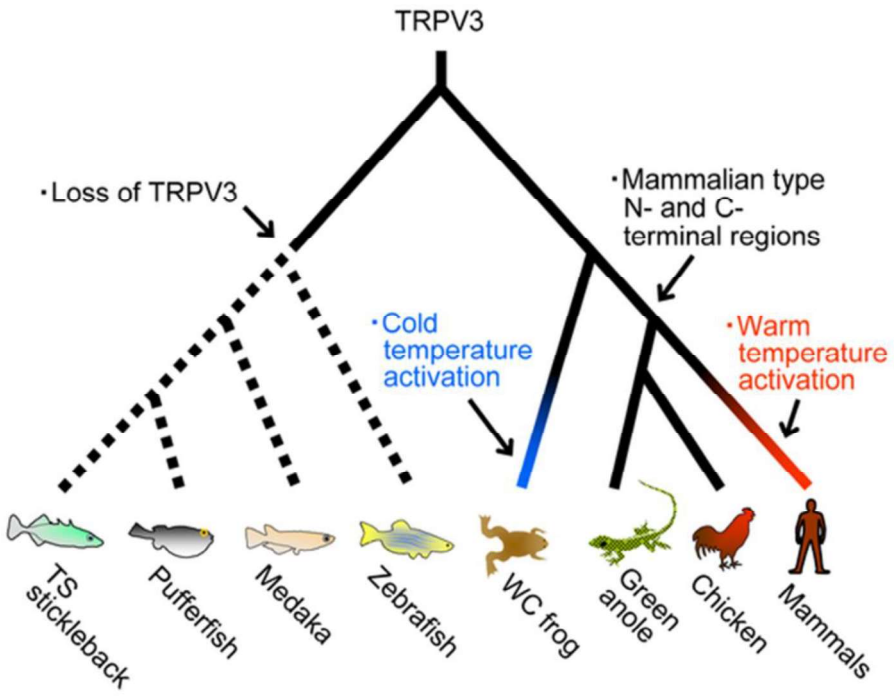

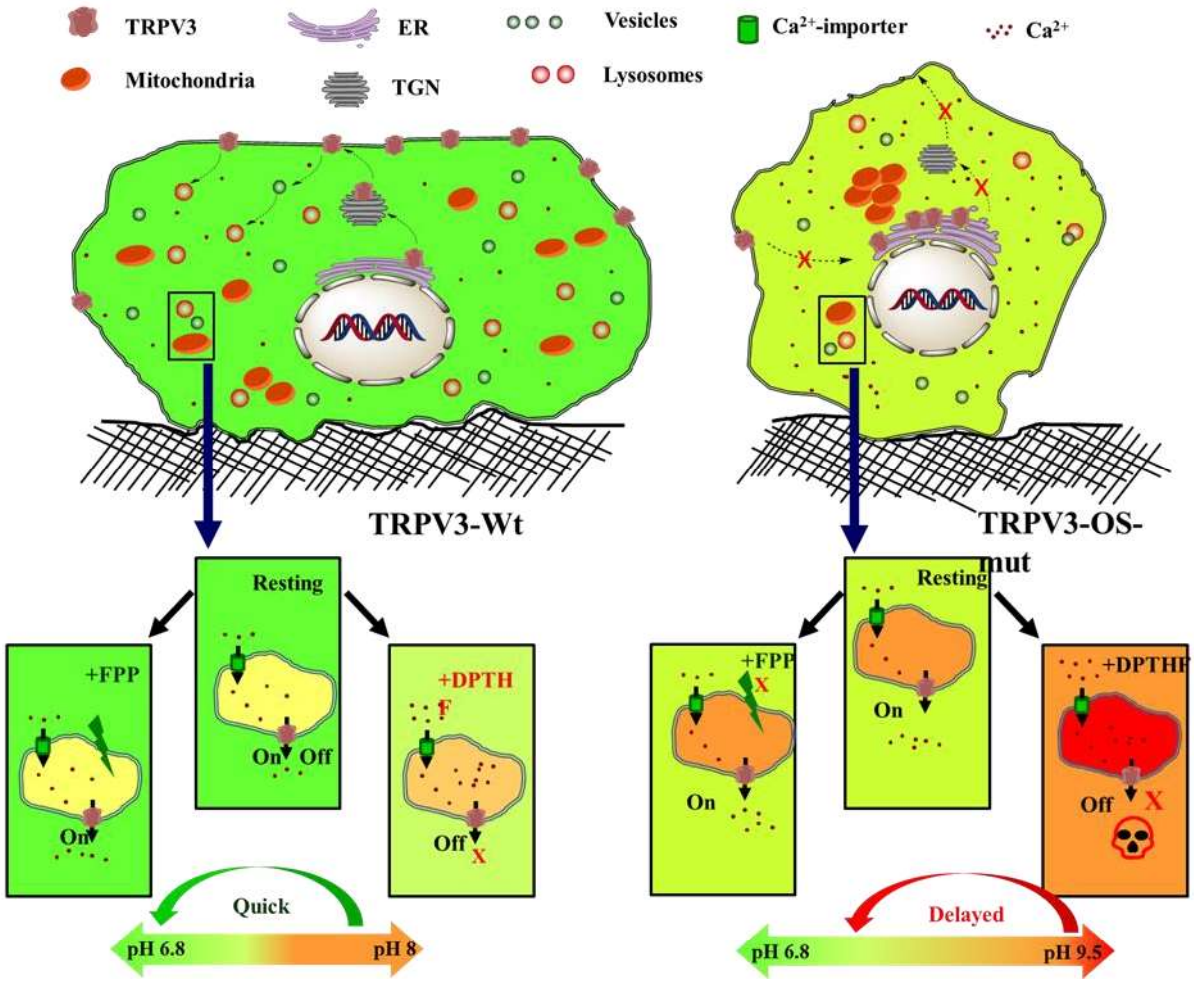

Figure 98. A plausible model demonstrating the importance of TRPV3 in regulation of intracellular pH and Ca^{2+} homeostasis. TRPV3-Wt localizes in the membrane while OS-mutants are primarily retained in the ER and affect vesicular trafficking as well as surface expression of other membrane proteins. This cause poor cell adhesion and clustering of mitochondria which in turn results in reduced cell size and increased cellular deformities. TRPV3-Wt as well as OS-mutants are present in the intracellular compartments and regulate Ca^{2+}-buffering activities by these organelles. Cells expressing OS-mutants have much reduced number of lysosomes, higher intracellular pH, and robust increment in intracellular Ca^{2+} upon pharmacological inhibition of TRPV3 by DPTHF. In intracellular organelles TRPV3 mostly act as Ca^{2+}-leaky channels in physiological temperature. Cells expressing OS-mutants have reduced number of functional lysosomes and impaired/delayed Ca^{2+}-buffering activity which correlates well with the impaired pH maintenance capacity of cytosol as well as within the intracellular organelles.

mutant shows an abrupt Ca^{2+} response after TRPV3 inhibition while activation doesn't change much. This could be due to the gating properties of the mutants that are "constitutively active" in nature.

3.3.6. Importance of TRPV3 in the regulation of lysosomal pH regulation:

Lysosome pH regulation is a complex process which is regulated by many proteins including transporter, pumps, channels etc. These all modules act synergistically and maintain the pH balance in lysosome and cytoplasm. The importance of TRP channels in the regulation of lysosome pH and function is coming from the evidence that mutation in TRPML1 has been associated with lysosomal storage disease called mucolipidosis type IV [95]. Our Ca^{2+} and pH imaging experiment largely suggest that TRPV3 might play as an exporter from lysosome to cytoplasm **(Fig. 98)**. It has been reported a long time ago that lysosomal Ca^{2+} and pH share a complex relationship. It has been suggested that change in the lysosome Ca^{2+} level does not change its pH but increased lysosome pH may reduce its Ca^{2+} level. Overall how TRPV3 mediated Ca^{2+} and pH regulation is not very well studied but based on some of live cell Ca^{2+} and pH imaging experiments indicate that TRPV3 plays as a molecular route for Ca^{2+} release from lysosome to cytoplasm, that is why inhibition of TRPV3 results in the increased Ca^{2+} level in the intracellular organelle including lysosome and mitochondria **(Fig. 98)**.

	TRPML3	Plasma membrane, early/late endosomes	pH regulated Ca^{2+} channel	[429-431]
Vanilloid				
	TRPV2 TRPV3 TRPV5 TRPV6	Early endosome Lysosome Recycling endosome	Ca^{2+} channel Ca^{2+} channel Ca^{2+} channel	[432] [244, 272] [433]

3.3.5. Importance of TRPV3 in intracellular Ca^{2+} regulation:

Although there is very less information available about the involvement of TRPV3 in intracellular Ca^{2+} regulation, however it is well accepted that physical stimuli such as temperature and different chemical stimuli modulate TRPV3 activity. For example, heating of keratinocyte in culture results in the release of ATP in the medium which acts on the nearby sensory nerve and activates different signaling cascade. Also, this extracellular ATP increases the TRPV3 mediated current due to the decrease in the level of PIP_2 [226]. Role of TRPV3 in the phosphatidylinositol metabolisms results in the Ca^{2+}-influx and also change the level of PIP_2 [226]. TRPV3 and PIP_2 cross talk is also supported by the fact that Voltage- and temperature-dependent activation of TRPV3 is potentiated by receptor-mediated PIP_2 hydrolysis. Two basic amino acid residues (R696A and K705A) in TRP domain are important for this PIP_2 binding with TRPV3 [226]. Other possible signaling molecules which activate TRPV3 are H^+ and FPP [225]. TRPV3 activation in skin keratinocyte also results in the modulation of several physiological functions such as inhibition of cell proliferation, induction of apoptosis, modulation of cell differentiation, inhibition of hair growth, and important in cutaneous barrier formation. More particularly it regulates the growth factor signaling by means of direct complex formation with TGF-α and EGFR. The stable cells expressing OS

Table 12. Localization and physiological function of endosomal ion transport. (Taken from [416].

Family	Name	Localization	Transport activity	References
CIC				
	ClC-3	Late endosomes (brain)	$2Cl^-/H^+$ transport	[417-420]
	ClC-4	Early/recycling endosomes	$2Cl^-/H^+$ transport	[418, 421]
	ClC-5	Early/recycling endosomes	$2Cl^-/H^+$ transport	[421]
	ClC-6	Late endosomes (brain)	$2Cl^-/H^+$ transport	[419, 420, 422]
	ClC-7	Lysosome	$2Cl^-/H^+$ transport	[421]
NHE				
	NHE-6	Early/recycling endosomes (brain)	K^+ or Na^+/H^+ transport	[419, 420, 423, 424]
	NHE-7	Plasma membrane, Golgi, endosomes	K^+ or Na^+/H^+ transport	[425]
	NHE-8	K+ or Na+/H+ transport 58	K^+ or Na^+/H^+ transport	[426]
	NHE-9	**?**	K^+ or Na^+/H^+ transport	
TPC				
	TPCN1	Lysosome	NAADP-responsive Ca^{2+} channel	[427]
	TPCN2	Lysosome (muscle)	NAADP-responsive Ca^{2+} channel	[427, 428]
Mucolipins				
	TRPML1	Lysosome (endosome?)	Cation H^+ channel	[429]
	TRPML2	Lysosome (endosome?)	Not characterized	[429]

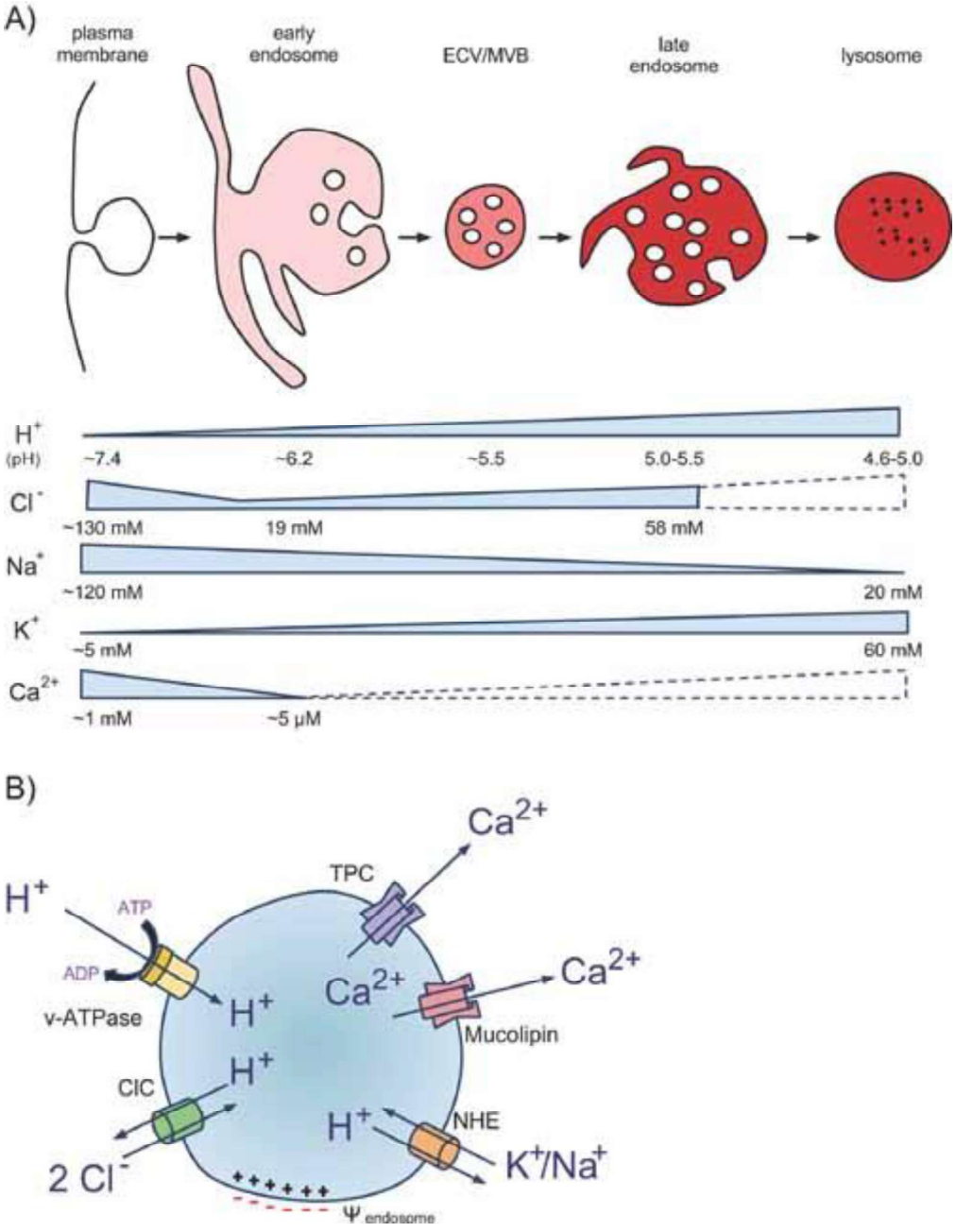

Figure 97. Schematic representation of ionic gradient across across endolysosomal compartment. a. The figure summarizes the change in ionic gradient during the endocytic pathway. From formation of endocytic vesicle to formation of mature lysosome acidification continuously increases. **b.** The figure shows the major transporters involve in the regulation and maintenance of ionic composition in endolysosome compartment. Taken from [416].

3.3.4. Comparison of TRPV3 with other lysosomal ion channels:

Lysosome has a large number of ion channels and proteins which maintain its acidic pH and cellular neutral pH. Different ions like H^+, Cl^-, Na^+, K^+ and Ca^{2+} plays important role in the regulation of endolysosomal pH gradient **(Fig. 97)**. These includes H^+-pump, CIC-7 antiporter, $H^+/K^+/Na^+$ antiporter, Na^+ channel, K^+ channel, and Ca^{2+} leak channels which act together and maintain this balance [413]. Some of Ca^{2+} channels, namely TPCs are present in endolysosomal compartments which also play a role in endosomal pH regulation [414, 415]. Other TRP channels which are present in endolysosome are TRPML family members, namely TRPML1, TRPML2 and TRPML3. These mucolipin family members play important role in the lysosome function. Mutation in TRPML1 leads to lysosome storage disorder mucolipidosis type IV [95]. The Ca^{2+} imaging experiment in HaCaT cell expressing TRPV3-Wt or OS mutant reveals that activation of TRPV3 by FPP does not shows any significant increment in intracellular Ca^{2+}-levels, especially in the case of OS-mutants. This effect could be the consequence of the fact that these mutants are "constitutively active" and therefore activation does not lead to any further change. However, pharmacological inhibition of TRPV3 by DPTHF results in increased Ca^{2+}-level in intracellular organelles as well as in the cytosol in TRPV3-Wt expressing cells. This observation suggests that TRPV3 might be acting as a Ca^{2+} efflux from these intracellular compartments.

Table 11. Examples of dileucine-based and tyrosine-based sorting signals. (Taken from [412].

DXXLL MPR300/CI-MPR	SFHDDS**D**ED**LL**
MPR46/CD-MPR	EESEER**D**DH**LL**
Sortilin	GYHDDS**D**ED**LL**
SorLA/SORL1	ITGFSD**D**VP**MV**
GGA1 (1)	ASVSLL**D**DEL**M**
GGA1 (2)	ASSGLD**D**LD**LL**
GGA2	VQNPSA**D**RN**LL**
GGA3	NALSWL**D**EE**LL**
[DE]XXXL[LI] LIMP-II	D**E**RAP**LI**
NPC1	T**E**RER**LL**
Mucolipin-1	S**E**TER**LL**
Sialin	T**D**RTP**LL**
GLUT8	E**E**TQP**LL**
Invariant chain (Ii) (1)	D**D**QRD**LI**
Invariant chain (Ii) (2)	N**E**QLP**ML**
YXXØ LAMP-1	G**Y**QT**I**
LAMP-2A	G**Y**EQ**F**
LAMP-2B	GYQTL
LAMP-2C	G**Y**QS**V**
CD63	G**Y**EV**M**
CD68	A**Y**QA**L**
Endolyn	N**Y**HT**L**
DC-LAMP	G**Y**QR**I**
Cystinosin	G**Y**DQ**L**
Sugar phosphate exchanger 2	G**Y**KE**I**
Acid phosphatase	G**Y**RH**V**

3.3.2. TRPV3 as a Lysosomal protein:

Although TRPV3 is known to be present in the plasma membrane, not much is reported about the intracellular localization of TRPV3. Through this study, and by several methodologies, this thesis work has demonstrated that TRPV3 is a lysosomal protein and it regulates many subcellular functions such as cellular trafficking, Ca^{2+} and pH homoeostasis. Stable cell lines expressing Wt and OS mutants show colocalization of GFP-tagged TRPV3-Wt or OS mutants with LysoTracker Red, a dye that stains functional lysosomes. Also, *in silico* data suggest that TRPV3 has four lysosomal targeting signal sequence on its N-terminus, and these LTS also show colocalization with lysosome in the live cell. Further biochemical fractionation study from goat brain also reveals that this TRPV3 is present in a lysosomal fraction. Our results match with another report which indicates that TRPV3 may act as a lysosomal protein. It is also important to mention that degradation of plasma membrane TRPV3 is regulated by Sorting Nexin (SNX11), a lysosomal protein [244].

3.3.3. Lysosomal target sequence in TRPV3:

By insilico analysis, we were able to identify that total four lysosomal targeting sequences are present in TRPV3 and all are present in the N-terminal region. Previously it has been reported that lysosomal transmembrane protein sorting requires the presence of dileucine-based motifs, DXXLL or [DE]XXXL[LI], and tyrosine-based motifs, YXXØ [410, 411]. The N-terminus of TRPV3 contains four different (322-DMILL-326), (134-ELVELL-139), (229-DIAALL-234), (276-EIVQLL-281) lysosomal targeting sequence. When expressed as GFP-tagged protein, all these fragments localize to the lysosome and therefore suggest that each of these sequences can serves as independent lysosomal targeting sequence. These sequences are conserved throughout the vertebrate evolution and essentially during last 450-500 million year ago.

3.3. The importance of TRPV3 in the regulation of subcellular functions:

3.3.1. TRPV3 in vesicle recycling:

Vesicular trafficking of membrane proteins is an important step for regulation of different cellular mechanism. Very recently in 2016 one report revealed that the sorting nexin 11 (SNX11) which is a vesicular trafficking protein downregulates the level of the TRPV3 plasma membrane protein [244]. Also, exogenous expression of SNX11 in HEK293 results in the decreased level of TRPV3 protein as well as TRPV3-medaited currents. The importance of SNX11 in the cellular trafficking of TRPV3 has been shown recently. SNX11 helps targeting of TRPV3 from plasma membrane to the lysosome for its degradation [244]. There are large number of TRPV3 mediated direct and indirect effects on keratinocyte have been reported **(Fig. 96)**.

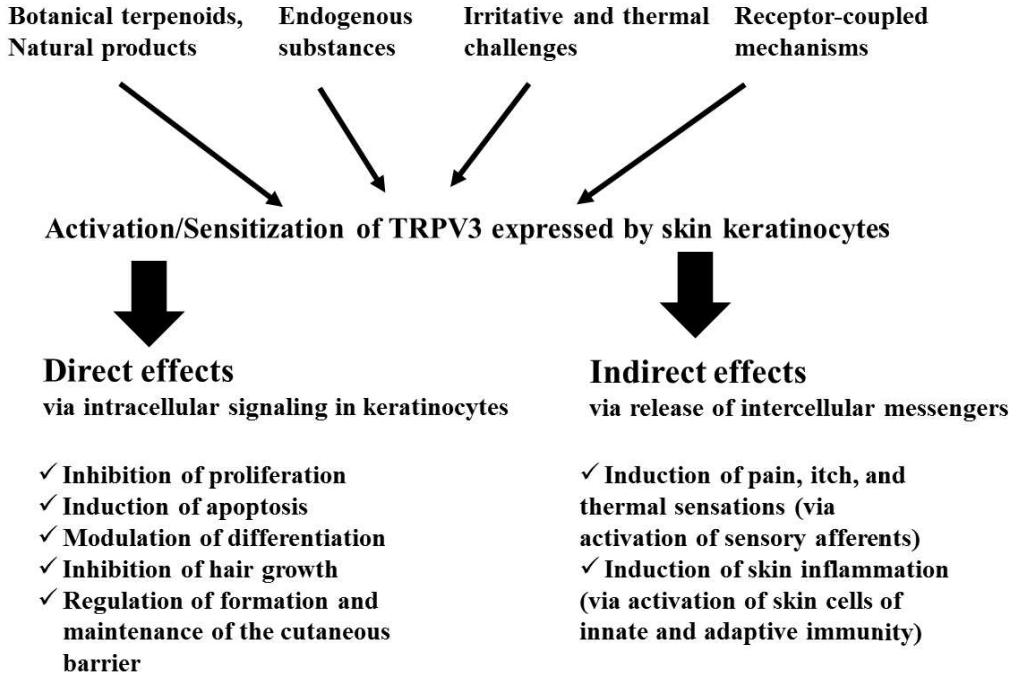

Figure 96. TRPV3 mediated different functions in skin keratinocyte. Activation of TRPV3 in skin by exogenous and endogenous agents result in TRPV3 mediated Ca^{2+} influx to the keratinocyte. TRPV3 activation results in inhibition of keratinocytes proliferation, induces cellular apoptosis and modulates epidermal differentiation, hair growth and barrier functions. Other mechanism includes release of many secondary messenger such as ATP, prostaglandin E2, nitric oxide, which acts on the neighbouring cells and initiates downstream signaling events. Taken from [70].

Wt as well as OS mutants (as GFP-tagged proteins) confirm that these fusion proteins are present in the lysosome as observed in stable cell lines. Also, endogenous TRPV3 is detected in the lysosomal fraction isolated from goat brain extract, suggesting that TRPV3 acts as a lysosomal protein. TRPV3 also has four lysosomal targeting sequences in its N-terminal region. These lysosomal targeting sequence (LTS) are conserved in all vertebrates and are functional. Live cell imaging of these LTS in HaCaT cells also shows colocalization with LysoTracker Red. These results in general suggest that TRPV3 is targeted to lysosome and acts as a lysosomal protein. Along with this report, there is a recent report which also suggests that TRPV3 as a lysosomal protein and degradation of plasma membrane TRPV3 is regulated by Sorting Nexin (SNX11) [244].

Surprisingly we have found that OS mutant expressing cells show reduced number of functional lysosome and with restricted movement when compared to the cells expressing TRPV3-Wt. The OS mutants are “constitutively active” in nature and therefore damages the structure and function of the lysosomes. Indeed, in stable cell lines expressing the Wt or OS mutants show altered cytoplasmic pH and Ca^{2+} buffering abilities. These evidences altogether suggest that TRPV3 is a lysosomal protein and changes its structure-function-regulation causes abnormalities to the lysosomal function.

such as hyper-IgE level and increased T cells [393]. Apart from these, there is not much known about the molecular mechanism of this disease. In continuation to that, in this thesis work we have characterized these mutants along with the Wt in HaCaT cell, an epithelial keratinocyte cell line [409]. Expression of the mutant's cause damage to the intracellular cell organelles such as ER, Golgi, Mitochondria, and Lysosome [272]. OS mutant expressing cells shows reduced surface expression of membrane proteins while Wt cells show normal membrane localization of TRPV3 as well as other membrenae proteins. For example, OS mutant expressing cells show no surface expression of TRPV1. We have also observed that OS mutant expressing cells have impaired cell adhesion abilities (they are not able to grow on the glass surface properly) while Wt expressing cells show better cell adhesion on the glass surface. ATP is a well-known secondary messenger which acts as a purinergic compound and induce itching signal [256]. The stable cell lines expressing TRPV3-Wt and different OS mutants were tested for their ATP release and inhibition of TRPV3 cause more ATP release in the medium. However, the detailed signaling events involved in such is not very clear.

3.2.5. OS as a lysosomal disorder:

Transient transfection in HaCaT cell with TRPV3-Wt and OS mutants reveal that the OS mutants damage intracellular organelle structure and functions. We have also found presence of very less number of functional lysosome and mitochondria in the OS expressing cell. OS patients shows hair loss, bone lose, and impaired cutaneous barrier formation. All these symptoms shown by OS patients are directly regulated through TRPV3. Other OS symptoms includes pain, itch, thermal sensation, and skin inflammation, these symptoms are also indirect consequence of altered TRPV3 function. TRPV3 activation also cause inhibition of cellular proliferation and induction of apoptosis. All these OS symptoms shown by patients are due to the constitutive activation of TRPV3 which results in the altered subcellular function. Other experiments include Colocalization experiment in stable cell lines expressing TRPV3-

related to OS present in human population are marked in the TRPV3 structure **(Fig. 94).** Analysis of different missense variants of hTRPV3 has been shown in **(Fig. 95).**

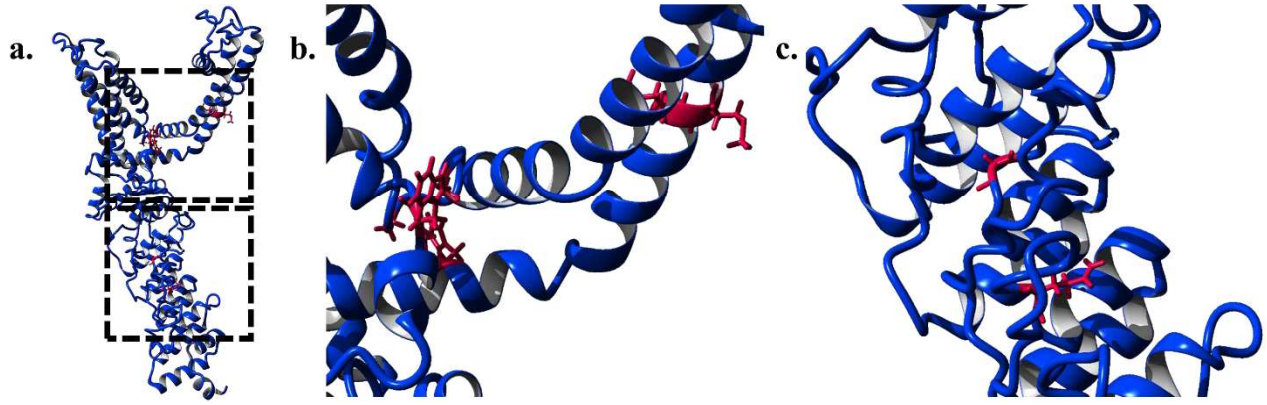

Figure 94. Schematic representation of OS mutant in TRPV3 structure. a. Shows human TRPV3 structure depicting the OS point mutants (Gly573Ala, Gly573Cys, Gly573Ser, Try692Gly, Met672lle, Gly573Val, Gly568Asp, Gly568Val, Gln580Pro, Trp521Ser, Gly568Cys, Leu673Phe). **b-c.** Shows zoom up image.

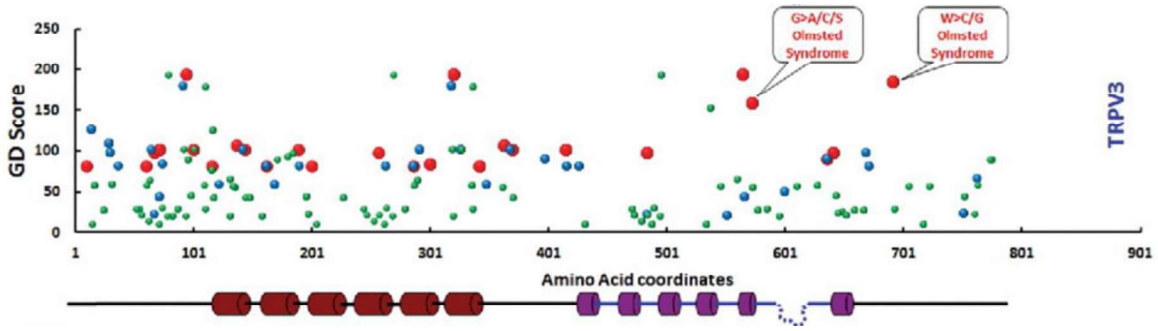

Figure 95. Analysis of missense variants of hTRPV3. Mutational analysis of TRPV3 ion channels on the basis of Grantham Deviation, SIFT and PolyPhen 2 Score are shown. The deleterious mutations reported in the 2504 (1000G Phase3 v5 Reference) genomes from 26 different ethnic populations were plotted in X-axis (labelled as the amino acid coordinates) and GD scores of the respective mutations were plotted in Y-axis. The red spheres denote mutations which are most likely damaging the structure function relationship of TRPV3 according to all three mutation prediction methods (GD, SIFT and PolyPhen), the blue spheres denote the mutations which are probably damaging according to only two of these methods and the green spheres denote ones which are probably damaging according to only one of these methods. Figure taken from [408].

3.2.4. Effect of TRPV3 mutations in cellular level:

The constitutively active TRPV3 OS mutants cause high cell death and increased apoptosis [72, 243]. Also, the patients having these mutants show immunological phenotype

endogenous stimuli, release of many secondary messengers and inflammatory mediators which act on sensory neuron. Taken from [406].

3.2.3. TRPV3 in OS:

A large number of mutation in TRPV3 have been reported since 2012. The first report was from Beijing, China, where author have identified a de novo mutation (Gly573Ser in TRPV3) in a patient suffering from OS. Exome sequencing of five different individuals who were affected with *Olmsted Syndrome* suggests that missense mutation in TRPV3 were found associated with this disorder. In this study authors have reported that Gly573Ser were found in three patients, Gly573Cys in one patient, and Trp692Gly in one patient [243]. In 2012, another case study from India revealed a boy who is positive for a mutation in TRPV3 [392]. This study reported Gly573Ser mutation by exom sequencing and Sanger sequencing [392]. In 2014 one report from France, identified a girl (who was affected with *Olmsted Syndrome*) as a positive for the de novo heterozygous mutation in TRPV3 [394]. In this study, they have reported that Leu673Phe is mutated in TRPV3 [395]. In 2014 one case study from Israel have reported mutation in TRPV3 at position Trp521Ser which is associated with *Olmsted Syndrome* [396]. Another case study from Tehran, Iran have reported a boy suffering from *Olmsted Syndrome* who is positive for a mutation in TRPV3, especially at position Trp692Cys [397]. In 2015 one study from China was reported where a male patient suffering from focal palmoplantar keratoderma is reported to be positive for a mutation in TRPV3, especially at position Gln580Pro [407]. Three different individuals have been found to be positive for *Olmsted Syndrome* where three homozygous recessive mutation have been reported. In one patient TRPV3 substitution mutation was identified at the position Trp521Ser. Two more positions are Gly568Cys and Gln216-Gly262del reported in two brothers [395]. Different point mutation

3.2.2. Molecular players involved in OS:

Clinical symptoms of OS overlap with skin carcinoma (PPK). One of the important gene, namely LOR has been associated with the pathogenesis of hereditary diseases such as mutilating Palmoplantar Keratoderma (PPK) [404]. The LOR gene codes for the Loricrin protein (a major protein component of the cornified cell envelope) and this protein is found in terminally differentiated epidermal cells. This is important to mention that recent reports have failed to detect any mutation in LOR gene [390] in OS patients. Also, other important genes for skin function such as KRT1 (Keratin 1), KRT10 (Keratin 10) and GJB2 (Gap junction protein beta 2) and SLURP1 (Secreted Ly-6/uPAR-related protein 1) were not found to be affected in patients suffering from OS. Instead, mutation in membrane-bound transcription factor protease site 2 (MBTPS2) has been associated with *Olmsted Syndrome* [405]. In recent reports related to *Olmsted Syndrome* every patient was found normal with respect to the above-mentioned genes. Considering all these reports, mutation in TRPV3, a non-selective cation channel turned out to be highly significant as a molecular cause of OS. Other intermediate signaling molecule which act downstream of TRPV3 are neuropeptides, proinflammatory cytokines, growth factors such as TGF-α, NO, PGE, ATP **(Fig. 93)**.

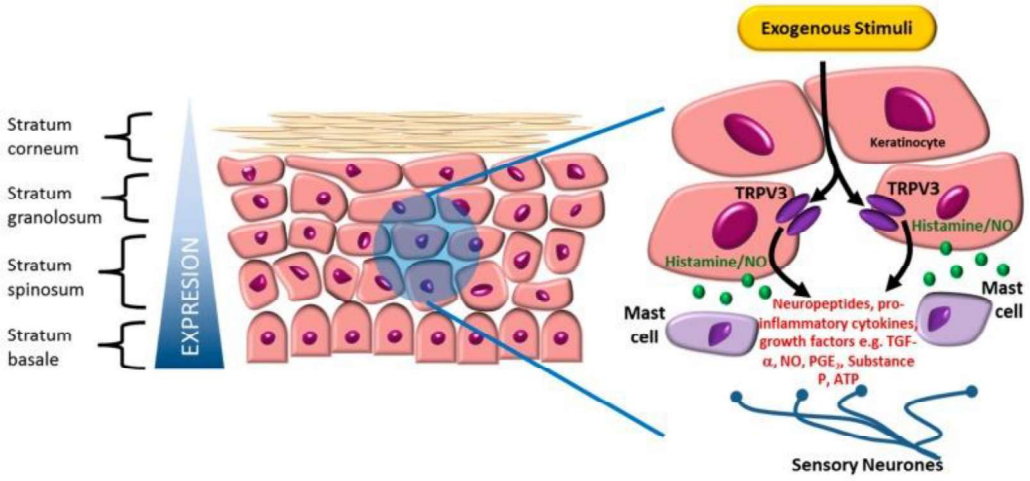

Figure 93. Schematic representation of expression and function of TRPV3 in skin. Epidermal keratinocyte and hair follicles expresses abundant TRPV3. Expression of TRPV3 increases under certain condition such as

[397]	NR	NR	NR	Dystrophic/absent	S	S	NR
[398]	NR	NR	NR	NR	NR	NR	NR
Family 1	M	Lesion border	Hands and feet	Koilonychia; thin plates	Absent	S	Absent
Family 2	Absent	Lesion border; distal digits (hands)	Feet	Normal	Absent	S	Absent
Family 3	M	Lesion border	Feet	Koilonychia; thin plates; onychoschizia	S	S	Present
Family 4	NR	Lesion border	NR	Onychoschizia	NR	S	Absent
Family 5	M	Lesion border; dorsal feet	Feet	Koilonychia; thin plates; onychoschizia	Absent	S	Absent
Family 6	NR	Lesion border	No	Normal	NR	S	Absent

Abbreviations: M, mild; Mod, moderate; NR, not reported; S, severe.

[1]Individual families.

[2]Individuals.

[399]	-	17p13.2	palmoplantar keratoderma	-	-	Present	sparse scalp hair
[400]	-	p.Gly568Val	palmoplantar keratoderma	-	-	Present	Present
[401]	-	p.Gly573Val	palmoplantar keratoderma	-	-	Present	Present
[402]	AD	p.Met672Ile	palmoplantar keratoderma	-	-	Present	Present
[403]	-	17p13.2	palmoplantar keratoderma	-		Present	Present
Report	**Follicular keratosis**	**Erythema**	**Hyperhidrosis**	**Nails**	**Lesional itch**	**Lesional pain**	**Leukokeratosis**
Olmsted's patient	NR	Lesion border; dorsal hands	Hands	Thickened	NR	Present	NR
[243]	Scalp	Lesion border	NR	NR	S (4)2	Present	NR
[243]	Scalp	Lesion border	NR	NR	S	Present	NR
[243]	NR	Lesion border	NR	NR	S	Present	NR
[392]	NR	NR	NR	Dystrophy	No	"Functional impairment"	NR
[393]	NR	Lesion border	NR	Dystrophy	S	S	NR
[394]	NR	Erythromelalgia	Present	Thin, brittle	S	S	NR
[395]	M	Erythromelalgia	Present	Normal	S	S	NR
[396]	NR	Diffuse, palms and soles	NR	NR	Present	Present	Present

Table 10. Clinical findings in patients with mutations in TRPV3 Adapted from [391]

Report	Inheritance	*TRPV3* mutation	Plantar keratoderma	Palmar keratoderma	Pseudoainhum	Periorificial keratoderma	Hair
Olmsted's patient			Diffuse-S	Diffuse-S	Present	Present	Dry
[243]	AD	p.Gly573Ser (4)1	M(1)2; Mod(1); S(2)	M(1)2; Mod(1); S(2)	Present	M(1)2; Mod(1); S(2)	Alopecia - M(1); Mod (1); S (2)
[243]	AD	p.Gly573Cys (1)	M	M	Absent	M	Alopecia - M
[243]	AD	p.Trp692Gly (1)	Mod	Mod	Present	Mod	Alopecia - M
[392]	AD	p.Gly573Ser (1)	Diffuse-S	Diffuse-S	Present	M	Fine-dry
[393]	AD	p.Gly573Ala (1)	Diffuse-S	Diffuse-S	Absent	S	Alopecia-S
[394]	AD	p.Leu673Phe (1)	Diffuse-S	Diffuse-S	Absent	Absent	Fine, dry
[395]	AR	p.Gly568Cys; p.Gln216_Gly262del (1)	Diffuse-S (1); Focal-Mod(1)	NR	Absent	Absent	Fine-dry
[396]	AR	p.Trp521Ser (1)	Diffuse-S	Diffuse-S	Absent	Present	Sparse
[397]	AD	p.Trp692Cys (1)	Diffuse-S	Diffuse-S	Present	Present (Mod)	Sparse; fragile
[398]	AD	p.Gln580Pro (1)2	Focal-Mod	Focal-Mod	Absent	Absent	Normal
Family 1	AD	p.Gly573Cys (1)	Focal-S	Focal-M	Absent	Absent	Fine
Family 2	AD	p.Gly568Val (1)	Focal-Mod	Focal-M	Absent	M	Normal
Family 3	AD	p.Gly568Asp (2)2	Focal-Mod	M	Absent	M	Fine
Family 4	AD	p.Gly568Asp (1)	Focal-Mod	Focal-M	Absent	NR	Normal
Family 5	AD	p.Gly573Ser (1)	Focal-Mod	M/transient	Absent	M/transient	Fragile, sparse
Family 6	AD	p.Gly573Ser (1)	Focal-Mod	M	Absent	Absent	Normal

3.2 TRPV3 and Olmsted Syndrome:

3.2.1. OS as a rare genetic disorder:

OS was first time reported in 1927 [375]. Since then worldwide around 80 patients have been detected with this syndrome. Initially, it was believed that this disorder is restricted to male only, but current reports suggest that females are equally prone to this syndrome. It is a rare disorder of defective keratinization which is congenital and sporadic in nature. Patients suffering from this disorder shows clinical symptoms of bilateral mutilating palmoplantar keratoderma and periorificial keratotic plaques **(Fig. 92)** [376-382]. Other features include severe itching at the affected regions of the body, impaired hair growth, loss of hearing and often loss of terminal portion of the limbs, auto-amputation of digits, loss-of-bones and/or osteonecrosis **(Fig. 92)** [377, 383, 384]. Until now there is no treatment for this disease as treatments with different agents such as salicylic acid, urea, boric acid, shale oil, retinoic acids, corticosteroids, anti-microbial drugs, antihistamines, Vitamin-E, Vitamin-A and other emollients failed to improve the pathological conditions [383]. Surgical removals of affected skin and autografting have also been unsuccessful due to the recurrence of the disorder [385-389]. The occurrence of this disorder is rare, and hallmarks of OS represent the fact that excludes this disorder from other syndromes of keratoderma. This disorder shares etiological similarity with another skin syndrome such as palmoplantar keratoderma (PPK). Indeed, there are reports of co-occurrence of squamous cell carcinoma and adenocarcinoma of the lung in certain cases of OS [390]. Patients suffering from this shows higher susceptibility to develop epidermal tumours [388]. Above mentioned features make this syndrome clinically important.

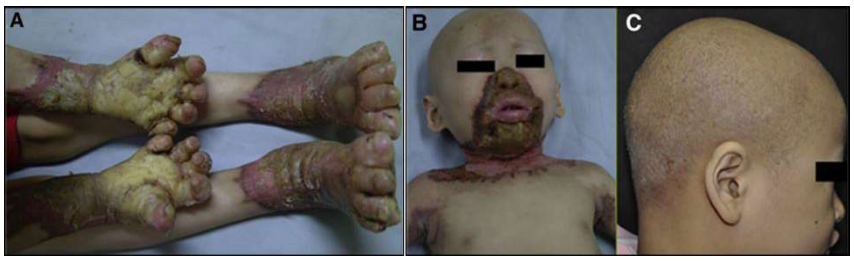

Figure 92. Shows patient suffering from *Olmsted Syndrome*. Gain-of-function mutations of TRPV3 results in the constitutive opening of channel. Characteristic feature includes bilateral mutilating palmoplantar keratoderma, periorificial keratotic plaques, and diffuse hair loss with follicular papules. Taken from [243].

Neuritogenesis is a complex event which is regulated by many signaling molecules including Ca^{2+} gradient along with different other signaling molecules such as PKC, PKA, cAMP, PIP_2 etc. Such process may involve other signaling pathways as well. Indeed, our work suggests that activation of TRPV2 results in phosphotyrosination of proteins present in the cell edges. This strongly suggests the involvement of Tyrosine-kinase in this process. However, there is a possibility that other kinases may be involved in this complex mechanism. Indeed, previous reports have suggested the involvement of MAPK, ERK, and other kinases in neuritogenesis process [171]. Involvement of cAMP pathway in this signaling event is also possible [163, 358].

The presence of TRPV2 in a special subcellular structure such as neurites growth cone was studied, other than TRPV2 there are some other TRPV members were also reported in these subcellular structures such as TRPV1 and TRPV4.

agreement with previous reports suggesting the importance of TRPV2 in neuritogenesis [171, 278]. These previous studies were mainly performed using another neuronal cell line PC12 in presence and absence of nerve growth factors, also activated by mechanical stimuli or by membrane stretching [171, 278]. Use of these nerve growth factor and membrane stretch allows activation of different signaling pathways so it is very difficult to conclude the actual role of TRPV2. Also, TRPV2 knockdown studies using siRNA results in a reduction in NGF-induced neurite outgrowth, at least in in vitro culture conditions [171]. Our experiments in this work are by using the neuronal cell line F11 cell line in presence and absence of specific agonist and antagonist. Use of pharmacological activator and inhibitor suggest that activation of TRPV2 induces neurite initiation and branching. However, once the neurites are initiated, the actual lengths are independent of the TRPV2 expression level.

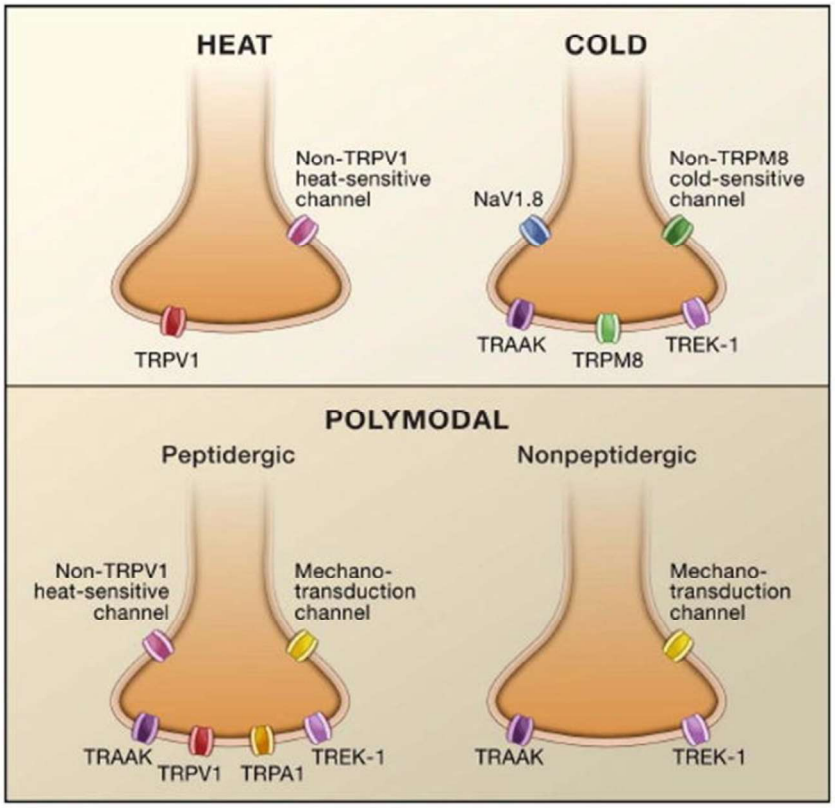

Figure 91. Nociceptor expresses different ion channel. Mainly nociceptor subtype which senses and detect the stimuli possess polymodality. Like, heat, cold and mechanosensitive afferents mainly express TRPV1, TRPM8 and TRPV4 respectively with some other sensors such as sodium and potassium channel which is essential for propagation of action potential. Taken from [373].

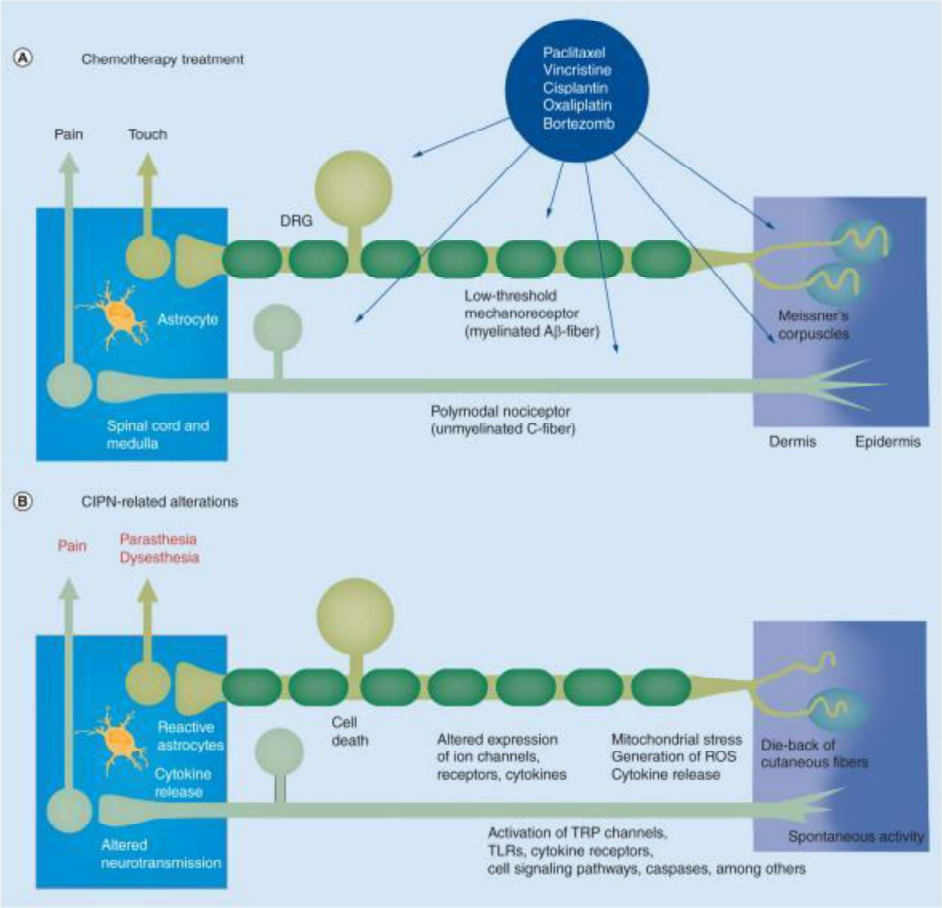

Figure 90. Schematic representation of chemotherapy-induced peripheral neuropathy. A. The figure represents different chemotherapy agents such as vincristine, paclitaxel, bortezomib and oxaliplatin which acts on many neuronal and glial targets. B. The figure represents different possibilities how these cells act and modulate their function in case of Chemotherapy-induced peripheral neuropathy. As a result of chemotherapy, neuronal and glial cells cause astrocytes activation and increased cytokine release which in turn alter signaling events in primary afferents fibres. CIPN (Chemotherapy-induced peripheral neuropathy), DRG (Dorsal root ganglion), ROS (Reactive oxygen species), TLR (Toll-like receptor), TRP (Transient receptor potential), Taken from [374].

3.1.11. Importance of study:

Importance of TRPV channel in neuritogenesis and different neuronal function are very well reported. Localization and distribution of TRPV2 in very specific subsets of the F11 cell such as growth cone, filopodia, neurite suggest a very specific function of TRPV2 in these neurons because these structures are important for the cell adhesion, cell-cell contact, cell spreading etc. These subcellular processes are precisely regulated by the multiple signaling molecules including TRPV ion channel protein **(Fig. 91)**. Any abnormality in these signaling processes leads to the development of different pathophysiological conditions. This work is in

neuropathic pain in the cancer patients by altering the microtubule cytoskeleton [366-369]. Another cytoskeletal stabilizing drug Vincristine cause the neuropathic pain in the cancer patients [367, 368, 370, 371]. Evidence suggest that microtubule stabilisation or destabilisation by Taxol, Paclitaxel or Nocodazole, Colchicine respectively could alter the pain thresholds and in particular be the primary cause of CIPN [162, 284]. Such findings link microtubule cytoskeletal in the context of chronic pain and the non-selective Ca^{2+} ion channels (TRP). Previously TRPV1 and TRPV4 have been shown to interact with microtubule cytoskeleton [196, 199]. Also, these channels stabilise as well as regulate the dynamics of microtubule cytoskeleton. Involvement of another Vanilloid member TRPV2 also have been reported in CIPN due to its high threshold activation temperature. Also, differential distribution of TRPV2 in sensory neurone and presence in neurotrophin-3 dependent DRG neuron suggest its possible role in the pain sensation [372] **(Fig. 89)**.

3.1.10. The importance of TRPV2 in neuropathic pain and other forms of pain:

Large number of evidence suggest that cancer patient during chemotherapy treatment develop chronic pain. This chronic pain develops as a result of the use cytoskeletal stabilising drugs such as Taxol, Vincristine, Paclitaxel, Bortezomib and Oxaliplatin etc. Patient suffering from this type of pain are called as chemotherapy induced peripheral neuropathy (CIPN) **(Fig. 90)**.

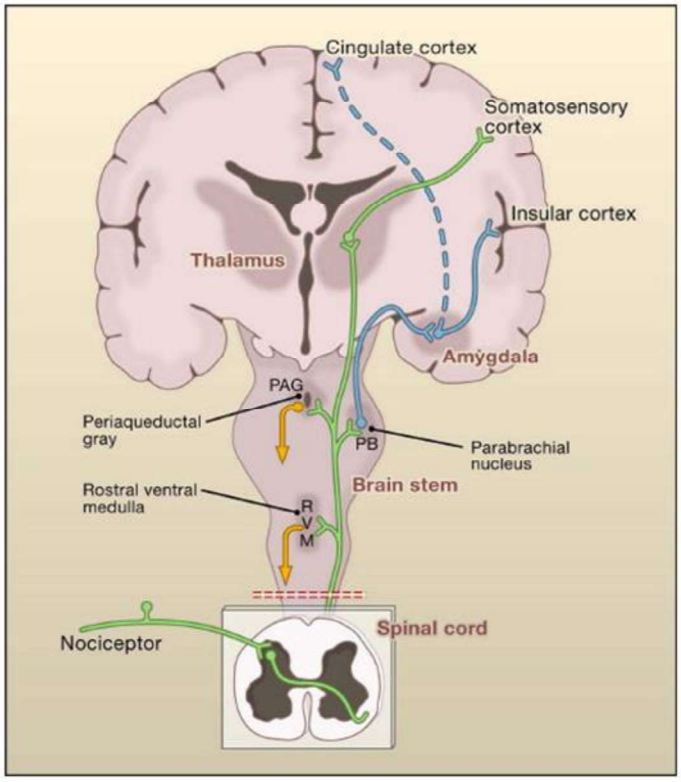

Figure 89. Pain perception and signaling. Noxious stimuli captured through nociceptor present on the tissue or site of injury carry the message to the spinal cord through DRG neurons, from there message are passed to the somatosensory cortex via the thalamus. Taken from [373].

Pathophysiology of CIPN can be for several reasons, but either loss of sensory terminal in the skin or excessive neurite sprouting can also be involved in the development CIPN. Microtubule cytoskeleton along with Ca^{2+}, Na^{+} and K^{+} ion channels play central role in the CIPN. Previously it has been discussed that TRPV1 and tubulin complex may play therapeutic role in the CIPN [162, 284]. Microtubule stabilising drug, namely Paclitaxel, cause severe

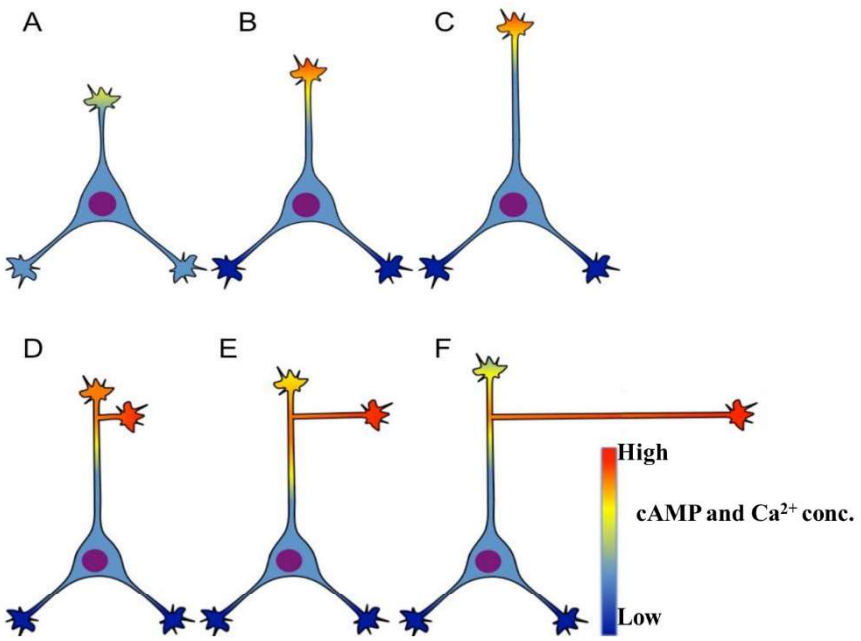

Figure 88. Signaling events involved in neuritogenesis. Image A shows undifferentiated cell with multiple neurites, one of these neurites have higher cAMP concentration, as a result this neurite through its own signaling mechanism deplete cAMP concentration in nearby neurites. As a result, it grows faster. Image D shows one of branch fast growing neurite have higher cAMP concentration, again through its own signaling mechanism it grows more faster and forms an axon. Adapted from [358].

In case of the neuronal cell, specific functions such as filopodial dynamics, growth cone formation, neurite initiation, neurite extension, neurite turning, and neurite branching are critical, and relevant for neuronal plasticity [359, 360]. Such processes are important for neuron-neuron contact formation and neuronal circuit formation which is essential for several physiological and sensory functions [360]. Indeed, such processes are very precise and regulated by multiple factors and often misregulation of such processes leads to the development of different pathophysiological conditions. For example, insufficient neuritogenesis may trigger neurodegeneration while excess sprouting may lead to hypersensitivity [361, 362]. Similarly, deletion of certain types of sensory neurons results in altered sensory functions [363-365].

3.1.8. Regulation of cytoskeleton and cell morphology by TRPV2:

Regulation of cell dynamics, cell adhesion, cell spreading, and cell-cell contact formation are essential events in the regulation of cytoskeleton. All these events are largely dependent on the Ca^{2+} gradient, Ca^{2+} dynamics and Ca^{2+} oscillation in the cellular system. This suggests the involvement of TRP ion channel in these different cellular processes. In this regard, previously it has been shown that membrane stretch-dependent activation of TRPV2 results in translocation of TRPV2 from an intracellular pool to the membrane and also it shows high accumulation of TRPV2 at the site of mechanical stimulation [238]. This study shows the importance of TRPV2 in functions of DRG neurons, such as axon elongation, neuronal guidance, cell-cell contact formation. Although membrane protrusions such as neurites, growth cone, filopodia are enriched with actin cytoskeleton, presence of microtubule cytoskeleton there is well established. Presence of tubulin as well as different types of modified tubulin including markers for stable and dynamic microtubule in such dynamic structures have also been shown [196]. In this regards our study shows that TRPV2-Ct interacts with both actin and tubulin cytoskeleton, and also interacts with different modified tubulin. All this suggest that TRPV2 have very important role in the regulation of sub-membranous cytoskeleton and therefore different cellular processes.

3.1.9. The importance of changes in neuronal morphology and neuritogenesis process in different forms of pain:

Neuronal processes such as filopodia, lamellipodia, growth cone, and neurites are very precisely regulated by the growth factors, different secondary messengers including Ca^{2+}, PKA, PKC, cAMP, PIP_2 etc **(Fig. 88)**.

GABAA	Signaling	[346]
CD2	T-cell activation	[347]
STIM1	Calcium signaling	[348]
CLIC (p64-related)	Signaling, transport	[349]
heag2 channel	Signaling, ion conductivity	[350]
Asx	MT dynamics	[351]
Connexin 43	Cell–cell communication	[352]
CAR	Cell migration	[353]
PMCA	Signaling, brain function?	[354]
TRPN1	Signal transduction	[355]
NOMPC	Cells of the sound-sensing organ of Drosophila	[356]

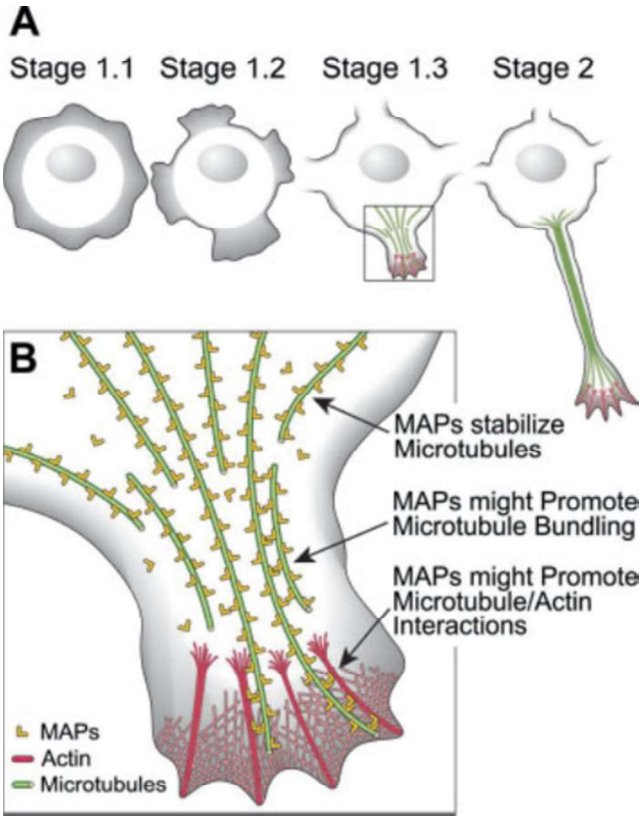

Figure 87. Stages involves in neuritogenesis. Starts with the formation of uniform lamellipodium layer, followed by small protrusion comes out from the cell and form a segmented lamellipodium, one of lamellipodium elongates in length and stabilised by the microtubules and microtubule-associated proteins (enlarge view). Taken from [357].

justified by the fact that often disruption of microtubule cytoskeleton or knockdown of TRPV channels results in same phenotypes suggesting that in case of certain forms of nociception, TRPV channels and microtubule cytoskeleton acts as a signaling complex [316]. Study of these complexes reveal the presence of different cytoskeletal components on the signaling complex formed by ion channels being present in the membrane **(Tab. 9)**. Such as α and β tubulin, kinesin, actin, myosin II and myosin V are present in such complexes [311, 312, 317-319].

Table 9. TRP channel and microtubule cytoskeleton Adapted from [320].

Name	**Function**	**References**
Polycystin-2 (PC2)	Signaling	[321, 322]
TRPV1	MT dynamics, signaling	[196, 269]
TRPV4	MT dynamics, signaling	[199, 323]
TRPC1	Translocation	[200, 201]
TRPC5	Signaling	[202]
TRPC6	Signaling	[202]
NMDA	MT dynamics, synaptic MT reorganization	[324]
VDAC	Apoptosis, mitochondrial signaling,	[325-328]
Na^+, K^+-ATPase pump	Signaling, development of brain?	[329, 330]
MGluR1	Signaling	[331, 332]
MGluR7	Signaling	[333]
G-Protein coupled receptors	Signaling	[334-337]
P2X(2)	Transport, signaling?	[338, 339]
Slo1	Transport	[340]
Ras	Signaling	[341, 342]
Estrogen Receptor A	Signaling	[343]
H^+-ATPase	Glucose uptake in yeast	[344]
GRK2	MT dynamics, signaling.	[345]

		filopodia, lamellipodia		
TRPV1	Actin cytoskeleton	Regulate neuronal morphology such as growth cone, filopodia, lamellipodia	Neuronal cells	[266, 269]

In agreement with other published reports, this study also demonstrate that TRPV2-Ct interacts with actin present in goat brain lysate. Further live cell imaging also shows that actin and TRPV2 colocalizes in F11 neuronal cell line. Our live cell imaging results followed by chemical modulation largely indicates essential role of TRPV2 in the regulation of neuronal morphology of F11 cell. Live cell imaging data also indicates that TRPV2 activation results in the actin reorganization. All these studies indicate that TRPV2 interacts with tubulin and TRPV2-actin interaction may have broad implication in the regulation subcellular signaling events.

3.1.7. TRPV2 interaction with tubulin:

Presence of microtubule cytoskeleton near submembranous region and interaction of microtubule cytoskeletal proteins with the transmembrane proteins have been reported by several research groups and such cross talks are important for submembranous dynamics which offers a field of active research. For example, so far, a large number of transmembrane proteins are known to interact with αβ-tubulin dimers [202, 308-315]. Regulatory role of microtubule and microtubule-associated proteins and their plasma membrane localization has also been demonstrated. All these studies have suggested the essential function of microtubule in the context of "membrane tubulin", a special sub-fraction of tubulin which is physically present in different membrane fractions. The interesting aspect about this is that microtubule cytoskeleton interacts with different proteins at the membrane and form dynamic signaling complex/s which initiate/s different signaling events **(Fig. 87)** [162, 195-197, 199, 266, 269, 316]. This is

soluble actin as well as with polymerized actin [199]. The interaction of actin with TRPV4-Ct is competitive with the interaction of tubulin as both actin and tubulin binds to the same domain [199]. Similarly, PC2 channels interaction with alpha-actinins, which is an actin-binding and actin-bundling proteins have been shown. Interestingly PC2 channels N and C terminus both interact with alpha-actinins and plays crucial role in the cell adhesion, organisation of cytoskeleton, proliferation and migration [277].

There is large no. of evidence which suggest that TRP channel are regulated through actin cytoskeleton. Such as, TRPC family members TRPC1, TRPC3, TRPC4, and TRPC5. TRPC family members have shown to form store operated Ca^{2+} channel (SOC) which activated upon the Ca^{2+} depletion from internal stores **(Tab. 8)**. This depleted Ca^{2+} is replenished by the actin mediated activation of these channel. Another Member which is regulated through actin is TRPP family member (TRPP2 and TRPP3). Some of members of Vanilloid family are also regulated through actin cytoskeleton such as, TRPV2 and TRPV4. Large no of evidence suggest that these two members plays essential role in the maintenance of neuronal structure such as growth cone, filopodia, lamellipodia and neuritogenesis process.

Table 8. TRP channel and actin cytoskeleton Adapted from [203].

TRP	Cytoskeletal structure/protein	Function	Cell type	Reference
TRPC1	Actin cytoskeleton	Regulation of SOCE	Human platelets, pancreatic acinar cells	[300-303]
TRPC1	Actin cytoskeleton	Cytoskeletal rearrangement and shape changes	Rat pulmonary arterial endothelial cells	[304]
TRPC1, TRPC3, TRPC4	Actin cytoskeleton	Surface expression	Neutrophils	[305]
TRPC4	Protein 4.1	Activation of ISOC	Endothelial cells	[306]
TRPC4, TRPC5	EBP50/NHERF	Regulation of SOCE	HEK293 cells expressing TRPC4	[307]
TRPP3	α-Actinin	Activation of channel function	Canine kidney cells	[277]
TRPV2	Actin cytoskeleton	Neuritogenesis	Different cell type	[171, 238, 278]
TRPV4	Actin cytoskeleton	Regulate neuronal morphology such as growth cone,	Neuronal cells	[199]

secondary messenger molecule such as PIP_2, Ca^{2+}, cAMP etc. [171]. These secondary messengers and their gradient in the developing neurite cause enhanced neuritogenesis.

This study demonstrates that TRPV2 interacts with large no. of molecules and is involved in signaling events that regulates the complex process of neuritogenesis, perticularly initiation of new neurites and branching **(Fig. 86)**.

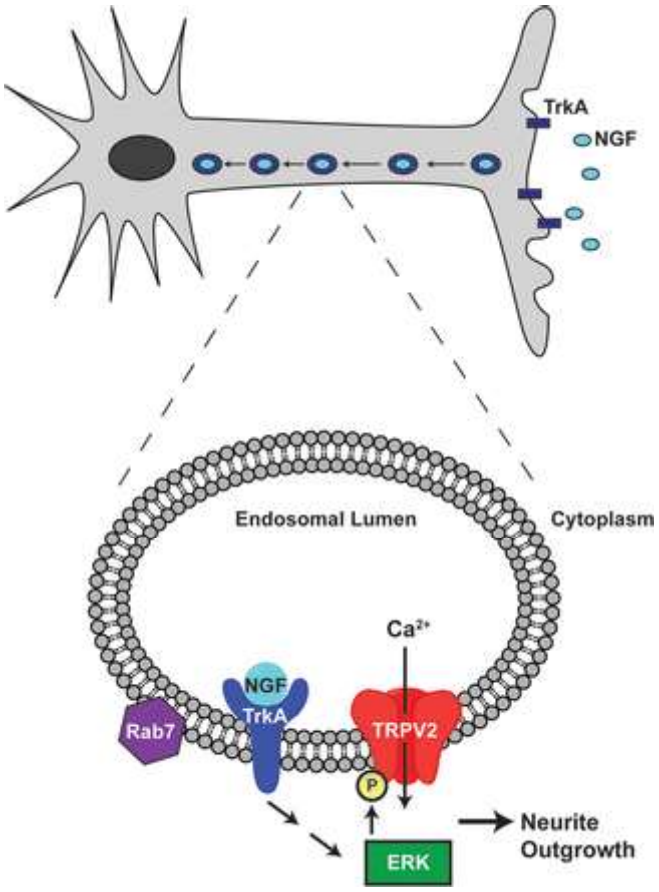

Figure 86. Different signaling molecules involved in the neuritogenesis. NGF activates downstream signaling molecules such as TrkA, ERK, and TRPV2 which increases the TRPV2 expression and enhanced neurite formation.Taken from [171]

3.1.6. TRPV2 interaction with actin:

Previously several ion channels were demonstrated to interact with actin. For example, TRPV4 not only co-localizes with actin-ribs in the lamellipodial regions, but also interact with

phosphorylation through ERK [171]. This may also suggest that these residues being in the cytoplasmic domain are accessible to these kinases.

It has been shown that mechanical stimulation of TRPV2 causes molecular interaction with the actin cytoskeleton and enhances growth cone motility [278]. They have explored the subcellular distribution of TRPV2 and found that it accumulates in very high amount at growth cone surface. More particularly the mechanical stimulated sites show increased accumulation of TRPV2. Taken together, importance of TRPV2 in the neuronal functions is established, though the molecular mechanism/s is/are remained to explore.

3.1.5. Signaling events involved in TRPV2-induced neuritogenesis:

Neuritogenesis is a complex process, which involves molecules that can be classified in different categories: the growth factors (and chemical attractants and repellents), ion channels and receptors at the membrane that can sense different physical and chemical stimuli, Ca^{2+}-binding and regulatory proteins, extracellular adhesion molecules, intracellular cytoskeleton and their regulatory molecules, and different kinases.

For example, growth factor binds to the receptor present on the surface of membrane and activates different signaling molecule like kinases, interacting proteins and secondary messengers. In case of TRPV2, Nerve Growth Factor (NGF) and Insulin like growth factor-1 (IGF-1) regulates its activity. The NGF-induced TRPV2 activity results in enhanced neurite outgrowth while silencing of TRPV2 does the opposite effect in PC12 cells [171]. IGF-1 results in the activation of Ca^{2+} entry pathways which is a prerequisite for neuritogeneis and cell cycle progression.

Different kinases phosphorylate TRPV2 such as Protein Kinase A (PKA) and Extracellular Signal Regulated Kinase (ERK) modulates its activity and as a result activates

expression has been detected in central nervous system (CNS) with compare to other Vanilloid members [282]. Extensive research work has revealed that abundant TRPV2 expression has been found in supraoptic nucleus, paraventricular nucleus, arcuate nucleus, nucleus of the solitary tract, hypoglossal nucleus, and nucleus ambiguous. Presence of TRPV2 in these specific positions of brain suggest its involvement in the osmoregulation, autonomic regulation and cardiovascular regulation [299]. Other few specific regions where TRPV2 expression has been abundant are spinal cord, trigeminal ganglia, and dorsal root ganglion where it helps in the transmission of noxious stimuli [121, 217, 279, 281].

3.1.4. TRPV2 in neuritogenesis:

Neuritogenesis is a complex process which involves the different signaling molecules. There are reports which suggest the importance of TRPV2 in neuritogenesis [171, 238, 278]. Shibasaki et al have reported the expression of TRPV2 in embryonic mice. In their study, they have shown that TRPV2 is present in the spinal motor neuron and DRG neuron on the day 10.5. At that time, the localization of TRPV2 is very specific and observed only in the growth cone and axon shafts of a subsets of neurons only [238]. The authors have shown that membrane stretch-dependent activation of TRPV2 is a key regulator for axon-outgrowth [238]. In a similar study, Cohen et al. has shown that TRPV2 is regulated by Nerve Growth Factor (NGF) and mitogen-activated protein kinase (MAPK) which increases neurite outgrowth [171]. Interestingly they have identified that multiple ERK phosphorylation sites are present in TRPV2 and mutagenesis of these phosphorylation sites results in reduced neurite length and less TRPV2-mediated Ca^{2+} signals. All these phosphorylation sites (Ser6, Ser37, Ser47, and Ser760) are present on the -N and C-terminus cytoplasmic domain and so far, no phosphorylation sites have been detected in the loop region. Further experiments reveal that mutation of all four sites to Ala (S6A, S37A, S47A, and S760A) results in reduced TRPV2

In a rat model, it has been shown that vincristine-mediated neuropathy cause microtubule disorientation and axonal swelling in unmyelinated sensory axons [285]. Also, follow up reports from the same group suggests that vincristine induces painful peripheral neuropathy in rat model which damages the cytoskeleton of large diameter sensory neurons and myelinated axons [286]. Involvement of TRPV ion channel in cancer has been reported by multiple groups. Especially, the role of TRPV2 in several types of cancer including liver, bladder, and prostate cancer has been studied [290-294]. These studies suggest that in different types of cancer cells, TRPV2 is over expressed in both protein and in mRNA level. Like human hepatocarcinoma cells (HepG2) show high TRPV2 expression [291, 292]. Bladder cancer cell line also shows the presence of TRPV2 in mRNA and protein level [290]. In case of prostate cancer cells, TRPV2 has been detected too. However, metastatic cancer cells show higher mRNA expression compare to solid tumour/s [293]. In bladder cell and leukaemic cell line, splice variants of TRPV2 (Δ529-663) and (Δ551-663) have been found respectively. These short variants have been proposed to act as a dominant negative mutant *per se* [290]. In this study we establish that TRPV2 interacts with tubulin and different modified tubulin through its C-terminal region, both in presence and absence of Ca^{2+}. TRPV2 seem to interact with polymerized microtubule also. Interaction with modified tubulin in different extent also suggest that TRPV2 may share complex relationship with "tubulin-code" [295-298]. Such findings can provide important clue to the chemotherapy-induced peripheral neuropathy and other cellular toxicities, such as loss-of-immune cells, reduced sperm count etc.

3.1.3. Localization of TRPV2 in specific regions of neurons:

High level expression in neuron and localization of TRPV2 in different subsets of neurons like growth cone, suggest the important role of TRPV2 in the neuronal outgrowth. Previous studies suggest that activation of TRPV2 through membrane stretch increases the intracellular Ca^{2+}-level which cause axon outgrowth [238]. More particularly high TRPV2

fiber sensory neurons [64-69, 251]. TRPV2 expression is relatively high in medium- and large-diameter primary afferents, mainly in myelinated A- and C-fiber sensory neurons which are devoid of TRPV1 [64-69, 251]. TRPV2 seem to be important for neuronal functions that are relevant at early ages such as neuronal migration, neuritogenesis and neuronal contact formation. Indeed, not only in adult neurons, but also at the time of neural development (from the day 10.5 to 13.5), TRPV2 expression has been reported in DRG and spinal motor neurons [238]. Transcriptome analysis of mature mouse forebrain suggests that among all TRPV members, TRPV2 have the relatively highest expression [282] **(Fig. 85)**.

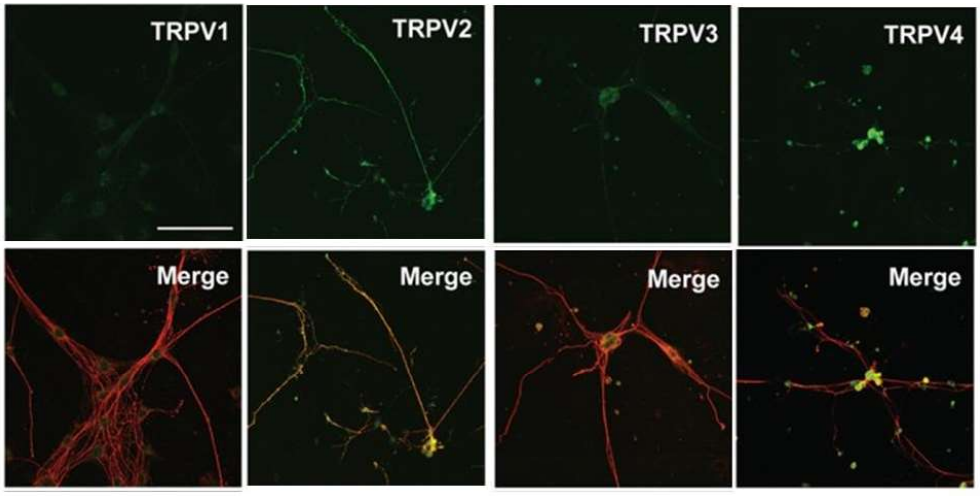

Figure 85. Expression of different thermo TRPV channels in the rat DRG neuron. Immune-stained with TRPV antibodies (Green) and β III tubulin (Red), scale bar is represented 100μm. (Adapted and modified from [171].

3.1.2. Importance of TRPV2 in cancer, pain and other pathophysiology:

TRPV2 is involved in several important physiological functions. Such as cross talk between microtubule seem to be important for TRPV2 function. Previously, several reports have suggested the essential role of microtubules in the transmission of nociceptive signals [275, 283-286]. Expression of TRPV2 in immune cells also indicate that TRPV2 may be important for neuro-immune interaction too [27, 287-289].

3.1. *TRPV2 and Cytoskeleton:*

The importance of cytoskeletal elements mainly actin and microtubules in the maintenance and regulation of cellular integrity and different cellular functions are well known [274]. In case of neurons, the cytoskeleton plays important role in the regulation of neuronal structure, migration and contact formations. Such events in turn determine the overall neuronal and physiological functions. In many cases, these neuronal circuits and functions are tightly inter-linked with complex physiological functions such as sensory functions. In this context, the previous studies have pointed that the cross talk between ion channels and cytoskeleton are important for several physiological functions. Indeed, several proteomic and biochemical studies have pointed that TRP channels interact with components that belong to cytoskeleton [134, 152, 196, 199, 203, 266, 269, 275-278]. For example, physical interaction of TRPV1 and TRPV4 with tubulin has been demonstrated by different studies and by different methodologies [196, 199, 266, 269]. TRPV1-tubulin interaction towards the complex formation and subsequent regulation of cell morphology by the same TRPV1-tubulin complex has implications in growth cone movement, neuritogenesis, neuron-neuron contact formation, filopodial dynamics and synaptogenesis events [134]. In agreement with such functions and regulations, this work establishes the physical interaction of TRPV2 with microtubule and actin cytoskeleton. The findings suggest implication of TRPV2 in the regulation of cell functions, such as regulation of cytoskeletal dynamics which in turn affects neuritogenesis and neurite branching.

3.1.1. Expression of TRPV2 in specific neurons:

Presence of TRPV2 in a specific subset of DRG neurons has been reported before [121, 217, 279]. For example, expression of TRPV2 in DRG and trigeminal ganglia has been reported [217, 280, 281]. Expression and distribution of TRPV2 have been reported in medium- and large-diameter primary afferents more particularly in myelinated A- and non-myelinated C-

In this thesis work, the importance of TRPV2 in neuritogenesis, actin and tubulin as an interacting partner of TRPV2 have been characterized. A detailed discussion about TRPV2 in neuritogenesis has been discussed in (chapter 3.1). Also, pathophysiological importance and characterization of the OS causing TRPV3 mutants has been discussed in (chapter 3.2). The importance of TRPV3 in the regulation of intracellular organelle has been discussed in (chapter 3.3). Cholesterol-mediated TRPV3 regulation has been discussed in the context of TRPV3-Wt and OS mutants in (chapter 3.4).

Chapter 3

Discussion

- TRPV2-Ct also interact with tubulin and different modified tubulin from cattle brain extract.
- TRPV2-Ct directly interacts with β-III tubulin (a neuronal marker).
- TRPV2 is present in Synaptosome and Synaptic junction protein fraction from Rat brain.
- TRPV3-OS mutants show reduced surface expression and affect cell size, morphology and cell adhesion.
- Expression of OS mutants alter the distribution of subcellular organelles such as ER, Golgi, Lysosome and Mitochondria.
- OS mutant alters mitochondrial potentiality.
- OS mutant show reduced lysosome number and movement.
- TRPV3 is present in lysosome and mitochondrial fraction isolated from cattle brain.
- TRPV3 contain different cholesterol binding motif and TRPV3 bind to cholesterol in closed conformation.
- OS mutant shows reduced binding to cholesterol.

In this thesis work, functional presence of TRPV2 in neuronal cell was established and its association with cytoskeletal proteins actin and tubulin have been characterized in details. TRPV2 regulates the Ca^{2+} level in the F11 cell. Other interacting proteins which regulate the activity of TRPV2 can be discovered in near future and how these proteins regulate neuritogenesis process together will shade molecular mechanism of neuritogenesis process in details. These finding may have broad implication in many neurodegenerative disorder.

TRPV3-OS mutants and their pathophysiological importance have been characterized. In near future TRPV3 interacting protein from lysosomal and mitochondria need to be discovered. This may help to understand the pathophysiology of OS. Future work will aim to characterize the other OS mutants and how these mutants damage the cellular machinery.

Conclusion and future prospect:

This thesis work unveils the importance of Transient Receptor Potential Vanilloid (TRPV) subfamily members TRPV2 and TRPV3 in the context of neuritogenesis and pathophysiology. Both of these members are relatively less explored in Vanilloid family. Presence and distribution of these ion channels largely vary in the neuronal and non-neuronal tissues where these channels regulate many physiological processes. In this study, TRPV2 driven neuritogenesis have been studied in the F11 cell (Neuronal cell line). And how cytoskeletal components mainly actin and tubulin play critical role in such processes that has been investigated.

Previously mutation in Vanilloid family member TRPV3 has been linked with a pathophysiology known as *Olmsted Syndrome* (OS). But very few reports are there which explains how these mutants of TRPV3 affect subcellular organelle functions. In this thesis work, we have reported that TRPV3-OS mutants largely affect mitochondrial and lysosomal functions in keratinocyte cell HaCaT. Also, the presence of TRPV3 in lysosome have been reported and its importance in the regulation of different subcellular function such as pH balance and Ca^{2+} homeostasis has been studied.

Thesis finding:

- TRPV2 regulates cell morphology in the neuronal and non-neuronal cell.
- TRPV2 is functionally present in the F11 cell line and its pharmacological activation enhances neuritogenesis.
- Pharmacological inhibition of TRPV2 results in the cell retraction.
- Increased phospho-Tyrosination have been observed after long-term TRPV2 activation.
- TRPV2 colocalizes with the actin cytoskeleton and its C-terminus interact with actin from cattle brain extract.

Chapter 4

Conclusion and Future prospect

cormorant, little egret, Dalmatian pelican, crested ibis, golden-collared manakin, downy woodpecker, common cuckoo, Anna's hummingbird, red-legged seriema, sunbittern, barn owl, hoatzin, red-throated loon, yellow-throated sandgrouse), reptiles (Green sea turtle, American alligator, Chinese alligator, Western painted turtle, Burmese python), amphibians (western clawed frog) and from fish (elephant shark,) sequences were taken. LWI residues were determined and the percentage content of Arg and Tyr was calculated. The different values (Arg%, Tyr% and their total % content) were plotted and statistical significance derived (non-parametric T test or one-way ANNOVA, wherever applicable) in Graphpad Prism 6 (www.graphpad.com).

5.2.9.9. Structural alignment and mutation of residues:

Mutating Gly 573 to Cys, Ser and Ala was done with the 'SwapRes' command in YASARA. The mutated side chains were optimized with a rotamer library in the SCWALL method in YASARA. This approach optimizes Side-Chain Conformations with ALL available methods [456-459]. Structural alignment of TRPV3 in closed and open confirmation was done using MUSTANGG program in YASARA using default values.

5.2.9.6. Identification of CRAC, CARC and CCM motifs of TRPV3:

To identify the presence of cholesterol binding motifs in hTRPV3, a sequence wide search of the protein was done manually for Cholesterol recognition amino acid consensus (CRAC) motifs (L/V-X¬(1-5)-Y-X(1-5)-R/K) and CARC (Inverted CRAC) motifs and CCM motif (R/K-X-(7-10)-W/Y-X(4)-I/V/L). We have analysed 11 CRAC motifs and 12 CARC (Inverted CRAC) motifs and 1 CCM motif in TRPV3.

5.2.9.7. Docking of cholesterol on closed and open structures of hTRPV3:

Docking of cholesterol on closed and open conformations of hTRPV3 was performed using VINA [455] keeping default parameters. The setup was done with the YASARA molecular modeling program [456].The best hit of 25 runs was manually chosen. A flexible docking was performed, i.e. the ligand's internal degrees of freedom were taken into account. Cholesterol interaction with TRPV3 as revealed by docking experiments were excluded if the interactions are either with very low binding energy, or with thermodynamically unfavourable orientations (such as OH group located at the middle of the membrane), or binds in areas which does not have apparently any specific target motifs or TM-Loop regions.

5.2.9.8. Frequency calculation of Arg, Tyr and Ser residues in the lipid water interface:

Different mammals (Human, Mouse, pygmy chimpanzee, rat, thirteen-lined ground squirrel, blind mole rat, Bactrian camel, prairie vole, prairie deer mouse, golden hamster, lesser Egytian jerboa, degu, naked mole-rat, aardvark, Cape golden mole, Cape elephant shrew, platypus, dog, domestic cat, water buffalo, wild yak, American buffalo, sheep, sperm whale, pig, European shrew, bat, black flying fox, golden snub-nosed monkey, small Madagascar hedgehog, Killer whale, Horse), birds (chicken, northern fulmar, Adelie penguin, emperor penguin, great

5.2.9.3. Membrane representation and SeqLogo generation:

Graphical representation of hTRPV3 with the determined LWI residues used in this study was prepared with *Protter-visuaize proteoforms* [451]. SeqLogos were generated with the Weblogo webserver (http://weblogo.berkeley.edu/) [452, 453].

5.2.9.4. Boxplot of the small amino acid stretch sequences of TRPV3:

Distance Matrix generation using MEGA 5. The alignments of all the lipid-water interface regions and different CRAC, CARC and CCM motifs were saved and then analysed with MEGA 5 software package [152, 454]. The pairwise matrices were generated to measure the pairwise distance between two different amino acid sequences in a group of aligned sequences. In distance estimation analysis method, Bootstrap method was chosen for variance estimation (Bootstrap value = 1000), amino acid substitution method was set to p-distance model, to treat the gaps or missing data, pairwise deletion model was chosen. The distance matrices thus generated showed the respective pairwise distance of all sequences in a group.

5.2.9.5. Statistical Tests:

The pairwise distance values from the matrices generated were imported in "R" software package and box-plots were generated for different regions and motifs of TRPV3 to evaluate the evolutionary relationship and differential selection pressure between these regions. To check the reliability and significance of the data generated, the Kruskal-Wallis test of variance was performed in "R" for all groups. The median values of each group were also calculated using "R" and outliers denoted subsequently and represented in the box plots. The graphical representation (box plots) depicts divergence of a particular domain or motif and the Y-axis represents the divergence of those regions, so lower values in the Y-axis represents higher level of conservation of the proteins.

5.2.9. Methods related to *in-silico* study:

5.2.9.1. Sequence Retrieval, Alignment and Structure retrieval:

TRPV3 sequences of different species were retrieved from National Centre for Biotechnology Information (NCBI) database [447, 448]. Details of each gene and protein are given in tabular form (**Tab 1**). The sequence alignment was done by using MUSCLE alignment software with its default values [449, 450]. The working structures of rTRPV1 were downloaded from the PDB (https://www.rcsb.org/pdb). 3J5P was used as closed conformation of rTRPV1 for building homology model of closed hTRPV3, using default programs in Yasara software and 3J5R was used as the open conformation for the same.

5.2.9.2. Embedding the TRPV3 structures in PEA or POPC membrane and determining the LWI residues:

Lipid bilayer made of PEA or POPC without any cholesterol or with 30% cholesterol were prepared *in silico* separately. The closed structure (3J5P) was imported into YASARA and was 'cleaned', hydrogen bonding network was optimized and force field parameters were added [46]. The open and closed conformation of TRPV3 was inserted in to these lipid bilayers separately. *In silico* membrane with different compositions of required size was built and the protein structure was embedded within it followed by a 250ps equilibration simulation was run, during which the membrane is artificially stabilized while it adapts to the protein. For all analysis, the temperature of the *in silico* system was maintained at 298 K. From the embedded structure, the lipid-water interface (LWI) residues were determined as the 5 residues (both in the N- and in the C-terminal regions) of all the 6 transmembrane helices of the closed structure of hTRPV3. Homologous regions were identified in the human TRPV3 sequence by aligning with MUSCLE alignment tool (**Tab 1**).

software). Calculation of cell size, morphology, cell shape, neurite number etc. was calculated manually using LSM image examiner. Image resolution and labeling were done by Adobe Photoshop software.

5.2.8. Flow cytometry:

To check the expression level of different cytoplasmic kinase and cAMP transcription factor CREB, cells were stained with specific antibody mentioned above. Followed by flow cytometric analysis. Stained cells were washed three time with the FACS buffer before acquisition. Acquisition was performed with FACS Calibur (BD Biosciences). Analysis of data was performed by using CELL QUEST PRO software (BD Biosciences).

was added. Live cell imaging was performed using 63X oil immersion objective at 25ºC. Different genetically encoded proteins (GFP and RFP) and cell permeant dyes such as LysoTracker Red, MitoTracker Red etc. were used to observe cellular dynamics and organelle movement.

5.2.7.3. Studying growth cone dynamics using live cell imaging:

To analyse the effect of TRP channels activation/ inhibition on growth cone, F11 cells were seeded on 25 mm glass coverslips. Approximately 24 hours after seeding, GFP/RFP-tagged proteins (such as TRPV2-GFP and mCherry-tubulin, etc.) were expressed in F11 cells by transient transfection. To visualize the localization of TRPV2, F11 cells expressing TRPV2-GFP were maintained in complete medium. Effect of TRPV2 activation or inhibition on growth cone was studied by visualizing TRPV2-GFP expressing cells. Probenecid (250 μM) and Tranilast (75 μM) was added to the complete medium during imaging as an activator and inhibitor of TRPV2 respectively. For experiments aimed at monitoring the colocalization of tubulin and TRPV2, mCherry-tubulin and TRPV2-GFP were co-expressed in F11 cells by co-transfection. Two days after transfection mCherry-tubulin-positive cells were monitored for this purpose. All live cell images were captured with the help of a time series program. A confocal laser-scanning microscope (Zeiss LSM780) with a 63X-objective was used to capture the images. All live cell imaging was done at standard room temperature (25°C). Images were analyzed later with the Zeiss LSM image examiner software.

5.2.7.4. Image processing, analysis, and quantification by different software:

All confocal images were processed with LSM image examiner software. Live cell time series images, movies depicting changes in the Ca^{2+} levels were subjected to intensity calculation and image processing were performed by using Image J and Fiji software's. Changes in lysosomal movement and numbers were calculated by using TrackMate (Fiji

For fixed cell imaging, the cells were grown on 12 mm glass coverslip and 24 hours after seeding, LysoTracker Red dye was added to the media at a concentration of 500 nM and incubated for 30 minutes. This was followed by a wash with 1X PBS and the cells were subsequently fixed with 4% PFA at RT.

5.2.7. Methods related to Immunocytochemistry and microscopy:

5.2.7.1. Immunocytochemistry:

For immunocytochemistry, cells were grown and/or transfected on glass coverslips. 24 to 48 hours after seeding or transfection, the cells were fixed with 2% paraformaldehyde at room temperature (RT), followed by permeabilization with 0.1% Triton X-100 in 1X PBS for 5 minutes. Subsequently the cells were gently washed with 0.1% PBS-T for 5 minutes. The cells were blocked with 5% bovine serum albumin (BSA). After blocking, the cells were incubated with primary antibody for 1 hour at RT. The primary antibody was added in a solution of 5% BSA and 0.1% PBS-T (1:1). The cells were then washed three times with 0.1% PBS-T. Cells were further incubated with secondary antibody diluted in PBS-T buffer and BSA (1:1). After incubation with secondary antibody, the cells were washed three times with 0.1% PBS-T buffer. Subsequently, DAPI was added in PBS-T buffer at 1:2000 dilution for 20 minutes. Finally, the cells were washed with PBS-T for three times. Coverslips containing the stained cells were mounted onto glass slides with fluoromount G (Southern Biotech). Alexa-594-labelled Phalloidin was used to label and visualize the actin cytoskeleton. Images were taken with a confocal laser-scanning microscope (Zeiss LSM780) with a 63X-objective and analyzed by the Zeiss LSM image examiner software.

5.2.7.2. Live cell imaging:

Live cell imaging was performed using inverted confocal microscope. After seeding the cells on 25 mm cover glass, coverslip was transferred to a metal chamber and slowly media

yields green fluorescence at 530±15 nm. While at higher mitochondrial potential, it forms J-aggregates yields red fluorescence and emission at 590±17 nm [446]. It exhibits potential dependent accumulation in mitochondria which results in the change in emission spectrum from green (529 nm) to red (590 nm). Lower ratio of green/red correlates with lower membrane potential while higher green/red ratio correlates with higher mitochondrial membrane potential. Subsequently the cells were washed with 1X PBS and coverslips were used for live cell imaging by confocal microscope (Zeiss LSM780).

5.2.6.5. MitoTracker Red staining in adherent cells:

Adherent cells (HaCaT and F11) were grown and/or transfected on 12 mm glass coverslips. After 24 hours of seeding or transfection, MitoTracker Red (1 μM) was added to cells for 20 minutes. Subsequently the cells were either washing with 1X PBS and used for live cell imaging or cells were fixed by 4% PFA at RT. MitoTracker Red is a cell permeable dye, accumulates in mitochondria in live cell. Accumulation of MitoTracker Red depends on mitochondrial membrane potential and also it is an aldehyde fixable dye which retain even after fixation. It exhibits excitation maxima of 580±10 nm and emission maxima of 620±10 nm.

5.2.6.6. LysoTracker Red staining in adherent cells:

HaCaT and F11 cells were grown on 25 mm glass coverslips in 35 mm culture dish. After 24 hours of seeding, LysoTracker Red (500 nM) was added to cells for 30 minutes. This was followed by washing with 1X PBS and subsequently coverslips were taken for live cell imaging by confocal microscope (Zeiss LSM780). LysoTracker Red is a fluorescent dye that consists of a fluorophore attached with a weak base, which is partially protonated at pH 7. This enables LysosTracker Red to freely permeate inside cells. This dye is highly selective for acidic organelles. LysoTracker Red exhibits an excitation maximum at 590 nm and emission maxima at 620 nm.

5.2.6.2. Generation of a stable TRPV3-Wt and OS mutant expressing HaCaT cell line:

HaCaT cells were seeded in a 6-well plate without glass coverslip and after 24 hours of seeding, plasmid DNA encoding Wt-TRPV3 or OS mutant in GFP vector were transfected into HaCaT cell. Around 24 hours after transfection, the cells were subject to selection by using antibiotic G-418 (100µg-600µg). Antibiotic concentration was gradually increased in the culture after several passages. After 15-20 days of selection, cells were confirmed by immunofluorescence and/or western blot analysis for the expression of TRPV3.

5.2.6.3. Ca^{2+}-imaging of adherent cells:

Adherent cells (HaCaT and F11) were seeded on 25 mm coverslip in 35 mm dishes and kept in CO_2 incubator at 37°C. After 24 hours, Ca^{2+}-sensing dye Fluo-4 AM (5 µM) which is a non-fluorescent form of acetoxymethyl ester was added in culture dishes for 40 minutes. Upon addition, due to esterase activity inside the cell, this acetoxymethyl group gets cleaved off and it binds to Ca^{2+} and emits fluorescence [445]. Fluo-4 AM shows excitation maxima at 488 nm and emission maxima at 520 nm, for which an argon laser was used. Subsequently, cells were gently washed two times with PBS (1X) and then cells were used for live cell imaging. Live cell imaging was performed with confocal microscope 488 nm argon laser and fluorescence microscope. During the imaging, Specific drugs for TRPV2 or TRPV3 were added without disturbing the cells.

5.2.6.4. JC-1 (Ratiometric dye) staining in adherent cells:

Adherent cells (HaCaT and F11) were seeded in 25 mm coverslip. Around 24 hours after seeding, JC-1 (5 µM) dye was added to these cells and incubated for 40 minutes at 37°C in a CO_2 incubator. JC-1 is a cell permeant cationic dye widely used to monitor mitochondrial potentiality. Mainly at very low mitochondrial potential JC-1 remains as a monomer which

at RT either in the presence or absence of 1 mM $CaCl_2$, followed by centrifugal separation of pellet (MT) and supernatant (free dimer) at 40000 RPM/30minutes/35°C.

In another experiment, the interaction of MBP-TRPV2-Ct with tubulin dimer were analyzed. For that 90 µg of purified tubulin dimer was mixed with MBP-TRPV2-Ct approximately 5µg in a total volume of 20 µl was incubated in PEM-S buffer (20mM PIPES, pH 6.8, 0.2mM $MgCl_2$, 1 mM EGTA and 100mM NaCl supplemented by 1 µM Taxol®, 5 mM GTP and 1 mM ATP) for 30 minutes at 37°C, to form microtubules (MT). Subsequently, the mixture was centrifuged at 40000 RPM/30minutes/35°C and supernatant (free dimer) and pellet (MT) was separated. Samples were then subjected to SDS-PAGE and followed by western blot detection for interacting partner.

Before starting the experiment purified proteins were centrifuged at high speed 40000 RPM/35°C/ 30minutes, in order to remove the protein aggregates, if any. Subsequently, the supernatant was collected and used for the co-sedimentation experiment.

5.2.6. Methods related to cell biology:

5.2.6.1. Cell culture and transfection:

F11 cells were cultured in Ham's F12 medium supplemented with 10% FBS, 2mM L-glutamine, 100 µg/ml streptomycin, 100 U/ml penicillin. The cells were grown in a humidity controlled incubator maintained with 5% CO_2 at 37°C. HaCaT, HEK, Neuro2A, and SaOS2 cells were maintained in DMEM media supplemented with 10% (v/v) FBS, 2mM L-glutamine, 100 µg/ml streptomycin, 100 U/ml penicillin, in a humidity controlled incubator with 5% CO_2 at 37°C. For transient transfection, lipofectamine (Invitrogen) was used according to manufacturer's protocol.

5.2.5.3. Blot overlay:

For blot overlay experiments, PVDF membrane was charged in methanol and washed with 1X PBS. Subsequently, the membrane was placed on a dot blot apparatus and different concentrations of cholesterol were spotted on PVDF membrane. The experiment was executed by connecting the dot blot apparatus with a vacuum pump and different concentrations of cholesterol were spotted on same area size through sudden suction. Subsequently, the membrane was blocked with 5% BSA in PBS pH 7.4 for 1 hour. After that the membranes were incubated overnight at 4ºC with different proteins representing specific fragments of TRPV3-Wt or/ mutants. Post incubation, the membranes were washed thrice with PBS buffer (for 5 minutes each). Subsequently, membranes were incubated with primary anti-MBP antibody (1:30,000 in blocking buffer and 1X PBS) for 1 hour at 4°C and then washed with 1X PBS thrice for 5 minutes each. Secondary antibody conjugated to horseradish peroxidase (1:10,000, GE healthcare) was applied to the membrane and incubated for 1 hour at room temperature. The membrane was washed thrice with 1X PBS. Bound protein was visualized by adding an equal amount of substrate and luminol solution to the membranes and the chemiluminescence signal was detected using Chemi Doc (Bio-Rad).

5.2.5.4. Co-sedimentation assay with Taxol®-stabilized microtubules and GTP-induced microtubules:

In order to study the interaction with polymerised microtubules, 90 µg of tubulin dimer in a total volume of 50 µl were incubated in PEM-S buffer (20mM PIPES, pH 6.8, 0.2mM $MgCl_2$, 1 mM EGTA and 100mM NaCl) supplemented with 1 µM Taxol®, 5 mM GTP and 1 mM ATP) for 30 minutes at 37°C, to form microtubules (MT). The MT was separated from unpolymerized tubulin dimer by centrifugation at 40000 RPM/30minutes/35°C. Subsequently, 5 µg of purified MBP-TRPV2-Ct or MBP alone was added to the same amount of polymerized microtubules. The purified proteins were incubated with Taxol®-stabilized MTs for 30 minutes

solution was made by adding 100 µL of PBS and 900 µL of Bradford reagent. All measurements were acquired using a Beckman Coulter spectrophotometer at 595 nm.

5.2.5. Methods related to protein interaction:

5.2.5.1. MBP-Pull-down assay for identifying TRPV2 interacting proteins:

For interaction studies MBP-fusion proteins or MBP alone were expressed in *E. coli*. Bacterial cells expressing these proteins were lysed and centrifuged. The cleared cell lysates were applied to amylose resin (NEB) beads, incubated for 1 Hour at RT and were washed thrice with PEMS buffer. Approximately 0.2 ml of amylose resin with the bound fusion protein was incubated with 0.1 ml of goat brain extract (1mg/ml protein) for 3 hours, either in the presence or absence of Ca^{2+} (1 mM). Post incubation with goat brain extract, the beads were washed again (3 times) using PEMS buffer. The proteins bound to amylose resin beads were eluted by adding 20 mM maltose to it. Eluted samples were analyzed by 10% SDS-PAGE according to Laemmli [441].

5.2.5.2. Other pull-down assays to characterize TRPV2-Tubulin interaction:

To find out direct interaction between TRPV2-Ct and tubulin, 50 µl of amylose beads bound to MBP-TRPV2-Ct and only MBP were incubated with 90 µg of αβ-tubulin in PEM-S buffer (50 mm PIPES; pH 6.8, 1mM EGTA, 0.2 mM MgCl2 and 100mM NaCl) with (1mM) or without presence of Ca^{2+}. To find out direct interaction between actin and TRPV2 fragments, 50 µl of amylose beads bound with MBP-TRPV2-Ct and MBP-LacZ were incubated with 30µg of purified actin. Proteins were dissolved in PEM-S buffer and binding experiments were carried out either in the presence or absence of free Ca^{2+} (1mM). Eluted samples were subjected to SDS page and followed by western blot.

minutes at 37°C. Resultant pellet was again subjected to depolymerisation in ice-cold PEM buffer and homogenised in a glass homogeniser. Depolymerisation mixture was incubated on ice for 30 minutes. This was followed by centrifugation at 45000 RPM at 4°C for 30 minutes to get a clear soluble extract with enriched tubulin dimer and very low amount of microtubule-associated proteins. This clear mixture was passed through a column packed with phosphocellulose. Different fractions were eluted which varied in their enrichment for tubulin. Protein concentration of the purified tubulin was measured, distributed in aliquots, followed by snap chilling of aliquots in liquid N_2 and stored at –80°C for long-term use.

5.2.4.2. Prokaryotic expression and purification of MBP-fusion proteins:

BL21DE3 strain of *E. coli* was transformed by heat shock with plasmids containing the coding regions corresponding to cytosolic domains or different transmembrane domain with/without loops of different TRP channels (such as for TRPV2, TRPV3, and TRPV4). Isopropyl thiogalactoside (IPTG) was added to *E. coli* cells to induce the expression of proteins for 2 hours. Subsequently, cells were harvested by centrifugation and lysed by freezing and thawing cycles in lysis buffer (PBS pH 7.4, lysozyme and protease inhibitor cocktail). The lysed extracts were cleared by centrifugation at 100,000 × g in a 45Ti or 70Ti (according to volume of protein lysate) rotor for 2 hours. The cleared lysate was applied to amylose resin beads for binding and washed thoroughly. Bound protein was eluted with 20 mM maltose in elution buffer (50mM PIPES, pH 6.8, 100 mM NaCl, 1 mM EGTA and 0.2 mM $MgCl_2$).

5.2.4.3. Protein estimation:

Protein concentration of samples were estimated using Bradford reagent [444]. Purified BSA proteins (20, 40, 60, 80 and 100 µg) were made in 100 µL of PBS solution. Subsequently, 900 µL of Bradford reagent (Sigma-Aldrich) was added to the tubes containing different BSA concentrations and incubated for 5 minutes after which the OD was measured at 595 nm. Blank

80°C for long-term storage. All isolation procedure and centrifugation steps were carried out at 4°C.

5.2.4. Methods related to protein purification:

5.2.4.1. Purification of Tubulin:

Tubulin dimers were purified from cattle brain according to [443] with minor modifications. Freshly collected brain tissue were collected from slaughter house in ice-cold PBS. Meninges were immediately removed in the ice-cold buffer. Subsequently clean brain tissue was homogenized in PEM buffer (50 mM PIPES: pH 6.8, 1mM EGTA, 0.2 mM MgCl2) with complete protease inhibitor cocktail. For better tubulin preparation and higher yield, homogenization of the brain was done within 1 hour from the time of collecting cattle brain. Homogenate was immediately centrifuged at 12000 RPM and 4°C for 60 minutes. Collected supernatant was again centrifuged at higher speed 29000 RPM and 4°C for 30 minutes to get clear supernatant. 100 ml of glycerol was added to 250 ml of clear supernatant in presence of ATP and GTP at 37°C in a water bath. ATP and GTP was added as solid powder at a final concentration of 1.5mM and 0.1mM respectively. Extra $MgCl_2$ was also added to make the final concentration to 4mM. Subsequently Taxol®1 μM was added to the solution to enhance the polymerization of microtubule. After 20-30 minutes the solution appeared turbid. Polymerised microtubule mixture was centrifuged at 45000 RPM for 60 minutes at 37°C to get a gelatinous pellet. To induce depolymerization of microtubule, the gelatinous pellet was resuspended in ice-cold PEM buffer, followed by homogenisation in glass homogeniser and incubated on ice for 30 minutes. This resulted in cold-induced depolymerisation of microtubule. This depolymerisation mixture was centrifuged at 45000 RPM for 60 minutes at 4°C to remove the chunky pellet. This supernatant represents recyclable tubulin and associated proteins. Again, solid GTP at a final concentration of 0.5 mM and extra $MgCl_2$ at final concentration of 4 mM were added to this clear supernatant and incubated at 37°C for a second round of polymerization. Polymerisation mixture was again centrifuged at 45000 RPM for 30

membrane blots were “stripped-off” by incubating the blots in a stripping-buffer at 50°C for 30 minutes and re-probed again with a different primary antibody.

Buffers and solutions required:

Transfer buffer: 0.1% SDS, 20% (v/v) MeOH, 48 mM TRIS/HCl, 39 mM Glycine

Ponceau Red solution: 5% (w/v) Ponceau S dye, 5% (v/v) Acetic acid

TBS-T: 20 mM Tris, 150 mM NaCl. 0.1% (w/v) Tween-20

Stripping buffer: 1% SDS, 20 mM TRIS/HCl (pH 6.8), 1% (v/v) β-Mercaptoethanol

5.2.3.4. Isolation of lysosome from Goat brain:

Fresh and adult goat brains were obtained from a local slaughterhouse and immediately collected in ice-cold homogenisation buffer. The meninges were separated from brain and immediately tissues were taken to the laboratory in isotonic cold lysosome isolating buffer (10 mM HEPES, 1 mM EDTA, 320 mM sucrose, pH 7.4). Isolation of lysosome was performed by the method established previously with some minor modifications [442]. Briefly, goat brain was homogenized in lysosome isolating buffer containing a complete protease inhibitor cocktail (Sigma-Aldrich). After homogenization, the homogenate was equally distributed in centrifuge tubes and centrifuged at 1000g for 10 minutes. The supernatant (S1, which contain lysosome and other cell organelles) was collected in a separate tube and the pellet was homogenized again in lysosome isolating buffer with 5-7 strokes of the pestle. The homogenized sample was centrifuged again at 1000g for 10 minutes. The supernatant fractions (S1′) were pooled and centrifuged at 10,000g for 20 minutes to get crude mitochondrial-lysosomal pellet fraction (P1, brown in color) and supernatant fraction (S2). Loosely attached pellet contain lysosome which was separated gently from mitochondrial pellet fraction. The Loosely attached fraction (lysosome) was mixed with the same buffer and centrifuged again at 10,000g for 20 minutes. Again, the loosely attached pellet was collected as lysosome fraction. Subsequently, the lysosomal pellet was resuspended in isolating buffer, aliquoted and kept at -

destained gel, blue protein bands can be seen against a clear background. The gels were scanned with a scanner attached to a computer. The original dye front, consisting of bromophenol blue dye, disappeared during the process. Due to the fact that bromophenol blue acts as a pH indicator, it turned to light yellow color under acidic conditions, prior to being washed out. The limitation with Coomassie blue staining is that it may not stain proteins that are present in a very low amount as well as proteins with high carbohydrate content.

5.2.3.3. Western blot analysis:

After proteins were separated by SDS-PAGE, the proteins were electrotransferred on a PVDF membrane by the semi-dry method. Initially, unfixed gels were incubated for a short time in a transfer buffer. Whatman paper and PVDF membranes were also soaked in the same transfer buffer. Primarily, the gel was placed on the PVDF membrane and two layers of Whatman papers were placed on both sides of the gel-membrane combination. To make the whole transfer-set air bubbles free, the entire set was rolled by a glass rod over it. Finally, this combination was placed on a transfer apparatus in such a way that the gel is connected to the cathode while the membrane is connected to the anode. The apparatus was connected to a power supply and the electrotransfer was done at a constant current of 50 mAmp (for a single gel) for 1 hour. The transfer efficiency of proteins from the gel to membrane was confirmed by staining the membranes with Coomassie solution. Further, the membranes were blocked with 5% non-fat milk dissolved in 1X TBS-T buffer. After blocking, the membrane was incubated with primary antibody in TBST buffer for 1 hour at room temperature/overnight at 4°C. This was followed by washing with TBST buffer 3 times. The membrane was further incubated with secondary antibody in TBST buffer for 1 hour. Finally, the membranes were again washed with TBST buffer for 3 times. Subsequently, the membrane was developed through chemiluminescence method (Super Signal™ West Femto Maximum Sensitivity Substrate, Thermo Scientific) and detected by chemidoc apparatus (Bio-Rad). In some experiments, the

case of Western blot analysis, the unfixed gel was used to transfer the proteins to a PVDF membrane.

Buffers required:

SDS-PAGE running buffer (1X): 196 mM glycine, 0.1% SDS, 50 mM Tris-HCl (pH 8.3)

Laemmli protein loading buffer (5X): 62.5 mM Tris HCl (pH 6.8), 5% β-mercaptoethanol (v/v), 50% Glycerol (v/v), 2% SDS (w/v), 0.1% (w/v) Bromo phenol Blue. Volume was adjusted by adding water.

Resolving gel mixture: 10% Bis-Acrylamide (v/v), 375 mM Tris HCl (pH 8.8), 0.1% SDS (w/v), 0.1% Ammonium persulfate, 0.005% TEMED in water.

Stacking gel mixture: 4% Bis-Acrylamide (v/v), 125 mM Tris HCl (pH 6.8), 0.1% SDS (w/v), 0.1% Ammonium persulfate, 0.005% TEMED in water.

30% Bis-Acrylamide stock solution, 10% APS stock solution, 100% TEMED solution, 10% SDS solution and 1.5 M Tris-HCl (pH 8.8) solution (for separating gel)/or 0.5M M Tris-HCl (pH 6.8, for stacking gel) were used to prepare separating and stacking solutions. APS and TEMED were added just prior to pouring the gels.

5.2.3.2. Coomassie staining of the protein bands in gel:

For Coomassie staining; generally, 0.1% Coomassie Brilliant blue dye dissolved in 50% methanol, 10% glacial acetic acid was used to stain the proteins in a gel after separated by SDS-PAGE. Acidified methanol precipitates the proteins. Staining was usually done overnight with agitation in staining solution. The agitation causes circulation of dye, enhances penetration, and ensures uniformity of staining. The dye penetrates the entire gel but it only sticks permanently to the proteins. After staining of the gel it was transferred in de-staining solution composed of acetic acid/methanol. Gentle agitation helps to wash out excess dye. To get better result, it is important to destain the gel in two steps, starting with 50% methanol, 10% acetic acid for 1-2 hours, then using 7% methanol, 10% acetic acid to get a desired staining. Because of higher methanol content, the first solution shrinks the gel, squeezing out much of the liquid component, and the gel swells and clears in the second solution. In a properly stained-

5.2.3. Methods related to protein chemistry:

5.2.3.1. Separation of denatured proteins by SDS-PAGE:

For electrophoretic separation of proteins, SDS-PAGE was performed with 10% acrylamide gels in a Biorad mini-apparatus if not mentioned otherwise. Use of sodium dodecyl sulfate (SDS), a strong anionic detergent helps in the separation of denatured protein and that's why it is termed as SDS-PAGE. A discontinuous polyacrylamide gel is used as a support medium to separate the denatured proteins according to their molecular size. SDS-PAGE as a useful technique for protein separation was first introduced by U.K. Laemmli [441]. To make the protein samples compatible for SDS-PAGE separation, protein samples were completely denatured by adding Laemmli protein loading buffer in 1:4 v/v (from a 5X stock of Laemmli protein loading buffer) and followed by heating the mixture at 95°C for 5 minutes. SDS-PAGE cassettes were prepared by using a pair of clean glass plate (10 cm wide and 7 cm high) separated by a pair of spacer (1 mm thick). Around 5 ml of resolving gel was filled into the cassettes and was allowed to polymerise. A thin layer of water was slowly added to the top of resolving gel layer to make the upper layer of resolving gel smooth. After polymerization of resolving gel, the added water was slowly decanted and stacking gel mixture (~ 2 ml) was poured on top of the resolving gel. A 10 well or 15 well comb was inserted within the stacking gel to form wells for loading protein samples. Once the stacking gel gets polymerized, combs were removed slowly without disrupting the wells. The cassette was then inserted into electrophoresis chamber vertically and was filled with an electrophoresis running buffer. The denatured protein samples were loaded into the wells using a Hamilton syringe. The apparatus was connected to a constant current source (10 mAmp) for electrophoresis. Bromophenol blue (used as the tracking dye) added in the protein loading buffer helps in the visualization of migrated proteins in the gel. When the dye-front reached almost end, electrophoresis was stopped, and the separated proteins in the gel were visualized by Coomassie blue staining. In

minutes at 4°C. The pellet obtained was again resuspended in 6 ml of TfbII buffer. Bacterial cells suspended in TfbII buffer were eventually aliquoted in microcentrifuge tubes. These competent cells containing tubes were snap-chilled in liquid nitrogen and stored in -80°C for further use.

Solutions and buffer required:

LB media: 10g Bacto Tryptone, 5g Bacto Yeast extract, 10g NaCl dissolved in 1 liter of double distilled water and autoclave at 121°C at 15 lbs for 20 minutes.

TfbI buffer: Rubidium Chloride (100 mM), Manganese Chloride (50 mM), Potassium Acetate (30 mM), Calcium Chloride (10 mM), Glycerol (15%). Adjust to pH 5.8 with dilute acetic acid (0.2%; 1.0 M). Filter sterilize (Do not autoclave) and store at 4ºC.

TfbII buffer: MOPS (10 mM), Rubidium Chloride (10 mM), Calcium Chloride (75 mM), Glycerol (15%). Adjust pH to 6.5 with KOH. Filter sterilize (Do not autoclave) and store at 4ºC.

5.2.2.3. Transformation of *E. coli*:

For transformation of *E. coli,* competent cells (DH5α or DE3 strain) containing aliquots were taken out from -80°C and thawed in ice for 10 minutes. Purified plasmid DNA (~100 ng/µl) or ligated DNA products were then added to 50 µl of competent cell containing vials. This mixture was incubated for 10 minutes in ice. After incubation, this mixture was given a heat shock at 42ºC for 45 seconds by dipping the tube in a water bath. Immediately after heat shock, the tube was kept in ice for 2 minutes. After subsequent cooling, 800 µL of LB media was added to the mix. The cells were allowed to grow for 1 hour at 37°C and 220 RPM in incubator-shaker with constant shaking. After 1 hour, the bacterial suspension was centrifuged at 13,500 RPM for 30 seconds. The resulting pellet was resuspended in 100 µL supernatant and plated on LB plates containing the desired antibiotic. Subsequently the plates were kept at 37°C for 12 hours and single colonies were obtained after 12 hours of incubation.

5.2.2. Competent *E. coli* cell preparation:

5.2.2.1. $CaCl_2$ Method:

The protocol mentioned below is followed for the preparation of Competent *E. coli* cells (both DE3 and DH5α strains). A single colony of bacterial cell from an LB plate streaked with either of the above-mentioned *E. coli* strain was incubated in 3 ml of Luria-Bertani (LB) broth and grown overnight at 37ºC and 220 RPM. One ml of this starter culture was added to 100 ml of fresh LB liquid medium and was incubated at 37°C and 220 RPM to make a broth culture. The cells were grown until the culture broth reaches an OD (at 600 nm) of 0.4-0.5. Subsequently the cells were incubated on ice for 10 minutes and centrifuged at 3000 RPM for 5 minutes at 4°C. The resulting pellet was resuspended in 30 ml of ice-cold $CaCl_2$ (100 mM) solution and further incubated for 30 minutes on ice. The suspension was further centrifuged for 5 minutes at 4°C at 5000 RPM. Finally, the pellet was resuspended in ice-cold $CaCl_2$ (100 mM) solution supplemented with 10% glycerol, distributed in tubes and stored at -80°C.

5.2.2.2. RbCl method:

A single colony of *E. coli* bacteria (DH5α or DE3) was added to 3 ml of Luria-Bertani (LB) broth and was grown overnight at 37°C in a shaker (220 RPM). From this starter culture, 1ml inoculum was added to 100 ml of fresh LB liquid medium and incubated at 37°C and 220 RPM. The cells were grown until the broth reached an OD (at 600 nm) of 0.4-0.5. Bacterial culture was then incubated in ice for 10 minutes and centrifuged at 4500 RPM for 10 minutes at 4°C. After centrifugation, supernatant was discarded and the entire 100 ml culture was pelleted by centrifugation again. The pellet was resuspended in 30 ml of TfbI buffer and incubated on ice for 15 minutes. Subsequently the cells were centrifuged at 4000 RPM for 5

5.2.1.4. Restriction digestion of dsDNA:

Approximately 1µg of dsDNA was used for restriction digestion in 20 µl reaction mixtures. In restriction digestion mixture, specific restriction buffer was added at a concentration of 1X and double distilled autoclaved water. Depending on the enzyme activity, restriction enzymes were added at the ratio of 1 unit /µg of DNA. The reaction mixture was incubated at 37°C for 3 hours or overnight, depending on the activity of the enzymes. For doubled restriction digestion, a compatible buffer was selected according to the manufacturer's (NEB) instruction.

5.2.1.5. Ligation of dsDNA:

After restriction digestion of insert and vector, it was first checked on 0.8% agarose gel and the bands of proper sizes were cut out from the gel. The dsDNA was further purified from the gel by using DNA gel extraction kit (Qiagen) according to the manufacturer's protocol. The concentration of both insert and vector DNA were estimated using Nanodrop (Thermo Scientific). Depending upon their respective concentrations, insert DNA: vector DNA was added to the ligation mix in a ratio of 3:1. Apart from insert and vector DNA, T4 DNA ligase compatible buffer (1X) was also added to the ligation mix and double distilled autoclaved water was added to make up the final reaction volume. At the last T4-DNA ligase was added to the reaction mixture and it was incubated for 12 hours at 16°C.

dNTPs (10mM) = 2µl

10x buffer = 2.5µl

H_2O = 17µl

Enzyme = 1µl

Total Volume = 25µl

The mixture was subjected to a temperature change in an Eppendorf thermocycler instrument as described below.

Step	**Process**	**Temperature and duration**
1.	Denaturation	95°C for 5 minutes
2	Denaturation	94°C for 30 sec
3	Annealing	55°C for 30 sec
4	Extension	72°C for 1 minutes/Kb
5	Repeat step 2 for 29 Cycles	
6	Extension	72°C for 10 minutes
7	End and store	4°C

All PCR-amplified DNA were further confirmed by agarose gel electrophoresis.

buffer. DNA samples were mixed with loading buffer and were subsequently loaded into sample wells. The apparatus was connected to a constant current source. The tracking dyes (mixture of Bromophenol blue and Xylene Cyanol) present in the DNA loading buffer helps in visualization of movement of DNA in the gel after migration. After adequate migration, the DNA fragment/s were visualized by using an ultraviolet transilluminator (DNA emits fluorescence in response to UV excitation due to the incorporation of Ethidium Bromide during electrophoresis). Subsequent gel images were photographed by a camera and attached to a gel documentation system.

Solutions and buffer required:

(1X) TAE buffer: 40mM Tris/Acetic acid, pH7.8; 1mM EDTA pH 8.0

(5X) DNA loading buffer: 40% (w/v) Sucrose, 240mM Tris/Acetic acid, pH7.8, 5mM EDTA, pH 0.8, 0.25% (w/v) Bromophenol blue, 0.25% (w/v) Xylene Cyanol FF.

5.2.1.3. Polymerase chain reaction (PCR): To prepare different constructs in particular expression vectors, PCR reactions were performed to precisely amplify the different coding regions with specific restriction sites at the ends. This was done in cases when a specific insert had to be cloned from one expression vector to another. PCR master mix contains Template DNA, specific forward and reverse primer, dNTPs, Taq buffer 1X, Taq DNA polymerase and miliQ water. The PCR master mix was kept for PCR amplification. All PCR reactions were carried out using following conditions mentioned below. Taq DNA-polymerase (NEB) was used as an enzyme.

PCR reaction conditions:

Forward Primer (100 nM) = 1µl

Reverse Primer (100 nM) =1µl

Template = 0.5 µl

5.2. Methods

5.2.1. Methods related to molecular biology:

5.2.1.1. Construct preparation: DNA fragments corresponding to the required coding regions were obtained either by restriction digestion of the available cDNA or amplified by PCR using a set of specific primers. PCR-amplified DNA and vector were subsequently digested by restriction enzyme/s to produce cohesive overhanging ends. Restriction enzyme-digested insert/s and vector/s were purified from agarose gel by using DNA purification kits. Subsequently, the purified insert and vector pair were ligated. The ligated product was transformed into *E. coli*. Transformed *E. coli* cells were selected on a LB plate containing specific antibiotic. Plasmid DNA was isolated from those colonies by using plasmid DNA purification kits. Miniprep plasmid DNA was further analysed for the presence of insert by means of restriction digestion analysis, PCR amplification and finally confirmed by sequencing.

5.2.1.2. Agarose gel electrophoresis: Separation of dsDNA was performed on horizontal agarose gel electrophoresis apparatus in the presence of 1X TAE buffer. Agarose-gel was prepared at a concentration ranging from (0.8-1.2%) by mixing agarose powder with electrophoresis buffer (1X TAE). The solution was then heated in a microwave oven until all the agarose melted. Choice of the gel percentage depends on the length of the dsDNA subjected to separation. Ethidium Bromide (EtBr, at a final concentration of 0.1 to 0.5 μg/ml) was added to the liquefied gel to facilitate visualization of DNA. Casting tray was kept on the workbench with proper leveling. After slight cooling, the molten gel was poured into a casting tray containing a sample comb and was allowed to solidify at room temperature (25°C). Once the gel becomes solidified, the comb was removed from the gel without destroying the bottom of the wells. The gel was placed into the electrophoresis chamber, covered with electrophoretic

5.1.13. Primers:

No.	Sequence	Use	Construct
1	GAT***GGATCC***GCCATCTTCCTGCTGAGACCC	FP	TRPV3-LOOP1+TM3
	GAT***GTCGAC***TTAGCAGGCGAGGTACTCTTTGT	RP	
2	GAT***GGATCC***CTGCAGCTCCTAGGGAGGATGT	FP	TRPV3-TM2+LOOP1
	GAT***GTCGAC***TTAAAAGACAAAGTGGAACCAGGCA	RP	
3	GAT***GGATCC***TACAAAGAGTACCTCGCCTGC	FP	TRPV3-TM4+LOOP2
	GAT***GTCGAC***TTACAAGAACTTCAGAACATCATGCAA	RP	
4	GAT***GGATCC***TATACGCGGGGTTTCCAGTC	FP	TRPV3-LOOP2+TM5
	GAT***GTCGAC***TTAGGGACACTTCTCGATCAGC	RP	
5	GAT***GGATCC***CTCCTCAACATGCTCATTGCTC	FP	TRPV3-Ct
	GAT***GTCGAC***CTACACCGAGGTTTCCGGGAA	RP	
6	GAGAGCGAACGCATC**G**GGCGCCTGCAGAG	FP	TRPV3-W692G
	CTCTGCAGGCGCC**C**GATGCGTTCGCTCTC	RP	
7	CGGGGTTTCCAGTCCATGG**C**CATGTACAGC	FP	TRPV3-G573A
	GCTGTACATG**G**CCATGGACTGGAAACCCCG	RP	
8	***AATTCT***GACATGATCCTACTG***GCGGCCGC***G	FP	V3(AA322-326) DMILL
	GATCCGCGGCCGCCAGTAGGATCATGTCAG	RP	
9	***AATTCT***GAGTTGGTAGAGTTGCTG***GCGGCCGC***G	F	V3(AA134-139) ELVELL
	GATCCGCGGCCGCCAGCAACTCTACCAACTCAG	RP	
10	***AATTCT***GACATCGCAGCCCTGCTC***GCGGCCGC***G	FP	V3(229-234) DIAALL
	GATCCGCGGCCGCGAGCAGGGCTGCGATGTCAG	RP	
11	***AATTCT***GAGATTGTGCAGCTGCTG***GCGGCCGC***	FP	V3(276-281) EIVQLL
	GATCC**GCGGCCGC**CAGCAGCTGCACAATCTCAG	RP	

Bold & Italics: Restriction enzyme in primer; **Only Bold:** Point mutation in Primer. FP and RP represent Forward primer and reverse primer respectively.

TRPV3-mutant-GFP (OS)	pCMV6-AC-GFP	Mammalian	Dr. Yong Yang [243]
cAMP-sensor (H189)	mTurquoiseΔ-Epac	Mammalian	Prof. Kees Jalink [440]
cAMP-sensor (H187)	mTurquoiseΔ-Epac	Mammalian	Prof. Kees Jalink [440]

5.1.12. TRPV3 Constructs used in this study:

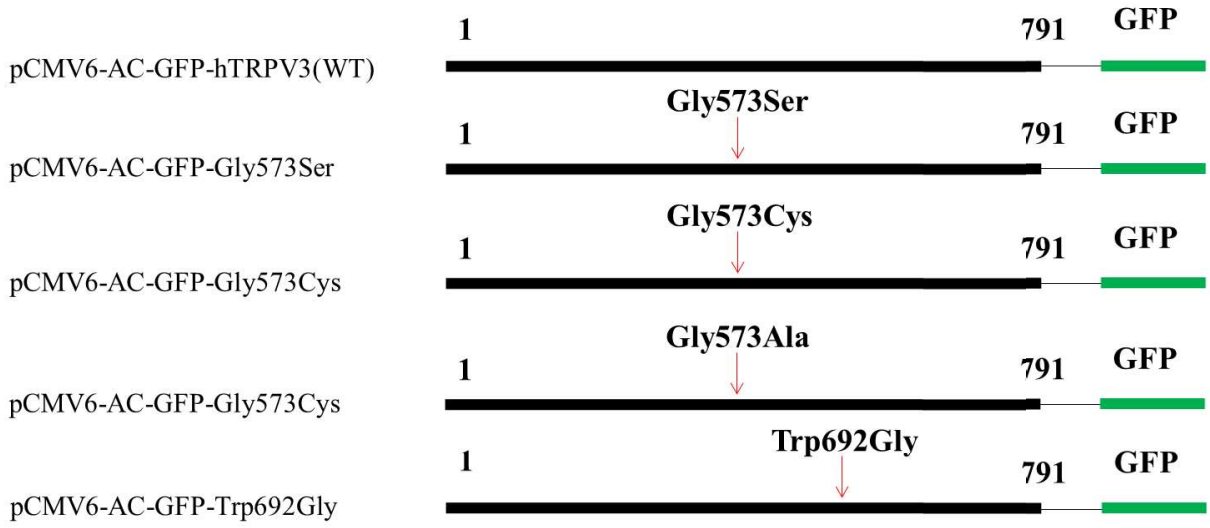

5.1.9. Cell line:

Cell lines	Source
F11	Prof. F. Hucho (FU, Berlin)
HaCaT	Prof. F. Hucho (FU, Berlin)
HeLa	Prof. F. Hucho (FU, Berlin)
HEK	Prof. F. Hucho (FU, Berlin)
CHOK1-Mock	Prof. Jon D Levine (UCSF, USA)
Neuro-2a	Prof. H. H. ropers (MPI Mol Gen, Berlin)
Saos-2	NCCS Pune, India

5.1.10. Bacterial cell line:

Bacterial cell line	Source
BL21DE3pLys	CG-Lab, NISER
DH5α	CG-Lab, NISER

5.1.11. Constructs:

Constructs used	Vector	Expression system	Source
TRPV2-GFP	pCDNA3.1	Mammalian	Prof. F. Hucho (FU, Berlin) [25]
TRPV3-GFP	pCMV6-AC-GFP	Mammalian	Dr. Yong Yang [243]
Tubulin-mCherry	pDSRed-Monomer	Mammalian	BD-Clontech
Actin-RFP	pDSRed-Monomer	Mammalian	BD-Clontech
MBP-TRPV2-Ct	pMalc2x	*E. Coli*	Prof. F. Hucho (FU, Berlin) [25]
MBP-TM2-L2-TM3-TRPV3	pMalc5x	*E. Coli*	CG lab, NISER
MBP-TM4-L4-TM5-TRPV3	pMalc5x	*E. Coli*	Prepared in CG lab
MBP-TM4-L4-TM5-TRPV3-G573C	pMalc5x	*E. Coli*	Prepared in CG lab
MBP-TM4-L4-TM5-TRPV3-G573S	pMalc5x	*E. Coli*	Prepared in CG lab
MBP-TM4-L4-TM5-TRPV3-G573A	pMalc5x	*E. Coli*	Prepared in CG lab

5.1.6. Secondary antibody used in western blotting:

Description	Host	Source	Dilution
HRP labeled anti-mouse	Donkey	GE Healthcare	1:10,000
HRP labeled anti-rabbit	Donkey	GE Healthcare	1:10,000

5.1.7. Blocking peptide:

Peptide Sequence	Blocking activity against	Source
C-terminus (824-838aa) EDAEVFKDSMVPGEK	TRPV1	Alomone
C-terminus (735-750aa) KKNPTSKPGKNSASEE	TRPV2	Alomone
1st extracellular loop (464-478aa) REEEAIPHPLALTHK	TRPV3	Alomone

5.1.8. Vectors:

Vectors	Source
pCDNA3.1	Prof. Jon D Levine (UCSF, San Francisco)
pDSRed-Monomer	Invitrogen (Carlsbad, California, USA)
pEGFPN3	Prof. J. Berreiter-Hahn (Frankfurt, Germany)
pGEX6P1	Dr. P V Alone (NISER, India)
pMALc2x	NEB (Ipswich, England)
mitoDsRed	Clontech (Mountain View California, USA)
pMALc5x	NEB (Ipswich, England)
Actin-RFP	Clontech (Mountain View California, USA)
Tubulin-mCherry	Prof. R. Y. Tsien (Sen Diego, California)
pCMV6-AC-GFP	Dr. Yong Yang (Peking University, Beijing, China)

Mo: mouse monoclonal; **Rb:** rabbit polyclonal; **WB:** Western Blot; Dilution with respect to Western Blot analysis.

5.1.4. Secondary antibody used in immunofluorescence:

Description	Host	Source	Dilution
Alexa-594-labelled anti-mouse	Chicken	Molecular Probe	1:750
Alexa-594-labelled anti-rabbit	Chicken	Molecular Probe	1:750
Alexa-488-labelled anti-rabbit	Chicken	Molecular Probe	1:750
Alexa-488-labelled anti-mouse	Chicken	Molecular Probe	1:750
Alexa-647 labeled anti-mouse	Chicken	Molecular Probe	1:500
Alexa-647 labeled anti-rabbit	Chicken	Molecular Probe	1500

5.1.5. Dyes used for live and fixed cells:

LysoTracker Red		Molecular Probe	500 nM
MitoTracker Red		Molecular Probe	1µM
JC1		Molecular Probe	1µM
Fluo4		Molecular Probe	3µM
DAPI		Molecular Probe	1:2000
BCECF		Molecular Probe	1µM

ECL	Thermoscientific
Bradford protein estimation kit	Sigma
SDS-PAGE protein marker High range	Thermoscientific
1 kb DNA ladder	Fermentas
100 bp DNA ladder	Fermentas
Restriction Enzyme	NEB, Fermentas
T4 DNA ligase	NEB

5.1.3. Primary antibody used:

Antibodies	**Host**	**Source**	**Application/s**	**Dilution**
Hsp60	Mo	Abcam	WB, IF	1:500
MBP	Mo	NEB	WB	1:30,000
E-cadherin		Merk Millipore	WB, IF	1:500
Calnexin	Rb	Abcam	WB, IF	1:500
Lamp1	Rb	Sigma	WB, IF	1:500
GM130	Rb	Sigma	WB, IF	1:500
β-Tubulin	Mo	Sigma	WB, IF	1:500
α-Tubulin	Mo	Sigma	WB, IF	1:500
β-III tubulin	Mo	Sigma	WB, IF	1:500
Acetylated tubulin	Mo	Sigma	WB, IF	1:500
Polyglutamylated tubulin	Mo	Sigma	WB, IF	1:500
Tyrosinated tubulin	Mo	Sigma	WB, IF	1:500
GAPDH	Rb		WB	1:30,000
PhosphoTyrosine	Rb	Sigma	WB, IF	1:500
Actin	Mo	Abcam	WB, IF	1:500
TRPV1-Ct	Rb	Alomone	WB, IF	1:500
TRPV2-Ct	Rb	Alomone	WB, IF	1:500
TRPV3-Ext. loop	Rb	Alomone	WB, IF	1:500
Anti CREB	Rb	Cell signaling technology	WB,	1:500
P-CREB	Rb	Cell signaling technology	WB	1:500
FES	Rb	Cell signaling technology	WB	1:500
FER	Mo	Cell signaling technology	WB	1:500

JC-1	Sigma – Aldrich
Kanamycin	MP biomedical
LB powder	Himedia
Maltose	Sigma – Aldrich
Methanol	Merck
MitoTracker Red	Invitrogen
$MgCl_2$	Sigma – Aldrich
NADH	Sigma – Aldrich
$NaBH_4$	MP biomedical
PMSF	Sigma – Aldrich
PIPES	Sigma – Aldrich
Probenecid	Sigma – Aldrich
Potassium phosphate monobasic	Sigma – Aldrich
PVDF membrane	Millipore
Ponceau S	Sigma – Aldrich
Potassium Hydroxide	Sigma – Aldrich
Skimmed milk powder	Himedia
Sodium Chloride	Sigma – Aldrich
Sodium Dodecyl Sulphate	Sigma – Aldrich
Sodium Hydroxide	Sigma – Aldrich
Sucrose	Sigma – Aldrich
TEMED	Sigma – Aldrich
Tranilast	Sigma – Aldrich
Tris base	Sigma – Aldrich
Triton X100	Sigma – Aldrich
Tryptone	Himedia
Tween 20	Sigma – Aldrich
Whatman paper	Whatman
Xylene cyanol	Sigma – Aldrich
Yeast extracts	Himedia

5.1.2. Kits and Markers:

Plasmid DNA isolation (maxi prep) kit	Qiagen
Plasmid DNA isolation (mini prep) kit	Qiagen
Gel extraction kit	Qiagen
Lipofectamine Cell transfection kit	Invitrogen

5.1. Material

5.1.1. Chemicals used:

Chemical used	Source
Acetic Acid	Merck Millipore
Acrylamide	Sigma – Aldrich
Agar	Himedia
Agarose	Lonza
Ampicillin	Sigma – Aldrich
Amylose resin	NEB
APS (Ammonium persulphate)	Sigma – Aldrich
β-mercaptoethanol	Sigma – Aldrich
Bis-acrylamide	Sigma – Aldrich
Bromophenol Blue	Sigma – Aldrich
BSA	Sigma – Aldrich
Cover Slip	Fisher
Complete protease inhibitor	Sigma – Aldrich
Coomassie Brilliant Blue G250	MP biomedical
DAPI	Invitrogen
Dipotassium phosphate	Sigma – Aldrich
DMSO	Sigma – Aldrich
dNTPs	NEB
DPTHF	Sigma – Aldrich
DTT	Sigma – Aldrich
EDTA	Sigma – Aldrich
EGTA	Sigma – Aldrich
Ethanol	Merck
FPP	Sigma – Aldrich
Ethidium Bromide	Sigma – Aldrich
Fluoromount G	Southern Biotechnology
Glutamate	MP biomedical
Paraformaldehyde	Sigma – Aldrich
Glycerol	Sigma – Aldrich
Glycine	Sigma – Aldrich
Hydrogen Chloride	Merck
HEPES	Sigma – Aldrich
IPTG	MP biomedical

Chapter 5

Material and Method

452. Crooks, G.E., et al., *WebLogo: a sequence logo generator.* Genome Res, 2004. **14**(6): p. 1188-90.
453. Schneider, T.D. and R.M. Stephens, *Sequence logos: a new way to display consensus sequences.* Nucleic Acids Res, 1990. **18**(20): p. 6097-100.
454. Tamura, K., et al., *MEGA5: molecular evolutionary genetics analysis using maximum likelihood, evolutionary distance, and maximum parsimony methods.* Mol Biol Evol, 2011. **28**(10): p. 2731-9.
455. Trott, O. and A.J. Olson, *AutoDock Vina: improving the speed and accuracy of docking with a new scoring function, efficient optimization, and multithreading.* J Comput Chem, 2010. **31**(2): p. 455-61.
456. Krieger, E., et al., *Improving physical realism, stereochemistry, and side-chain accuracy in homology modeling: Four approaches that performed well in CASP8.* Proteins, 2009. **77 Suppl 9**: p. 114-22.
457. Canutescu, A.A., A.A. Shelenkov, and R.L. Dunbrack, Jr., *A graph-theory algorithm for rapid protein side-chain prediction.* Protein Sci, 2003. **12**(9): p. 2001-14.
458. Dunbrack, R.L., Jr. and F.E. Cohen, *Bayesian statistical analysis of protein side-chain rotamer preferences.* Protein Sci, 1997. **6**(8): p. 1661-81.
459. Konagurthu, A.S., et al., *MUSTANG: a multiple structural alignment algorithm.* Proteins, 2006. **64**(3): p. 559-74.

427. Zong, X., et al., *The two-pore channel TPCN2 mediates NAADP-dependent Ca(2+)-release from lysosomal stores.* Pflugers Arch, 2009. **458**(5): p. 891-9.
428. Tugba Durlu-Kandilci, N., et al., *TPC2 proteins mediate nicotinic acid adenine dinucleotide phosphate (NAADP)- and agonist-evoked contractions of smooth muscle.* J Biol Chem, 2010. **285**(32): p. 24925-32.
429. Zeevi, D.A., A. Frumkin, and G. Bach, *TRPML and lysosomal function.* Biochim Biophys Acta, 2007. **1772**(8): p. 851-8.
430. Kim, H.J., et al., *The Ca(2+) channel TRPML3 regulates membrane trafficking and autophagy.* Traffic, 2009. **10**(8): p. 1157-67.
431. Martina, J.A., B. Lelouvier, and R. Puertollano, *The calcium channel mucolipin-3 is a novel regulator of trafficking along the endosomal pathway.* Traffic, 2009. **10**(8): p. 1143-56.
432. Saito, M., P.I. Hanson, and P. Schlesinger, *Luminal chloride-dependent activation of endosome calcium channels: patch clamp study of enlarged endosomes.* J Biol Chem, 2007. **282**(37): p. 27327-33.
433. van de Graaf, S.F., et al., *Direct interaction with Rab11a targets the epithelial Ca2+ channels TRPV5 and TRPV6 to the plasma membrane.* Mol Cell Biol, 2006. **26**(1): p. 303-12.
434. Escriba, P.V., et al., *Membranes: a meeting point for lipids, proteins and therapies.* J Cell Mol Med, 2008. **12**(3): p. 829-75.
435. Grouleff, J., et al., *The influence of cholesterol on membrane protein structure, function, and dynamics studied by molecular dynamics simulations.* Biochim Biophys Acta, 2015. **1848**(9): p. 1783-95.
436. Simons, K. and R. Ehehalt, *Cholesterol, lipid rafts, and disease.* J Clin Invest, 2002. **110**(5): p. 597-603.
437. Chen, X. and M.D. Resh, *Cholesterol depletion from the plasma membrane triggers ligand-independent activation of the epidermal growth factor receptor.* J Biol Chem, 2002. **277**(51): p. 49631-7.
438. Baier, C.J., J. Fantini, and F.J. Barrantes, *Disclosure of cholesterol recognition motifs in transmembrane domains of the human nicotinic acetylcholine receptor.* Sci Rep, 2012. **1**: p. 69.
439. Fantini, J. and F.J. Barrantes, *How cholesterol interacts with membrane proteins: an exploration of cholesterol-binding sites including CRAC, CARC, and tilted domains.* Front Physiol, 2013. **4**: p. 31.
440. Klarenbeek, J., et al., *Fourth-generation epac-based FRET sensors for cAMP feature exceptional brightness, photostability and dynamic range: characterization of dedicated sensors for FLIM, for ratiometry and with high affinity.* PLoS One, 2015. **10**(4): p. e0122513.
441. Laemmli, U.K., *Cleavage of structural proteins during the assembly of the head of bacteriophage T4.* Nature, 1970. **227**(5259): p. 680-5.
442. Graham, J.M., *Isolation of lysosomes from tissues and cells by differential and density gradient centrifugation.* Curr Protoc Cell Biol, 2001. **Chapter 3**: p. Unit 3 6.
443. Shelanski, M.L., F. Gaskin, and C.R. Cantor, *Microtubule assembly in the absence of added nucleotides.* Proc Natl Acad Sci U S A, 1973. **70**(3): p. 765-8.
444. Bradford, M.M., *A rapid and sensitive method for the quantitation of microgram quantities of protein utilizing the principle of protein-dye binding.* Anal Biochem, 1976. **72**: p. 248-54.
445. Gee, K.R., et al., *Chemical and physiological characterization of fluo-4 Ca(2+)-indicator dyes.* Cell Calcium, 2000. **27**(2): p. 97-106.
446. Reers, M., et al., *Mitochondrial membrane potential monitored by JC-1 dye.* Methods Enzymol, 1995. **260**: p. 406-17.
447. Wheeler, D.L., et al., *Database resources of the National Center for Biotechnology Information.* Nucleic Acids Res, 2006. **34**(Database issue): p. D173-80.
448. Wheeler, D.L., et al., *Database resources of the National Center for Biotechnology Information.* Nucleic Acids Res, 2007. **35**(Database issue): p. D5-12.
449. Edgar, R.C., *MUSCLE: multiple sequence alignment with high accuracy and high throughput.* Nucleic Acids Res, 2004. **32**(5): p. 1792-7.
450. Edgar, R.C., *MUSCLE: a multiple sequence alignment method with reduced time and space complexity.* BMC Bioinformatics, 2004. **5**: p. 113.
451. Omasits, U., et al., *Protter: interactive protein feature visualization and integration with experimental proteomic data.* Bioinformatics, 2014. **30**(6): p. 884-6.

401. Zhi, Y.P., et al., *Two familial cases of Olmsted-like syndrome with a G573V mutation of the TRPV3 gene.* Clin Exp Dermatol, 2016. **41**(5): p. 510-3.
402. Ni, C., et al., *A novel mutation in TRPV3 gene causes atypical familial Olmsted syndrome.* Sci Rep, 2016. **6**: p. 21815.
403. Agarwala, M.K., et al., *Olmsted syndrome in an Indian male with a new de novo mutation in TRPV3.* Br J Dermatol, 2016. **174**(1): p. 209-11.
404. Ishida-Yamamoto, A., et al., *Mutant loricrin is not crosslinked into the cornified cell envelope but is translocated into the nucleus in loricrin keratoderma.* J Invest Dermatol, 2000. **115**(6): p. 1088-94.
405. Haghighi, A., et al., *A missense mutation in the MBTPS2 gene underlies the X-linked form of Olmsted syndrome.* J Invest Dermatol, 2013. **133**(2): p. 571-3.
406. Broad, L.M., et al., *TRPV3 in Drug Development.* Pharmaceuticals (Basel), 2016. **9**(3).
407. He, Y., et al., *A gain-of-function mutation in TRPV3 causes focal palmoplantar keratoderma in a Chinese family.* J Invest Dermatol, 2015. **135**(3): p. 907-9.
408. Ghosh, A., et al., *Why individual thermo sensation and pain perception varies? Clue of disruptive mutations in TRPVs from 2504 human genome data.* Channels (Austin), 2016. **10**(5): p. 339-345.
409. Boukamp, P., et al., *Normal keratinization in a spontaneously immortalized aneuploid human keratinocyte cell line.* J Cell Biol, 1988. **106**(3): p. 761-71.
410. Bonifacino, J.S. and L.M. Traub, *Signals for sorting of transmembrane proteins to endosomes and lysosomes.* Annu Rev Biochem, 2003. **72**: p. 395-447.
411. Letourneur, F. and R.D. Klausner, *A novel di-leucine motif and a tyrosine-based motif independently mediate lysosomal targeting and endocytosis of CD3 chains.* Cell, 1992. **69**(7): p. 1143-57.
412. Braulke, T. and J.S. Bonifacino, *Sorting of lysosomal proteins.* Biochim Biophys Acta, 2009. **1793**(4): p. 605-14.
413. Ishida, Y., et al., *A model of lysosomal pH regulation.* J Gen Physiol, 2013. **141**(6): p. 705-20.
414. Galione, A., et al., *The acid test: the discovery of two-pore channels (TPCs) as NAADP-gated endolysosomal Ca(2+) release channels.* Pflugers Arch, 2009. **458**(5): p. 869-76.
415. Morgan, A.J. and A. Galione, *NAADP induces pH changes in the lumen of acidic Ca2+ stores.* Biochem J, 2007. **402**(2): p. 301-10.
416. Scott, C.C. and J. Gruenberg, *Ion flux and the function of endosomes and lysosomes: pH is just the start: the flux of ions across endosomal membranes influences endosome function not only through regulation of the luminal pH.* Bioessays, 2011. **33**(2): p. 103-10.
417. Hara-Chikuma, M., et al., *ClC-3 chloride channels facilitate endosomal acidification and chloride accumulation.* J Biol Chem, 2005. **280**(2): p. 1241-7.
418. Mohammad-Panah, R., et al., *The chloride channel ClC-4 contributes to endosomal acidification and trafficking.* J Biol Chem, 2003. **278**(31): p. 29267-77.
419. Su, A.I., et al., *A gene atlas of the mouse and human protein-encoding transcriptomes.* Proc Natl Acad Sci U S A, 2004. **101**(16): p. 6062-7.
420. Wu, C., et al., *BioGPS: an extensible and customizable portal for querying and organizing gene annotation resources.* Genome Biol, 2009. **10**(11): p. R130.
421. Wellhauser, L., C. D'Antonio, and C.E. Bear, *ClC transporters: discoveries and challenges in defining the mechanisms underlying function and regulation of ClC-5.* Pflugers Arch, 2010. **460**(2): p. 543-57.
422. Ignoul, S., et al., *Human ClC-6 is a late endosomal glycoprotein that associates with detergent-resistant lipid domains.* PLoS One, 2007. **2**(5): p. e474.
423. Gilfillan, G.D., et al., *SLC9A6 mutations cause X-linked mental retardation, microcephaly, epilepsy, and ataxia, a phenotype mimicking Angelman syndrome.* Am J Hum Genet, 2008. **82**(4): p. 1003-10.
424. Garbern, J.Y., et al., *A mutation affecting the sodium/proton exchanger, SLC9A6, causes mental retardation with tau deposition.* Brain, 2010. **133**(Pt 5): p. 1391-402.
425. Kagami, T., et al., *Identification and biochemical characterization of the SLC9A7 interactome.* Mol Membr Biol, 2008. **25**(5): p. 436-47.
426. Lawrence, S.P., et al., *The sodium/proton exchanger NHE8 regulates late endosomal morphology and function.* Mol Biol Cell, 2010. **21**(20): p. 3540-51.

373. Basbaum, A.I., et al., *Cellular and molecular mechanisms of pain.* Cell, 2009. **139**(2): p. 267-84.
374. Boyette-Davis, J.A., E.T. Walters, and P.M. Dougherty, *Mechanisms involved in the development of chemotherapy-induced neuropathy.* Pain Manag, 2015. **5**(4): p. 285-96.
375. HC., O., *Keratoderma palmaris et plantaris congenitalis: Report of a case showing associated lesions of unusual location.* Am J Dis Child, 1927. **33**: p. 757–64.
376. Requena, L., et al., *Olmsted syndrome: report of a case with study of the cellular proliferation in keratoderma.* Am J Dermatopathol, 2001. **23**(6): p. 514-20.
377. Batra, P. and N. Shah, *Olmsted syndrome--a rare syndrome with oral manifestations.* Oral Surg Oral Med Oral Pathol Oral Radiol Endod, 2004. **97**(5): p. 599-602.
378. Kumar, P., P.K. Sharma, and H.K. Kar, *Olmsted syndrome.* Indian J Dermatol, 2008. **53**(2): p. 93-5.
379. Mevorah, B., et al., *Olmsted syndrome: mutilating palmoplantar keratoderma with periorificial keratotic plaques.* J Am Acad Dermatol, 2005. **53**(5 Suppl 1): p. S266-72.
380. Tharini, G.K., et al., *Olmsted syndrome: report of two cases.* Indian J Dermatol, 2011. **56**(5): p. 591-3.
381. Vosynioti, V., et al., *A case of Olmsted syndrome.* Eur J Dermatol, 2010. **20**(6): p. 837-8.
382. Yaghoobi, R., et al., *Olmsted syndrome in an Iranian family: report of two new cases.* Arch Iran Med, 2007. **10**(2): p. 246-9.
383. Al-Mutairi, N., et al., *Olmsted syndrome: report of a new case with unusual features.* Clin Exp Dermatol, 2005. **30**(6): p. 640-2.
384. Poulin, Y., H.O. Perry, and S.A. Muller, *Olmsted syndrome--congenital palmoplantar and periorificial keratoderma.* J Am Acad Dermatol, 1984. **10**(4): p. 600-10.
385. Armstrong, A.P. and N. Percival, *Olmsted's syndrome.* J R Soc Med, 1997. **90**(2): p. 81-2.
386. Atherton, D.J., C. Sutton, and B.M. Jones, *Mutilating palmoplantar keratoderma with periorificial keratotic plaques (Olmsted's syndrome).* Br J Dermatol, 1990. **122**(2): p. 245-52.
387. Kress, D.W., et al., *Olmsted syndrome. Case report and identification of a keratin abnormality.* Arch Dermatol, 1996. **132**(7): p. 797-800.
388. Larregue, M., et al., *Olmsted syndrome: report of two new cases and literature review.* J Dermatol, 2000. **27**(9): p. 557-68.
389. Lucker, G.P. and P.M. Steijlen, *The Olmsted syndrome: mutilating palmoplantar and periorificial keratoderma.* J Am Acad Dermatol, 1994. **31**(3 Pt 1): p. 508-9.
390. Ogawa, F., et al., *Olmsted syndrome with squamous cell carcinoma of extremities and adenocarcinoma of the lung: failure to detect loricrin gene mutation.* Eur J Dermatol, 2003. **13**(6): p. 524-8.
391. Wilson, N.J., et al., *Expanding the Phenotypic Spectrum of Olmsted Syndrome.* J Invest Dermatol, 2015. **135**(11): p. 2879-83.
392. Lai-Cheong, J.E., et al., *Recurrent heterozygous missense mutation, p.Gly573Ser, in the TRPV3 gene in an Indian boy with sporadic Olmsted syndrome.* Br J Dermatol, 2012. **167**(2): p. 440-2.
393. Danso-Abeam, D., et al., *Olmsted syndrome: exploration of the immunological phenotype.* Orphanet J Rare Dis, 2013. **8**: p. 79.
394. Duchatelet, S., et al., *Olmsted syndrome with erythromelalgia caused by recessive transient receptor potential vanilloid 3 mutations.* Br J Dermatol, 2014. **171**(3): p. 675-8.
395. Duchatelet, S., et al., *A new TRPV3 missense mutation in a patient with Olmsted syndrome and erythromelalgia.* JAMA Dermatol, 2014. **150**(3): p. 303-6.
396. Eytan, O., et al., *Olmsted syndrome caused by a homozygous recessive mutation in TRPV3.* J Invest Dermatol, 2014. **134**(6): p. 1752-4.
397. Kariminejad, A., et al., *Olmsted syndrome in an Iranian boy with a new de novo mutation in TRPV3.* Clin Exp Dermatol, 2014. **39**(4): p. 492-5.
398. He, Y., et al., *A gain-of-function mutation in TRPV3 causes focal palmoplantar keratoderma in a Chinese family.* J Invest Dermatol, 2014. **135**(3): p. 907-9.
399. Konathan, R. and S.K. Alur, *Olmsted Syndrome in a Family.* Int J Trichology, 2017. **8**(4): p. 168-170.
400. Nagai, H., et al., *Identification of a heterozygous p.Gly568Val missense mutation in the TRPV3 gene in a Japanese patient with Olmsted syndrome: In silico analysis of TRPV3.* J Dermatol, 2017. **44**(9): p. 1059-1062.

349. Suginta, W., et al., *Chloride intracellular channel protein CLIC4 (p64H1) binds directly to brain dynamin I in a complex containing actin, tubulin and 14-3-3 isoforms.* Biochem J, 2001. **359**(Pt 1): p. 55-64.
350. Wray, D., *Intracellular regions of potassium channels: Kv2.1 and heag.* Eur Biophys J, 2009. **38**(3): p. 285-92.
351. Kramer, J. and R.S. Hawley, *The spindle-associated transmembrane protein Axs identifies a membranous structure ensheathing the meiotic spindle.* Nat Cell Biol, 2003. **5**(3): p. 261-3.
352. Giepmans, B.N., et al., *Gap junction protein connexin-43 interacts directly with microtubules.* Curr Biol, 2001. **11**(17): p. 1364-8.
353. Fok, P.T., et al., *The Coxsackie and adenovirus receptor binds microtubules and plays a role in cell migration.* J Biol Chem, 2007. **282**(10): p. 7512-21.
354. Monesterolo, N.E., et al., *Activation of PMCA by calmodulin or ethanol in plasma membrane vesicles from rat brain involves dissociation of the acetylated tubulin/PMCA complex.* FEBS J, 2008. **275**(14): p. 3567-79.
355. Shin, J.B., et al., *Xenopus TRPN1 (NOMPC) localizes to microtubule-based cilia in epithelial cells, including inner-ear hair cells.* Proc Natl Acad Sci U S A, 2005. **102**(35): p. 12572-7.
356. Liang, X., et al., *NOMPC, a member of the TRP channel family, localizes to the tubular body and distal cilium of Drosophila campaniform and chordotonal receptor cells.* Cytoskeleton (Hoboken), 2011. **68**(1): p. 1-7.
357. Dotti, C.G., C.A. Sullivan, and G.A. Banker, *The establishment of polarity by hippocampal neurons in culture.* J Neurosci, 1988. **8**(4): p. 1454-68.
358. Hutchins, B.I., *Competitive outgrowth of neural processes arising from long-distance cAMP signaling.* Sci Signal, 2010. **3**(118): p. jc1.
359. Dehmelt, L. and S. Halpain, *Actin and microtubules in neurite initiation: are MAPs the missing link?* J Neurobiol, 2004. **58**(1): p. 18-33.
360. Sainath, R. and G. Gallo, *Cytoskeletal and signaling mechanisms of neurite formation.* Cell Tissue Res, 2015. **359**(1): p. 267-78.
361. Kuner, R., *Central mechanisms of pathological pain.* Nat Med, 2010. **16**(11): p. 1258-66.
362. Neumann, S., et al., *Inflammatory pain hypersensitivity mediated by phenotypic switch in myelinated primary sensory neurons.* Nature, 1996. **384**(6607): p. 360-4.
363. Huang, E.J., et al., *Targeted deletion of numb and numblike in sensory neurons reveals their essential functions in axon arborization.* Genes Dev, 2005. **19**(1): p. 138-51.
364. Zappia, K.J., et al., *Sensory Neuron-Specific Deletion of TRPA1 Results in Mechanical Cutaneous Sensory Deficits.* eNeuro, 2017. **4**(1).
365. Zhou, X., et al., *Deletion of PIK3C3/Vps34 in sensory neurons causes rapid neurodegeneration by disrupting the endosomal but not the autophagic pathway.* Proc Natl Acad Sci U S A, 2010. **107**(20): p. 9424-9.
366. Bhalla, K.N., *Microtubule-targeted anticancer agents and apoptosis.* Oncogene, 2003. **22**(56): p. 9075-86.
367. Lee, J.J. and S.M. Swain, *Peripheral neuropathy induced by microtubule-stabilizing agents.* J Clin Oncol, 2006. **24**(10): p. 1633-42.
368. White, J.G. and G.H. Rao, *Effects of a microtubule stabilizing agent on the response of platelets to vincristine.* Blood, 1982. **60**(2): p. 474-83.
369. Jaggi, A.S. and N. Singh, *Mechanisms in cancer-chemotherapeutic drugs-induced peripheral neuropathy.* Toxicology, 2012. **291**(1-3): p. 1-9.
370. Grisold, W., G. Cavaletti, and A.J. Windebank, *Peripheral neuropathies from chemotherapeutics and targeted agents: diagnosis, treatment, and prevention.* Neuro Oncol, 2012. **14 Suppl 4**: p. iv45-54.
371. Mora, E., et al., *Vincristine-induced peripheral neuropathy in pediatric cancer patients.* Am J Cancer Res, 2016. **6**(11): p. 2416-2430.
372. Tamura, S., Y. Morikawa, and E. Senba, *TRPV2, a capsaicin receptor homologue, is expressed predominantly in the neurotrophin-3-dependent subpopulation of primary sensory neurons.* Neuroscience, 2005. **130**(1): p. 223-8.

324. van Rossum, D., J. Kuhse, and H. Betz, *Dynamic interaction between soluble tubulin and C-terminal domains of N-methyl-D-aspartate receptor subunits.* J Neurochem, 1999. **72**(3): p. 962-73.
325. Carre, M., et al., *Tubulin is an inherent component of mitochondrial membranes that interacts with the voltage-dependent anion channel.* J Biol Chem, 2002. **277**(37): p. 33664-9.
326. Rostovtseva, T.K. and S.M. Bezrukov, *VDAC regulation: role of cytosolic proteins and mitochondrial lipids.* J Bioenerg Biomembr, 2008. **40**(3): p. 163-70.
327. Rostovtseva, T.K., et al., *Interfacial polar interactions affect gramicidin channel kinetics.* Biophys J, 2008. **94**(4): p. L23-5.
328. Rostovtseva, T.K., et al., *Membrane lipid composition regulates tubulin interaction with mitochondrial voltage-dependent anion channel.* J Biol Chem, 2012. **287**(35): p. 29589-98.
329. Casale, C.H., A.D. Alonso, and H.S. Barra, *Brain plasma membrane Na+,K+-ATPase is inhibited by acetylated tubulin.* Mol Cell Biochem, 2001. **216**(1-2): p. 85-92.
330. Vladimirova, N.M., et al., *Interaction between tubulin and Na+,K+-ATPase in brain stem neurons.* Biochemistry (Mosc), 2002. **67**(4): p. 503-9.
331. Ciruela, F. and R.A. McIlhinney, *Metabotropic glutamate receptor type 1alpha and tubulin assemble into dynamic interacting complexes.* J Neurochem, 2001. **76**(3): p. 750-7.
332. Ciruela, F., et al., *Interactions of the C terminus of metabotropic glutamate receptor type 1alpha with rat brain proteins: evidence for a direct interaction with tubulin.* J Neurochem, 1999. **72**(1): p. 346-54.
333. Saugstad, J.A., et al., *Interaction between metabotropic glutamate receptor 7 and alpha tubulin.* J Neurochem, 2002. **80**(6): p. 980-8.
334. Popova, J.S., et al., *Tubulin, Gq, and phosphatidylinositol 4,5-bisphosphate interact to regulate phospholipase Cbeta1 signaling.* J Biol Chem, 1997. **272**(10): p. 6760-5.
335. Roychowdhury, S., et al., *G protein alpha subunits activate tubulin GTPase and modulate microtubule polymerization dynamics.* J Biol Chem, 1999. **274**(19): p. 13485-90.
336. Roychowdhury, S. and M.M. Rasenick, *G protein beta1gamma2 subunits promote microtubule assembly.* J Biol Chem, 1997. **272**(50): p. 31576-81.
337. Sarma, T., et al., *Heterotrimeric G-proteins associate with microtubules during differentiation in PC12 pheochromocytoma cells.* FASEB J, 2003. **17**(8): p. 848-59.
338. Gendreau, S., J. Schirmer, and G. Schmalzing, *Identification of a tubulin binding motif on the P2X2 receptor.* J Chromatogr B Analyt Technol Biomed Life Sci, 2003. **786**(1-2): p. 311-8.
339. Guimaraes, M.Z., *Isoform specificity of P2X2 purinergic receptor C-terminus binding to tubulin.* Neurochem Int, 2008. **52**(1-2): p. 314-20.
340. Ma, D., et al., *Differential trafficking of carboxyl isoforms of Ca2+-gated (Slo1) potassium channels.* FEBS Lett, 2007. **581**(5): p. 1000-8.
341. Chen, Z., et al., *The C-terminal polylysine region and methylation of K-Ras are critical for the interaction between K-Ras and microtubules.* J Biol Chem, 2000. **275**(52): p. 41251-7.
342. Thissen, J.A., et al., *Prenylation-dependent association of Ki-Ras with microtubules. Evidence for a role in subcellular trafficking.* J Biol Chem, 1997. **272**(48): p. 30362-70.
343. Azuma, K., et al., *Analysis of estrogen receptor alpha signaling complex at the plasma membrane.* FEBS Lett, 2004. **577**(3): p. 339-44.
344. Campetelli, A.N., et al., *Activation of the plasma membrane H-ATPase of Saccharomyces cerevisiae by glucose is mediated by dissociation of the H(+)-ATPase-acetylated tubulin complex.* FEBS J, 2005. **272**(22): p. 5742-52.
345. Haga, K., et al., *GTP-binding-protein-coupled receptor kinase 2 (GRK2) binds and phosphorylates tubulin.* Eur J Biochem, 1998. **255**(2): p. 363-8.
346. Item, C. and W. Sieghart, *Binding of gamma-aminobutyric acidA receptors to tubulin.* J Neurochem, 1994. **63**(3): p. 1119-25.
347. Offringa, R. and B.E. Bierer, *Association of CD2 with tubulin. Evidence for a role of the cytoskeleton in T cell activation.* J Biol Chem, 1993. **268**(7): p. 4979-88.
348. Grigoriev, I., et al., *STIM1 is a MT-plus-end-tracking protein involved in remodeling of the ER.* Curr Biol, 2008. **18**(3): p. 177-82.

301. Redondo, P.C., et al., *Evidence for secretion-like coupling involving pp60src in the activation and maintenance of store-mediated Ca2+ entry in mouse pancreatic acinar cells.* Biochem J, 2003. **370**(Pt 1): p. 255-63.
302. Rosado, J.A., S. Jenner, and S.O. Sage, *A role for the actin cytoskeleton in the initiation and maintenance of store-mediated calcium entry in human platelets. Evidence for conformational coupling.* J Biol Chem, 2000. **275**(11): p. 7527-33.
303. Rosado, J.A. and S.O. Sage, *Activation of store-mediated calcium entry by secretion-like coupling between the inositol 1,4,5-trisphosphate receptor type II and human transient receptor potential (hTrp1) channels in human platelets.* Biochem J, 2001. **356**(Pt 1): p. 191-8.
304. Moore, T.M., et al., *Store-operated calcium entry promotes shape change in pulmonary endothelial cells expressing Trp1.* Am J Physiol, 1998. **275**(3 Pt 1): p. L574-82.
305. Itagaki, K., et al., *Cytoskeletal reorganization internalizes multiple transient receptor potential channels and blocks calcium entry into human neutrophils.* J Immunol, 2004. **172**(1): p. 601-7.
306. Cioffi, D.L., S. Wu, and T. Stevens, *On the endothelial cell I(SOC).* Cell Calcium, 2003. **33**(5-6): p. 323-36.
307. Tang, Y., et al., *Association of mammalian trp4 and phospholipase C isozymes with a PDZ domain-containing protein, NHERF.* J Biol Chem, 2000. **275**(48): p. 37559-64.
308. Ambudkar, I.S. and H.L. Ong, *Organization and function of TRPC channelosomes.* Pflugers Arch, 2007. **455**(2): p. 187-200.
309. Huber, A., et al., *The transient receptor potential protein (Trp), a putative store-operated Ca2+ channel essential for phosphoinositide-mediated photoreception, forms a signaling complex with NorpA, InaC and InaD.* EMBO J, 1996. **15**(24): p. 7036-45.
310. Li, H.S. and C. Montell, *TRP and the PDZ protein, INAD, form the core complex required for retention of the signalplex in Drosophila photoreceptor cells.* J Cell Biol, 2000. **150**(6): p. 1411-22.
311. Meng, X. and J.A. Wilkins, *Compositional characterization of the cytoskeleton of NK-like cells.* J Proteome Res, 2005. **4**(6): p. 2081-7.
312. Nebl, T., et al., *Proteomic analysis of a detergent-resistant membrane skeleton from neutrophil plasma membranes.* J Biol Chem, 2002. **277**(45): p. 43399-409.
313. Sanxaridis, P.D., et al., *Light-induced recruitment of INAD-signaling complexes to detergent-resistant lipid rafts in Drosophila photoreceptors.* Mol Cell Neurosci, 2007. **36**(1): p. 36-46.
314. Shieh, B.H. and M.Y. Zhu, *Regulation of the TRP Ca2+ channel by INAD in Drosophila photoreceptors.* Neuron, 1996. **16**(5): p. 991-8.
315. Voltz, J.W., E.J. Weinman, and S. Shenolikar, *Expanding the role of NHERF, a PDZ-domain containing protein adapter, to growth regulation.* Oncogene, 2001. **20**(44): p. 6309-14.
316. Goswami, C., *Structural and functional regulation of growth cone, filopodia and synaptic sites by TRPV1.* Commun Integr Biol, 2011. **3**(6): p. 614-8.
317. Foster, L.J., C.L. De Hoog, and M. Mann, *Unbiased quantitative proteomics of lipid rafts reveals high specificity for signaling factors.* Proc Natl Acad Sci U S A, 2003. **100**(10): p. 5813-8.
318. Ishmael, J.E., et al., *Nonmuscle myosins II-B and Va are components of detergent-resistant membrane skeletons derived from mouse forebrain.* Brain Res, 2007. **1143**: p. 46-59.
319. Lee, N., et al., *Expression and characterization of human transient receptor potential melastatin 3 (hTRPM3).* J Biol Chem, 2003. **278**(23): p. 20890-7.
320. Goswami, C., *TRPV1-tubulin complex: involvement of membrane tubulin in the regulation of chemotherapy-induced peripheral neuropathy.* J Neurochem, 2012. **123**(1): p. 1-13.
321. Li, Q., et al., *Polycystin-2 cation channel function is under the control of microtubular structures in primary cilia of renal epithelial cells.* J Biol Chem, 2006. **281**(49): p. 37566-75.
322. Montalbetti, N., et al., *Polycystin-2 cation channel function in the human syncytiotrophoblast is regulated by microtubular structures.* J Physiol, 2007. **579**(Pt 3): p. 717-28.
323. Huai, J., et al., *Interaction of transient receptor potential vanilloid 4 with annexin A2 and tubulin beta 5.* Neurosci Lett, 2012. **512**(1): p. 22-7.

278. Sugio, S., et al., *Transient receptor potential vanilloid 2 activation by focal mechanical stimulation requires interaction with the actin cytoskeleton and enhances growth cone motility.* FASEB J, 2017. **31**(4): p. 1368-1381.
279. Park, K.S., et al., *Identification and functional characterization of ion channels in CD34(+) hematopoietic stem cells from human peripheral blood.* Mol Cells, 2011. **32**(2): p. 181-8.
280. Ahluwalia, J., H. Rang, and I. Nagy, *The putative role of vanilloid receptor-like protein-1 in mediating high threshold noxious heat-sensitivity in rat cultured primary sensory neurons.* Eur J Neurosci, 2002. **16**(8): p. 1483-9.
281. Ichikawa, H. and T. Sugimoto, *Vanilloid receptor 1-like receptor-immunoreactive primary sensory neurons in the rat trigeminal nervous system.* Neuroscience, 2000. **101**(3): p. 719-25.
282. Cahoy, J.D., et al., *A transcriptome database for astrocytes, neurons, and oligodendrocytes: a new resource for understanding brain development and function.* J Neurosci, 2008. **28**(1): p. 264-78.
283. Alessandri-Haber, N., et al., *Transient receptor potential vanilloid 4 is essential in chemotherapy-induced neuropathic pain in the rat.* J Neurosci, 2004. **24**(18): p. 4444-52.
284. Dina, O.A., et al., *Role of the sensory neuron cytoskeleton in second messenger signaling for inflammatory pain.* Neuron, 2003. **39**(4): p. 613-24.
285. Tanner, K.D., J.D. Levine, and K.S. Topp, *Microtubule disorientation and axonal swelling in unmyelinated sensory axons during vincristine-induced painful neuropathy in rat.* J Comp Neurol, 1998. **395**(4): p. 481-92.
286. Topp, K.S., K.D. Tanner, and J.D. Levine, *Damage to the cytoskeleton of large diameter sensory neurons and myelinated axons in vincristine-induced painful peripheral neuropathy in the rat.* J Comp Neurol, 2000. **424**(4): p. 563-76.
287. Entin-Meer, M., et al., *The transient receptor potential vanilloid 2 cation channel is abundant in macrophages accumulating at the peri-infarct zone and may enhance their migration capacity towards injured cardiomyocytes following myocardial infarction.* PLoS One, 2014. **9**(8): p. e105055.
288. Hassan, S., et al., *Cannabidiol enhances microglial phagocytosis via transient receptor potential (TRP) channel activation.* Br J Pharmacol, 2014. **171**(9): p. 2426-39.
289. Santoni, G., et al., *The role of transient receptor potential vanilloid type-2 ion channels in innate and adaptive immune responses.* Front Immunol, 2013. **4**: p. 34.
290. Caprodossi, S., et al., *Transient receptor potential vanilloid type 2 (TRPV2) expression in normal urothelium and in urothelial carcinoma of human bladder: correlation with the pathologic stage.* Eur Urol, 2008. **54**(3): p. 612-20.
291. Liu, G., et al., *Clinical significance of transient receptor potential vanilloid 2 expression in human hepatocellular carcinoma.* Cancer Genet Cytogenet, 2010. **197**(1): p. 54-9.
292. Vriens, J., et al., *TRPV channels and modulation by hepatocyte growth factor/scatter factor in human hepatoblastoma (HepG2) cells.* Cell Calcium, 2004. **36**(1): p. 19-28.
293. Monet, M., et al., *Role of cationic channel TRPV2 in promoting prostate cancer migration and progression to androgen resistance.* Cancer Res, 2010. **70**(3): p. 1225-35.
294. Yamada, T., et al., *TRPV2 activation induces apoptotic cell death in human T24 bladder cancer cells: a potential therapeutic target for bladder cancer.* Urology, 2010. **76**(2): p. 509 e1-7.
295. Janke, C., *The tubulin code: molecular components, readout mechanisms, and functions.* J Cell Biol, 2014. **206**(4): p. 461-72.
296. Verhey, K.J. and J. Gaertig, *The tubulin code.* Cell Cycle, 2007. **6**(17): p. 2152-60.
297. Wehenkel, A. and C. Janke, *Towards elucidating the tubulin code.* Nat Cell Biol, 2014. **16**(4): p. 303-5.
298. Yu, I., C.P. Garnham, and A. Roll-Mecak, *Writing and Reading the Tubulin Code.* J Biol Chem, 2015. **290**(28): p. 17163-72.
299. Nedungadi, T.P., et al., *Expression and distribution of TRPV2 in rat brain.* Exp Neurol, 2012. **237**(1): p. 223-37.
300. Redondo, P.C., et al., *A role for cofilin in the activation of store-operated calcium entry by de novo conformational coupling in human platelets.* Blood, 2006. **107**(3): p. 973-9.

253. Deng, H.X., et al., *Scapuloperoneal spinal muscular atrophy and CMT2C are allelic disorders caused by alterations in TRPV4.* Nat Genet, 2010. **42**(2): p. 165-9.
254. Landoure, G., et al., *Mutations in TRPV4 cause Charcot-Marie-Tooth disease type 2C.* Nat Genet, 2010. **42**(2): p. 170-4.
255. Katanosaka, Y., et al., *TRPV2 is critical for the maintenance of cardiac structure and function in mice.* Nat Commun, 2014. **5**: p. 3932.
256. Mandadi, S., et al., *TRPV3 in keratinocytes transmits temperature information to sensory neurons via ATP.* Pflugers Arch, 2009. **458**(6): p. 1093-102.
257. Huang, S.M., et al., *TRPV3 and TRPV4 ion channels are not major contributors to mouse heat sensation.* Mol Pain, 2011. **7**: p. 37.
258. da Silva, J.S. and C.G. Dotti, *Breaking the neuronal sphere: regulation of the actin cytoskeleton in neuritogenesis.* Nat Rev Neurosci, 2002. **3**(9): p. 694-704.
259. Dent, E.W. and F.B. Gertler, *Cytoskeletal dynamics and transport in growth cone motility and axon guidance.* Neuron, 2003. **40**(2): p. 209-27.
260. Feng, Y. and C.A. Walsh, *Protein-protein interactions, cytoskeletal regulation and neuronal migration.* Nat Rev Neurosci, 2001. **2**(6): p. 408-16.
261. Lambert de Rouvroit, C. and A.M. Goffinet, *Neuronal migration.* Mech Dev, 2001. **105**(1-2): p. 47-56.
262. Bamburg, J.R. and G.S. Bloom, *Cytoskeletal pathologies of Alzheimer disease.* Cell Motil Cytoskeleton, 2009. **66**(8): p. 635-49.
263. McMurray, C.T., *Neurodegeneration: diseases of the cytoskeleton?* Cell Death Differ, 2000. **7**(10): p. 861-5.
264. Pawson, T. and J.D. Scott, *Signaling through scaffold, anchoring, and adaptor proteins.* Science, 1997. **278**(5346): p. 2075-80.
265. Peterson, B.Z., et al., *Calmodulin is the Ca2+ sensor for Ca2+ -dependent inactivation of L-type calcium channels.* Neuron, 1999. **22**(3): p. 549-58.
266. Goswami, C., H. Schmidt, and F. Hucho, *TRPV1 at nerve endings regulates growth cone morphology and movement through cytoskeleton reorganization.* FEBS J, 2007. **274**(3): p. 760-72.
267. Li, Y., et al., *Essential role of TRPC channels in the guidance of nerve growth cones by brain-derived neurotrophic factor.* Nature, 2005. **434**(7035): p. 894-8.
268. Wang, J., et al., *Acute hypoxia increases intracellular [Ca2+] in pulmonary arterial smooth muscle by enhancing capacitative Ca2+ entry.* Am J Physiol Lung Cell Mol Physiol, 2005. **288**(6): p. L1059-69.
269. Goswami, C. and T. Hucho, *TRPV1 expression-dependent initiation and regulation of filopodia.* J Neurochem, 2007. **103**(4): p. 1319-33.
270. Brunton, V.G., I.R. MacPherson, and M.C. Frame, *Cell adhesion receptors, tyrosine kinases and actin modulators: a complex three-way circuitry.* Biochim Biophys Acta, 2004. **1692**(2-3): p. 121-44.
271. Mitra, S.K., D.A. Hanson, and D.D. Schlaepfer, *Focal adhesion kinase: in command and control of cell motility.* Nat Rev Mol Cell Biol, 2005. **6**(1): p. 56-68.
272. Yadav, M. and C. Goswami, *TRPV3 mutants causing Olmsted Syndrome induce impaired cell adhesion and nonfunctional lysosomes.* Channels (Austin), 2016. **11**(3): p. 196-208.
273. Cao, E., et al., *TRPV1 structures in distinct conformations reveal activation mechanisms.* Nature, 2013. **504**(7478): p. 113-8.
274. Wickstead, B. and K. Gull, *The evolution of the cytoskeleton.* J Cell Biol, 2011. **194**(4): p. 513-25.
275. Clark, K., J. Middelbeek, and F.N. van Leeuwen, *Interplay between TRP channels and the cytoskeleton in health and disease.* Eur J Cell Biol, 2008. **87**(8-9): p. 631-40.
276. Han, P., et al., *Capsaicin causes protein synthesis inhibition and microtubule disassembly through TRPV1 activities both on the plasma membrane and intracellular membranes.* Biochem Pharmacol, 2007. **73**(10): p. 1635-45.
277. Li, Q., et al., *Direct binding of alpha-actinin enhances TRPP3 channel activity.* J Neurochem, 2007. **103**(6): p. 2391-400.

227. Denda, M., et al., *Effects of skin surface temperature on epidermal permeability barrier homeostasis.* J Invest Dermatol, 2007. **127**(3): p. 654-9.
228. Mandadi, S., et al., *Increased sensitivity of desensitized TRPV1 by PMA occurs through PKCepsilon-mediated phosphorylation at S800.* Pain, 2006. **123**(1-2): p. 106-16.
229. Gaudet, R., *TRP channels entering the structural era.* J Physiol, 2008. **586**(15): p. 3565-75.
230. Owsianik, G., et al., *Structure-function relationship of the TRP channel superfamily.* Rev Physiol Biochem Pharmacol, 2006. **156**: p. 61-90.
231. Peralvarez-Marin, A., P. Donate-Macian, and R. Gaudet, *What do we know about the transient receptor potential vanilloid 2 (TRPV2) ion channel?* FEBS J, 2013. **280**(21): p. 5471-87.
232. Erler, I., et al., *Trafficking and assembly of the cold-sensitive TRPM8 channel.* J Biol Chem, 2006. **281**(50): p. 38396-404.
233. Lishko, P.V., et al., *The ankyrin repeats of TRPV1 bind multiple ligands and modulate channel sensitivity.* Neuron, 2007. **54**(6): p. 905-18.
234. Phelps, C.B., et al., *Insights into the roles of conserved and divergent residues in the ankyrin repeats of TRPV ion channels.* Channels (Austin), 2007. **1**(3): p. 148-51.
235. Fuchs, E. and S. Raghavan, *Getting under the skin of epidermal morphogenesis.* Nat Rev Genet, 2002. **3**(3): p. 199-209.
236. Zhang, X., L. Li, and P.A. McNaughton, *Proinflammatory mediators modulate the heat-activated ion channel TRPV1 via the scaffolding protein AKAP79/150.* Neuron, 2008. **59**(3): p. 450-61.
237. Ma, X., et al., *Electrophysiological properties of heteromeric TRPV4-C1 channels.* Biochim Biophys Acta, 2011. **1808**(12): p. 2789-97.
238. Shibasaki, K., et al., *TRPV2 enhances axon outgrowth through its activation by membrane stretch in developing sensory and motor neurons.* J Neurosci, 2010. **30**(13): p. 4601-12.
239. Link, T.M., et al., *TRPV2 has a pivotal role in macrophage particle binding and phagocytosis.* Nat Immunol, 2010. **11**(3): p. 232-9.
240. Iwata, Y., et al., *A novel mechanism of myocyte degeneration involving the Ca2+-permeable growth factor-regulated channel.* J Cell Biol, 2003. **161**(5): p. 957-67.
241. Yoshioka, T., et al., *Impact of the Gly573Ser substitution in TRPV3 on the development of allergic and pruritic dermatitis in mice.* J Invest Dermatol, 2009. **129**(3): p. 714-22.
242. Kottgen, M., et al., *TRPP2 and TRPV4 form a polymodal sensory channel complex.* J Cell Biol, 2008. **182**(3): p. 437-47.
243. Lin, Z., et al., *Exome sequencing reveals mutations in TRPV3 as a cause of Olmsted syndrome.* Am J Hum Genet, 2012. **90**(3): p. 558-64.
244. Li, C., et al., *Sorting Nexin 11 Regulates Lysosomal Degradation of Plasma Membrane TRPV3.* Traffic, 2016. **17**(5): p. 500-14.
245. Qin, N., et al., *TRPV2 is activated by cannabidiol and mediates CGRP release in cultured rat dorsal root ganglion neurons.* J Neurosci, 2008. **28**(24): p. 6231-8.
246. Neeper, M.P., et al., *Activation properties of heterologously expressed mammalian TRPV2: evidence for species dependence.* J Biol Chem, 2007. **282**(21): p. 15894-902.
247. Chung, M.K., et al., *2-aminoethoxydiphenyl borate activates and sensitizes the heat-gated ion channel TRPV3.* J Neurosci, 2004. **24**(22): p. 5177-82.
248. Vennekens, R., G. Owsianik, and B. Nilius, *Vanilloid transient receptor potential cation channels: an overview.* Curr Pharm Des, 2008. **14**(1): p. 18-31.
249. Vogt-Eisele, A.K., et al., *Monoterpenoid agonists of TRPV3.* Br J Pharmacol, 2007. **151**(4): p. 530-40.
250. Vriens, J., G. Appendino, and B. Nilius, *Pharmacology of vanilloid transient receptor potential cation channels.* Mol Pharmacol, 2009. **75**(6): p. 1262-79.
251. Yamamoto, Y. and K. Taniguchi, *Immunolocalization of VR1 and VRL1 in rat larynx.* Auton Neurosci, 2005. **117**(1): p. 62-5.
252. Watanabe, A., et al., *Role of the Nh (Non-hair) mutation in the development of dermatitis and hyperproduction of IgE in DS-Nh mice.* Exp Anim, 2003. **52**(5): p. 419-23.

203. Smani, T., et al., *Cytoskeletal and scaffolding proteins as structural and functional determinants of TRP channels.* Biochim Biophys Acta, 2014. **1838**(2): p. 658-64.
204. Martinac, B., *The ion channels to cytoskeleton connection as potential mechanism of mechanosensitivity.* Biochim Biophys Acta, 2014. **1838**(2): p. 682-91.
205. Liman, E.R., *TRPM5 and taste transduction.* Handb Exp Pharmacol, 2007(179): p. 287-98.
206. Shen, Y., et al., *A transient receptor potential-like channel mediates synaptic transmission in rod bipolar cells.* J Neurosci, 2009. **29**(19): p. 6088-93.
207. Lange, M., et al., *The Transient Receptor Potential (TRP) Channel Family in Colletotrichum graminicola: A Molecular and Physiological Analysis.* PLoS One, 2016. **11**(6): p. e0158561.
208. Myers, B.R., C.J. Bohlen, and D. Julius, *A yeast genetic screen reveals a critical role for the pore helix domain in TRP channel gating.* Neuron, 2008. **58**(3): p. 362-73.
209. Tsuruda, P.R., D. Julius, and D.L. Minor, Jr., *Coiled coils direct assembly of a cold-activated TRP channel.* Neuron, 2006. **51**(2): p. 201-12.
210. Saito, S., et al., *Evolution of vertebrate transient receptor potential vanilloid 3 channels: opposite temperature sensitivity between mammals and western clawed frogs.* PLoS Genet, 2011. **7**(4): p. e1002041.
211. Saito, S., et al., *Analysis of transient receptor potential ankyrin 1 (TRPA1) in frogs and lizards illuminates both nociceptive heat and chemical sensitivities and coexpression with TRP vanilloid 1 (TRPV1) in ancestral vertebrates.* J Biol Chem, 2012. **287**(36): p. 30743-54.
212. Gavva, N.R., et al., *Molecular determinants of vanilloid sensitivity in TRPV1.* J Biol Chem, 2004. **279**(19): p. 20283-95.
213. Tewksbury, J.J. and G.P. Nabhan, *Seed dispersal. Directed deterrence by capsaicin in chilies.* Nature, 2001. **412**(6845): p. 403-4.
214. Siemens, J., et al., *Spider toxins activate the capsaicin receptor to produce inflammatory pain.* Nature, 2006. **444**(7116): p. 208-12.
215. Caterina, M.J. and D. Julius, *The vanilloid receptor: a molecular gateway to the pain pathway.* Annu Rev Neurosci, 2001. **24**: p. 487-517.
216. Tominaga, M. and D. Julius, *Capsaicin receptor in the pain pathway.* Jpn J Pharmacol, 2000. **83**(1): p. 20-4.
217. Caterina, M.J., et al., *A capsaicin-receptor homologue with a high threshold for noxious heat.* Nature, 1999. **398**(6726): p. 436-41.
218. Bang, S., et al., *Transient receptor potential V2 expressed in sensory neurons is activated by probenecid.* Neurosci Lett, 2007. **425**(2): p. 120-5.
219. De Petrocellis, L., et al., *Effects of cannabinoids and cannabinoid-enriched Cannabis extracts on TRP channels and endocannabinoid metabolic enzymes.* Br J Pharmacol, 2011. **163**(7): p. 1479-94.
220. Hu, H.Z., et al., *2-aminoethoxydiphenyl borate is a common activator of TRPV1, TRPV2, and TRPV3.* J Biol Chem, 2004. **279**(34): p. 35741-8.
221. Juvin, V., et al., *Pharmacological characterization and molecular determinants of the activation of transient receptor potential V2 channel orthologs by 2-aminoethoxydiphenyl borate.* Mol Pharmacol, 2007. **72**(5): p. 1258-68.
222. Monet, M., et al., *Lysophospholipids stimulate prostate cancer cell migration via TRPV2 channel activation.* Biochim Biophys Acta, 2009. **1793**(3): p. 528-39.
223. Nie, L., et al., *Inhibition of proliferation of MCF-7 breast cancer cells by a blocker of Ca(2+)-permeable channel.* Cell Calcium, 1997. **22**(2): p. 75-82.
224. Bang, S., et al., *Isopentenyl pyrophosphate is a novel antinociceptive substance that inhibits TRPV3 and TRPA1 ion channels.* Pain, 2011. **152**(5): p. 1156-64.
225. Cao, X., et al., *Intracellular proton-mediated activation of TRPV3 channels accounts for the exfoliation effect of alpha-hydroxyl acids on keratinocytes.* J Biol Chem, 2012. **287**(31): p. 25905-16.
226. Doerner, J.F., H. Hatt, and I.S. Ramsey, *Voltage- and temperature-dependent activation of TRPV3 channels is potentiated by receptor-mediated PI(4,5)P2 hydrolysis.* J Gen Physiol, 2011. **137**(3): p. 271-88.

177. Nilius, B., et al., *Regulation of the Ca2+ sensitivity of the nonselective cation channel TRPM4.* J Biol Chem, 2005. **280**(8): p. 6423-33.
178. Okada, T., et al., *Molecular and functional characterization of a novel mouse transient receptor potential protein homologue TRP7. Ca(2+)-permeable cation channel that is constitutively activated and enhanced by stimulation of G protein-coupled receptor.* J Biol Chem, 1999. **274**(39): p. 27359-70.
179. Premkumar, L.S. and G.P. Ahern, *Induction of vanilloid receptor channel activity by protein kinase C.* Nature, 2000. **408**(6815): p. 985-90.
180. Venkatachalam, K., F. Zheng, and D.L. Gill, *Regulation of canonical transient receptor potential (TRPC) channel function by diacylglycerol and protein kinase C.* J Biol Chem, 2003. **278**(31): p. 29031-40.
181. Zhang, L. and D. Saffen, *Muscarinic acetylcholine receptor regulation of TRP6 Ca2+ channel isoforms. Molecular structures and functional characterization.* J Biol Chem, 2001. **276**(16): p. 13331-9.
182. Foster, M.W., D.T. Hess, and J.S. Stamler, *S-nitrosylation TRiPs a calcium switch.* Nat Chem Biol, 2006. **2**(11): p. 570-1.
183. Takahashi, N., D. Kozai, and Y. Mori, *TRP channels: sensors and transducers of gasotransmitter signals.* Front Physiol, 2012. **3**: p. 324.
184. Yoshida, T., et al., *Nitric oxide activates TRP channels by cysteine S-nitrosylation.* Nat Chem Biol, 2006. **2**(11): p. 596-607.
185. Wirkner, K., et al., *Characterization of rat transient receptor potential vanilloid 1 receptors lacking the N-glycosylation site N604.* Neuroreport, 2005. **16**(9): p. 997-1001.
186. Clapham, D.E., *Calcium signaling.* Cell, 1995. **80**(2): p. 259-68.
187. Minke, B. and B. Cook, *TRP channel proteins and signal transduction.* Physiol Rev, 2002. **82**(2): p. 429-72.
188. Minke, B. and M. Parnas, *Insights on TRP channels from in vivo studies in Drosophila.* Annu Rev Physiol, 2006. **68**: p. 649-84.
189. Montell, C., *Drosophila TRP channels.* Pflugers Arch, 2005. **451**(1): p. 19-28.
190. Spassova, M.A., et al., *Calcium entry mediated by SOCs and TRP channels: variations and enigma.* Biochim Biophys Acta, 2004. **1742**(1-3): p. 9-20.
191. Montell, C., *Visual transduction in Drosophila.* Annu Rev Cell Dev Biol, 1999. **15**: p. 231-68.
192. Rohacs, T., B. Thyagarajan, and V. Lukacs, *Phospholipase C mediated modulation of TRPV1 channels.* Mol Neurobiol, 2008. **37**(2-3): p. 153-63.
193. Runnels, L.W., L. Yue, and D.E. Clapham, *The TRPM7 channel is inactivated by PIP(2) hydrolysis.* Nat Cell Biol, 2002. **4**(5): p. 329-36.
194. Ufret-Vincenty, C.A., et al., *Localization of the PIP2 sensor of TRPV1 ion channels.* J Biol Chem, 2011. **286**(11): p. 9688-98.
195. Goswami, C. and T. Hucho, *Submembraneous microtubule cytoskeleton: biochemical and functional interplay of TRP channels with the cytoskeleton.* FEBS J, 2008. **275**(19): p. 4684-99.
196. Goswami, C., et al., *Identification and characterization of a Ca2+ -sensitive interaction of the vanilloid receptor TRPV1 with tubulin.* J Neurochem, 2004. **91**(5): p. 1092-103.
197. Goswami, C., et al., *Rapid disassembly of dynamic microtubules upon activation of the capsaicin receptor TRPV1.* J Neurochem, 2006. **96**(1): p. 254-66.
198. Storti, B., et al., *Intact microtubules preserve transient receptor potential vanilloid 1 (TRPV1) functionality through receptor binding.* J Biol Chem, 2012. **287**(10): p. 7803-11.
199. Goswami, C., et al., *Importance of non-selective cation channel TRPV4 interaction with cytoskeleton and their reciprocal regulations in cultured cells.* PLoS One, 2010. **5**(7): p. e11654.
200. Bollimuntha, S., E. Cornatzer, and B.B. Singh, *Plasma membrane localization and function of TRPC1 is dependent on its interaction with beta-tubulin in retinal epithelium cells.* Vis Neurosci, 2005. **22**(2): p. 163-70.
201. Bollimuntha, S., et al., *TRPC1-mediated inhibition of 1-methyl-4-phenylpyridinium ion neurotoxicity in human SH-SY5Y neuroblastoma cells.* J Biol Chem, 2005. **280**(3): p. 2132-40.
202. Goel, M., et al., *Proteomic analysis of TRPC5- and TRPC6-binding partners reveals interaction with the plasmalemmal Na(+)/K(+)-ATPase.* Pflugers Arch, 2005. **451**(1): p. 87-98.

152. Sardar, P., et al., *Conservation of tubulin-binding sequences in TRPV1 throughout evolution.* PLoS One, 2012. **7**(4): p. e31448.
153. De Petrocellis, L. and V. Di Marzo, *Lipids as regulators of the activity of transient receptor potential type V1 (TRPV1) channels.* Life Sci, 2005. **77**(14): p. 1651-66.
154. Rohacs, T., *Phosphoinositide regulation of TRP channels.* Handb Exp Pharmacol, 2014. **223**: p. 1143-76.
155. Trebak, M., et al., *The TRPC3/6/7 subfamily of cation channels.* Cell Calcium, 2003. **33**(5-6): p. 451-61.
156. Zitt, C., et al., *Expression of TRPC3 in Chinese hamster ovary cells results in calcium-activated cation currents not related to store depletion.* J Cell Biol, 1997. **138**(6): p. 1333-41.
157. Jansson, E.T., et al., *Effect of cholesterol depletion on the pore dilation of TRPV1.* Mol Pain, 2013. **9**: p. 1.
158. Klein, A.H., et al., *Eugenol and carvacrol excite first- and second-order trigeminal neurons and enhance their heat-evoked responses.* Neuroscience, 2014. **271**: p. 45-55.
159. Klein, A.S., A. Tannert, and M. Schaefer, *Cholesterol sensitises the transient receptor potential channel TRPV3 to lower temperatures and activator concentrations.* Cell Calcium, 2014. **55**(1): p. 59-68.
160. Hofmann, T., et al., *TRPM5 is a voltage-modulated and Ca(2+)-activated monovalent selective cation channel.* Curr Biol, 2003. **13**(13): p. 1153-8.
161. Launay, P., et al., *TRPM4 is a Ca2+-activated nonselective cation channel mediating cell membrane depolarization.* Cell, 2002. **109**(3): p. 397-407.
162. Goswami, C. and L. Goswami, *Filamentous microtubules in the neuronal spinous process and the role of microtubule regulatory drugs in neuropathic pain.* Neurochem Int, 2010. **57**(5): p. 497-503.
163. Nishiyama, M., et al., *Cyclic AMP/GMP-dependent modulation of Ca2+ channels sets the polarity of nerve growth-cone turning.* Nature, 2003. **423**(6943): p. 990-5.
164. Phelps, C.B., et al., *Differential regulation of TRPV1, TRPV3, and TRPV4 sensitivity through a conserved binding site on the ankyrin repeat domain.* J Biol Chem, 2010. **285**(1): p. 731-40.
165. Holakovska, B., et al., *Characterization of calmodulin binding domains in TRPV2 and TRPV5 C-tails.* Amino Acids, 2011. **40**(2): p. 741-8.
166. Jeske, N.A., et al., *A-kinase anchoring protein mediates TRPV1 thermal hyperalgesia through PKA phosphorylation of TRPV1.* Pain, 2008. **138**(3): p. 604-16.
167. Numazaki, M., et al., *Direct phosphorylation of capsaicin receptor VR1 by protein kinase Cepsilon and identification of two target serine residues.* J Biol Chem, 2002. **277**(16): p. 13375-8.
168. Bhave, G., et al., *cAMP-dependent protein kinase regulates desensitization of the capsaicin receptor (VR1) by direct phosphorylation.* Neuron, 2002. **35**(4): p. 721-31.
169. Li, L., R. Hasan, and X. Zhang, *The basal thermal sensitivity of the TRPV1 ion channel is determined by PKCbetaII.* J Neurosci, 2014. **34**(24): p. 8246-58.
170. Stokes, A.J., et al., *A TRPV2-PKA signaling module for transduction of physical stimuli in mast cells.* J Exp Med, 2004. **200**(2): p. 137-47.
171. Cohen, M.R., et al., *Nerve Growth Factor Regulates Transient Receptor Potential Vanilloid 2 via Extracellular Signal-Regulated Kinase Signaling To Enhance Neurite Outgrowth in Developing Neurons.* Mol Cell Biol, 2015. **35**(24): p. 4238-52.
172. Bhave, G., et al., *Protein kinase C phosphorylation sensitizes but does not activate the capsaicin receptor transient receptor potential vanilloid 1 (TRPV1).* Proc Natl Acad Sci U S A, 2003. **100**(21): p. 12480-5.
173. Por, E.D., et al., *PP2B/calcineurin-mediated desensitization of TRPV1 does not require AKAP150.* Biochem J, 2010. **432**(3): p. 549-56.
174. Zhang, D., et al., *Mast-cell degranulation induced by physical stimuli involves the activation of transient-receptor-potential channel TRPV2.* Physiol Res, 2012. **61**(1): p. 113-24.
175. Fan, H.C., X. Zhang, and P.A. McNaughton, *Activation of the TRPV4 ion channel is enhanced by phosphorylation.* J Biol Chem, 2009. **284**(41): p. 27884-91.
176. Thoppil, R.J., et al., *TRPV4 channels regulate tumor angiogenesis via modulation of Rho/Rho kinase pathway.* Oncotarget, 2016. **7**(18): p. 25849-61.

128. Krakow, D., et al., *Mutations in the gene encoding the calcium-permeable ion channel TRPV4 produce spondylometaphyseal dysplasia, Kozlowski type and metatropic dysplasia.* Am J Hum Genet, 2009. **84**(3): p. 307-15.
129. Rock, M.J., et al., *Gain-of-function mutations in TRPV4 cause autosomal dominant brachyolmia.* Nat Genet, 2008. **40**(8): p. 999-1003.
130. Nilius, B. and G. Owsianik, *Channelopathies converge on TRPV4.* Nat Genet, 2010. **42**(2): p. 98-100.
131. Dong, X.P., X. Wang, and H. Xu, *TRP channels of intracellular membranes.* J Neurochem, 2010. **113**(2): p. 313-28.
132. Morenilla-Palao, C., et al., *Regulated exocytosis contributes to protein kinase C potentiation of vanilloid receptor activity.* J Biol Chem, 2004. **279**(24): p. 25665-72.
133. Goel, M., W.G. Sinkins, and W.P. Schilling, *Selective association of TRPC channel subunits in rat brain synaptosomes.* J Biol Chem, 2002. **277**(50): p. 48303-10.
134. Goswami, C., et al., *TRPV1 acts as a synaptic protein and regulates vesicle recycling.* J Cell Sci, 2010. **123**(Pt 12): p. 2045-57.
135. Venkatachalam, K., C.O. Wong, and M.X. Zhu, *The role of TRPMLs in endolysosomal trafficking and function.* Cell Calcium, 2015. **58**(1): p. 48-56.
136. Jordt, S.E. and D. Julius, *Molecular basis for species-specific sensitivity to "hot" chili peppers.* Cell, 2002. **108**(3): p. 421-30.
137. Liedtke, W. and J.M. Friedman, *Abnormal osmotic regulation in trpv4-/- mice.* Proc Natl Acad Sci U S A, 2003. **100**(23): p. 13698-703.
138. Chuang, H.H., et al., *Bradykinin and nerve growth factor release the capsaicin receptor from PtdIns(4,5)P2-mediated inhibition.* Nature, 2001. **411**(6840): p. 957-62.
139. Huang, S.M., et al., *An endogenous capsaicin-like substance with high potency at recombinant and native vanilloid VR1 receptors.* Proc Natl Acad Sci U S A, 2002. **99**(12): p. 8400-5.
140. Bang, S., et al., *Farnesyl pyrophosphate is a novel pain-producing molecule via specific activation of TRPV3.* J Biol Chem, 2010. **285**(25): p. 19362-71.
141. Colton, C.K. and M.X. Zhu, *2-Aminoethoxydiphenyl borate as a common activator of TRPV1, TRPV2, and TRPV3 channels.* Handb Exp Pharmacol, 2007(179): p. 173-87.
142. Gao, L., et al., *Selective potentiation of 2-APB-induced activation of TRPV1-3 channels by acid.* Sci Rep, 2016. **6**: p. 20791.
143. Bang, S., et al., *17(R)-resolvin D1 specifically inhibits transient receptor potential ion channel vanilloid 3 leading to peripheral antinociception.* Br J Pharmacol, 2012. **165**(3): p. 683-92.
144. Chung, M.K., A.D. Guler, and M.J. Caterina, *Biphasic currents evoked by chemical or thermal activation of the heat-gated ion channel, TRPV3.* J Biol Chem, 2005. **280**(16): p. 15928-41.
145. Watanabe, H., et al., *Activation of TRPV4 channels (hVRL-2/mTRP12) by phorbol derivatives.* J Biol Chem, 2002. **277**(16): p. 13569-77.
146. Vincent, F., et al., *Identification and characterization of novel TRPV4 modulators.* Biochem Biophys Res Commun, 2009. **389**(3): p. 490-4.
147. Parnas, M., et al., *Membrane lipid modulations remove divalent open channel block from TRP-like and NMDA channels.* J Neurosci, 2009. **29**(8): p. 2371-83.
148. Parnas, M., M. Peters, and B. Minke, *Linoleic acid inhibits TRP channels with intrinsic voltage sensitivity: Implications on the mechanism of linoleic acid action.* Channels (Austin), 2009. **3**(3): p. 164-6.
149. Goswami, C. and M.S. Islam, *Transient Receptor Potential channels: What's happening? Reflections in the wake of the 2009 TRP Meeting, Karolinska Institutet, Stockholm.* Channels (Austin), 2010. **4**(2): p. 124-35.
150. Stotz, S.C., et al., *Citral sensing by Transient [corrected] receptor potential channels in dorsal root ganglion neurons.* PLoS One, 2008. **3**(5): p. e2082.
151. Majhi, R.K., et al., *Expression of temperature-sensitive ion channel TRPM8 in sperm cells correlates with vertebrate evolution.* PeerJ, 2015. **3**: p. e1310.

103. Vaca, L. and A. Sampieri, *Calmodulin modulates the delay period between release of calcium from internal stores and activation of calcium influx via endogenous TRP1 channels.* J Biol Chem, 2002. **277**(44): p. 42178-87.
104. Cui, J., et al., *CaT1 contributes to the stores-operated calcium current in Jurkat T-lymphocytes.* J Biol Chem, 2002. **277**(49): p. 47175-83.
105. Voets, T., et al., *CaT1 and the calcium release-activated calcium channel manifest distinct pore properties.* J Biol Chem, 2001. **276**(51): p. 47767-70.
106. Yue, L., et al., *CaT1 manifests the pore properties of the calcium-release-activated calcium channel.* Nature, 2001. **410**(6829): p. 705-9.
107. Cheng, X., et al., *TRP channel regulates EGFR signaling in hair morphogenesis and skin barrier formation.* Cell, 2010. **141**(2): p. 331-43.
108. Ferby, I., et al., *Mig6 is a negative regulator of EGF receptor-mediated skin morphogenesis and tumor formation.* Nat Med, 2006. **12**(5): p. 568-73.
109. Murillas, R., et al., *Expression of a dominant negative mutant of epidermal growth factor receptor in the epidermis of transgenic mice elicits striking alterations in hair follicle development and skin structure.* EMBO J, 1995. **14**(21): p. 5216-23.
110. Kanzaki, M., et al., *Translocation of a calcium-permeable cation channel induced by insulin-like growth factor-I.* Nat Cell Biol, 1999. **1**(3): p. 165-70.
111. Geraldo, S. and P.R. Gordon-Weeks, *Cytoskeletal dynamics in growth-cone steering.* J Cell Sci, 2009. **122**(Pt 20): p. 3595-604.
112. Xu, X.Z. and P.W. Sternberg, *A C. elegans sperm TRP protein required for sperm-egg interactions during fertilization.* Cell, 2003. **114**(3): p. 285-97.
113. Gallio, M., et al., *The coding of temperature in the Drosophila brain.* Cell. **144**(4): p. 614-24.
114. Kwon, Y., et al., *Fine thermotactic discrimination between the optimal and slightly cooler temperatures via a TRPV channel in chordotonal neurons.* J Neurosci. **30**(31): p. 10465-71.
115. Rosenzweig, M., K. Kang, and P.A. Garrity, *Distinct TRP channels are required for warm and cool avoidance in Drosophila melanogaster.* Proc Natl Acad Sci U S A, 2008. **105**(38): p. 14668-73.
116. Geng, J., et al., *Molecular evolution of the infrared sensory gene TRPA1 in snakes and implications for functional studies.* PLoS One, 2011. **6**(12): p. e28644.
117. Bellono, N.W., et al., *UV light phototransduction activates transient receptor potential A1 ion channels in human melanocytes.* Proc Natl Acad Sci U S A, 2013. **110**(6): p. 2383-8.
118. Bolcskei, K., et al., *Investigation of the role of TRPV1 receptors in acute and chronic nociceptive processes using gene-deficient mice.* Pain, 2005. **117**(3): p. 368-76.
119. Caterina, M.J., et al., *Impaired nociception and pain sensation in mice lacking the capsaicin receptor.* Science, 2000. **288**(5464): p. 306-13.
120. Marics, I., et al., *Acute heat-evoked temperature sensation is impaired but not abolished in mice lacking TRPV1 and TRPV3 channels.* PLoS One, 2014. **9**(6): p. e99828.
121. Park, U., et al., *TRP vanilloid 2 knock-out mice are susceptible to perinatal lethality but display normal thermal and mechanical nociception.* J Neurosci, 2011. **31**(32): p. 11425-36.
122. Che, H., et al., *Functional TRPV and TRPM channels in human preadipocytes.* Pflugers Arch, 2014. **466**(5): p. 947-59.
123. Cheung, S.Y., et al., *Activation of transient receptor potential vanilloid 3 channel suppresses adipogenesis.* Endocrinology, 2015. **156**(6): p. 2074-86.
124. Ryskamp, D.A., et al., *TRPV1 and Endocannabinoids: Emerging Molecular Signals that Modulate Mammalian Vision.* Cells, 2014. **3**(3): p. 914-38.
125. Chavez, A.E., C.Q. Chiu, and P.E. Castillo, *TRPV1 activation by endogenous anandamide triggers postsynaptic long-term depression in dentate gyrus.* Nat Neurosci, 2010. **13**(12): p. 1511-8.
126. Lowin, T. and R.H. Straub, *Cannabinoid-based drugs targeting CB1 and TRPV1, the sympathetic nervous system, and arthritis.* Arthritis Res Ther, 2015. **17**: p. 226.
127. Auer-Grumbach, M., et al., *Alterations in the ankyrin domain of TRPV4 cause congenital distal SMA, scapuloperoneal SMA and HMSN2C.* Nat Genet, 2010. **42**(2): p. 160-4.

78. Liedtke, W., et al., *Vanilloid receptor-related osmotically activated channel (VR-OAC), a candidate vertebrate osmoreceptor.* Cell, 2000. **103**(3): p. 525-35.
79. Nilius, B. and G. Droogmans, *Ion channels and their functional role in vascular endothelium.* Physiol Rev, 2001. **81**(4): p. 1415-59.
80. Strotmann, R., et al., *OTRPC4, a nonselective cation channel that confers sensitivity to extracellular osmolarity.* Nat Cell Biol, 2000. **2**(10): p. 695-702.
81. Wissenbach, U., et al., *Trp12, a novel Trp related protein from kidney.* FEBS Lett, 2000. **485**(2-3): p. 127-34.
82. Chung, M.K., H. Lee, and M.J. Caterina, *Warm temperatures activate TRPV4 in mouse 308 keratinocytes.* J Biol Chem, 2003. **278**(34): p. 32037-46.
83. Fernandez-Fernandez, J.M., et al., *Maxi K+ channel mediates regulatory volume decrease response in a human bronchial epithelial cell line.* Am J Physiol Cell Physiol, 2002. **283**(6): p. C1705-14.
84. Jia, Y., et al., *Anandamide induces cough in conscious guinea-pigs through VR1 receptors.* Br J Pharmacol, 2002. **137**(6): p. 831-6.
85. Bezzerides, V.J., et al., *Rapid vesicular translocation and insertion of TRP channels.* Nat Cell Biol, 2004. **6**(8): p. 709-20.
86. Greka, A., et al., *TRPC5 is a regulator of hippocampal neurite length and growth cone morphology.* Nat Neurosci, 2003. **6**(8): p. 837-45.
87. Singh, B.B., et al., *VAMP2-dependent exocytosis regulates plasma membrane insertion of TRPC3 channels and contributes to agonist-stimulated Ca2+ influx.* Mol Cell, 2004. **15**(4): p. 635-46.
88. Nadler, M.J., et al., *LTRPC7 is a Mg.ATP-regulated divalent cation channel required for cell viability.* Nature, 2001. **411**(6837): p. 590-5.
89. Schmitz, C., et al., *Regulation of vertebrate cellular Mg2+ homeostasis by TRPM7.* Cell, 2003. **114**(2): p. 191-200.
90. Takezawa, R., et al., *Receptor-mediated regulation of the TRPM7 channel through its endogenous protein kinase domain.* Proc Natl Acad Sci U S A, 2004. **101**(16): p. 6009-14.
91. Corey, D.P., et al., *TRPA1 is a candidate for the mechanosensitive transduction channel of vertebrate hair cells.* Nature, 2004. **432**(7018): p. 723-30.
92. Mochizuki, T., et al., *PKD2, a gene for polycystic kidney disease that encodes an integral membrane protein.* Science, 1996. **272**(5266): p. 1339-42.
93. Bargal, R., et al., *Identification of the gene causing mucolipidosis type IV.* Nat Genet, 2000. **26**(1): p. 118-23.
94. Bassi, M.T., et al., *Cloning of the gene encoding a novel integral membrane protein, mucolipidin-and identification of the two major founder mutations causing mucolipidosis type IV.* Am J Hum Genet, 2000. **67**(5): p. 1110-20.
95. Sun, M., et al., *Mucolipidosis type IV is caused by mutations in a gene encoding a novel transient receptor potential channel.* Hum Mol Genet, 2000. **9**(17): p. 2471-8.
96. Nilius, B. and G. Owsianik, *The transient receptor potential family of ion channels.* Genome Biol, 2011. **12**(3): p. 218.
97. Minke, B., *TRP channels and Ca2+ signaling.* Cell Calcium, 2006. **40**(3): p. 261-75.
98. Tiruppathi, C., et al., *Ca2+ signaling, TRP channels, and endothelial permeability.* Microcirculation, 2006. **13**(8): p. 693-708.
99. Berridge, M.J., P. Lipp, and M.D. Bootman, *The versatility and universality of calcium signalling.* Nat Rev Mol Cell Biol, 2000. **1**(1): p. 11-21.
100. Goswami, C., et al., *Estrogen destabilizes microtubules through an ion-conductivity-independent TRPV1 pathway.* J Neurochem, 2011. **117**(6): p. 995-1008.
101. Prakriya, M. and R.S. Lewis, *CRAC channels: activation, permeation, and the search for a molecular identity.* Cell Calcium, 2003. **33**(5-6): p. 311-21.
102. Freichel, M., et al., *Lack of an endothelial store-operated Ca2+ current impairs agonist-dependent vasorelaxation in TRP4-/- mice.* Nat Cell Biol, 2001. **3**(2): p. 121-7.

53. Nilius, B., et al., *Transient receptor potential cation channels in disease.* Physiol Rev, 2007. **87**(1): p. 165-217.
54. Pedersen, S.F., G. Owsianik, and B. Nilius, *TRP channels: an overview.* Cell Calcium, 2005. **38**(3-4): p. 233-52.
55. Liedtke, W., et al., *Mammalian TRPV4 (VR-OAC) directs behavioral responses to osmotic and mechanical stimuli in Caenorhabditis elegans.* Proc Natl Acad Sci U S A, 2003. **100 Suppl 2**: p. 14531-6.
56. Gees, M., B. Colsoul, and B. Nilius, *The role of transient receptor potential cation channels in Ca2+ signaling.* Cold Spring Harb Perspect Biol, 2010. **2**(10): p. a003962.
57. Kumari, S., et al., *Influence of membrane cholesterol in the molecular evolution and functional regulation of TRPV4.* Biochem Biophys Res Commun, 2015. **456**(1): p. 312-9.
58. Kastenhuber, E., et al., *Phylogenetic analysis and expression of zebrafish transient receptor potential melastatin family genes.* Dev Dyn, 2013. **242**(11): p. 1236-49.
59. Gracheva, E.O., et al., *Molecular basis of infrared detection by snakes.* Nature, 2010. **464**(7291): p. 1006-11.
60. Julius, D., *From peppers to peppermints: natural products as probes of the pain pathway.* Harvey Lect, 2005. **101**: p. 89-115.
61. Patapoutian, A., et al., *ThermoTRP channels and beyond: mechanisms of temperature sensation.* Nat Rev Neurosci, 2003. **4**(7): p. 529-39.
62. Kobayashi, K., et al., *Distinct expression of TRPM8, TRPA1, and TRPV1 mRNAs in rat primary afferent neurons with adelta/c-fibers and colocalization with trk receptors.* J Comp Neurol, 2005. **493**(4): p. 596-606.
63. Tominaga, M., et al., *The cloned capsaicin receptor integrates multiple pain-producing stimuli.* Neuron, 1998. **21**(3): p. 531-43.
64. Gibbs, J.L., J.L. Melnyk, and A.I. Basbaum, *Differential TRPV1 and TRPV2 channel expression in dental pulp.* J Dent Res, 2011. **90**(6): p. 765-70.
65. Hamamoto, T., et al., *Localization of transient receptor potential channel vanilloid subfamilies in the mouse larynx.* Acta Otolaryngol, 2008. **128**(6): p. 685-93.
66. Hamamoto, T., et al., *Localization of transient receptor potential vanilloid (TRPV) in the human larynx.* Acta Otolaryngol, 2009. **129**(5): p. 560-8.
67. Koike, S., et al., *Distribution of vanilloid receptors in the rat laryngeal innervation.* Acta Otolaryngol, 2004. **124**(4): p. 515-9.
68. Lewinter, R.D., et al., *Immunoreactive TRPV-2 (VRL-1), a capsaicin receptor homolog, in the spinal cord of the rat.* J Comp Neurol, 2004. **470**(4): p. 400-8.
69. Ma, Q.P., *Vanilloid receptor homologue, VRL1, is expressed by both A- and C-fiber sensory neurons.* Neuroreport, 2001. **12**(17): p. 3693-5.
70. Nilius, B., T. Biro, and G. Owsianik, *TRPV3: time to decipher a poorly understood family member!* J Physiol, 2014. **592**(2): p. 295-304.
71. Valdes-Rodriguez, R., S.B. Kaushik, and G. Yosipovitch, *Transient receptor potential channels and dermatological disorders.* Curr Top Med Chem, 2013. **13**(3): p. 335-43.
72. Borbiro, I., et al., *Activation of transient receptor potential vanilloid-3 inhibits human hair growth.* J Invest Dermatol, 2011. **131**(8): p. 1605-14.
73. Ishibashi, T., et al., *Expression of transient receptor potential vanilloid (TRPV) 1, 2, 3, and 4 in mouse inner ear.* Acta Otolaryngol, 2008. **128**(12): p. 1286-93.
74. Mergler, S., et al., *TRPV channels mediate temperature-sensing in human corneal endothelial cells.* Exp Eye Res, 2010. **90**(6): p. 758-70.
75. Moqrich, A., et al., *Impaired thermosensation in mice lacking TRPV3, a heat and camphor sensor in the skin.* Science, 2005. **307**(5714): p. 1468-72.
76. Peier, A.M., et al., *A heat-sensitive TRP channel expressed in keratinocytes.* Science, 2002. **296**(5575): p. 2046-9.
77. Ueda, T., et al., *TRPV3, a thermosensitive channel is expressed in mouse distal colon epithelium.* Biochem Biophys Res Commun, 2009. **383**(1): p. 130-4.

27. Majhi, R.K., et al., *Functional expression of TRPV channels in T cells and their implications in immune regulation.* FEBS J, 2015. **282**(14): p. 2661-81.
28. Wagner, S.A., et al., *A proteome-wide, quantitative survey of in vivo ubiquitylation sites reveals widespread regulatory roles.* Mol Cell Proteomics, 2011. **10**(10): p. M111 013284.
29. Peier, A.M., et al., *A TRP channel that senses cold stimuli and menthol.* Cell, 2002. **108**(5): p. 705-15.
30. Smith, G.D., et al., *TRPV3 is a temperature-sensitive vanilloid receptor-like protein.* Nature, 2002. **418**(6894): p. 186-90.
31. Xu, H., et al., *TRPV3 is a calcium-permeable temperature-sensitive cation channel.* Nature, 2002. **418**(6894): p. 181-6.
32. Caterina, M.J., et al., *The capsaicin receptor: a heat-activated ion channel in the pain pathway.* Nature, 1997. **389**(6653): p. 816-24.
33. Cao, E., et al., *TRPV1 channels are intrinsically heat sensitive and negatively regulated by phosphoinositide lipids.* Neuron, 2013. **77**(4): p. 667-79.
34. Dopico, A.M., A.N. Bukiya, and A.K. Singh, *Large conductance, calcium- and voltage-gated potassium (BK) channels: regulation by cholesterol.* Pharmacol Ther, 2012. **135**(2): p. 133-50.
35. Lukacs, V., et al., *Promiscuous activation of transient receptor potential vanilloid 1 (TRPV1) channels by negatively charged intracellular lipids: the key role of endogenous phosphoinositides in maintaining channel activity.* J Biol Chem, 2013. **288**(49): p. 35003-13.
36. Morales-Lazaro, S.L., et al., *Structural determinants of the transient receptor potential 1 (TRPV1) channel activation by phospholipid analogs.* J Biol Chem, 2014. **289**(35): p. 24079-90.
37. Morales-Lazaro, S.L., S.A. Simon, and T. Rosenbaum, *The role of endogenous molecules in modulating pain through transient receptor potential vanilloid 1 (TRPV1).* J Physiol, 2013. **591**(13): p. 3109-21.
38. Morenilla-Palao, C., et al., *Lipid raft segregation modulates TRPM8 channel activity.* J Biol Chem, 2009. **284**(14): p. 9215-24.
39. Yoo, S., J.Y. Lim, and S.W. Hwang, *Sensory TRP channel interactions with endogenous lipids and their biological outcomes.* Molecules, 2014. **19**(4): p. 4708-44.
40. Cheng, W., et al., *Heteromeric heat-sensitive transient receptor potential channels exhibit distinct temperature and chemical response.* J Biol Chem, 2012. **287**(10): p. 7279-88.
41. Hellwig, N., et al., *Homo- and heteromeric assembly of TRPV channel subunits.* J Cell Sci, 2005. **118**(Pt 5): p. 917-28.
42. Hoenderop, J.G., et al., *Homo- and heterotetrameric architecture of the epithelial Ca2+ channels TRPV5 and TRPV6.* EMBO J, 2003. **22**(4): p. 776-85.
43. Kobori, T., et al., *The transient receptor potential channels TRPP2 and TRPC1 form a heterotetramer with a 2:2 stoichiometry and an alternating subunit arrangement.* J Biol Chem, 2009. **284**(51): p. 35507-13.
44. Montell, C., *The history of TRP channels, a commentary and reflection.* Pflugers Arch, 2011. **461**(5): p. 499-506.
45. Moiseenkova-Bell, V.Y., et al., *Structure of TRPV1 channel revealed by electron cryomicroscopy.* Proc Natl Acad Sci U S A, 2008. **105**(21): p. 7451-5.
46. Liao, M., et al., *Structure of the TRPV1 ion channel determined by electron cryo-microscopy.* Nature, 2013. **504**(7478): p. 107-12.
47. Owsianik, G., et al., *Permeation and selectivity of TRP channels.* Annu Rev Physiol, 2006. **68**: p. 685-717.
48. Ellinor, P.T., et al., *Ca2+ channel selectivity at a single locus for high-affinity Ca2+ interactions.* Neuron, 1995. **15**(5): p. 1121-32.
49. Zubcevic, L., et al., *Cryo-electron microscopy structure of the TRPV2 ion channel.* Nat Struct Mol Biol, 2016. **23**(2): p. 180-186.
50. Huynh, K.W., et al., *Structure of the full-length TRPV2 channel by cryo-EM.* Nat Commun, 2016. **7**: p. 11130.
51. Damann, N., T. Voets, and B. Nilius, *TRPs in our senses.* Curr Biol, 2008. **18**(18): p. R880-9.
52. Montell, C., *The TRP superfamily of cation channels.* Sci STKE, 2005. **2005**(272): p. re3.

Reference:

1. Cosens, D.J. and A. Manning, *Abnormal electroretinogram from a Drosophila mutant.* Nature, 1969. **224**(5216): p. 285-7.
2. Montell, C. and G.M. Rubin, *Molecular characterization of the Drosophila trp locus: a putative integral membrane protein required for phototransduction.* Neuron, 1989. **2**(4): p. 1313-23.
3. Minke, B., *Drosophila mutant with a transducer defect.* Biophys Struct Mech, 1977. **3**(1): p. 59-64.
4. Minke, B., C. Wu, and W.L. Pak, *Induction of photoreceptor voltage noise in the dark in Drosophila mutant.* Nature, 1975. **258**(5530): p. 84-7.
5. Clapham, D.E., *TRP channels as cellular sensors.* Nature, 2003. **426**(6966): p. 517-24.
6. Montell, C., et al., *Rescue of the Drosophila phototransduction mutation trp by germline transformation.* Science, 1985. **230**(4729): p. 1040-3.
7. Hofmann, T., et al., *Subunit composition of mammalian transient receptor potential channels in living cells.* Proc Natl Acad Sci U S A, 2002. **99**(11): p. 7461-6.
8. Cai, X., *Unicellular Ca2+ signaling 'toolkit' at the origin of metazoa.* Mol Biol Evol, 2008. **25**(7): p. 1357-61.
9. Chang, Y., et al., *Properties of the intracellular transient receptor potential (TRP) channel in yeast, Yvc1.* FEBS Lett, 2010. **584**(10): p. 2028-32.
10. Matsuura, H., et al., *Evolutionary conservation and changes in insect TRP channels.* BMC Evol Biol, 2009. **9**: p. 228.
11. Wheeler, G.L. and C. Brownlee, *Ca2+ signalling in plants and green algae--changing channels.* Trends Plant Sci, 2008. **13**(9): p. 506-14.
12. Denis, V. and M.S. Cyert, *Internal Ca(2+) release in yeast is triggered by hypertonic shock and mediated by a TRP channel homologue.* J Cell Biol, 2002. **156**(1): p. 29-34.
13. Zhou, X.L., et al., *The transient receptor potential channel on the yeast vacuole is mechanosensitive.* Proc Natl Acad Sci U S A, 2003. **100**(12): p. 7105-10.
14. de Bono, M., et al., *Social feeding in Caenorhabditis elegans is induced by neurons that detect aversive stimuli.* Nature, 2002. **419**(6910): p. 899-903.
15. Stowers, L., et al., *Loss of sex discrimination and male-male aggression in mice deficient for TRP2.* Science, 2002. **295**(5559): p. 1493-500.
16. Zhang, Y., et al., *Coding of sweet, bitter, and umami tastes: different receptor cells sharing similar signaling pathways.* Cell, 2003. **112**(3): p. 293-301.
17. Arias-Darraz, L., et al., *A transient receptor potential ion channel in Chlamydomonas shares key features with sensory transduction-associated TRP channels in mammals.* Plant Cell, 2015. **27**(1): p. 177-88.
18. Fujiu, K., et al., *Mechanoreception in motile flagella of Chlamydomonas.* Nat Cell Biol, 2011. **13**(5): p. 630-2.
19. Martinac, B., Y. Saimi, and C. Kung, *Ion channels in microbes.* Physiol Rev, 2008. **88**(4): p. 1449-90.
20. Julius, D., *TRP channels and pain.* Annu Rev Cell Dev Biol, 2013. **29**: p. 355-84.
21. Frias, B. and A. Merighi, *Capsaicin, Nociception and Pain.* Molecules, 2016. **21**(6).
22. Tominaga, M., *[Thermosensitive TRP channels and brain function].* Nihon Shinkei Seishin Yakurigaku Zasshi, 2016. **36**(2): p. 37-41.
23. Barnhill, J.C., et al., *RGA protein associates with a TRPV ion channel during biosynthesis and trafficking.* J Cell Biochem, 2004. **91**(4): p. 808-20.
24. Bavassano, C., et al., *Identification of voltage-gated K(+) channel beta 2 (Kvbeta2) subunit as a novel interaction partner of the pain transducer Transient Receptor Potential Vanilloid 1 channel (TRPV1).* Biochim Biophys Acta, 2013. **1833**(12): p. 3166-75.
25. Jahnel, R., et al., *Dual expression of mouse and rat VRL-1 in the dorsal root ganglion derived cell line F-11 and biochemical analysis of VRL-1 after heterologous expression.* Eur J Biochem, 2003. **270**(21): p. 4264-71.
26. Kobayashi, Y., et al., *Identification and characterization of GSRP-56, a novel Golgi-localized spectrin repeat-containing protein.* Exp Cell Res, 2006. **312**(16): p. 3152-64.

Chapter 6

Bibliography